# The role of the tumour microenvironment in arginine deprivation in malignant pleural mesothelioma

A thesis submitted for the degree of Doctor of Philosophy at the University of London

**Dr. Melissa Phillips**

Clinical Research Fellow

Centre for Molecular Oncology
Barts Cancer Institute
Queen Mary University of London
EC1M 6BQ
UK

# Declaration

I, Melissa Phillips, confirm that the work presented in this thesis is my own. Where information has been derived from other sources, I confirm that this has been indicated in the thesis.

Signed:

Date:

# Acknowledgements


## Supervisors

**Dr Peter Szlosarek**
Clinical Senior Lecturer and Honorary Consultant in Medical Oncology, Centre for Molecular Oncology, Barts Cancer Institute.

**Professor Frances Balkwill OBE**
Centre Lead, Centre for Cancer and Inflammation, Barts Cancer Institute.

## Principle co-worker

| | |
|---|---|
| **Mr Ramsay Khadeir** | Laboratory Technician, Centre for Molecular Oncology. Provided support throughout final year of my PhD. |

## Co-workers

| | |
|---|---|
| **Dr Essam Ghazaly** | Post-doctoral Research Assistant, Centre for Haemato-Oncology. Performed Mass Spectrometry analysis |
| **Dr Pedro-Maria Casado** | Post-doctoral Research Assistant, Centre for Haemato-Oncology. Prepared cell lysates for Proteomic analysis |
| **Dr Pedro Cutillas** | Reader in Cell Signalling and Proteomics, Centre for Haemato-Oncology. Performed Proteomic analysis |
| **Mr Andrew Clear** | Research Assistant, Centre for Haemato-Oncology. Gave extensive advice and training on Ariol Imaging Analysis for quantification of macrophages |
| **Mr George Elia** | Pathology Manager, Pathology Services. Performed immunohistochemistry using the Ventana Classic automated system |

| | |
|---|---|
| **Dr Barbara Delage** | Post-doctoral Research Assistant, Centre for Molecular Oncology. Performed initial experiments for Affymetrix analysis |
| **Dr Laura Tookman** | Clinical Research Fellow, Centre for Molecular Oncology. Gave training on confocal microscopy for immunofluorescence analysis. |
| **Ms Julie Andow Cleaver** | Animal Technician, Centre for Molecular Oncology. Gave training in intraperitoneal (IP) injections in mice and performed all IP injections in the SB225002 pilot study. |
| **Dr Ming Yuan** | Post-doctoral Research Assistant, Centre for Molecular Oncology. Performed all subcutaneous injections of tumour cells into mice for *in vivo* studies. |
| **Dr Rebecca Pike** | Performed live cell sorting of co-cultured cells for proteomics and gave extensive training in FACS analysis. |

# Collaborations

**Dr Nico van Rooijen**

Department of Molecular Cell Biology, Vrije Universiteit, Amsterdam.
Provided Liposomal Clodronate and Liposomal phosphate buffered saline (PBS).

**Polaris Pharmaceuticals**
San Diego, USA.
Provided ADI-PEG20.

# Funding

This work was supported by a joint grant from the Medical Research Council (MRC), the British Lung Foundation (BLF), and the Mick Knighton Mesothelioma Research Fund (MKMRF). Funding was also provided by the Barts and the London Charity.

# With special thanks

First and foremost I would like to thank my PhD supervisor, Dr Peter Szlosarek, for allowing me to follow this project into exciting new areas and for providing support and encouragement throughout. I would also like to thank Dr Sarah Martin's group for their advice and guidance throughout the course of my PhD. In particular, I would like to thank Dr Gemma Bridge and Dr Sukaina Rashid. Special thanks must also go to Dr Mike Allen, Dr Katherine Bridge and Dr Alice Shia for experimental advice and scientific chats which were much appreciated. I would like to thank Dr Tyson Sharp, Head of Molecular Oncology and Professor Iain McNeish, former Head of Molecular Oncology, for their general help and guidance over the years.

Finally, a big thank you to my family for all their patience and understanding.

# Dedication

I would like to dedicate this work to the late Mr Roger Parker MS FRCS. Thank you for everything.

# Abstract

Approximately 50% of all malignant pleural mesotheliomas (MPM) are deficient in argininosuccinate synthetase (ASS1), the rate-limiting enzyme in arginine biosynthesis, and are sensitive to arginine deprivation. This discovery in MPM has been translated into the clinic using the arginine depletor pegylated arginine deiminase (ADI-PEG20), which showed a halving in the risk of disease progression in a randomised phase II study. However, unstudied to date, stromal resistance to ADI-PEG20 may reduce its efficacy. Here, I studied the effect of macrophages, abundant in mesothelioma, on the tumour cytotoxicity of ADI-PEG20.

A distinct pro-inflammatory cytokine gene expression signature involved in macrophage recruitment and activation was identified and validated in ADI-PEG20-treated ASS1 negative MPM cell lines. *In vivo* induction of pro-inflammatory cytokines was also seen in ADI-PEG20-treated patient plasma. Notably, *in vitro* co-culture experiments demonstrated a significant increase in ASS1 negative MPM cell viability upon co-culture with macrophages in the presence of ADI-PEG20. This was accompanied by a significant increase in ASS1 expression in co-cultured macrophages, with a corresponding increase in argininosuccinate lyase (ASL) expression in co-cultured tumour cells and a doubling in levels of the arginine precursor, argininosuccinate, in cell supernatant. The addition of argininosuccinate to tumour cell media rescued ASS1 negative MPM cells from ADI-PEG20 cytotoxicity, while the macrophage-mediated resistance to ADI-PEG20 was abrogated following ASL knockdown in MPM cells. Finally, xenograft studies demonstrated a significant reduction in tumour volume in mice treated with ADI-PEG20 in combination with macrophage depletion, compared with ADI-PEG20 alone.

Collectively, the data indicate that as a result of metabolic ‘cross-talk’ between macrophages and ASS1 negative MPM cells, macrophages mediate MPM resistance to ADI-PEG20 via the provision of argininosuccinate. My studies provide a rationale for combining ADI-PEG20 with an inhibitor of macrophage recruitment in the treatment of ASS1-deficient mesothelioma.

# Table of Contents

List of Figures ..... 14

List of Tables ..... 19

Abbreviations ..... 20

Publications ..... 25

Chapter 1. Introduction ..... 27

1.1 Malignant Pleural Mesothelioma ..... 27

1.1.1 Aetiology and Pathogenesis ..... 27

1.1.2 Incidence ..... 32

1.1.3 Clinical Presentation ..... 33

1.1.4 Diagnosis ..... 33

1.1.5 Current therapeutic strategies ..... 35

1.2 Tumour metabolism: an emerging cancer 'hallmark' ..... 46

1.3 Amino acid deprivation as an anti-cancer therapeutic strategy ..... 47

1.3.1 Asparagine ..... 47

1.3.2 Arginine ..... 47

1.3.3 Strategies for arginine depletion ..... 56

1.3.4 Arginine Deprivation: pre-clinical data ..... 57

1.3.5 Arginine deprivation: clinical data ..... 59

1.3.6 Resistance to arginine depletion ..... 62

1.4 Tumour microenvironment ..... 65

1.4.1 Cells of the tumour stroma ..... 66

1.5 Macrophage Biology ..... 72

1.5.1 Macrophage development ..... 72

1.5.2 Macrophage activation and phenotypic diversity ..... 72

1.5.3 The arginine metabolome and macrophages ..... 75

1.5.4 Macrophages, cancer cells and the tumour microenvironment ..... 77

1.5.5 TAM and mesothelioma ..... 88

1.5.6 TAM and therapeutic resistance in cancer ..... 90

1.6 Hypothesis ..... 93

1.7 Thesis aims ..... 94

Chapter 2. Materials and Methods ..... 95
2.1 Cell Culture ..... 95
2.1.1 Tumour cell lines (MSTO, Ju77, 2591, H28 and H226) ..... 95
2.1.2 Human monocyte-derived macrophages ..... 96
2.1.3 Freezing and thawing cells ..... 101
2.2 Transfection techniques ..... 101
2.2.1 ASS1 overexpression ..... 101
2.2.2 ASL/XBP1 SiRNA transfection ..... 102
2.3 Reagents ..... 102
2.3.1 ADI-PEG20 ..... 102
2.3.2 Liposomal Clodronate and Liposomal PBS ..... 103
2.3.3 Tunicamycin ..... 103
2.3.4 SB225002 ..... 103
2.3.5 Recombinant human cytokines ..... 103
2.3.6 Argininosuccinic Acid (ASA) ..... 104
2.4 Cell viability assays (MTS) ..... 104
2.4.1 ADI-PEG20 ..... 104
2.4.2 Liposomal Clodronate (CLIP) ..... 105
2.4.3 ADI-PEG20 plus argininosuccinic acid (ASA) ..... 105
2.5 Real-time PCR analysis ..... 105
2.5.1 RNA extraction ..... 105
2.5.2 RNA analysis ..... 106
2.5.3 Reverse transcription of RNA to yield cDNA ..... 106
2.5.4 Quantitative RT-PCR (qRT-PCR) ..... 107
2.6 Western Blot ..... 108
2.6.1 Protein Extraction ..... 108
2.6.2 Protein concentration assay ..... 109
2.6.3 Western Blotting ..... 109
2.7 Enzyme-linked immunosorbent assay (ELISA) ..... 111
2.7.1 Cell Supernatants ..... 111
2.7.2 Human Plasma ..... 114
2.8 Immunostaining ..... 116
2.8.1 Immunohistochemistry ..... 116
2.8.2 Immunofluorescence ..... 117

2.9 Flow Cytometry ..... 120
2.9.1 FACS antibody staining of co-cultured tumour cells ..... 120
2.9.2 FACS antibody staining of monocytes ..... 120
2.9.3 FACS antibody staining of macrophages ..... 121
2.9.4 FACS antibody staining of co-cultured cells for live sorting ..... 121
2.9.5 FACS analysis ..... 122
2.10 Preparation of supernatant for Mass Spectrometry analysis ..... 122
2.11 Preparation of cells for proteomics analysis ..... 123
2.12.1 Co-culture experiments to assess tumour viability ..... 123
2.12.2 Co-culture experiments for qRT-PCR and Western blot analysis ..... 124
2.12.3 Co-culture experiments for mass spectrometry ..... 124
2.12.4 Co-culture experiments for Proteomics ..... 125
2.13 Cytokine Stimulation of macrophages ..... 126
2.13.1 Determining the optimal concentration of individual cytokines ..... 126
2.13.2 Cytokine stimulation of macrophages ..... 126
2.13.3 Cytokine stimulation of tumour cells ..... 126
2.14 *In vitro* assays to validate the Affymetrix data ..... 127
2.14.1 ADI-PEG20 ..... 127
2.14.2 Arginine-deficient media ..... 127
2.15 Animal Studies ..... 127
2.15.1 Mouse xenograft model ..... 127
2.15.2 Mesotheliomal cell preparation and transplantation ..... 128
2.15.3 Injections ..... 128
2.15.4 Treatment schedules ..... 128
2.15.5 Mesothelioma tumour progression assessment ..... 130
2.15.6 Sacrifice and tumour removal ..... 130
2.16 Statistical analysis ..... 130

Chapter 3. ADI-PEG20 induces pro-inflammatory cytokine production by ASS1-negative malignant mesothelioma cells ..... 132
3.1 Introduction ..... 132
3.2 Aims ..... 133
3.3 ADI-PEG20 causes cell death in ASS1 negative mesothelioma cells ..... 134

3.4 Validation of the pro-inflammatory gene expression signature induced by ADI-PEG20 treatment ..... 136
3.5 Arginine-deficient media replicates the cytokine response in ASS1 negative mesothelioma cells ..... 141
3.6 Endoplasmic reticulum stress induces pro-inflammatory cytokine response 144
3.7 *In vivo* induction of pro-inflammatory cytokines by ADI-PEG20 ..... 156
3.8 Discussion ..... 166

Chapter 4. Macrophages promote resistance to ADI-PEG20 in ASS1 negative mesothelioma ..... 174
4.1 Introduction ..... 174
4.2 Aims ..... 175
4.3 Mesothelioma is enriched with ASS1-expressing macrophages ..... 176
4.4 Quantification of macrophage number in ASS1 'high' and ASS1 'low' mesothelioma ..... 178
4.5 Macrophages mediate resistance to ADI-PEG20 in ASS1 negative mesothelioma cells *in vitro* ..... 179
4.6 ADI-PEG20 exposure leads to coordinate up-regulation of ASS1 in macrophages and ASL in tumour cells ..... 189
4.7 Tumour-derived pro-inflammatory cytokines induced by ADI-PEG20 modulate macrophage ASS1 expression ..... 197
4.8 Co-cultured macrophages secrete argininosuccinate following ADI-PEG20 202
4.9 Argininosuccinate rescues ASS1 negative mesothelioma cells from ADI-PEG20-induced cytoxicity ..... 205
4.10 Macrophage-mediated resistance to ADI-PEG20 is reversed by tumoural ASL knockdown ..... 207
4.11 Proteomic analysis of arginine-labelled peptides in ASS1 negative tumour cells cultured alone and with macrophages ..... 210
4.12 Analysis of macrophage phenotype in the presence and absence of ADI-PEG20 ..... 213
4.13 Discussion ..... **219**

Chapter 5. Macrophage depletion potentiates the cytotoxic effect of ADI-PEG20 *in vivo* ..... 229
5.1 Introduction ..... 229

5.2 Aims ..... 230
5.3 CXCR2 expression is up-regulated in co-cultured macrophages following ADI-PEG20 treatment ..... 231
5.4 CXCR2 blockade fails to prevent up-regulation of macrophage ASS1 in response to ADI-PEG20 ..... 233
5.5 CXCR2 blockade has no effect on the anti-tumour efficacy of ADI-PEG20 *in vivo*. ..... 235
5.6 Liposomal Clodronate (CLIP) does not affect tumour cell viability *in vitro* ... 237
5.7 Macrophage depletion enhances the cytotoxic effect of ADI-PEG20 *in vivo* 239
5.8.....ADI-PEG20 stimulates recruitment of macrophages into ASS1 negative xenografts ..... 241
5.9 Discussion ..... 244
Chapter 6. Conclusions and future research ..... 252
6.1 Summary ..... 252
6.2 Conclusions ..... 253
6.3 Future work ..... 254
6.3.1 Alternative methods of targeting macrophages ..... 254
6.3.2 Assessment of ADI-PEG20 in combination with chemotherapy ..... 255
6.3.3 Further assessment of the regulation of ASL ..... 256
6.3.4 Further Proteomics analysis of the macrophage-mediated resistance pathway ..... 257
6.3.5 Assessment of the effect of arginine depletion on other stromal cells within the MPM tumour microenvironment ..... 257
Bibliography ..... 259
Appendix ..... 298

# List of Figures

Figure 1.1 Axial computed tomography (CT) scan.....38
Figure 1.2. Arginine utilisation within the tumour cell.....50
Figure 1.3. Arginine deprivation: mechanisms of action and proposed resistance mechanisms. .....64
Figure 1.4. Reciprocal interactions of tumour cells with stromal cells in the tumour microenvironment.....70
Figure 1.5. The differentiation pathways of 'classically'-activated M1 macrophages and 'alternatively'-activated M2 macrophages .....74
Figure 1.6. Schematic representation of TAM 1 and TAM 2 metabolic pathways .....76
Figure 1.7. The various pro-tumoural effector functions of TAM. .....86
Figure 2.1. Diagram demonstrating the different layers following Ficoll separation...97
Figure 2.2. Flow cytometry analysis assessing the % of CD14 positive cells following MACS selection.....97
Figure 3.1. A) ASS1 expression in a panel of MPM cell lines; B) Response of ASS1 negative cells toADI-PEG20 treatment ..... 135
Figure 3.2. Validation of the pro-inflammatory gene expression by qRT-PCR.....138
Figure 3.3. Assessment of pro-inflammatory cytokines by ELISA (ASS1 negative MPM cells only).....139
Figure 3.4. Pro-inflammatory gene expression signature induced by arginine-deficient media in ASS1 negative MPM cells lines.....142
Figure 3.5. Pro-inflammatory cytokine response induced by arginine-deficient media in ASS1 negative MPM cells.....143
Figure 3.6. Validation of the up-regulation of ER stress marker XBP1.....146
Figure 3.7. Up-regulation of XBP1 mRNA at 24 hours following TM treatment. .....147
Figure 3.8. Pro-inflammatory cytokine gene expression in a panel of mesothelioma cell lines at 24hrs following TM treatment. ..... 148
Figure 3.9. Confirmation of XBP1 knockdown in ASS1 negative MPM cell lines 2591 and MSTO at 24hrs by qRT-PCR.....149
Figure 3.10. ADI-PEG20-induced pro-inflammatory cytokine gene expression signature following XBP1 silencing in ASS1 negative cells (qRT-PCR).....151

Figure 3.11. Tumour cell viability in XBP1 knockdown ASS1 negative cell lines at 24hrs following ADI-PEG20 treatment. ..... 153
Figure 3.12. NFκB phosphorylation following ADI-PEG20 treatment in ASS1 negative MPM cell lines..... 155
Figure 3.13. Diagrammatic summary of ADAM trial design..... 157
Figure 3.14. Plasma concentrations of pro-inflammatory cytokines at baseline and following 1st administration of ADI-PEG20..... 161
Figure 3.15. Plasma concentrations of pro-inflammatory cytokines at baseline and the 9 week follow-up for patients in both trial groups..... 163
Figure 3.16. Difference in plasma concentrations of pro-inflammatory cytokines in patients receiving ADI-PEG20 (Arm B) whose disease progressed at 9 week follow up compared with those who showed stable disease or a partial response ..... 164
Figure 3.17. ER stress and activation of the UPR: implication in the inflammatory response following ADI-PEG20 treatment..... 169
Figure 4.1 A+B. Human mesothelioma is enriched with ASS1 expressing macrophages..... 177
Figure 4.2. Percentage of CD68 positive macrophages in human mesothelioma tissue. ..... 178
Figure 4.3. Tumour cell viability at 4 days post ADI-PEG20 treatment. ..... 180
Figure 4.4. 2591 tumour cell viability following ADI-PEG20 treatment..... 182
Figure 4.5. MSTO tumour cell viability following ADI-PEG20 treatment..... 184
Figure 4.6. Ju77 tumour cell viability following ADI-PEG20 treatment. ..... 186
Figure 4.7. Macrophage viability at 4 days post ADI-PEG20 treatment..... 188
Figure 4.8. Increase in ASS1 expression in co-cultured macrophages at 48 hours following treatment with ADI-PEG20..... 190
Figure 4.9. Macrophage ASL expression at 48 hours following ADI-PEG20 treatment..... 191
Figure 4.10. ASS1 expression in MSTO tumour cells cultured alone and with macrophages ± ADI-PEG20 treatment..... 193
Figure 4.11. Tumoural ASL expression ± ADI-PEG20 treatment..... 195
Figure 4.12 A. Induction of ASS1 in macrophages by pro-inflammatory cytokines (qRT-PCR). ..... 198
Figure 4.12 B. Induction of ASS1 in macrophages by pro-inflammatory cytokines

(western blot).....198
Figure 4.13. ASL expression in MSTO mesothelioma cells ± pro-inflammatory cytokines.....200
Figure 4.14. ASL expression in MSTO mesothelioma cells ± ADI-PEG20 and argininosuccinic acid (ASA).....201
Figure 4.15. Arginine and Citrulline in supernatant of co-cultured cells ± ADI-PEG20. ..... 203
Figure 4.16. Argininosuccinate in supernatant of co-cultured cells ± ADI-PEG20...204
Figure 4.17. Effect of argininosuccinate on MSTO cell viability treated with ADI-PEG20. ..... 206
Figure 4.18. SiRNA knockdown of tumoural ASL mRNA expression. .....208
Figure 4.19. MSTO cell viability following ASL mRNA knockdown and ADI-PEG20. .....208
Figure 4.20. MSTO tumour cell viability following ASL mRNA knockdown and ADI-PEG20. ..... 209
Figure 4.21. Proteomic analysis identifying the percentage of arginine labelled peptides present in MSTO tumour cells following ADI-PEG20 treatment.....211
Figure 4.22. Cell surface marker expression in macrophages cultured alone and with MSTO tumour cells ±ADI-PEG20.....215
Figure 4.23. Macrophage cell surface marker expression ± ADI-PEG20. .....216
Figure 4.24. Induction of IL-10 mRNA expression in co-cultured macrophages ± ADI-PEG20. ..... 217
Figure 4.25. Co-cultured macrophage arginase expression following ADI-PEG20 treatment..... 218
Figure 4.26. Proposed mechanism of macrophage-mediated resistance to ADI-PEG20 in ASS1 negative mesothelioma. ..... 221
Figure 5.1. Co-cultured macrophage CXCR2 expression following ADI-PEG20 treatment..... 232
Figure 5.2. Co-cultured macrophage ASS1 expression following ADI-PEG20 treatment and CXCR2 blockade.....234
Figure 5.3. CXCR2 blockade plus ADI-PEG20 in vivo.....236
Figure 5.4. MSTO cell viability at 6 days following treatment with CLIP.....238

Figure 5.5. ADI-PEG20 combined with macrophage depletion suppression in the MSTO xenograft model. ..... 240
Figure 5.6. Difference in macrophage number in xenograft tumours following ADI-PEG20 treatment. ..... 242
Figure 5.7. F4/80 expression in mouse xenografts ..... 243

# List of Tables

Table 1.1. Markers frequently used in the diagnosis of mesothelioma. .....34
Table 1.2. Summary of ASS1 expression in tumours .....55
Table 1.3. Completed clinical studies of single agent ADI-PEG20 in advance cancer

.....61
Table 2.1. Primary antibodies used for Western Blotting .....111
Table 2.2. Secondary antibodies used for Western Blotting.....111
Table 2.3. Standard range and Minimum Detection Dose (MDD) for each of the cytokines analysed.....112
Table 2.4. Standard curve range for each cytokine. .....115
Table 2.5. Primary antibodies used for Immunostaining.....118
Table 3.1. Gene expression analysis using the Affymetrix U133 plus 2.0 microarray platform. .....137
Table 3.2. Gene expression analysis using the Affymetrix U133 plus 2.0 microarray platform. .....144
Table 5.1.MacrophageTherapeuticTargeting.....250

# Abbreviations

| | |
|---|---|
| ABT | Androgen blockade therapy |
| ADAM | Arginine deiminase and mesothelioma |
| ADC | Arginine decarboxylase |
| ADI | Arginine deiminase |
| ALL | Acute lymphoblastic leukaemia |
| ANOVA | Analysis of variance |
| APC | Adenomatous Polyposis Coli |
| AP1 | Activator protein 1 |
| ARG | Arginase |
| ASA | Argininosuccinic acid |
| ASCO | American Society of Clinical Oncology |
| ASL | Argininosuccinate lyase |
| ASS1 | Argininosuccinate synthetase-1 |
| ATF6 | Activating Transcription Factor 6 |
| ATP | Adenosine triphosphate |
| BAP1 | BRCA1- associated protein-1 |
| BiP | Immunoglobulin heavy-chain-binding protein |
| BSA | Bovine serum albumin |
| BSC | Best supportive care |
| CAF | Cancer associated fibroblasts |
| CAT | Cationic amino acid transporter |
| Cav-1 | Caveolin-1 |
| CDKN2A/ARF | Cyclin-dependent kinase inhibitor 2A/alternative reading frame |
| CDKN2B | Cyclin-dependent kinase inhibitor 2B |
| CCL | C-C chemokine ligand |
| CCND2 | Cyclin D2 |
| CLIP | Liposomal clodronate |
| CPS1 | Carbamoylphosphate synthetase I |
| CSF-1 | Colony-stimulating factor-1 |
| CT | Computed Tomography |

| | |
|---|---|
| CTGF | Connective tissue growth factor |
| CTLA-4 | Cytotoxic T-lymphocyte antigen 4 |
| CXCL | Chemokine (C-X-C motif) ligand |
| CXCR | Chemokine (C-X-C motif) receptor |
| DHFR | Dihydrofolate reductase |
| DMEM | Dulbecco's Modified Eagle Medium |
| DMSO | Dimethyl sulphoxide |
| EC | Endothelial cell |
| ECM | Extracellular matrix |
| EDTA | Ethylenediaminetetraacetic acid |
| EGF | Epidermal Growth Factor |
| EGFR | Epidermal Growth Factor Receptor |
| ELISA | Enzyme linked immunosorbent assay |
| EMT | Epithelial mesenchymal transition |
| EPP | Extrapleural pneumonectomy |
| ER | Endoplasmic reticulum |
| ERK | Extracellular signal-regulated kinases |
| FACS | Fluorescence-activated cell sorting |
| FAK | Focal adhesion kinase |
| FBS | Fetal Bovine Serum |
| 18-FDG-PET | 18F-deoxyglucose-positron emission tomography |
| FFPE | Formulin-fixed paraffin embedded |
| FGF-2 | Fibroblast-growth factor 2 |
| FH | Fumarate hydratase |
| GBM | Glioblastoma multiforme |
| GDH | Glutamine dehydrogenase |
| GLS1 | Glutaminase |
| GM-CFUs | Granulocyte/ macrophage colony-forming units |
| HCC | Hepatocellular carcinoma |
| HER2 | Human epidermal growth factor receptor 2 |
| HGF | Hepatocyte Growth Factor |
| HIF1α | Hypoxia inducible factor 1-α |
| HLA | Human leukocyte antigen |
| HMGB-1 | High-mobility group protein B1 |

| | |
|---|---|
| HPLC | High performance liquid chromatography |
| HR | Hazard ratio |
| HUVEC | Human umbilical vein endothelial cells |
| IDH1/2 | Isocitrate dehydrogenase-1/2 |
| IFN | Interferon |
| IGF | Insulin-like Growth Factor |
| IKK | IκB kinase |
| IL- | Interleukin |
| IMIG | International Mesothelioma Interest Group |
| IMRT | Intensity-modulated radiation therapy |
| IRE-1 | Inositol Requiring 1 |
| JNK | C-Jun N-terminal kinase |
| LPS | Lipopolysaccharide |
| MACS | Magnetic-activated cell sorting |
| MAP | Mitogen activated protein |
| MARS | Mesothelioma and Radical Surgery study |
| M-CFUs | Macrophage colony-forming units |
| Mdm2 | Mouse double minute 2 homolog |
| MDSC | Myeloid-derived suppressor cell |
| MHC | Major histocompatibility complex |
| MM | Malignant melanoma |
| MMP | Matrix metalloproteinase |
| MOA | Mechanism of action |
| MPM | Malignant pleural mesothelioma |
| MR | Mannose receptor |
| MT1A | Metallothionein 1A |
| mTORC1 | Mammalian target of rapamycin complex 1 |
| MW | Molecular weight |
| NF2 | Neurofibromatosis type 2 |
| NF-kB | Nuclear factor kappa-light-chain-enhancer of activated B cells |
| NK | Natural Killer |
| NO | Nitric oxide |
| NOHA | N hydroxy L-arginine |
| NOS | Nitric oxide synthase |

| | |
|---|---|
| NPC | Nasopharyngeal carcinoma |
| NRF2 | Nuclear factor-erythroid-derived 2-related factor 2 |
| OAT | Ornithine aminotransferase |
| OBD | Optimum biological dose |
| ORF | Open reading frame |
| OS | Overall survival |
| OTC | Ornithine transcarbamylase |
| PBMC | Peripheral blood mononuclear cells |
| PBS | Phosphate buffered saline |
| P/D | Pleurectomy/decortication |
| PDA | Pancreatic ductal adenocarcinoma |
| PD-1 | Programmed death 1 receptor |
| PDGF-AA | Platelet-derived growth factor-AA |
| PD-L1 | Programmed death 1 ligand |
| PEG | Polyethylene Glycol |
| PERK | PKR-like ER kinase |
| PFS | Progression free survival |
| PG | Prostaglandin |
| PI3K | Phosphoinositide-3 kinase |
| PLIP | PBS-containing liposomes |
| PMR | Partial metabolic response |
| PR | Partial response |
| PTEN | Phosphatase and tensin homolog |
| PyMT | Polyoma Middle T oncoprotein |
| RASSF1 | Ras association domain family member 1 |
| pRb | Retinoblastoma protein |
| RCC | Renal cell cancer |
| RCF | Relative centrifugal force |
| RNAi | RNA interference |
| RNS | Reactive nitrogen species |
| ROS | Reactive oxygen species |
| RPM | Revolutions per minute |
| RPMI | Roswell Park Memorial Institute media |
| RR | Response Rate |

| | |
|---|---|
| RT | Radiotherapy |
| RTK | Receptor tyrosine kinase |
| qRT-PCR | Real-Time quantitative reverse transcription polymerase chain reaction |
| SD | Stable disease |
| SDH | Succinate dehydrogenase |
| SEM | Standard error of the mean |
| SILAC | Stable isotope labelling with amino acids in cell culture |
| SiRNA | Small interfering RNA |
| α-SMA | Alpha-smooth muscle actin |
| SV40 | Simian Virus 40 |
| TAM | Tumour associated macrophage |
| TCA | Tricarboxylic acid |
| TCR | T cell receptor |
| TEC | Tumour endothelial cells |
| TGFβ | Transforming Growth Factor beta |
| TKI | Tyrosine kinase inhibitor |
| TLR | Toll-like receptor |
| TM | Tunicamycin |
| TMA | Tissue microarray |
| TME | Tumour microenvironment |
| TNFα | Tumour necrosis factor alpha |
| TNM | Tumour Node Metastasis |
| TRAF2 | TNF receptor-associated factor 2 |
| TS | Thymidylate synthase |
| UCD | Urea Cycle Disorder |
| UPR | Unfolded protein response |
| VATS | Video-assisted thoracoscopy |
| VEGF | Vascular Endothelial Growth Factor |
| XBP1 | X-box binding protein 1 |

# Publications

To date, the following papers have been published that relate to work described in this thesis:

Phillips MM, Sheaff MT, Szlosarek PW (2013) 'Targeting arginine-dependent cancers with arginine-degrading enzymes.' Cancer Res Treat 45(4); 251-262

Szlosarek PW, Luong P, Phillips MM *et al* (2013) 'Metabolic response to pegylated arginine deiminase in mesothelioma with promoter methylation of argininosuccinate synthetase'. JCO 31(7); e111-e113.

# Chapter 1. Introduction

## 1.1 Malignant Pleural Mesothelioma

Malignant pleural mesothelioma (MPM) is an aggressive inflammatory malignancy arising from the mesothelial surface of the pleural cavity. It is characterised by insidious growth, high primary chemoresistance, and a uniformly poor prognosis, with median overall survival ranging between 9 and 12 months and a 5-year survival of less than 5% (1, 2).

### 1.1.1 Aetiology and Pathogenesis

#### *1.1.1.1 Asbestos*

Exposure to the asbestos group of silicate minerals is the principle risk factor for the development of MPM. The group of minerals categorized as 'asbestos' are divided into two basic structural types: amphibole and serpentine. Chrysotile is the only serpentine asbestos, and exists as a long, curly, and pliable fiber most suitable for making fabrics. Amphibole fibers are short, straight, and stiff, and have been used to make pipes and tiles. The major commercial amphiboles are amosite, crocidolite, and anthophyllite. Mixtures of chrysotile and amphiboles were used to produce an array of roofing, insulation, and fire-proofing materials. The larger amphibole minerals are reported as having the greatest carcinogenicity (3).

The first convincing evidence of a link between asbestos and MPM was reported in 1960 in South Africa. Wagner and his colleagues described asbestos exposure in 33 cases of MPM in South African mine workers (4). Later, several studies from the USA, Europe, Australia and Japan verified asbestos inhalation as the aetiological risk factor of MPM (5-8). Despite this, due to its extraordinary fire resistant properties, there was widespread use of asbestos around the world, predominantly in the shipbuilding and construction industries, until the end of the 1970's. Industrial

use of asbestos was then largely eliminated in developed countries, but it is still present today in countless buildings, where it is used as insulation and a fire retardant (3).

The mechanism of asbestos-induced MPM is not fully understood but it is generally believed that asbestos inhalation leads to the deposition of fibers deep in the lung parenchyma, with eventual migration and implantation of these fibers into the lining of the pleura. As the fibers are too large to be cleared by pulmonary macrophages, a chronic state of inflammation ensues during which the secretion of free radicals causes genotoxic damage, facilitating the transformation of normal mesothelial cells to malignant cells, a process frequently referred to as 'frustrated phagocytosis' (9). It was recently discovered that asbestos induces necrotic cell death, causing an increase in extracellular high-mobility group protein B1 (HMGB-1). HMGB-1 release triggers a chronic inflammatory response, macrophage accumulation and the secretion of tumour necrosis factor alpha (TNFα), which in turn activates NF-kB, leading to the survival of mesothelial cells that have accumulated asbestos induced genetic damage (10). Production of reactive oxygen species (ROS) from the high iron content within asbestos fibers and direct damage to DNA by these fibers are also accepted pathogenic features of asbestos exposure (11). In addition, MPM has a dysfunctional epigenetic background, with a number of epigenetic events having been observed which may contribute to MPM carcinogenesis. Importantly, asbestos has been shown to influence the epigenetic regulation of a number of critical genes, with methylation of p16, CDKN2B and RASSF1 significantly associated with asbestos exposure (12). The methylation of MT1A has also been correlated with asbestos burden (13), and, furthermore, increased asbestos burden has been associated with increased hypermethylation of cell cycle genes such as APC and CCND2 (14). A number of methylation profiles have been linked to reduced overall survival in MPM (15).

However, it is unknown why the transformation of asbestos-injured cells into MPM occurs in only 2% to 10% of individuals exposed to asbestos. Conversely, up to 80% of MPM patients have a documented history of asbestos exposure. In addition, there does not appear to be a linear dose-response relationship between asbestos exposure and MPM, meaning that the amount of exposure does not correlate with

increased risk of disease. Instead, some individuals are thought to be more susceptible to asbestos (16). This suggests a complex relationship between environment, biology and genetics in the pathogenesis of MPM.

#### *1.1.1.2 Endemic Eronite exposure*

The possibility of a specific gene-environment interaction was raised following the observation of high MPM rates in the Cappadocian villages of Turkey (17). This region is rich in the highly carcinogenic mineral erionite, which causes MPM in animal models and has been detected in the lungs of local people. Pedigree analysis in affected families indicates a genetic susceptibility that is inherited in an autosomal dominant pattern (18).

#### *1.1.1.3 Ionising radiation*

Long-term effects of ionising radiation have also been aetiologically linked to MPM, although in a much smaller group of individuals than the asbestos exposed. Indeed, the risk of developing MPM was found to be significantly higher in cases previously exposed to α-particle-emitting agents, such as the radioactive contrast Thorotrast (used in the 1950's) (19). Moreover, it is well-documented that mesothelioma is more common in testicular cancer and Hodgkin's lymphoma survivors who have been treated with external radiotherapy (20, 21). However, today, due to better understanding of the risks of developing secondary cancers, together with improved alternative therapies for these cancers, these treatments are used much less frequently.

#### *1.1.1.4 Simian Virus 40*

Simian Virus 40 (SV40), a rhesus monkey DNA virus likely introduced to humans from contaminated Salk polio vaccines produced between 1955 and 1978 (22), has, too, been implicated as a cofactor in the causation of MPM (16). SV40 acts as a potent oncogenic virus for human and rodent cells by blocking tumour suppressor genes (23, 24). It has been reported that up to 60% of human mesotheliomas

contain SV40 DNA (25). However, despite a number of studies illustrating the malignant transformation potential of this virus *in vitro* and in animal studies of MPM (16, 26-28), the interpretation of the repeated finding of SV40 in human MPM is still controversial.

#### *1.1.1.5 Molecular pathogenesis of MPM*

##### 1.1.1.5.1 Chromosomal alterations

Studies have shown that mesotheliomas have complex and variable chromosomal alterations (29), and only few features are shared between patients. Loss-of-heterozygosity analyses have demonstrated frequent deletions of specific sites within chromosome arms 1p, 3p, 6q, 9p, 13q, 15q and 22q. Three of these regions are most commonly altered, the tumour suppressors CDKN2A–ARF at 9p21, NF2 at 22q12 (30) and BAP1 at 3p21 (31).

###### *1.1.1.5.1.1 Cyclin-dependent kinase inhibitor 2A/alternative reading frame (CDKN2A/ARF) inactivation*

Homozygous deletion of the 9p21 region is frequently present in mesothelioma cell lines and tumour specimens. Loss of 9p21 results in loss of the INK4a/ARF locus, which encodes two distinct proteins, p16INK4a and p14ARF, translated from alternatively spliced mRNA. p16INK4a inhibits the cyclin-dependent kinase (CDK)-mediated inactivation of pRb. p14ARF stabilizes p53 through its actions on Mdm2. As the INK4a/ARF locus plays an important role in the activity of both the p53 and pRb tumour suppressor pathways, a single mutational event may lead to the functional loss of both of these two key regulatory pathways (32).

###### *1.1.1.5.1.2. Neurofibromatosis type 2 (NF2) inactivation*

The neurofibromatosis type 2 *(*NF2*)* gene encodes a tumour suppressor protein, merlin (moesin-ezrin-radixin-like protein). NF2 cancer syndrome is characterized by the development of tumours of the nervous system such as bilateral vestibular schwannomas at the eighth cranial nerve, spinal schwannomas and meningiomas

(33). It has been reported that 40–50% of MPM cases harbour an inactivating NF2 mutation, typically a separate subset to those with BAP1 loss (34, 35). As NF2 mutation is frequently detected in MPM, genetically engineered *Nf2*-knockout mouse models have been developed to confirm the significance of *NF2* inactivation on MPM pathogenesis. Asbestos-exposed *Nf2* (+/−) knockout mice exhibited markedly accelerated MPM tumour formation compared with asbestos-treated wild-type mice (36).

Merlin regulates multiple signal transduction cascades of the cells, including the mTOR pathway and Hippo signaling pathway. Indeed, merlin has been shown to be a negative regulator of mTORC1, with integrin-mediated adhesion to fibronectin being shown to promote mTORC1 signaling through the inactivation of merlin (37). In addition, the Merlin-Hippo signaling pathway, key to the regulation of cell division and promoting apoptosis, has been shown to be frequently inactivated in mesothelioma cells (38).

#### *1.1.1.5.1.3 BRCA1- associated protein-1 (BAP1) inactivation*

The nuclear protein, BAP1, has several proposed functions, including transcriptional regulation, chromatin regulation, and forming part of protein complexes that regulate cellular differentiation, gluconeogenesis, cell cycle checkpoints, transcription and apoptosis (39). The BAP1 gene is located on chromosome 3p21, a region that shows loss or deletion in many cancers, including 30–60% of mesotheliomas. In families who have the BAP1 mutation, there is a significantly increased incidence of a number of cancer-types, often developed at an earlier age than observed in the general population (39). A BAP1 cancer syndrome has therefore been proposed, including mesothelioma, uveal melanoma and cutaneous melanoma (40). Indeed, germ-line BAP1 mutations have been reported in families with unusually high incidence of mesothelioma (40) and in 25% of sporadic mesotheliomas (41), highlighting the importance of genetic factors in MPM susceptibility. However, its association with asbestos-induced carcinogenesis has not been established. BAP1 mutations appear to be significantly more common in epithelioid MPM (42, 43).

#### 1.1.1.5.2 Activation of oncogene cascades

##### *1.1.1.5.2.1 Receptor tyrosine kinases*

Receptor tyrosine kinases (RTKs) are commonly activated in malignant cells. Activation of RTKs via interaction with peptide growth factors leads to constitutive up-regulation of two major downstream cell signaling cascades, mitogen-activated protein (MAP) kinase and phosphoinositide-3 kinase (PI3K)-AKT pathways, which are critical for proliferation and/or survival of cells. Activation of several growth factors and their receptors has been shown to play an important role in the oncogenesis and progression of MPM, including Epidermal Growth Factor (EGF), Hepatocyte Growth Factor (HGF), Vascular Endothelial Growth Factor (VEGF), and Insulin-like Growth Factor (IGF) (44).

## 1.1.2 Incidence

Mesothelioma accounts for less than 1% of all cancers in the UK. However, although uncommon, it poses an increasing public health and economic problem. This is because incidence is still rising as a result of the widespread use of asbestos in the last century and the long latency period from the time of first exposure to development of MPM, which ranges from approximately 15 to 60 years (45). Indeed, incidence in men has increased 5-fold since 1980. Moreover, recent estimates expect more than a quarter of a million deaths caused by MPM in Western Europe over the next four decades (3, 46).

It is interesting to note here that Canada, which has one of the highest rates of MPM in the world, was a major producer and exporter of chrysotile asbestos. Remarkably, despite the universal ban on asbestos as proposed by the World Health Organisation and most developed countries, asbestos production in Canada did not cease until 2012 (47).

In addition, asbestos continues to pose a public health risk throughout the world due to its current and increasing use in industrializing nations. Thus, the worldwide

epidemic is in its beginning, and in countries that still produce and/or use asbestos, such as China, India, Russia, Zambia, Colombia and Kazakhstan, a steep rise in incidence is likely (48-50).

### 1.1.3 Clinical Presentation

The initial clinical presentation for most patients with MPM is progressive dyspnea and/or chest wall pain. There also may be a dry cough, weight loss, fever, fatigue, or night sweats. The disease is more frequently found unilaterally (95%), and located on the right side (60%). The majority of patients will have a documented history of asbestos exposure, with common prior occupational exposures including pipefitters, plumbers, carpenters, steamfitters, heavy construction or shipbuilding industry workers, and those working aboard ships (1). Due to occupational exposure, it is more common in men than in women (5:1) (51) and it is also more frequent in advanced age as a result of the long latency period, usually presenting in the 6$^{th}$ through 8$^{th}$ decades.

### 1.1.4 Diagnosis

An accurate diagnosis of MPM is important for optimal clinical management, including accessing industrial compensation.

MPM is divided into three major histological sub-types: sarcomatoid, biphasic and epithelioid. Epithelioid is the most common subtype and it is also associated with the best prognosis (52). To help distinguish between these subtypes, secondary carcinoma and other malignant tumours metastatic to serosal membranes, several immunohistochemical panels are available (53), of which calretinin is the most commonly used antibody, positive for mesothelioma with a reported sensitivity of 95% and specificity of 87% (54). Other useful antibodies include thrombomodulin and cytokeratin 5/6 (55). For a detailed summary of antibodies used, please see Table 1.1.

| Epithelioid mesothelioma | | Sarcomatoid mesothelioma | Markers differentiating mesothelioma *vs* reactive mesothelium[1] |
|---|---|---|---|
| **Mesothelial markers** | **Carcinoma markers** | | |
| Calretinin | CEA | Cytokeratin 7 | Desmin |
| Cytokeratin 5/6 | TTF-1 | Cytokeratin 8/18 | EMA |
| HBME-1 | CD15 (Leu-M1) | Cytokeratin CAM5.2 | p53 |
| Podoplanin (D2-40) | BG8 | Cytokeratin AE1/AE3 | GLUT-1 |
| WT-1 | B72.3 | MNF116 | IMP3 |
| Thrombomodulin | MOC31 | Cytokeratin 34BetaE12 | |
| | Ber-EP4 | Vimentin | |
| | E-cadherin | | |

**Table 1.1. Markers frequently used in the diagnosis of mesothelioma.** The antibody used depends on histological subtype, the differential diagnosis and the gender of the patient. A panel of four markers (two 'positive' and two 'negative' mesothelial markers), selected based upon availability and which ones yield good staining results in a given laboratory is recommended. Because of their specificity and sensitivity for mesotheliomas, the best combination appears to be calretinin and cytokeratin 5/6 (or WT1) for the positive markers and CEA and MOC-31 (or B72.3, Ber-EP4, or BG-8) for the negative markers. [1] FISH for deletion of p16/CDKN2A. Adapted from Ascoli 2015 (56).

However, to date no mesothelial marker has shown 100% sensitivity and specificity for MPM. This, in addition to the fact that MPM is uncommon, makes diagnosis difficult. Nevertheless, the identification of the three key genetic alterations CDKN2A/ARF, NF2 and BAP1, described in section 1.1.1.5.1, may help lead to the development of new diagnostic tools.

#### *1.1.4.1 Staging*

As with all malignancies, accurate staging in MPM is key to rational treatment planning. Many staging systems have been proposed but the most widely accepted is the TNM-type system of the International Mesothelioma Interest Group (IMIG) (55). A summary of the classification is described below:

***Stage I*** includes lymph node-negative patients with minimal tumour confined to the parietal pleura (stage Ia) or with minimal visceral pleural involvement (stage Ib).

***Stage II*** includes lymph node-negative patients with confluent superficial tumour on all pleural surfaces or involvement of the diaphragmatic muscle or lung parenchyma.

***Stage III*** includes patients with metastasis to hilar (N1) or ipsilateral mediastinal (N2) lymph nodes, or those with extension of tumour into the soft tissues of the chest wall, the endothoracic fascia, mediastinal fat or pericardium (T3 tumour).

***Stage IV*** includes patients who have locally advanced tumour invading the spine or ribs, the chest wall extensively, diaphragmatic spread, or contralateral pleural spread. Patients with stage IV disease also may have contralateral or supraclavicular lymph node involvement (N3) or distant metastases.

Stage III is the most common presenting stage, which means that, in many cases, therapeutic options are limited.

### 1.1.5 Current therapeutic strategies

#### *1.1.5.1 Surgery*

Surgical management of MPM falls into three categories. First, diagnostic surgery is often required, such as video-assisted thoracoscopy (VATS). Second, palliative

surgery can be performed to relieve symptoms, including partial pleurectomy with pleurodesis, or thoracoscopy with pleurodesis. Third, potentially curative surgery, carried out in specialist centres that employ multimodality approaches, including surgical resection, chemotherapy, and radiation, is an option in a few patients. In general, most stage I, and some stage II and III patients are considered potentially resectable. However, there are exceptions: whether a tumour is resectable is also based on subtype (many surgeons do not believe that sarcomatoid mesothelioma is helped by resection), the extent of spread into nearby tissues, and, importantly, the general fitness of the patient. Two forms of radical surgery have been performed since the late 1970s: extrapleural pneumonectomy (EPP), which involves removing the pleura, as well as the lung and diaphragm, on one side, and, more recently, a lung sparing resection of the pleura, now commonly referred to as pleurectomy decortication (P/D) (57). The role of surgery in the treatment of MPM has been the subject of much heated debate in the last few years, following the controversial Mesothelioma and Radical Surgery (MARS) study. In this randomised feasibility study, all 50 patients received chemotherapy and/or radiotherapy, and one group underwent EPP. The Hazard Ratio (HR) for overall survival (OS) between EPP and no EPP groups after adjustment for sex, histological subtype, stage and age, was 2.75 (p=0.016). Median survival was 14.4 months in the EPP group and 19.5 months in the no EPP group. The authors concluded that radical surgery in the form of EPP within trimodal therapy offers no benefit and possibly harms patients (58). Conclusions from the study have been contested and these criticisms rebutted since its publication in 2011. The debate is ongoing. In the meantime, MARS 2, another randomised feasibility study, has been recruiting to evaluate P/D following chemotherapy compared with chemotherapy alone. Results are awaited. The two surgical procedures have been directly compared in a retrospective analysis of 3000 patients. This showed that for stage II and III MPM, survival data is the same for both EPP and P/D, with P/D causing less impairment of quality of life. However, this analysis also showed that there may be an advantage in using EPP in Stage I patients, as in this small subgroup, median survival was 4 years following EPP and 2.5 years following P/D (59).

Selection bias, the difficulty of the surgery and the perioperative mortality rate together make the role of radical surgery controversial. The International

Mesothelioma Interest Group (IMIG) advise that surgical cytoreduction is indicated only when macroscopic complete resection is deemed achievable and that the type of surgery (EPP or P/D) depends on clinical factors and on individual surgical judgment and expertise.

As radical treatment is reserved only for a carefully selected subgroup of patients, palliative treatments become the principle of care for the vast majority of patients with MPM.

#### *1.1.5.2 Radiotherapy*

Radiotherapy (RT) has been studied in MPM for many years and overall results have been largely disappointing. The biggest limitation to radical radiotherapy is the diffuse nature of the tumour covering most of the pleural surfaces as well as the interlobular fissures. Indeed, treating the entire pleura requires a large radiation field, which significantly increases toxicity risks. Traditionally, adjuvant RT following EPP or P/D as part of multi-modality regimens has been given through anterior and posterior fields that encompass the entire involved hemithorax. More recently, complex intensity-modulated radiation therapy (IMRT) techniques have been explored, with early outcomes suggesting acceptable safety in appropriately selected patients. Newer methods such as Arc therapy or helical tomotherapy are rotational RT techniques that deliver radiation from even more beam angles than IMRT. They are ideally suited for spherical or circular targets and are therefore of particular interest in MPM (60). However, these have not yet been validated clinically and therefore future studies will need to test whether the theoretical advantages of newer RT techniques can be translated into clinical benefit for MPM patients.

#### *1.1.5.3 Chemotherapy*

Despite decades of clinical research, cytotoxic chemotherapy remains one of the few therapeutic options that has been proven to improve survival in patients with MPM.

#### 1.1.5.3.1 First line Chemotherapy

First line chemotherapy for MPM in routine practice has remained unchanged since 2003, when the pivotal phase III trial conducted by Vogelzang and colleagues (61) showed that the combination of cisplatin and pemetrexed gave a three month survival benefit over cisplatin alone, improving median survival from 9.3 to 12.1 months (p=0.02) in patients with advanced disease (See Figure 1.1). This modest survival increase was also associated with improvements in quality of life. A similar benefit was seen with the addition of raltitrexed to cisplatin, with survival increasing from 8.8 to 11.4 months (p=0.048), although objective radiological response rates were lower to this combination than to cisplatin and pemetrexed (62).

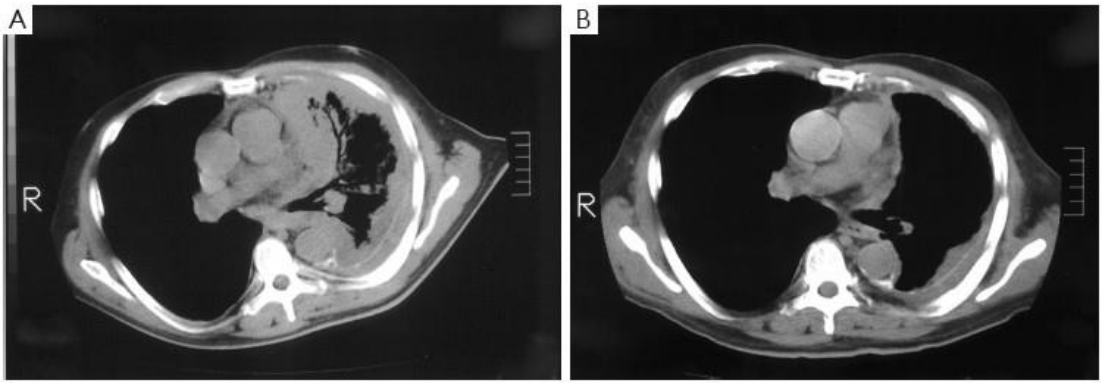


**Figure 1.1 Axial computed tomography (CT) scan.** Scan shows pre-treatment disease (A) and a partial response to chemotherapy with cisplatin and pemetrexed (B) after four cycles of treatment (adapted from Nowak (63)).

#### 1.1.5.3.2 Second Line chemotherapy

After first line chemotherapy, patients almost invariably experience disease recurrence or progression. Currently, there is no standard second line treatment and options are limited. However, a recent retrospective review of second-line chemotherapy found that disease control with second-line treatment was better in those patients who received pemetrexed, and those with a prolonged time to progression (≥12 months) after first-line therapy (64). Furthermore, patients re-treated with a platinum-pemetrexed combination had a lower risk of death than those treated with pemetrexed alone (HR =0.11, p<0.001). This therefore indicates that re-

treatment with pemetrexed plus a platinum is a rational option for second-line therapy in good performance status patients with previous disease control after pemetrexed-based treatment.

A variety of cytotoxic agents have some activity in second-line treatment, but none have had the appropriate randomised controlled design to determine which particular agent is the best choice. The lack of randomised designs also means that we do not know if survival benefits ensue from agents with modest objective radiological responses in the second-line setting. Single agent vinorelbine has a response rate (RR) of 16% and overall survival of 9.6 months as a second-line therapy (65). Combinations of gemcitabine and vinorelbine (RR 10%, OS 10.9 months, PFS 2.8 months) (66), gemcitabine and epirubicin (RR 13%, OS 9.3 months, PFS 6.3 months in a high dose group) (67), irinotecan, cisplatin, and mitomycin (RR 20%, OS 7.3 months, PFS 7.3 months) (68) and others have also been reported. The tolerability and response rate of single agent vinorelbine has meant that this is often the treatment of choice in clinical practice.

### *1.1.5.4 Targeted therapies*

#### 1.1.5.4.1 Molecular targeted therapy

In contrast to lung cancer, oncogenic driver mutations are absent in MPM. The development of targeted therapy therefore relies on the evaluation of pathways indirectly activated by the loss of tumour suppressor genes or targets associated with the disease phenotype. In line with this, various dysregulated molecular pathways have been identified in MPM in the past decade, including cell cycle regulation, apoptosis, growth factor pathways and angiogenesis. Subsequently, a number of novel agents targeting these pathways, which have shown promising activity in other cancers, have been trialled empirically in mesothelioma. Below is a summary of key molecular targets under investigation.

#### *1.1.5.4.1.1 Epidermal Growth Factor Receptor*

Epidermal Growth Factor Receptor (EGFR) is expressed by a variety of epithelial malignancies, and activation of the pathway interferes with apoptosis, uncontrolled cell proliferation and angiogenesis. EGFR overexpression in mesothelioma has been reported by several authors (69, 70). However, results from clinical trials have been disappointing: single agent treatment with EGFR tyrosine kinase inhibitors (TKIs) gefitinib and erlotinib showed no evidence of activity even as first-line treatment (71, 72).

#### *1.1.5.4.1.2 Vascular Endothelial Growth Factor*

Vascular endothelial growth factor (VEGF) is a key stimulator of both angiogenesis and neovascularisation of tumours. Agents inhibiting the VEGF receptor, in many cases in combination with other targets, have shown some evidence of activity in MPM in an unselected population, with response rates around 10% and PFS between 3 and 4 months (73-75). However, identifying which patients may benefit from these agents has been problematic, with no predictive factors yet identified.

The anti-VEGF monoclonal antibody bevacizumab has also been tested in a number of completed and ongoing trials. A randomised phase II trial of untreated mesothelioma patients compared cisplatin-gemcitabine alone or with bevacizumab. The addition of bevacizumab did not improve response, progression-free survival, or overall survival compared with chemotherapy alone. A potential benefit in patients with low circulating levels of VEGF was, however, suggested in subgroup analysis (76). More recently, a two-armed phase II/III trial compared the standard of care cisplatin and pemetrexed combination with or without bevacizumab as first-line treatment and maintenance in inoperable mesothelioma patients. Notably, results of this study revealed that pemetrexed and cisplatin combination with bevacizumab gave a significantly longer OS (median OS 18.8 months vs. 16.1 months without bevacizumab; adjusted HR 0.76, p=0.012) (77).

#### *1.1.5.4.1.3 Cyclin-dependent kinase inhibitor 2A (CDKN2A)*

MPM lacks expression of both CDKN2A encoded proteins p16 and ARF due to gene deletion or methylation (reviewed in section 1.1.1.5.1.1). Deletion in CDKN2A leads to loss of control of cyclin D-dependent kinases (CDK). Although only a very small number of MPM cases present with p53 mutations (42), deletion of CDKN2A leads to the hypothesis that these tumours may be dependent on G2 checkpoint and therefore vulnerable to a G2 checkpoint inhibition when combined with chemotherapy. In line with this hypothesis, the calmodulin-binding peptide (CBP501) was clinically tested in combination with cisplatin and pemetrexed in order to increase the sensitivity of mesothelioma cells to chemotherapy. In patients receiving CBP501 with chemotherapy, PFS of more than 4 months was achieved compared with 39% receiving chemotherapy alone (78).

#### *1.1.5.4.1.4 Neurofibromatosis type 2 (NF2)*

Loss of the tumour suppressor gene NF2 occurs in around 40% of patients (reviewed in section 1.1.1.5.1.2) (79). The resultant merlin loss affects a number of key pathways, including the activation of mTORC1 and focal adhesion kinase (FAK) pathways. Drugs that target these pathways are therefore being considered as potential therapeutic options.

A phase I trial evaluated the effect of the PI3K/mTOR inhibitor GDC0980 (dual PI3K/mTOR inhibitors are used due to the compensatory up-regulation of PI3K seen with mTOR inhibition alone). The preliminary result of the phase I extension cohort showed two objective responses among 26 patients with mesothelioma (80). A phase II trial studying the mTOR inhibitor, everolimus, showed no significant activity in unselected MPM patients, concluding that additional studies of everolimus in advanced MPM are not warranted (81).

The role of FAK inhibitors has also been recently studied (63). The COMMAND study, a phase II trial investigating the FAK inhibitor defactinib (VS-6063) in mesothelioma (NCT01870609), had been scheduled to complete in 2016; however, despite promising early results, the trial closed early due to poor efficacy data.

#### 1.1.5.4.2 Therapy targeting cell surface receptors

##### *1.1.5.4.2.1 Anti-mesothelin antibodies*

Mesothelin is a cell-surface glycoprotein that is present on normal mesothelial cells but overexpressed on the surface of mesothelioma. It is known that mesothelin binds to CA-125 and reports suggest that overexpression, which occurs prominently on epithelioid tumours but not on sarcomatoid tumours, may affect cell adhesion and/or invasion (82). Accordingly, a number of anti-mesothelin targeted therapies have been developed.

The chimeric IgG1 antibody Amataximab has recently been evaluated. Studies demonstrate that it blocks the binding of mesothelin to CA-125 (83) and that it is well tolerated in patients with MPM (84) Furthermore, a single arm phase II clinical trial in combination with pemetrexed and cisplatin reported median OS of 6.1 months and a median OS of 14.8 months, with a third of patients alive at the time of analysis (85)

SS1(dsFV)PE38 (SS1P) is an immunotoxin consisting of an anti-mesothelin antibody variable fragment linked to a cytotoxic fragment of *Pseudomonas* exotoxin A. It has been shown to be safe in a phase I trial, but only minor antitumor activity could be observed. Additionally, the development of neutralising antibodies was observed in 24% of patients and this prevented its use for more than one cycle (86). However, in a subsequent pilot study using immunosuppressive pretreatment with pentostatin and cyclophosphamide to prevent neutralising antibodies and allow delivery of more courses of treatment, 3 of 10 assessable patients demonstrated dramatic responses with subsequent chemotherapy (87). Another phase 1 trial of SS1P combined with chemotherapy (cisplatin and pemetrexed) is closed to recruitment and awaiting data analysis. (Clinicaltrials.gov NCT01445392).

#### 1.1.5.4.2 Immune checkpoint inhibitors

Tumours have evolved multiple mechanisms to evade immune destruction. One of these recognised escape mechanisms is expression of T cell inhibitory ligands such as cytotoxic T-lymphocyte antigen 4 (CTLA-4), the programmed death 1 ligand (PD-

L1) and the programmed death 1 receptor (PD-1). Immune checkpoint inhibitors block these T cell inhibitory mechanisms and allow T cells to resume their cytotoxic activity on cancer cells.

#### *1.1.5.4.3.1 Cytotoxic T lymphocyte antigen-4*

CTLA-4 is crucial for preserving host immune tolerance to established tumours. The CTLA-4 receptor sequesters CD80 and CD86 immune co-stimulatory signals provided by antigen-presenting cells, and this increases the activation threshold for T lymphocytes. The anti-CTLA-4 monoclonal antibody tremelimumab was investigated in pretreated patients in a phase II single-arm study: the primary endpoint of objective response rate was not met (88). However, responses to immune therapy can take appreciably longer to become apparent compared with other therapies. Furthermore, disease control was noted in 31% of the patients, and overall survival rates were 48% at 1 year and 37% at 2 years. Additionally, there is an ongoing randomised phase II trial in which pretreated patients are allocated to either single agent tremelimumab or placebo (89).

#### *1.1.5.4.3.2 Programmed death -1 receptor/ligand*

The programmed death receptor is found on the surface of T-cells and its stimulation leads to T-cell deactivation, therefore permitting escape from the immune system surveillance. Activation of this receptor occurs by a programmed death ligand 1 (PD-L1), which exists within the tumor microenvironment and on the surface of tumour cells. Monoclonal antibodies directed at the PD-L1 or PD1 receptors are currently being considered (90) . Indeed, preliminary results from the phase II trial of pembrolizumab in MPM were presented at ASCO 2015 (Clinicaltrials.gov NCT02399371). The authors reported a good safety and tolerability profile and revealed a 28% partial response (PR) rate, with 48% demonstrating stable disease (SD), giving an overall disease control rate of 76%.

#### 1.1.5.4.4 Vaccines

##### *1.1.5.4.4.1 Dendritic cell vaccines*

These are in the early stages of evaluation. In a pilot Phase I study, Hegmans and colleagues (91) vaccinated 10 patients with autologous dendritic cells. Each vaccine was composed of mature dendritic cells pulsed with autologous tumour lysate purified from pleural effusions or biopsy samples. In four patients, dendritic cell vaccination induced cytotoxic T cells. It was well tolerated and produced three partial responses with overall median survival of 19 months, which is encouraging. Results from a trial evaluating dendritic cell-based vaccination in combination with low-dose cyclophosphamide are awaited.

##### *1.1.5.4.4.2 CRS-207 vaccine*

CRS-207 is a genetically modified *Listeria monocytogenes* attenuated vaccine expressing mesothelin. Mesothelin acts as an antigen and stimulates activation of T-cells upon exposure to CRS-207 (92). A phase I trial evaluating this vaccine in combination with chemotherapy was presented at ASCO 2014 (Clinicaltrials.gov NCT01675765). Authors reported that CRS-207 can be safely combined with standard of care chemotherapy and showed encouraging anti-tumour activity with 9 out of 15 subjects having confirmed durable PR and 4 having SD (93). These results are considerably better than those expected with chemotherapy alone and warrant further evaluation.

#### 1.1.5.4.5 Gene therapy

Gene therapy usually involves administration of engineered viruses into which a gene of interest has been inserted, with the aim of inducing long term expression of the protein product of the inserted gene in the tissues. Two separate gene therapy approaches have been trialled in MPM, briefly described below.

#### *1.1.5.4.5.1 Suicide gene therapy*

This method uses engineered viruses that deliver transgenes encoding enzymes that metabolize prodrugs into toxic metabolites capable of destroying tumour cells. Multiple viral vectors have been investigated. A clinical trial of intrapleural herpes simplex virus thymidine kinase/ganciclovir enrolled 34 patients and reported minimal morbidity and a dose-dependent median survival as high as 15 months at the highest viral titers. Some patients experienced prolonged survival, suggesting induction of anti-tumour immunity in addition to the acute viral-mediated cytotoxicity (94).

#### *1.1.5.4.5.2 Cytokine gene therapy*

An alternative approach involves the delivery of viral vectors encoding specific cytokine genes that may exert a direct cytotoxic effect on tumour cells or may alter the immunologic response to the tumour. Although early trials of direct intrapleural administration of interleukin-2 (IL-2) demonstrated a response rate of almost 50%, with a median survival of 28 months in responders (95), subsequent interest has focused on gene therapy with interferon (IFN), which plays a critical role in activation of the immune system and can also have direct anti-tumour cytotoxic/cytostatic effects. Several clinical trials have evaluated adenoviral-mediated IFN (α and β) therapy in patients with MPM (96, 97). Survival ranged from 1–22 months with some long-term survival, but neutralising antibodies limited the ability to administer repeated treatments.

### *1.1.5.5 Summary*

Despite on-going research providing an increasing list of potential new therapies, progress has been slow. Consequently, MPM continues to impart a dismal prognosis to those diagnosed with the disease. With the incidence of MPM on the rise and the global burden of this devastating disease continuing to increase, novel therapeutic strategies that improve outcome are urgently needed.

## 1.2 Tumour metabolism: an emerging cancer 'hallmark'

A recently re-discovered biological 'hallmark' of cancer is energy re-programming, by which tumour cells adjust their metabolic and bioenergetic pathways for cell proliferation (98). In this way, tumour cells acquire distinct metabolic characteristics from normal cells, driven by a combination of genetic lesions and non-genetic factors such as the tumour microenvironment. Interest in tumour cell metabolism originated over 80 years ago, with Otto Warburg's seminal discovery that cancer cells display higher rates of glycolysis than their non-malignant counterparts, even in the presence of sufficient oxygen supply (99), despite this process being far less efficient in terms of net ATP production per molecule of glucose (100). This seemingly paradoxical phenomenon, termed the 'Warburg effect' or aerobic glycolysis, has subsequently been observed across many tumour types and often occurs in parallel with a significant increase in glucose uptake and consumption, a trend which forms the basis of 18F-deoxyglucose-positron emission tomography (18-FDG-PET) in cancer imaging today (101). The catabolism of glucose via aerobic glycolysis has in many ways become the 're-programmed' pathway that defines the altered cancer metabolism hallmark; however, there are many other metabolic pathways that may modulate tumour cell growth (102, 103). Understanding these changes and the advantage this gives the tumour in terms of development and maintenance remains an area of intense research and has significant clinical implications. Indeed, testing for metabolic genetic drivers such as mutations in Kreb's cycle genes (i.e., fumarate hydratase (FH), succinate dehydrogenase (SDH), isocitrate dehydrogenase-1/2 (IDH 1/2)) is already available, and antimetabolites, such as antifolates and pyrimidine analogues, are being effectively used in the oncology clinic (104). Furthermore, new PET tracers and antimetabolites are being devised that aim to exploit the differential biochemistry of sugars, lipids and amino acids in normal and malignant cells (105). Here, the focus is on the amino acid arginine, which has gained much clinical interest in recent years as an exciting cancer target, driven by the emergence of several novel arginine-depleting agents.

## 1.3 Amino acid deprivation as an anti-cancer therapeutic strategy

### 1.3.1 Asparagine

The rationale for targeting amino acids in cancer therapy was pioneered with the introduction of asparaginase in childhood leukemia over fifty years ago. In contrast to normal cells, leukemic cells are critically dependent on exogenous asparagine for growth (known as ‘auxotrophy’), due to lack of the biosynthetic enzyme asparagine synthetase (106). As a monotherapy, deamidation of asparagine to aspartate and ammonia by asparaginase, led to responses of up to 50% in early studies of patients with chemo-refractory leukemia (107). However, it was not until the advent of multimodality chemotherapy regimens containing asparaginase that the cure rate of acute lymphoblastic leukemia increased from 5% in the 1950's to the present 90%. Since its incorporation into treatment protocols in the 1970’s, asparaginase has remained a consistent component of paediatric acute lymphoblastic leukaemia (ALL) treatment regimens (108).

### 1.3.2 Arginine

Similarly, observations that various tumour cells are susceptible to arginine deprivation were made over 70 years ago (109). However, delay in the development of appropriate therapeutic methods has meant that the use of arginine depletion as a therapeutic strategy in the clinical setting has been more recent.

Arginine is a dibasic α amino acid first discovered over 100 years ago from lupin seedlings (110). Like asparagine, it is one of the 20 most common natural amino acids and is regarded as highly versatile. In addition to protein synthesis, it is involved in many diverse aspects of tumour metabolism, including the synthesis of nitric oxide (NO), polyamines (putrescine, spermine, spermidine), nucleotides, proline and glutamate (111, 112) (Figure 1.2). Arginine and a number of these ‘downstream’ molecules have been implicated in tumour development, with animal studies confirming a modulatory effect of arginine on tumourigenesis. Hence, mice

that either had transplantable tumours, or were genetically programmed to develop cancer, displayed enhanced tumour growth when fed an arginine rich diet (113, 114). In contrast, depletion of dietary arginine inhibited tumour growth (115).

#### *1.3.2.1 Sources and availability of arginine*

On an organismal level, diet and protein degradation are the main sources of plasma arginine, with only 5-15% (up to 30% in newborns) derived from *de novo* biosynthesis. Because normal cells are able to endogenously synthesise arginine in addition to utilising extracellular supplies, it is not classed as an essential dietary amino acid. However, in cases of catabolic stress (e.g. inflammation or infection) or conditions involving dysfunction of the kidneys or small intestine, levels of arginine may not suffice to meet metabolic demands. Accordingly, arginine is classified as a semi-essential or conditionally essential amino acid (110).

##### 1.3.2.1.1 Arginine transport systems

In most mammalian cells, arginine requirements are met primarily by uptake of extracellular arginine via specific transporters, with system y+, a high-affinity, Na+-independent transporter of arginine, postulated to be the main route of entry in the majority of cell types. Transporters in this system include those of the high affinity cationic amino acid transporter (CAT) family (part of the larger SLC7 gene family) (116). CAT1 is constitutively expressed and involved in uptake of arginine for basic metabolism. CAT2 is recognised as an inducible form, which includes the alternatively spliced isoform CAT2B, a high-affinity arginine transporter known to be abundant in macrophages. CAT3 and CAT4 have also been described: CAT3 is found in brain and thymus, and the function of CAT4 is unknown at this time.

#### 1.3.2.1.2 *De novo* arginine biosynthesis

Alternatively, endogenous synthesis of arginine in adults occurs via the intestinal-renal axis. Namely, citrulline is synthesised from glutamine, glutamate and proline in the mitochondria of enterocytes via a series of enzymatic reactions, released from the small intestine into the circulation, and taken up primarily by the proximal tubular cells of the kidney for arginine production. Besides the kidney, however, citrulline is also readily converted into arginine in nearly all cell types, including adipocytes, endothelial cells, enterocytes, macrophages, neurons, and myocytes (111). Under physiological conditions, the arginine biosynthetic pathway is organised according to tissue function: for example, as the urea cycle in the liver for elimination of nitrogenous waste, and as the nitric oxide (NO)-citrulline cycle in endothelial cells to generate NO, with arginine acting as an intermediary molecule (117).

Arginine is synthesised by two sequential enzymatic reactions in the urea cycle: argininosuccinate synthetase-1 (ASS1), which catalyses the condensation reaction of citrulline and aspartic acid to argininosuccinate, and argininosuccinate lyase (ASL), which catalyses the conversion of argininosuccinate to arginine with the production of fumarate, an intermediate in the tricarboxylic acid (TCA) cycle.

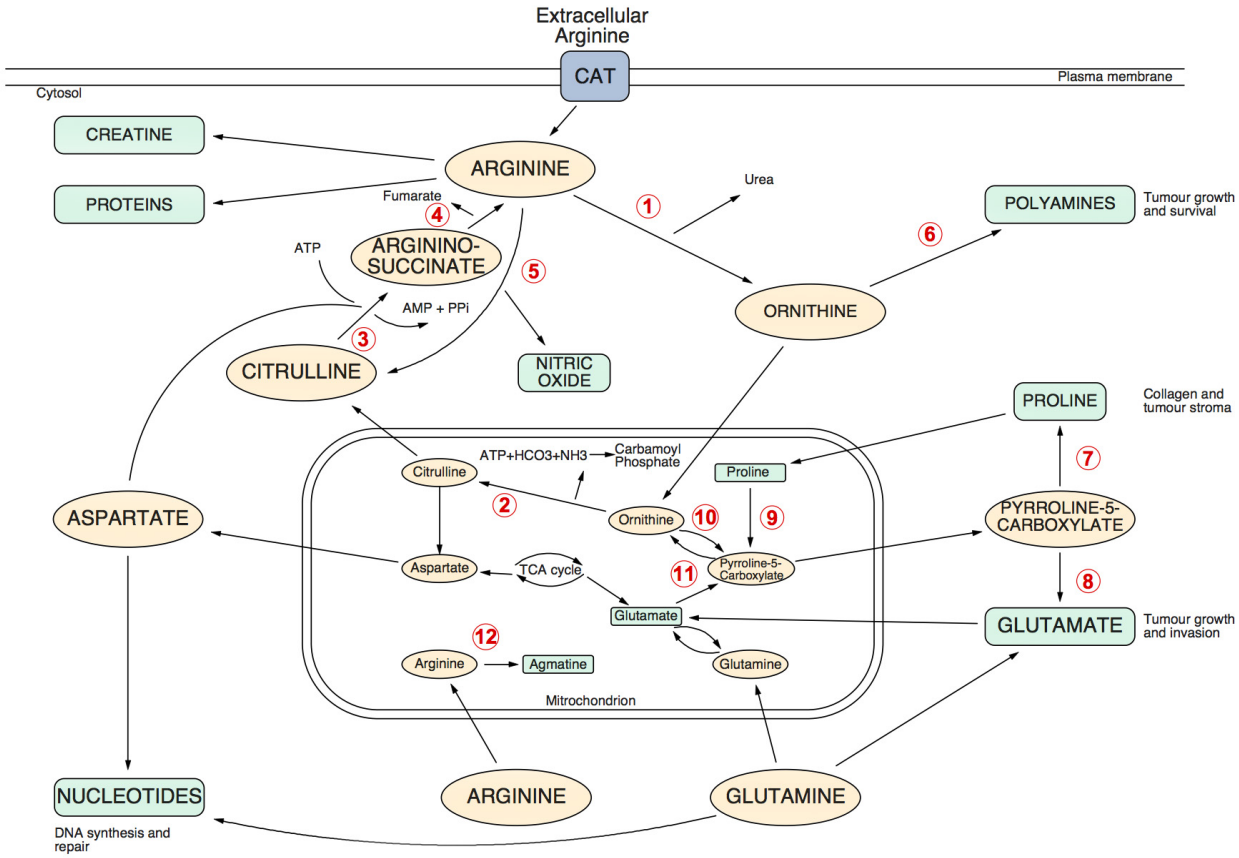


**Figure 1.2. Arginine utilisation within the tumour cell.** Arginine is a substrate for multiple metabolic and inflammatory pathways in health and disease (see text). Arginine may be sourced from the extracellular environment via the cationic amino acid transporter, or endogenously synthesised via ASS1. The subcellular locations of key enzymes are shown and enumerated in the figure as follows: 1, arginase; 2, ornithine transcarbamylase (OTC); 3, argininosuccinate synthetase (ASS1); 4, argininosuccinate lyase (ASL); 5; nitric oxide synthase; 6, ornithine decarboxylase; 7, pyrroline-5-carboxylate reductase; 8, pyrroline-5-carboxylate dehydrogenase; 9, proline oxidase (dehydrogenase); 10, ornithine aminotransferase; 11, pyrroline-5-carboxylate synthase; 12, arginine decarboxylase. Adapted from Delage *et al* (112)

#### 1.3.2.1.3 ASS1

The human ASS1 gene is located on chromosome 9, has 16 exons and a 1236 base-pair segment of open reading frame (ORF). The protein has 412 amino acids in total. It is a ubiquitous enzyme, expressed differentially and regulated according to cell type, differentiation status and function. For example, in the adult kidney, ASS1 is located in the cytosol of proximal tubules and is geared to arginine production, especially during starvation. Similarly, in the adult liver ASS1 expression is predominantly cytosolic, whereas in the endothelial cell it has been identified in caveolae, forming invaginations in the plasma membrane (117). Under physiologic conditions, hepatic ASS1 is hormonally regulated (e.g. cortisol, insulin, growth hormone, and glucagon). In contrast, expression of endothelial and inflammatory cell ASS1 is principally under the control of cytokines (IL-1, TNF-α, TGF-β) (112).

Much attention has been focused on ASS1 in recent years, as it is the rate-limiting enzyme in arginine biosynthesis. Indeed, several experimental models support a rate-limiting role for ASS1 in NO production. Xie and Gross overexpressed ASS1 in rat vascular smooth muscle cells and, following treatment with LPS/IFN-γ, noted a 3–4 fold increase in NO production, despite saturating levels of extracellular arginine (118). The reverse experiment using ASS1 RNAi, confirmed that not only was NO production in endothelial cells critically dependent on intact citrulline recycling, but also that abrogation of ASS1 resulted in apoptotic cell death.

##### *1.3.2.1.3.1 ASS1 deficiency and urea cycle disorders*

ASS1 is one of five catalytic enzymes of the urea cycle, which also includes carbamoylphosphate synthetase I (CPS1), ornithine transcarbamylase (OTC), argininosuccinic acid lyase (ASL) and arginase (ARG). As the urea cycle is the sole source of endogenous arginine, ornithine and citrulline and the principal mechanism for the clearance of waste nitrogen resulting from protein turnover, urea cycle disorders that result from inherited deficiencies in the enzymes of the urea cycle pathway are life-threatening. In ASS1 deficiency, the specific urea cycle disorder is Citrullinaemia Type 1. This is inherited in an autosomal recessive manner and the

estimated incidence is 1:250,000 (119). Severe deficiency or total absence of activity of ASS1 results in the accumulation of ammonia and other precursor metabolites during the first few days of life. Infants with a severe urea cycle disorder are normal at birth but rapidly develop cerebral oedema and the related signs of lethargy, anorexia, hyper- or hypoventilation, hypothermia, seizures, neurologic posturing, and coma. In milder (or partial) deficiencies, ammonia accumulation may be triggered by illness or stress at almost any time of life (120, 121). Early recognition and treatment of a urea cycle disorder is essential to prevent severe brain damage.

#### *1.3.2.1.3.2 ASS1 dysregulation in human cancers*

ASS1 was first cloned from a carcinoma cell line in 1981(122). Since then, various independent studies have revealed differential expression across a wide range of tumour tissues compared with corresponding normal epithelia, implying a key role for ASS1 in malignant disease (see Table 1.2 for details). Specifically, high levels of ASS1 mRNA and protein have been noted in malignant ovarian, gastric and colonic epithelium. In contrast, tumours often characterised by chemoresistance and poor clinical outcome, including melanoma, hepatocellular carcinoma (HCC), mesothelioma, renal cell carcinoma, and prostate cancer, exhibit loss of ASS1 expression (123-127) . Importantly, loss of this rate-limiting enzyme leads to a critical dependence on exogenous arginine for growth.

Epigenetic silencing, *via* methylation of the CpG islands within the ASS1 promoter, accounts for loss of ASS1 expression in some tumours studied to date, including mesothelioma (128). Other mechanisms identified include repression of the *ASS1* promoter by hypoxia-inducible factor-1alpha (HIF1α), detected in melanoma cells (129). Further work is required to ascertain additional mechanisms of loss.

The reason for down-regulation of tumoural ASS1 expression remains unclear and is an area of ongoing research. However, as a rate-limiting enzyme involved in providing arginine for various key metabolic pathways, it suggests that such loss provides a fundamental biological advantage for these tumours. Although ASS1

primarily functions as an enzyme, its non- enzymatic functions, such as tumour suppression, have recently been evaluated. It appears from several studies that the reprogramming of tumour arginine metabolism by switching off ASS1 supports a more aggressive phenotype driven by exogenous arginine. To illustrate this, reduced ASS1 expression was significantly correlated with the development of pulmonary metastasis after surgery and poor prognosis in patients with osteosarcoma, while over-expression of ASS1 inhibited tumour growth *in vitro (130)*. Furthermore, ASS1 deficiency was identified in half of patients with nasopharyngeal carcinomas (NPC), and it was associated with advanced tumour stage, high local recurrence rate and poor disease- free survival (131). Likewise, in ovarian cancer, ASS1 methylation was associated with significantly reduced overall survival and relapse-free survival and contributed to treatment failure (132), and, recently, it was reported that 40% of bladder tumours exhibited ASS1 deficiency, which was associated with worse disease-free and metastasis-free survival. Here, epigenetic silencing of ASS1 was shown to consistently enhance tumour proliferation and invasion (133), further indicating that ASS1 might be a novel metabolic tumour suppressor.

Several recent examples taken from the Kreb's cycle illustrate how loss of key metabolic enzymes promotes tumourigenesis: mutations of fumarate hydratase (FH) predisposing to leiomyosarcomas and papillary renal cell carcinomas; mutations of succinate dehydrogenase (SDH) leading to paragangliomas, phaechromocytomas and renal cell carcinomas; and isocitrate dehydrogenase (IDH) mutations described in more than 70% of low grade glioblastoma (IDH 1 and 2) and 10% of glioblastoma multiforme (IDH1) tumours (134). Recessive mutations have not been identified in tumoural ASS1. Nevertheless, as evident with the loss of FH and SDH, inactivation of ASS1 may be involved in sustaining the bioenergetic and biosynthetic needs of the tumour cell *via* diversion of critical intermediates. Pharmacological studies from our laboratory support the hypothesis that exogenous arginine is sparing for glutamine in the synthesis of pyrimidines, specifically in ASS1-negative tumour cells. Here, arginine depletion in ASS1-negative cells led to a distinct increase in intracellular glutamine whilst thymidine levels dropped secondary to inhibition of thymidylate synthase (TS) and dihydrofolate reductase (DHFR), emphasising the interdependence between exogenous arginine and glutamine for nucleotide synthesis. (133). Furthermore, a key study by Rabinovich et al recently

demonstrated that the decreased activity of ASS1 in various cancers supports proliferation of cells by facilitating pyrimidine synthesis via CAD (carbamoyl-phosphate synthase 2, aspartate transcarbamylase, and dihydroorotase complex) activation. They found that ASS1 deficiency in cancer increases cytosolic aspartate levels, which increases CAD activation by upregulating its substrate availability and by increasing its phosphorylation by S6K1 through the mTOR pathway, concluding that this novel mechanism provides a metabolic link between the urea cycle enzymes and pyrimidine synthesis (135)

Interestingly, it has also been reported that high ASS1 expression is associated with unfavourable disease-free survival in head and neck carcinoma (136). Taken together, results presented in this section all highlight the importance of dysregulated ASS1 expression in malignant disease.

#### 1.3.2.1.4 ASL

Less is known about the tumoural role of ASL, which is immediately downstream of ASS1 and catalyses the final step in arginine biosynthesis. It is apparent from inborn errors of metabolism that ASL is critical in synthesising arginine for NO production, with NO donors reversing the clinical picture of hypertension in children with ASL deficiency (137). More recently, ASL has been explored in cancer; up-regulation was noted in hepatocellular carcinoma, linked to increased aggressiveness mediated by NO and cyclin A2 signaling (138). There is also evidence that methylated ASL contributes to the arginine auxotrophy of glioblastoma multiforme, with loss of ASS1 and ASL conferring greater sensitivity to arginine depletion (139). In FH deficient renal cell cancer (RCC), where ASL is intact, the enzyme's activity is reversed producing high levels of argininosuccinate from arginine and fumarate. As argininosuccinate levels correlate with reversed ASL activity here, this has been suggested as a potential biomarker in FH null RCC and other tumours (140, 141). Although there is much less available data, the role of ASL in human cancer also appears to be dependent on tumour type. Further work is required to understand the role of ASL expression in human cancer.

| Tumour Type | ASS1 deficiency [a] |
|---|---|
| Bladder Cancer (133) | 45% |
| Breast Carcinoma (125, 142) | 9%<br>63.8% |
| Colorectal carcinoma (125) | 2% |
| Glioblastoma (139) | 36% |
| Head and Neck Carcinoma (136) | 56% |
| Hepatocellular Carcinoma (125) | 100% |
| Hodgkins Lymphoma (112) | 97% |
| Kidney carcinoma (125, 126) | 29%<br>100% |
| Malignant pleural mesothelioma (124, 143) | 63%<br>46% |
| Malignant melanoma (125, 144) | 100%<br>62.9% |
| Mixofibrosarcoma (145) | 44% |
| Non-hodgkins lymphoma (146) | 95% |
| Nasopharyngeal carcinoma (131) | 52% |
| Oesophageal carcinoma (147) | 19% |
| Osteosarcoma (130) | 63% |
| Ovarian cancer (125) | 4% |
| Pancreatic carcinoma (148) | 87% |
| Prostate carcinoma (127) | 100% |
| Retinoblastoma (149) | 0% |
| Sarcoma (125) | 22% |
| Seminoma (125) | 17% |
| Small cell lung carcinoma (150) | 44% |
| Squamous cell lung cancer (125) | 12% |
| Stomach carcinoma (125) | 0% |

**Table 1.2. Summary of ASS1 expression in tumours**

[a] ASS1 deficiency indicates the ratio of patients with absent/low expression of ASS1 at protein, mRNA and DNA levels, as determined by immunohistochemical staining, RT-PCR or methylation-specific PCR respectively, to all the patients enrolled. Adapted from Qiu *et al* (151)

### 1.3.3 Strategies for arginine depletion

Loss of ASS1 and the resulting arginine auxotrophy evident in various tumour types has been exploited as an ‘Achilles’ heel’ in recent years. Based on the asparaginase treatment paradigm, several arginine- catabolising enzymes have been evaluated for use in cancer therapy. In theory, a number of enzymes such as arginine deiminase (ADI), arginase, arginine decarboxylase (ADC) and the nitric oxide synthases (NOS) are potentially suitable for use as arginine depletors (152). However, various issues, including substrate specification, optimal pH and stability of individual enzymes for *in vivo* use, have meant that ADI and, to a lesser extent, arginase have come furthest along the path of clinical development.

#### *1.3.3.1 Arginine deiminase (ADI)*

ADI, an enzyme derived from Mycoplasma, degrades arginine into citrulline and ammonia. This is important as it allows cells with a functional ASS1 to re-cycle the citrulline back to arginine, thereby leaving ‘normal’ cells unaffected by arginine depletion whilst targeting ASS1 negative tumour cells. Currently, the commonly used ADI protein is derived from Mycobacterium arginini. At physiological status, 70% of the enzyme activity of ADI is reserved with an optimal pH of approximately 6.0–7.5 at 50 °C. However, in its native form it is strongly antigenic with a half-life of approximately 5 hours, which is clearly too short to be used *in vivo* (153). To help resolve these issues, ADI is conjugated with polyethylene glycol (PEG). The obtained ADI-PEG20 (Mw: 20,000Da) decreases antigenicity as well as dramatically increasing serum half life to 7 days, allowing weekly administration that reduces plasma arginine to undetectable levels (~2µmol/l) (154).

#### *1.3.3.2 Arginase*

Arginase is a manganese-containing enzyme that degrades arginine into ornithine and urea. Currently, two different subtypes of human arginases (arginase I and arginase II) have been identified, and they share 60% similarity in their amino acid sequence. Arginase I, which is mainly detected in the liver, has received more attention. Unlike ADI, human arginase I has no antigenicity. However, its optimal pH is 9.6, meaning it is less effective in human plasma. Compared with ADI, a large amount of arginase I is required to achieve arginine depletion (155). Therefore, recombinant human arginase I is also conjugated with PEG (Mw: 5,000Da) to formulate rhArg-PEG. This has an improved half-life time, increased from a few minutes to 3 days, and an improved Km value of arginine (Km is the concentration of substrate required to produce 50% of the maximal speed of activity of the enzyme), decreased from 6.0 to 2.9 mM, which makes rhArg-PEG usable in clinical application (156). However, animal toxicity testing indicates that citrulline supplementation is required since the ornithine produced by arginase cannot be recycled readily to citrulline (157).

ADI-PEG20 has been used more extensively in the pre-clinical and clinical setting and is therefore discussed in more detail below.

### 1.3.4 Arginine Deprivation: pre-clinical data

It is now well established that targeting extracellular arginine for degradation in the absence of ASS1 leads to cell death in arginine auxotrophs *in vitro* (112). More recent studies evaluating the efficacy of bioengineered arginine catabolising enzymes have confirmed that arginine depletion is also effective in various ASS1 – deficient xenograft models. Thus, in mice bearing subcutaneous malignant melanoma (MM) and hepatocellular carcinoma (HCC) xenograft tumours, ADI-PEG20 significantly suppressed tumour growth and extended animal survival time (123). The anti-tumour activity of ADI-PEG20 has also been validated in pancreatic cancer, prostate cancer, small cell lung cancer, lymphoma, head and neck cancer,

mesothelioma, bladder cancer, glioblastoma and breast cancer (127, 128, 131, 139, 142, 146, 150).

Whilst amino acid deprivation is known to induce nutritional starvation, the inhibitory effects of arginine depletors on tumour growth are not fully understood and remain an area of active investigation. ADI-PEG20 has been shown to down-regulate mammalian target of rapamycin (mTOR) and modulate phosphoinositide 3-kinase (PI3K) via suppression of phosphatase and tensin homolog (PTEN) in ASS1-negative tumour cells (104). In fact, arginine is one of two key amino acid regulators of mTOR—the other being leucine—and this could explain, in part, the ability of arginine depletors to critically impair protein synthesis (158). In addition to modulating tumour biomass via suppression of nucleotide and protein synthesis, arginine depletion also affects tumour cell motility via a NO and focal adhesion kinase (FAK)-dependent pathway; importantly, FAK activation has been linked to deprivation of several other amino acids including glutamine and tyrosine (159, 160). Interestingly, ADI was also identified in an anti-angiogenic screen and an anti-vascular effect has been confirmed both in HUVEC cells *in vitro* and in a xenograft melanoma study using fluorescence molecular tomography. Furthermore, ADI was anti- angiogenic and potentiated the effect of radiation in a neuroblastoma mouse model (161-163).

Having established an anti-tumour effect using ADI-PEG20 alone, investigators are increasingly evaluating the therapeutic efficacy of ADI-PEG20 in combination with other anti-tumour modalities. To date several preclinical combinatorial studies have shown additive and/or synergistic effects of arginine depletion with taxanes, 5-fluorouracil, pemetrexed, cytarabine, PI3K inhibitors, and modulators of autophagy using chloroquine and TRAIL (127, 133, 164, 165). For example, the combination of docetaxel and ADI-PEG20 exhibited synergistic effects in prostate cancer cells (127). ADI-PEG20 was also shown to potentiate the activity of pemetrexed in bladder cancer and mesothelioma (133), and more recently, Qui and colleagues (142) demonstrated a synergistic interaction between ADI-PEG20 and doxorubicin in breast cancer. Other interactions under investigation include the potentiation observed between arginine deprivation and radiotherapy in 3D spheroid models of arginine auxotrophic cell lines (166).

These results suggest that using ADI-PEG20 as part of a rational treatment combination may improve outcome in the clinical setting.

### 1.3.5 Arginine deprivation: clinical data

The initial phase I/II studies of ADI-PEG20 were performed in patients with HCC and melanoma, tumours with a high frequency of ASS1 loss (see Table 1.3). Encouraging response rates of between 25-47% were observed in these small studies, with good safety and tolerability (167, 168). The common adverse reactions have been self-limiting grade 1-2 injection site reactions. Diffuse skin rashes and arthralgia have also been recorded, although less frequently, and neutropenia, anaphylactoid reactions and serum sickness are rare (104). Following on from these studies, the latest ADI-PEG20 clinical trials in HCC and metastatic melanoma have recorded stable disease as the best response. Yang et al (169) performed a randomized phase II study of two different doses of ADI-PEG20 (320 IU/$m^2$ vs. 160 IU/$m^2$) in HCC showing that disease control rates were similar in both groups. A trend towards better survival was observed in patients with >4 weeks (10.0 months) compared with <4 weeks (5.8 months) of arginine deprivation. A global phase III trial is now underway using the 160 IU/$m^2$ dose (ClinicalTrials.gov Identifier: NCT01 287585) to confirm the therapeutic efficacy of ADI-PEG20 in HCC. Results are expected in 2016.

The role of ASS1 as a predictor of response to ADI-PEG20 has been explored only recently in clinical trials. The first prospective multi-centre randomised study of ADI-PEG20 in patients pre-selected for *ASS1* deficiency in cancer has recently been conducted in mesothelioma (the Arginine Deiminase And Mesothelioma or ADAM Phase II study). ADAM met its primary endpoint of an improvement in the progression-free survival in the best supportive care (BSC) plus ADI-PEG20 group compared to the BSC alone group of almost 6 weeks (p=0.02) (143). In addition, 46% of patients achieved partial metabolic response by PET-CT, with stable disease as the best radiographic response (170). The data support differential methylation as

the basis for the loss of ASS1 observed in mesothelioma, consistent with earlier cell line studies.

Following on from the ADAM trial, a phase I study evaluating ADI-PEG20 in combination with pemetrexed and cisplatin is currently recruiting patients with mesothelioma and other ASS1-deficient tumours (NCT0209690). In addition, several other ongoing clinical trials using ADI-PEG20 in combination are recruiting patients with advanced non-Hodgkin's lymphoma (NCT01910025), acute myeloid leukemia (NCT01910012), prostate cancer (NCT01497925), HER2 negative metastatic breast cancer (NCT01948843) and small cell lung cancer (NCT01266018) [Available from: https://clinicaltrials.gov]

Therefore, in summary, early signs suggest that arginine deprivation as a therapeutic strategy has the potential to make an impact across a broad range of human malignancies, including MPM.

| Study | Number of patients | Tumour type | Arginine depletor | Overall survival (months) | Response rate (best response) | Comments |
|---|---|---|---|---|---|---|
| Izzo et al, 2004 (168) | 19 | HCC | ADI-PEG20<br><br>Phase I/II | 13.7 | 47% (CR+PR) | Low toxicity |
| Glazer et al, 2010 (171) | 76 | HCC | ADI-PEG20<br><br>Phase II | 15.8‡ | SD only | [Arginine] plasma reduced for 50 days |
| Yang et al, 2010 (169) | 71 | HCC | Randomized Phase II:<br><br>160 or 320IU/$m^2$ of ADI-PEG20 | 7.3 | 31% (SD) | PFS 1.8 months; Heavily pre-treated patients |
| Ascierto et al, 2005 (167) | 39 | Melanoma | ADI-PEG20 Phase I/II | 15 | 25% (CR+PR) | Reduced NO synthesis consistent with MOA |
| Feun et al, 2012 (144) | 38 | Melanoma | ADI-PEG20 Phase II | 14.6 (ASS1-ve) vs 9.3 (ASS1+ve) months [p=0.374] | 11% (PR) in ASS1-ve only | PFS 3.6 ASS1-ve) vs 1.8 months (ASS1+ve), [p=0.025]; 74% ASS-ve frequency; ASS1 re-expression on relapse (n=2/2) |
| Ott et al, 2012 (172) | 31 | Melanoma | ADI-PEG20 Phase I/II | n/a | 25% early PMR; 29% (SD) | Prolonged SD in choroidal melanoma |
| Szlosarek et al, 2013(143) | 68 | Mesothelioma | Randomized Phase II in ASS1-ve patients:<br><br>ADI-PEG20+BSC (n=44)<br><br>vs.<br><br>BSC alone (n=24) | n/a | 46% early PMR; SD by modified RECIST | PFS 3.3 vs 1.9 months [p=0.02] favoring ADI-PEG20+BSC; *ASS1* methylation status correlated with IHC [p=0.025] |

**Table 1.3: Completed clinical studies of single agent ADI-PEG20 in advance cancer**. Adapted from Phillips et al (104).

‡ from diagnosis; PMR=partial metabolic response; MOA=mechanism of action; OBD=Optimal biological dose; n/a =not available

### 1.3.6 Resistance to arginine depletion

However, despite promising results observed in both pre-clinical and clinical studies as a targeted therapy for arginine auxotrophic tumours, drug resistance remains a significant challenge for effective use of arginine depletors. The underlying mechanisms of resistance to arginine deprivation are being explored, and several have recently been identified. These mechanisms are discussed below and are also summarised in Figure 1.3.

#### *1.3.6.1 Re-expression of ASS1*

Re-expression of ASS1 results in the re-cycling of citrulline back to arginine. This has been described by Manca and colleagues (173) who found that thirty-three percent of initial ASS1-deficient malignant melanoma tumours became ASS1-positive after ADI-PEG20 treatment, and therefore resistant to ADI-PEG20. ADI-PEG20 was reported to activate the Ras/PI3K/ERK signaling pathway in melanoma cells and increase the stability of the transcription factor c-Myc, which subsequently caused c-Myc accumulation and elevated ASS1 expression by binding to the ASS1 promoter (164).

#### *1.3.6.2 Autophagy*

Autophagy (‘self-eating’), leading to the provision of a temporary but finite supply of arginine via the breakdown of intracellular organelles (174), is also triggered by arginine deprivation, circumventing the depletion of arginine in several malignancies, including prostate cancer, lymphoma, glioblastoma multiforme, and melanoma (175-178)

#### *1.3.6.3 Drug-neutralising antibodies*

ADI derived from mycobacterium *arginini* is still immunogenic in humans even after pegylation. As a result, anti-ADI antibodies have been detected in patients enrolled

in clinical trials. For example, in a phase II clinical trial for the treatment of HCC patients, anti-ADI antibodies were detected after the administration of ADI-PEG20 and reached a plateau at day 50, which was accompanied by an arginine level that rebounded to baseline value (171). Although further investigations are needed to clarify the correlation between the onset/progression of the antibody and the therapeutic efficacy of ADI-PEG20, anti-ADI antibodies may contribute to the resistance to arginine deprivation.

#### *1.3.6.4. A role for the tumour microenvironment?*

Finally, the direct supply of arginine or its precursors by host cells within the tumour microenvironment (TME) may also be a resistance mechanism, as shown for other metabolites. For example, in acute lymphoblastic leukaemia (ALL), mesenchymal-derived stromal cells were reported to provide asparagine for asparaginase-resistant ALL cells (179, 180). Thus, the basis for the current work is that the tumour microenvironment may also influence MPM resistance to arginine deprivation.

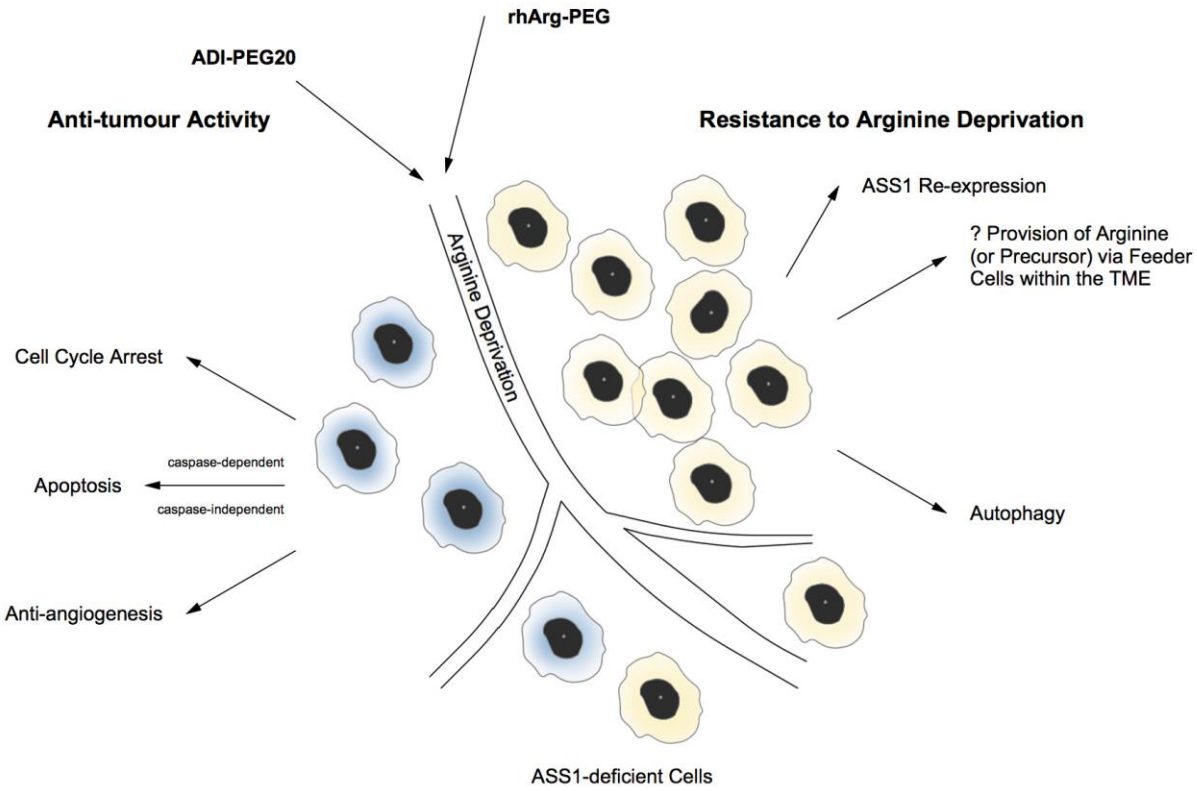


**Figure 1.3. Arginine deprivation: mechanisms of action and proposed resistance mechanisms.** Recognised mechanisms mediating the anti-tumour activity of arginine deprivation include induction of cell cycle arrest, apoptosis and inhibition of angiogenesis. On the other hand, ASS1 re-expression, enhanced glycolysis and autophagy have been reported to be associated with resistance to arginine deprivation. Additionally, cells within the TME may act as 'feeder cells' providing MPM cells with arginine (or its intermediates), thereby bypassing the effect of arginine depletion. Adapted from Qiu *et al* (151)

## 1.4 Tumour microenvironment

Tumours evolve in a complex, dynamic, and functionally multifaceted microenvironment that includes the cancer cells, stromal tissue (fibroblasts, neuroendocrine cells, adipose cells, immune and inflammatory cells, and the blood and lymphatic vascular network) as well as the surrounding extracellular matrix (181, 182). Physiologically, the stroma is an essential compartment in maintaining homeostasis of normal tissue, and in healthy individuals it acts physical barrier against tumour development; however, malignant cells provoke various changes within this environment to convert it into a pathological entity. Under such conditions, the stromal cells co-evolve with the cancer cells by being repeatedly re-educated or modified by the latter to produce a wide variety of cytokines, chemokines, growth factors, and proteinases, all of which can significantly promote cancer progression, invasion, metastasis and drug resistance (183, 184). Indeed, this 'transformed' tumour-promoting stroma, or tumour microenvironment (TME), is characterised by a remodeled matrix, reprogrammed metabolism, activated transcription, and altered synthesis of repair-associated proteins (185-187).

The concept of the tumour microenvironment was first suggested in the 1880's with Paget's assertion that the microenvironment plays a critical role in regulating the growth of metastases - his 'seed and soil' theory (188): it is now recognised as an integral part of tumour physiology, structure and function. Indeed, there has been much interest in recent years on developing drugs that target the TME, as, unlike cancer cells, stromal populations within the TME are genetically stable, and thus represent an attractive therapeutic target with minimal risk of treatment resistance and disease relapse.

### 1.4.1 Cells of the tumour stroma

The most widely studied stromal cells in solid tumours, including MPM, are cancer-associated fibroblasts (CAF), tumour endothelial cells (TEC) and tumour-infiltrating immune cells (T lymphocytes and tumour–associated macrophages (TAM)). These cell-types will therefore be reviewed below, with a more detailed discussion on macrophages, which are abundant in MPM and the main focus of my thesis. For a diagrammatic summary, please see Figure 1.4.

#### *1.4.1.1 Fibroblasts*

In normal tissue, fibroblasts are the predominant mesenchyme-derived cell type in the connective tissue stroma and are the primary producers of the extracellular matrix (ECM). Fibroblasts are responsible for the deposition of the fibrillar ECM—type I, type III, and type V collagen and fibronectin—and contribute to the formation of the basement membrane by secreting type IV collagen and laminin. Connective tissue and the ECM are continually remodeled through a dynamic process of ECM protein production and degradation by fibroblast-derived matrix metalloproteinases (MMPs). This turnover is, however, well regulated and controlled (189).

In cancer, fibroblasts are a major cellular component of the tumour microenvironment. Indeed, in some cancer types, fibroblasts comprise a larger proportion of cells within the tumour than the cancer cells themselves. Fibroblasts within tumours have an ‘activated’ phenotype, and therefore resemble fibroblasts in wound healing. They have been shown to assist in proliferation and progression of cancer through the secretion of growth factors, pro-inflammatory and pro-angiogenic cytokines, and extracellular matrix proteins, thereby permitting invasion and spread of cancer cells (190, 191). Moreover, it has recently been shown that certain secreted factors (the nutrients lactate, ketone bodies and glutamine) sustain the survival of hypoxic cancer cells and the growth of normoxic cancer cells by serving as a source of

energy and/or as intermediates to biosynthesis (192). This is discussed in more detail in Chapter 4.

Importantly, these cancer-associated fibroblasts (CAFs) are functionally and phenotypically distinct from normal fibroblasts. The difference between CAFs and physiologically activated fibroblasts is that CAFs are permanently activated, neither returning to a normal phenotype nor undergoing apoptosis and elimination (193). CAFs are recognised within tumor stroma by their spindyloid appearance and the expression of alpha-smooth muscle actin (α-SMA); characteristics shared by activated fibroblasts in wounds.

As with other solid tumours, CAFs are a major component of the MPM tumour microenvironment (194, 195). CAFs regulate tumour behavior through several mediators. For example, it was recently demonstrated using an *in vitro* co-culture model that MPM cell lines produced fibroblast-growth factor 2 (FGF-2) and platelet-derived growth factor-AA (PDGF-AA), and that these growth factors stimulated CAFs to produce hepatocyte growth factor (HGF), thus promoting tumour progression through a malignant cytokine network. Furthermore, the significant infiltration of CAFs and the simultaneous expression of these three cytokines were also detected in 51 clinical specimens obtained from patients with MPM (196). This highlights the importance of stromal fibroblasts in MPM tumour progression and suggests that these three cytokines may be potential therapeutic targets in MPM treatment.

#### *1.4.1.2 Endothelial Cells*

Endothelial cells (ECs) remain quiescent for years, but when tissues are deprived of oxygen or nutrients, they sprout to vascularise these tissues (angiogenesis) (197). Tumours require the formation of a complex vascular network to meet their metabolic and nutritional needs for growth, and the vessel formation generated by angiogenesis addresses these needs. VEGF is the principal factor involved in the formation of tumour vessels. It is secreted

directly by the tumour cells, and by fibroblasts and inflammatory cells in the stroma. VEGF is important for the activation of the ‘‘angiogenic switch’’ (98), which causes the usually quiescent vasculature to sprout new vessels and, in turn, aid tumour growth and proliferation (189). However, tumour vessels formed as a result of VEGF are abnormal; they are inconsistently distributed and irregularly shaped, incorrectly branched and tortuous, often ending blindly. They do not have the classic hierachical arrangement of arterioles, venules, and capillaries and often form arterio-venous shunts. They are also fenestrated and leaky, leading to high interstitial pressures, further exacerbating tissue hypoxia and stimulating additional VEGF production (198).

*In vitro* studies have shown that mesothelioma cell lines produce varying quantities of VEGF. In the MPM cells that produce large quantities, the interaction with endothelial cells seems to be particularly important. VEGF produced by MPM cells activates endothelial cells and induces angiogenesis, promoting tumour progression (199). In addition, by activating endothelial cells, VEGF induces hypervascular permeability to produce pleural effusion (200). Therapy targeting VEGF/endothelial cells may therefore be effective for MPM cells that produce large quantities of VEGF.

#### *1.4.1.3 T lymphocytes*

Infiltrating innate and adaptive immune cells comprise a large component of the TME. Key adaptive immune cells are the T lymphocytes. Many different T cell populations infiltrate the tumour; among these are the memory CD8+ T cells, which are capable of killing tumour cells and are generally associated with good prognosis (201). Indeed, a study to determine the impact of tumour infiltrating T lymphocytes on survival in MPM patients treated with induction chemotherapy followed by EPP found that patients with high levels of CD8+ tumour-infiltrating T lymphocytes demonstrated better survival than those with low levels (3-year survival: 83% versus 28%; p =0.06). Moreover, high levels

of CD8+ tumour-infiltrating lymphocytes were associated with a lower incidence of mediastinal node disease (p =0.004) and longer progression-free survival (p = 0.05) (202).

These CD8+ T cells are supported by CD4+ T Helper 1 cells, which are which are characterised by production of the cytokines interleukin-2 (IL-2) and interferon gamma (IFN-γ); high numbers of these in the TME are also associated with good prognosis. Conversely, other CD4+ T cell populations, such as the T Helper 2 cells, are thought to promote tumour growth. These tumour-promoting CD4+ T cells are commonly described as the immunosuppressive T regulatory (Tregs) cells (203). They exert an immune suppressive function through the production of IL-10,TGFβ and cell-mediated contact through CTLA-4, inhibiting recognition and clearance of tumour cells by the immune system (204). High numbers of Tregs in the TME correlate with worse prognosis in many types of cancer (205), including in MPM, where patients with high levels of CD4+ tumour-infiltrating lymphocytes were found to demonstrate a trend toward shorter survival (202).

#### *1.4.1.4 Macrophages*

Below is a detailed review of macrophage biology and the role these cells play in tumour development and therapeutic resistance. This is followed by a specific section focusing on macrophages in MPM.

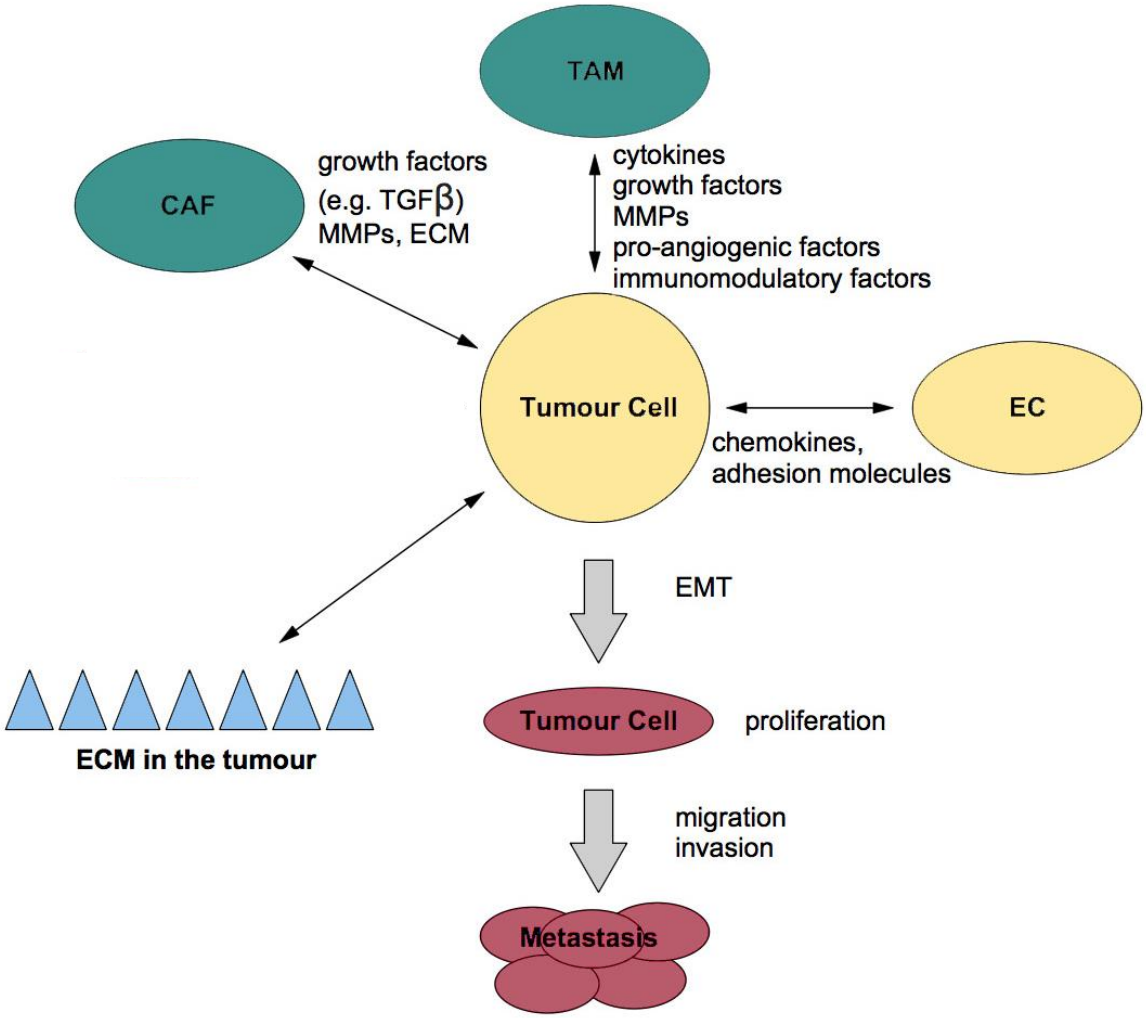


**Figure 1.4. Reciprocal interactions of tumour cells and stromal cells in the tumour microenvironment.** Tumour-associated macrophages (TAM), carcinoma- associated fibroblasts (CAF), endothelial cells (EC) and the extracellular matrix (ECM). These interactions are mediated by direct cell-to- cell contact and/or the release of cytokines, chemokines, growth factors, matrix metalloproteases (MMPs), and ECM proteins. Eventually this results in tumour cell proliferation, epithelial-mesenchymal transition (EMT), migration, invasion and the formation of metastases. For reasons of clarity, other stromal cell populations, e.g. lymphocytes and known interactions among different stroma cell populations are not shown. Adapted from Ungefroren *et al* (191)

## 1.5 Macrophage Biology

### 1.5.1 Macrophage development

Macrophages are a heterogeneous population of terminally differentiated, tissue-resident, innate myeloid cells. They exist in almost all tissues and play important roles in development and the maintenance of tissue homeostasis (206). Under non-pathological conditions, most resident macrophage populations derive from embryonic (yolk sac) progenitors and are maintained through local proliferation (207). Exceptions to this include intestinal, dermal and alveolar macrophages (208, 209). These macrophages differentiate from peripheral blood monocytes, which develop from common myeloid progenitor cells. These cells are identified as granulocyte/ macrophage colony-forming units (GM-CFUs) in the bone marrow. In response to a macrophage colony-forming factor, GM-CFUs sequentially give rise to macrophage colony-forming units (M-CFUs), monoblasts, and pro-monocytes. Subsequently, they move into the peripheral blood and differentiate into monocytes. Finally, the monocytes migrate into different tissues and replenish the populations of these tissue-specific macrophages (210, 211). Under pathological conditions there is evidence of both local proliferation and recruitment, depending on the tissue location and inflammatory insult (212).

### 1.5.2 Macrophage activation and phenotypic diversity

Macrophages display huge variation in phenotype, with specialised populations seen in different tissues. Well-described specialised resident tissue macrophages with distinct phenotypes include kuppfer cells (liver), osteoclasts (bone), microglia (brain), histiocytes (connective tissue) and alveolar macrophages (lung) (211). The phenotypic diversity in macrophages is influenced by activation signals from the surrounding microenvironment and can be strongly regulated by the products of T- lymphocytes, natural killer

(NK) cells and tumour cells, in particular interferon- gamma (IFN-γ) and a cytokine network involving IL-4, IL-10, IL-12, and IL-13, as well as tissue oxygen tension and pH (213). Macrophage activation states have been separated into two phenotypes, M1 or M2, which parallel the Th1/Th2 paradigm, and *in vitro* data has established that peripheral blood monocyte-derived macrophages can be polarized into M1 or M2 phenotypes (see Figure 1.5). This has also been validated *in vivo* for M1 macrophages, which are activated by IFN-γ or by bacterial cell wall-derived LPS, and predominate during acute inflammatory responses (214). M1, or 'classically activated' macrophages produce large quantities of pro-inflammatory cytokines (e.g. IL-1β, IL-12, and TNF-α), present antigens via increased expression of MHC class II molecules, and are implicated in the killing of pathogens and tumour cells (215, 216). In contrast, M2, or 'alternatively activated', macrophages (217) are characterised by increased production of IL-10, amplification of metabolic pathways that can suppress adaptive immune responses, and up-regulation of cell-surface scavenger receptors, such as mannose receptor (MRC1/CD206) and hemoglobin/aptoglobin scavenger receptor (CD163). As such, M2 macrophage activation moderates the inflammatory response and promotes tissue re-modeling/repair (including angiogenesis) (218, 219). Stimulation with IL-4, IL-13, TGFβ, IL-10, immune-complexes, glucocorticoid hormones, and agonists of certain TLRs or the IL-1R, drives macrophages toward an M2 phenotype (219).

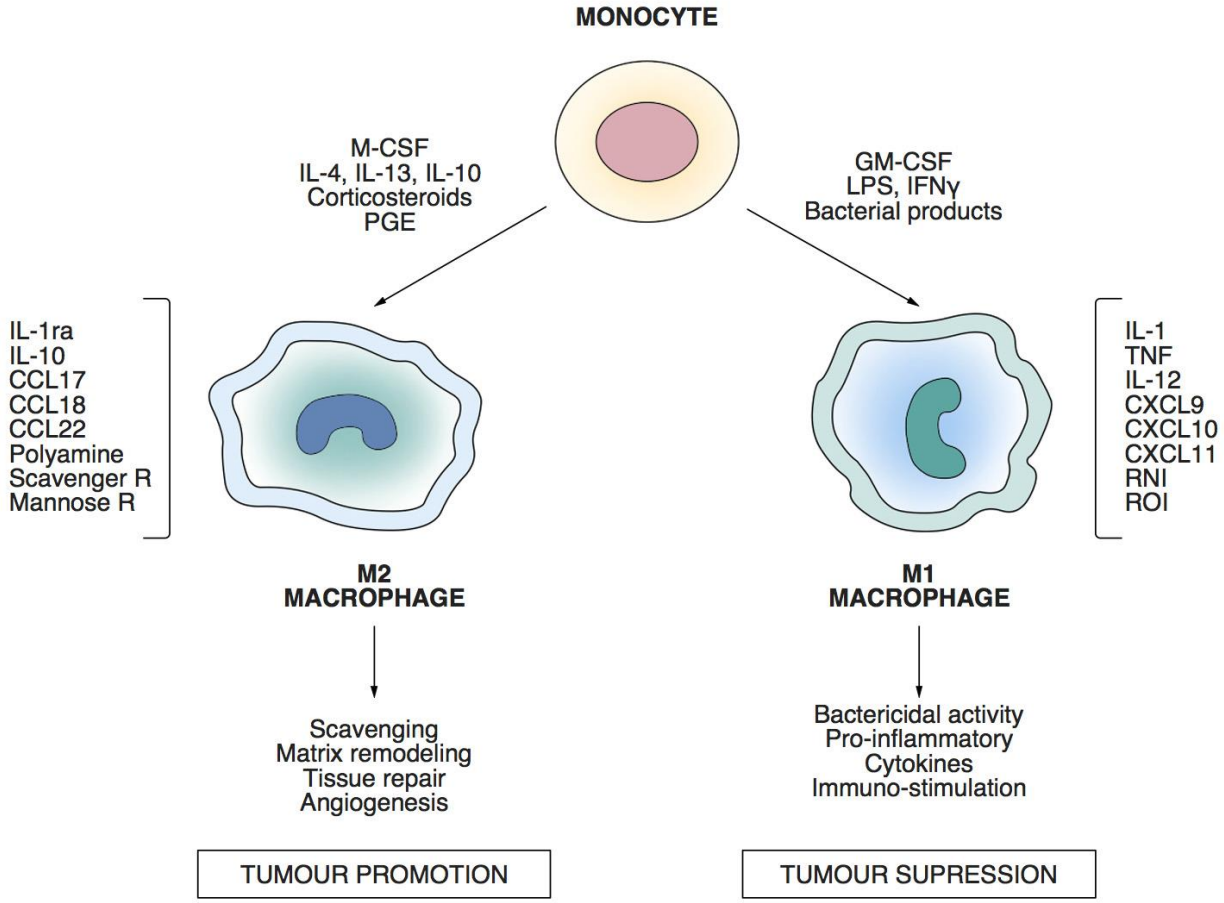


**Figure 1.5. The differentiation pathways of 'classically'-activated M1 macrophages and 'alternatively'-activated M2 macrophages**. Adapted from Quatromoni and Eruslanov (220)

However, whilst the M1-M2 classification system is useful when attempting to understand macrophage plasticity, it oversimplifies the diversity of macrophage phenotypes. Indeed, macrophage phenotype does not appear to be stereotyped or twofold in response to different stimuli, as may be assumed if incorrectly interpreting the M1-M2 model. Instead, macrophages often express a mixed M1/M2 phenotype; thus “M1” and “M2” polarisation should be considered as extreme ends of a continuum of activation states, with the position on this spectrum depending on the exact composition of the activating signals present in a given microenvironment (214, 221, 222). Furthermore, macrophages can also shift from one activation state to another, reflecting their dynamic interaction with the surrounding environment (223). The M1-M2 model remains, nonetheless, a useful tool for descriptive purposes and laboratory testing of the general principles of macrophage phenotype.

### 1.5.3 The arginine metabolome and macrophages

Importantly, each pathway of macrophage activation employs arginine as a key substrate. Indeed, arginine can be utilised by macrophages in a variety of metabolic pathways, with the differential catabolism via the inducible form of nitric oxide synthase (iNOS) and arginase being the best characterised to date. Th1-type cytokines transcriptionally up-regulate iNOS (M1 macrophages), and Th2-type cytokines activate arginase expression (M2 macrophages) (224, 225). Arginine utilisation can therefore directly affect the role of macrophages and the type of host immune response within the tumour microenvironment (Figure 1.6).

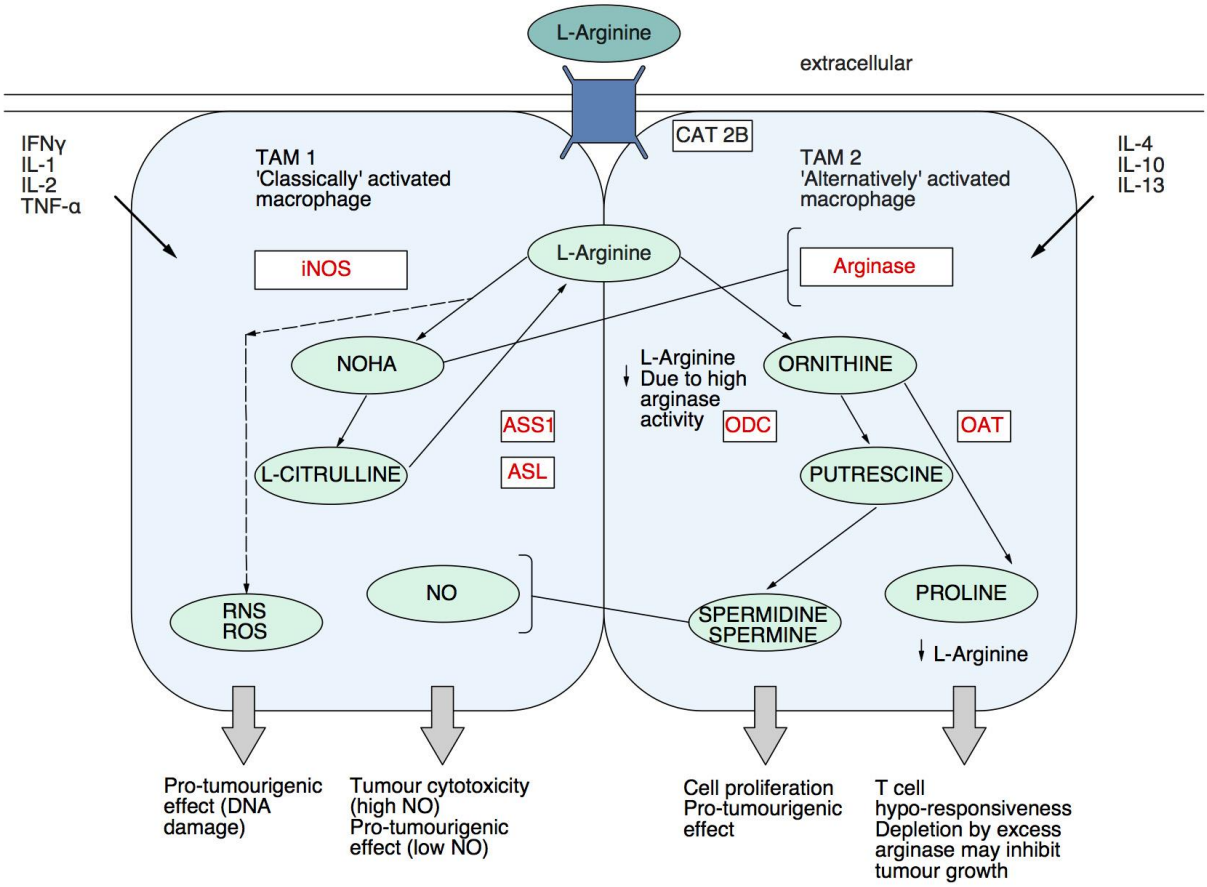


**Figure 1.6. Schematic representation of TAM 1 and TAM 2 metabolic pathways**. The activities of the enzymes in both 'classically' activated (M1), and 'alternatively' activated (M2) macrophages in the TME are illustrated. Solid arrows indicate the main enzymatic activity, whereas dashed arrows indicate alternative metabolic activity. In particular, when arginine concentrations are low (common within the TME), iNOS activity changes from the prevalent production of NO to the generation of superoxide and highly reactive nitrogen species (RNS). The T helper 1 cytokines (IFN γ) and T helper 2 cytokines (IL4, IL13) are the main inducers of iNOS and Arginase, respectively. Pro-inflammatory signals (such as IL1 and TNF α) and anti-inflammatory signals (IL10) can contribute to regulate the final balance between iNOS and arginase activity. Moreover, arginase and iNOS directly activate several biochemical circuits that negatively regulate each other. The depletion of L-arginine by overexpression of arginase reduces the activity of iNOS in the production of NO. Polyamines can also inhibit production of NO. Conversely, NOHA can inhibit arginase.
NOHA, N hydroxy L-arginine; OAT, ornithine aminotransferase; ODC, ornithine decarboxylase; RNS, reactive nitrogen species; ROS, reactive oxygen species; ASS1 argininosuccinate synthetase; ASL, argininosuccinate lyase. Adapted from Phillips M (226).

## 1.5.4 Macrophages, cancer cells and the tumour microenvironment

As detailed in the section above, a wide variety of signals can profoundly affect the function of macrophages. This section will focus on the role of macrophages in the tumour microenvironment.

### *1.5.4.1 Tumour-associated macrophages (TAM)*

#### 1.5.4.1.1 TAM origin and recruitment

Macrophages are a major component of the infiltrate of most tumours, where they are commonly termed tumour-associated macrophages (TAM). They represent a mature population of terminally differentiated myeloid lineage cells, derived from both local proliferation and bone marrow (BM) monocytes (212). Production of certain chemoattractants by tumour cells and stromal cells is essential to recruit and sustain large numbers of TAM. For instance, the C-C chemokine ligand 2 (CCL2) and colony-stimulating factor-1 (CSF-1) play a critical role in recruiting macrophages to neoplastic tissue. Indeed, CSF-1 was shown to selectively promote metastatic potential in mice with mammary tumours by regulating the infiltration and function of TAM. Here, it was reported that CSF-1 receptor expression was restricted to TAM at the tumour site (227). Similarly, it was reported that the recruitment of inflammatory monocytes, which express CCR2 (the receptor for chemokine CCL2), as well as the subsequent recruitment of metastasis-associated macrophages and their interaction with metastasising tumour cells, is dependent on CCL2. Inhibition of CCL2-CCR2 signalling blocks the recruitment of inflammatory monocytes, inhibits metastasis *in vivo* and prolongs the survival of mice bearing mammary tumours (228). Furthermore, in prostate cancer, CCL2 overexpression increased the growth of transplanted xenografts and increased macrophage accumulation *in vivo* (229). Other chemokines, including CCL3, CCL4, CCL5, CCL7, CCL8, CXCL8 and

CXCL12, and cytokines, including VEGF, platelet-derived growth factor (PDGF), and IL-10, are also reported to promote macrophage recruitment into tumours (230-233).

Over a decade ago, it was proposed that TAM are primarily polarized in the tumour microenvironment toward an M2-like phenotype and that this underlies their ability to aid tumour growth (215). This is also supported by clinical studies showing the predictive value of M2-macrophage associated markers, like CD163 (234). However, it is becoming increasingly evident that distinct macrophage subpopulations with variable phenotypes coexist in tumours and that their relative abundance changes with the tumour type (235, 236). To illustrate this, recent work has identified varying proportions of M1 (arginase low and iNOS high) and M2 (arginase high and iNOS low) TAM depending upon the type of chemically or genetically induced epithelial tumour murine model. For example, macrophages exhibited arginase (high), iNOS (low) polarisation in early stage chemically induced lung tumours, whereas a mixed population of M1 and M2 TAM was observed with late stage lung adenocarcinomas (237). Moreover, lung tumour regression secondary to the inactivation of the Kras or FGF10-driven transgene was associated with a switch from an arginase (high) iNOS (low) TAM polarisation to an arginase (low) iNOS (low) pulmonary macrophage phenotype (no polarisation). In contrast, studies of TAM associated with different stages of melanoma progression, revealed dominant iNOS expression in *in situ* and thin melanomas which declined with the development of thicker melanomas (238). This complexity implies significant TAM phenotypic diversity in different tumour microenvironments.

#### 1.5.4.1.2 Role of TAM in tumour progression

For many solid tumour types, high numbers of cells expressing macrophage-associated markers have generally been found to be correlated with poor clinical outcome (212, 239). There are exceptions; for example, it has been

reported that macrophages in colorectal cancer play an anti-tumour role, which leads to a good prognosis (240, 241). Indeed, TAM do express a series of pro-inflammatory cytokines such as IFN-γ, IL-1, and IL-6, which can activate type-1 T-cells associated with anti-tumour immune responses (240). As illustrated in Figure 1.6, M1-skewed TAM also generate nitric oxide (NO) and its derivative reactive nitrogen species (RNS) via iNOS, which at high levels can initiate tumour cell apoptosis and destroy emerging transformed cells (242, 243).

In addition, conflicting data exist for stomach, prostate and bone cancers, where both positive and negative outcome associations have been reported (239, 244). This may be related to the type/stage of cancer evaluated (e.g. Ewing sarcoma versus osteosarcoma), or to the type of analysis performed (e.g. quantification of stromal versus intra-tumoural macrophages). The use of different macrophage markers may also result in some discrepancy; for example CD68 represents a reasonably specific marker in murine macrophages and, in combination with F4/80, identifies the majority of TAM (212). However, in humans, CD68 expression is more widespread (245) and is therefore less useful for association studies, although it is commonly used.

In many other tumours, including breast, pancreas, ovarian, lung carcinoma, cutaneous melanoma, and, importantly, mesothelioma, TAM are considered to be pro-tumourigenic (220, 239, 246-249). Added to this, epidemiological studies have suggested that a macrophage-rich microenvironment will promote an aggressive tumour with a high metastatic potential (250). The next section will therefore focus on the pro-tumoural properties of TAM.

#### 1.5.4.1.3 Pro-tumoural mechanisms of TAM

The functional mechanisms underlying the tumour-promoting activities of TAM are summarised below and in Figure 1.7.

#### *1.5.4.1.3.1 Angiogenesis*

It is well established that the growth and spread of malignant tumours requires angiogenesis, and the majority of cancers and cancer models show increased tissue vascular density during transformation to the malignant state. Various cell types contribute to this “angiogenic switch” (121) of which macrophages are a major component (122). It appears that hypoxia plays a role in directing macrophages towards a pro-angiogenic phenotype, and so promoting tumour progression. Indeed, functional studies in mouse models of cancer provide evidence for a link between macrophages and the angiogenic switch. For instance, macrophage depletion is observed in CSF-1 constitutive genetic knockout mice, in which the Polyoma Middle T oncoprotein (PyMT) induced mammary tumours show a greatly attenuated angiogenic switch (251). Furthermore, there is evidence from this murine model of breast cancer that VEGF production by TAM is key to the angiogenic switch. Using transgenic VEGF-A op/op PyMT mice, VEGF over-expression at a benign stage in such macrophage-depleted mice produces increased angiogenesis and accelerates the transition to outright malignancy (252). Characterisation of angiogenic TAM show that they express TIE2. Genetic ablation of this population inhibits angiogenesis in a variety of models, including glioblastoma and the PyMT model (253). Interestingly, CSF-1 upregulates TIE2 on TAM (254), indicating a link between CSF-1, $TIE2^{+}$ macrophages and the induction of the angiogenic switch. There are now numerous additional reports of TAM affecting angiogenesis in a wide range of models, primarily xenograft models, highlighting this key protumoural role (255).

#### *1.5.4.1.3.2 Invasion and metastasis*

Tumour cell migration, particularly in epithelial tumours, relies on proteolytic destruction of the surrounding ECM to facilitate the escape of tumour cells

from the confines of the basement membrane. Common to all spreading tumours is the need for subsequent proteolysis of surrounding dense tissue stroma. Macrophages are potent producers of many proteases, including cathepsins, MMPs, and serine proteases (256). Increased production of MMPs is a feature of the M2 macrophage phenotype and is typical of TAM (257). Cathespin proteases remodel the ECM and release sequestered growth factors. Macrophage-specific depletion of cathepsins or urokinase plasminogen activator, results in reduced tumour cell invasion and inhibition of metastasis in mouse mammary tumour models (258, 259). Macrophages also produce other molecules that advance tumour cell invasion, including Osteonectin (known as SPARC) (260), which increases tumour cell-ECM interaction and thus migration, and TGFβ, that promotes EMT of the invading tumour cells (261).

#### *1.5.4.1.3.3 Immune-suppression*

Macrophages are central to many immune responses and under certain conditions, in particular during bacterial infection, they act as potent antigen presenting cells. However, within the tumour microenvironment, it appears that TAM assume an immune-regulatory role, suppressing anti-tumour immune responses. TAM can inhibit cytotoxic T-cell responses through several mechanisms. For example, they produce IL-10, which is commonly regarded as an anti-inflammatory, immunosuppressive cytokine that aids tumour escape from immune surveillance. TAM-derived IL-10 stimulates expression of the co-stimulatory molecule B7-H3 on tumour cells, and induces monocytes to express the co-stimulatory molecule PDL-1, both of which have been shown to suppress cytotoxic T-cell responses (262, 263). Furthermore, it was recently shown by Noman et al (264) that TAM in hypoxic tumour regions also up-regulate the expression of PDL-1 as a consequence of hypoxia inducible factor 1-α (HIF1α) signaling. This has also been demonstrated in HCC (262). Notably, the response rates in the PD-1/PD-L1 trials have been

shown to relate, at least partially, to PD-L1 expression in the stroma (265, 266), supporting a role for macrophages in blocking anti-tumour T cell responses. However, it is difficult to determine the exact impact of TAM PD-1 ligand expression on effector cell inhibition *in vivo*, since several cells within the TME express PD-L1.

In another study, a recruited macrophage population into mammary tumour xenografts suppressed immune responses through synthesis of prostaglandin-E2 and TGFβ (267). A similar response was also seen when macrophages were co-cultivated with mesothelioma cells: here, macrophages released a significant amount of prostaglandin-E2, stimulating the development of regulatory T cells, thereby promoting an immunosuppressive TME (268).

Several studies have found that chemokines secreted by macrophages also play an important role in immunosuppression. In human ovarian cancers, TAM produce CCL22, a chemokine that regulates the influx of regulatory T-cells (Tregs) that suppress cytotoxic T-cell responses. The abundance of these Tregs in ovarian cancer predicts poor survival (269). More recently, it was shown that in colorectal cancer CCL20 secreted by TAM also recruits Tregs (270).

In addition, TAM have been shown to secrete arginase into the microenvironment in different mouse cancer models (271), and the subsequent depletion of arginine in the TME can suppress T cell activity. Indeed, arginine is required for effective T cell function, and its depletion has been shown to inhibit the re-expression of the CD3ξ chain after internalization caused by antigen stimulation and T cell receptor (TCR) signaling, resulting in $CD8^+$ T cell unresponsiveness (272, 273). However, it is interesting to note that inhibition of arginase activity does not blunt *in vitro* suppressive functions of TAM (235).

The effect of TAM-derived arginase on reducing arginine within the TME also raises the question; can this method of arginine depletion cause cell death in

arginine auxotrophic tumour cells? This was recently evaluated in ASS1 negative melanoma (274), and results revealed that arginase depletion of arginine by TAM did result in the direct inhibition of B16-F1 melanoma cell proliferation *in vitro*. However, importantly, it was also noted that the ratio of macrophages (effector, E) to tumour (T) cells impacted tumour survival: low E:T ratios (<4:1) increased tumour growth, whereas only much higher E:T ratios (>10:1) elicited anti-tumour immunity. It was suggested that above a certain E:T ratio, macrophages release enough arginase to deplete arginine adequately from the TME to inhibit growth in arginine auxotrophic melanoma cells. However, at lower E:T ratios, more representative of the TME, the arginine depletion would be insufficient to have a negative effect on tumour growth, and instead the tumour promoting properties of TAM remain dominant.

Lastly, a subpopulation of macrophages found within hypoxic regions of tumours express low levels of major histocompatibility complex (MHC) II. The decrease in MHC II expression in this population supports an immunosuppressive phenotype (275).

#### *1.5.4.1.3.4 Tumour cell proliferation*

TAMs secrete an array of cytokines, chemokines and growth factors that can stimulate the differentiation and proliferation of other cells. Indeed, macrophage-elicited PDGF and TGFβ are known to stimulate the differentiation of fibroblasts and myofibroblasts. It seems plausible then, as postulated by Mantovani (276), that these and other growth factors might also promote the differentiation and proliferation of malignant cells. Furthermore, arginase generates urea and ornithine, the latter a precursor for various polyamines produced via ornithine decarboxylase (ODC), and proline via ornithine aminotransferase, thereby playing an important role in tumour cell proliferation and collagen production, respectively (112). Indeed, it has been demonstrated that TAM infiltration is positively correlated with the proliferation

of tumour cells in several tumours, such as breast cancer, endometrial cancer, and renal cell cancer (277, 278).

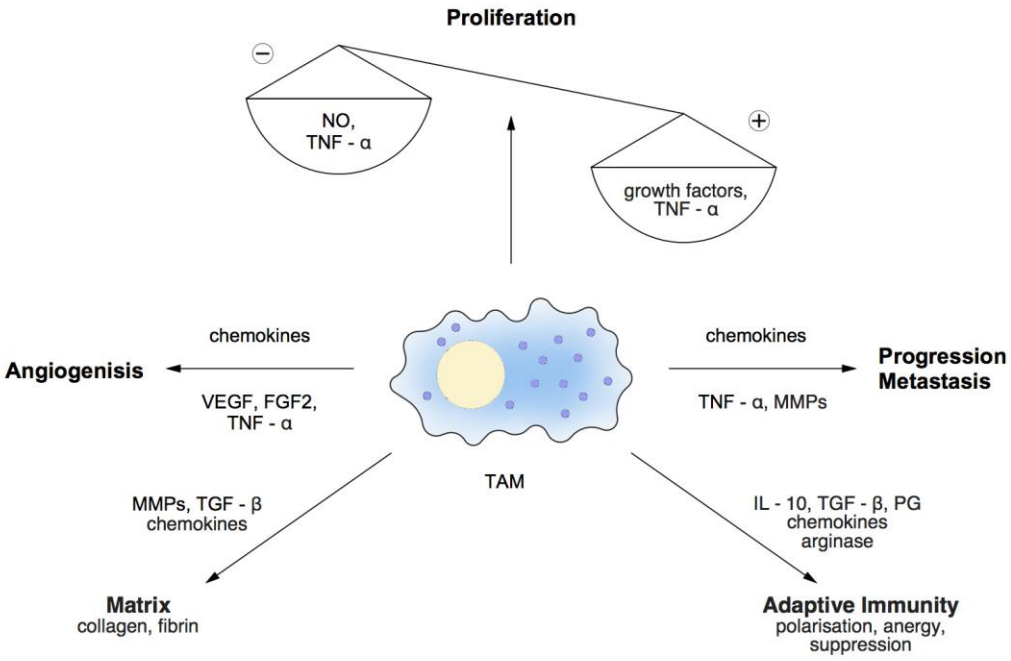


**Figure 1.7. The various pro-tumoural effector functions of TAM.** Abbreviations: FGF, fibroblast growth factor; IL, interleukin; MMP, matrix metalloproteinase; NO, nitric oxide; PG, prostaglandin; TAM, tumour-associated macrophage; TNF, tumor necrosis factor;
TGF, transforming growth factor; VEGF, vascular endothelial growth factor. Adapted from Mantovani *et al* (215)

#### *1.5.4.1.3.5 Summary*

TAMs are not a single uniform population; thus, their phenotype and role are not entirely consistent amongst cancers. Indeed, multiple specialised macrophage subpopulations within each tumour appear to have very different roles in supporting tumour progression. Therefore, detailed study of the specific features of TAM in individual tumour types is required in order to gain a better understanding of the role these phenotypically diverse cells play in different tumour microenvironments.

### 1.5.5 TAM and mesothelioma

Inflammation is an early and consistent feature of mesothelioma and macrophages are key regulators of the link between inflammation and cancer. Macrophages are involved in mesothelioma development from the initial introduction of asbestos fibres into the lung, when they are recruited and activated both by mesothelium-derived inflammatory factors and by the engulfment which they themselves undergo in an attempt to clear away the fibres. These events trigger a long-lasting inflammation, directly influencing mesothelioma tumourigenesis (279).

As with many other epithelial tumours, macrophages infiltrating the established mesothelioma tumour mass constitute the majority of infiltrating leukocytes, accounting for up to 30% of the solid mass (248). Indeed, Hegmans *et al* identified macrophages as the most representative immune cell type in human MPM biopsies (280), and Burt *et al* retrospectively reviewed 667 cases of MPM patients who underwent cytoreduction between 1989 and 2009, reporting that all the biopsies showed high levels of TAM infiltration, mainly characterised by the immunosuppressive phenotype expressing high levels of CD163, CD206 and IL-4 receptor α (248) . Similar findings were observed by Bielefeldt-Ohmann and colleagues (281), who demonstrated that TAM infiltrating mesothelioma in an orthotopic murine model exhibited low or absent expression of class-II MHC and integrins, indicating their polarisation towards an altered, immunosuppressive (M2) phenotype. Furthermore, it was recently demonstrated that C57 Black 6 (C57/B6) mice transplanted with malignant mesothelioma cells also had macrophages with an immunosuppressive phenotype that expressed arginase and F4/80, both in solid tumours and spheroids (282).

Notably, as for other solid tumours, high TAM counts are inversely correlated with the survival of patients with mesothelioma. The prognostic significance of both circulating blood monocytes and TAM was evaluated and it was found that higher numbers of circulating blood monocytes are associated with poor

survival in patients with both epithelial and non-epithelial mesothelioma and that a high TAM count was negatively correlated with the survival of patients with non-epithelioid mesothelioma, independent of tumour stage (248). A more recent study found that the macrophage CD163/CD68 ratio (representative of M2 phenotype) negatively correlated with overall survival in epithelioid mesothelioma (283).

The immunosuppressive nature of TAM in mesothelioma has been widely reported (280) (284). In addition, other pro-tumoural functions of TAM, including promotion of mesothelioma growth, invasion and metastasis, have also been described. For example, when investigating the effects of macrophage depletion on tumour progression, Veltman *et al*. reported that tumour weights in mice injected with lethal doses of AC29 tumour cells (a murine malignant mesothelioma cell line) were drastically decreased following macrophage depletion with liposomal clodronate (285). Miselis *et al* also demonstrated that macrophage depletion with liposomal clodronate significantly reduced the number of tumours, the area of tumour burden and the percentage of liver and lung metastasis in an orthotopic, immunocompetent murine model of diffuse peritoneal mesothelioma (282).

These studies identify TAM as abundant and important host-derived cells that contribute to development, growth, invasion and metastasis in mesothelioma.

#### *1.5.5.1 Myeloid-derived suppressor cells*

In addition to TAM, it is also important to mention a group of cells collectively called myeloid-derived suppressor cells (MDSC). These cells have been found to accumulate in some solid tumours, including MPM, during tumour progression and are recognised as being immunosuppressive. In mice, MDSC are defined as being CD11b+ and Gr1+, therefore incorporating a mixed population of both monocytic and granulocytic cells (286). The majority of these cells are granulocytic and will not be discussed here. The smaller group are Ly6C+ Ly6G –, and are monocytic in origin, therefore termed monocytic

MDSC (M-MDSC). These immunosuppressive cells display low expression of MHC class II and are also co-stimulatory molecule low or negative, indicating that they do not directly induce anti-T cell activity. Instead, they highly express TGF-β and arginase, promoting nonspecific immune suppression. In an orthotopic murine model of mesothelioma, it was found that MDSCs arise late in tumour development and their appearance is preceded by the accumulation of TAM and T cells. Furthermore, the expansion of the MDSC population was described as being concurrent with that of the tumour burden, leading to the hypothesis that MDSCs are required for tumour progression and outgrowth in MPM (287). It is currently unclear whether these cells accumulate in excessive numbers in tumours as a transient to mature macrophages (or TAM), or whether M-MDSC represent a monocyte-derived terminal sub-type. Regardless, these are important myeloid-derived cells that influence the immune response within the TME (286, 288).

### 1.5.6 TAM and therapeutic resistance in cancer

Despite increasing recognition of the involvement of macrophages in cancer invasion and progression, their role in mediating drug resistance has received comparatively little attention amongst researchers until recently. Earlier studies had suggested that the sensitivity of myelomas to melphalan and mitoxantrone may be influenced by macrophages (289, 290). More recently, a number of independent studies have revealed that macrophages can mediate chemotherapy resistance by modulating cellular immunity, providing survival factors, and/or activating anti-apoptotic pathways in tumour cells. For example, it was demonstrated that the response of mammary tumour-bearing mice to paclitaxel could be regulated by macrophages in CD8+ T-cell dependent mechanisms: here, the inhibition of TAM recruitment improved chemosensitivity, reduced tumour progression and reduced metastasis, associated with an increased survival of CD8+ T-cells (291). Furthermore, Shree *et al*. showed that cathepsin-expressing macrophages protect breast

cancer cells from cell death induced by the following chemotherapeutic drugs: taxol, etoposide and doxorubicin. They reported that the combination of anti-cathepsin with taxol treatment enhanced the anti-tumour efficacy, the late-stage survival and decreased metastatic burden compared to taxol alone in a breast cancer mouse model (292).

In addition, in pancreatic adenocarcinoma (PDA), macrophages were found to induce chemoresistance by reducing gemcitabine-induced apoptosis, via up-regulation of tumoural cytidine deaminase, the enzyme that metabolises gemcitabine (293).

It has also recently been reported that macrophage-derived TNF-α provides resistance to mitogen activated protein kinase (MAPK) pathway inhibitors in melanoma through NF-κβ- dependent expression of microphthalmia transcription factor (294). Inhibiting TNF-α signaling with IκB kinase inhibitors profoundly enhanced the efficacy of MAPK pathway suppression by targeting not only the melanoma cells but also the microenvironment. Another study reported that macrophages play a critical role in melanoma resistance to BRAF inhibitors, via the production of VEGF, which reactivates the MAPK pathway and stimulates cell growth (295).

On the other hand, there is also evidence that activation or re-activation of immune responses is a key component of the anti-neoplastic efficacy of drugs such as Doxorubicin (233). Specifically, in a model of breast cancer, Doxorubicin reduced the levels of MDSCs, improving the efficacy of adoptive transfer of T cells (296). Macrophages can also contribute in other ways to the modulation of tumour response to chemotherapy. For example, the antitumor activity of docetaxel involves the depletion of immunosuppressive (M2-like) TAM and the concomitant activation or expansion of antitumoral (M1-like) monocytes/MDSC in 4T1-Neu mammary tumour implants. Indeed, *in vitro* T cell assays showed that the docetaxel-treated M1-like monocytes/MDSC are able to enhance tumor-specific, cytotoxic T cell responses (297).

Therefore, it is clear that different mechanisms regulate TAM functions during chemotherapy and other forms of therapy, and this can either enhance or antagonize the activity of the anticancer drug, depending on the type of treatment and the tumour model (298). As TAM have been shown to nurture mesothelioma cells and promote tumour progression, could they also be responsible for mediating resistance to arginine depletion?

## 1.6 Hypothesis

Tumour-associated macrophages are an integral part of the interaction between cancer cells and their microenvironment.

My thesis is driven by the hypothesis that macrophages maintain the right metabolic environment in MPM to support tumour growth. Under conditions of arginine deprivation, this results in the provision of arginine (or its precursors) to the arginine auxotrophic tumour cells, thereby mediating resistance to ADI-PEG20.

## 1.7 Thesis aims

The aims of this thesis were to determine whether macrophages are critical modulators of the response of ASS1 negative MPM cells to the arginine-depleting agent ADI-PEG20, to establish how macrophages mediate tumoural resistance to ADI-PEG20 and, finally, to develop strategies to overcome macrophage-mediated MPM resistance to arginine depletion.

The specific aims of each chapter are detailed below.

Aims of Chapter 3:

- To validate the ADI-PEG20-induced pro-inflammatory gene expression signature identified in ASS1 negative mesothelioma cells
- To determine how ADI-PEG20 provokes a pro-inflammatory cytokine response in ASS1 negative mesothelioma cells
- To assess whether the *in vitro* pro-inflammatory cytokine response is relevant *in vivo*.

Aims of Chapter 4:

- To investigate whether macrophages are able to modulate the therapeutic response of ASS1 negative mesothelioma cells to ADI-PEG20
- To identify mechanisms behind the macrophage-mediated resistance

Aims of Chapter 5:

- To evaluate whether targeting macrophages in combination with ADI-PEG20 potentiates the cytotoxic effect of ADI-PEG20 *in vivo.*

# Chapter 2. Materials and Methods

## 2.1 Cell Culture

The tumour cell lines MSTO, H226 and H28 were obtained from American Type Culture Collection (ATCC; Manassas, USA), 2591 was obtained from Professor Pasi Janne (Harvard, USA), and Ju77 was obtained from Professor Ken O'Byrne (Dublin, Ireland). All cell lines were Short Tandem Repeat (STR) profiled to ensure quality and integrity. Buffy cones of lymphocyte-rich peripheral blood from healthy volunteers were obtained from the National Blood Service (Tooting, London). All cells were cultured at 37° in a humidified atmosphere of 5% $CO_2$.

### 2.1.1 Tumour cell lines (MSTO, Ju77, 2591, H28 and H226)

All tumour cell lines were maintained in endotoxin free-RPMI 1640 media supplemented with 10% heat-inactivated fetal bovine serum (FBS; Gibco® Life Technologies) in T175 flasks (Corning). Cells were split 1:6 when confluency of 80%-90% was reached. The cells were washed with phosphate buffered saline (PBS) and then incubated for up to five minutes at 37°C with 5mls of 1x trypsin-EDTA (Gibco®, Life Technologies). Once the majority of cells had detached from the flask the trypsin-EDTA was quenched by the addition of an equal volume of RPMI. Cells were collected and then pelleted by centrifugation for 5 min at 1500 rpm. Cells were then re-suspended in RPMI and seeded at a density of ~$1.5x10^6$ cells per T175 flask. Similar passage numbers were used for all experiments. Cell lines were tested monthly for mycoplasma infection.

## 2.1.2 Human monocyte-derived macrophages

### *2.1.2.1 Generation of macrophages from human peripheral blood mononuclear cells (PBMC)*

#### 2.1.2.1.1 Purification of leukocytes

Two 'Buffy cones' of lymphocyte-rich peripheral blood from healthy human donors were purchased from the National Blood Service and stored at 4ºC to maintain cell viability. Cones were always used within 24 hours of delivery. In a large 175cm$^3$ flask the combined 100ml volume of the two 'buffy cones' was added to 180mls of sterile PBS and mixed. 15mls of Ficoll-Paque$^{TM}$PLUS (a density gradient media used for the separation of PBMCs; GE Healthcare) was added to each of eight 50ml capacity polypropylene centrifuge tubes (Corning). 35ml volumes of 'buffy cone' mixture were carefully layered onto the Ficoll-Paque$^{TM}$PLUS at an oblique angle, using a pipette controller set to gravity powered expulsion only. The full tubes were then spun at 1200rcf for 60 minutes at 4ºC, set to decelerate slowly without a break.

Spun tubes were handled extremely carefully to avoid agitation and mixing of the separated layers. The lymphocyte–rich white layer was then aspirated from the middle, between the plasma above and the red cell-rich layer beneath, and mixed with sterile PBS in each of eight 50ml centrifuge tubes (see Figure 2.1). The tubes were spun at 1400rpm for 10 minutes and the supernatant aspirated and discarded. The pellet from each tube was re-suspended in Pharma Lyse$^{TM}$ (BD Biosciences) red cell lysis buffer and left for 5 minutes at room temperature, then spun at 1400rpm for 5 minutes. The supernatant was again aspirated and discarded.

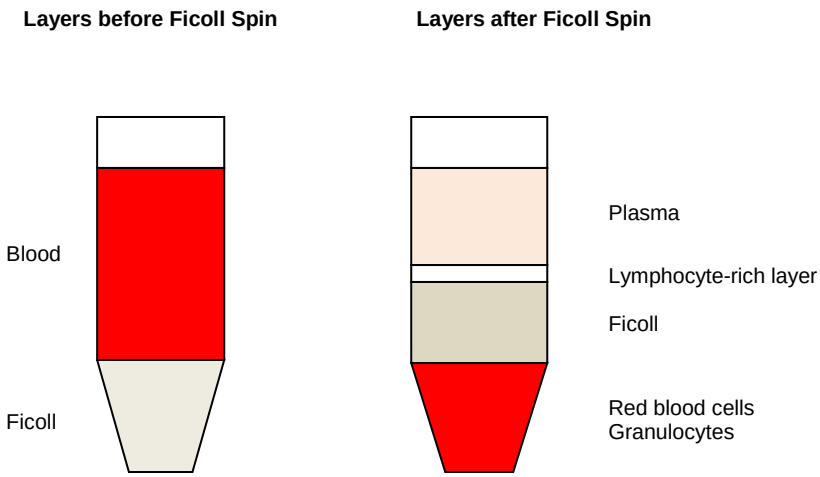


**Figure 2.1. Diagram demonstrating the different layers following Ficoll separation.** The lymphocyte-rich layer is shown in white.

#### 2.1.2.1.2 Magnetic bead and column positive selection of CD14+monocytes

MACS buffer was made up as follows:

| | |
|---|---|
| 500mls | PBS (without calcium and magnesium) |
| 2.5g | Bovine Serum Albumin |
| 2ml | 500mM EDTA |

This was mixed until fully dissolved, before sterile filtration.
The pellets were re-suspended and pooled in 50mls MACS buffer and a 550µl aliquot sampled to calculate cell number and viability by trypan blue exclusion assay using a Beckman Coulter Vi-CELL™ XR viability analyser. The remaining cells in MACS buffer were spun at 1400rpm for 5 minutes and re-suspended in MACS buffer at $1.25x10^8$cells/ml.

Human anti-CD14 MicroBeads (Miltenyi Biotec) were mixed with cells at a dose of 1ml per $5x10^8$ cells and placed at 4ºC to stain for 15 minutes.
This mixture was then made up to a total volume of 50mls with MACS buffer and spun at 1400rpm for 5 minutes, before re-suspending in 8mls of MACS buffer.

2 LS+ columns (Miltenyi Biotec) were placed into appropriate holders on a MidiMACS magnet and primed with 4mls each of MACS buffer. 4mls of CD14-labelled cell suspension was then passed through each column. 3 washes of 4mls each of MACS buffer were run through each column and the run-through was discarded. Each column was then individually removed from the magnet and vigorously flushed with 5mls MACS buffer, forcing through with a column plunger. This flush was collected, made up to 50mls with DMEM, and spun at 1400rpm for 5 minutes. The pellet was re-suspended in DMEM with 5% Human AB serum (Sigma-Aldrich) for differentiation into mature macrophages, and placed into 150mm x 25mm sterile cell culture dishes (Corning). A sample of cells was taken prior to transferring to the culture dishes for FACS analysis to assess the purity of CD14+ve cells (detailed in

section 2.9.2): >97% of cells were consistently CD14+ve by FACS analysis (see Figure 2.2). The culture dishes were incubated at 37ºc in 5% $CO_2$ for 8 days to allow differentiation.

After 8 days the differentiated macrophages were washed with warm PBS and gently detached using cold PBS and a cell scraper. The cell suspension was poured into a sterile flask and viable cells were counted from a 550µl aliquot using the Beckman Coulter Vi-CELL™ XR cell viability analyser. Mature macrophages were then ready for immediate use in co-culture experiments (see section 2.12)

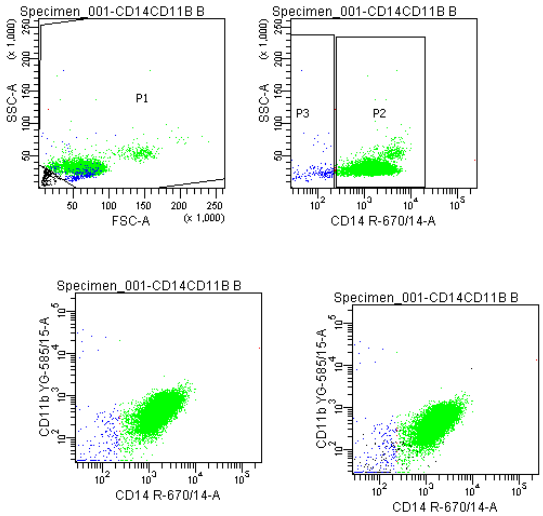


| Experiment Name: | | monocyte isolation x 2 nov | | | |
|---|---|---|---|---|---|
| Tube Name: | | CD14CD11B B | | | |
| Record Date: | | Nov 7, 2011 12:58:13 PM | | | |
| | | | | annexin ... | DAPI V-4... |
| Population | #Events | %Parent | %Grand ... | Mean | Mean |
| P1 | 10,000 | 98.1 | #### | 2 | 9 |
| Q1 | 0 | 0.0 | 0.0 | #### | #### |
| Q2 | 0 | 0.0 | 0.0 | #### | #### |
| Q3 | 10,000 | 100.0 | 98.1 | 2 | 9 |
| Q4 | 0 | 0.0 | 0.0 | #### | #### |
| Q1-1 | 0 | 0.0 | 0.0 | #### | #### |
| Q2-1 | 0 | 0.0 | 0.0 | #### | #### |
| Q3-1 | 10,000 | 100.0 | 98.1 | 2 | 9 |
| Q4-1 | 0 | 0.0 | 0.0 | #### | #### |
| P2 | 9,751 | 97.5 | 95.7 | 2 | 9 |
| P3 | 242 | 2.4 | 2.4 | 3 | 6 |

**Figure 2.2. Flow cytometry analysis assessing the % of CD14 positive cells following MACS selection.** Cells were prepared for flow cytometry as described in section 2.9.2. The raw data presented here is a representative example of cell purity obtained following monocyte isolation. The chart demonstrates that 97.5% (P2; green) of cells were CD14 positive.

#### *2.1.2.2 Matured macrophages*

Matured macrophages were maintained in endotoxin free-RPMI 1640 media supplemented with 10% heat-inactivated FBS, as for the tumour cell lines. Macrophages were used immediately in experiments once matured. They were not split as they were fully differentiated at the time of use.

### 2.1.3 Freezing and thawing cells

The following procedure was used to cryogenically store all tumour cell types used. Monocytes/macrophages were always used in experiments immediately after maturation and were therefore not cryogenically stored.

Live cell pellets were re-suspended in 45% RPMI, 45% FBS and 10% dimethyl sulphoxide (DMSO). The cell suspension was aliquoted into cryovials, which were insulated in polystyrene containers and placed at -80°C for 48 h before being transferred into liquid nitrogen for long term storage.

Frozen cells were recovered by placing a frozen cryovial immediately into a 37°C water bath until thawed. The thawed cell suspension was added to 10mls of pre- warmed RPMI and then spun at 1200rpm for five minutes. The supernatant was removed and the cell pellet was re-suspended in RPMI and placed into a T175 flask.

## 2.2 Transfection techniques

### 2.2.1 ASS1 overexpression

Human ASS1 cDNA was cloned into pIREShyg3 (Clontech Laboratories, UK) to produce ASS1 pIREShyg3. Ju77 cells were transfected with empty vector or ASS1 pIREShyg3 using Effectene (Qiagen) according to the manufacturer's instructions. Stable, pooled populations of transfectants were

obtained following selection with hygromycin (200µl/ml) for three to four weeks. Ju77 ASS1 overexpression was performed by Dr Barbara Delage.

### 2.2.2 ASL/XBP1 SiRNA transfection

SiRNA ASL (SMARTpool, Dharmacon) 20µM stock; SiRNA XBP1 SMARTpool, Dharmacon) 20µM stock; SiControl (Dharmacon) 100µM stock.

To establish ASL/XBP1 knockdown in the tumour cells, $2x10^4$ tumour cells were seeded in each well of a 6 well plate. After 24 hours (at approximately 30% confluent), either the SiRNA or SiControl was added at a concentration of 50nM to 1.5ml Eppendorfs containing 200µl of serum free RPMI media (one Eppendorf per well). 10µl of INTERFERin™ (Peqlab, Fareham, UK) was then added to each of the Eppendorfs and these were vortexed for 10 seconds. The Eppendorfs were then incubated at room temperature for 10 minutes. At the same time, media was removed from the cells and discarded. 2mls of RPMI 10% FBS was then added to each well followed by the addition of the 200µl of either SiRNA or SiControl into the appropriate wells and gently mixed. After 8 hours, the media was replaced with 2mls RPMI 10% FBS. Plates were incubated at 37ºc for either 24 hours (XBP1), or 48hrs and 96hrs (ASL). RNA was then extracted as described in section 2.5 to confirm knockdown.

## 2.3 Reagents

### 2.3.1 ADI-PEG20

ADI-PEG20 (Polaris Pharmaceuticals) is arginine deiminase (ADI), a *mycoplasma* – derived enzyme, formulated with polyethylene glycol (PEG) of 20,000 dalton molecular weight to increase the circulating half life and decrease antigenicity of ADI, that catabolises circulating arginine to yield citrulline and ammonia. This was used at a dose of 750ng/ml in all *in vitro*

experiments and at a dose of 5IU for all *in vivo* experiments unless otherwise specified.

### 2.3.2 Liposomal Clodronate and Liposomal PBS

Liposome preparations were obtained from Dr Nico van Rooijen, Department of Molecular Cell Biology, Vrije Universiteit, Amsterdam. Liposomes contained either clodronate at 7 mg/ml, or simply PBS as a vehicle control, which were manufactured by Dr van Rooijen as previously described (299). Animals were injected into the peritoneum with 200µl of Liposomal Clodronate (dichloromethylene bisphosphonate, CLIP), or vehicle control, unless otherwise specified.

### 2.3.3 Tunicamycin

Tunicamycin (Sigma-Aldrich) was used to induce endoplasmic reticulum stress at a dose of 5µg/ml.

### 2.3.4 SB225002

SB 225002 (Cayman Chemical) is a selective non-peptide inhibitor of CXCR2. This was dissolved in 100% ethanol to give a soluble concentration of 10mg/ml. The stock solution was then further diluted to give the desired concentration using sterile PBS to ensure any residual amount of ethanol was insignificant for use in experiments. Concentration used for *in vitro* experiments: 750nM. Concentration used for *in vivo* experiment: 1mg/kg SB225002 made up to 100µl in sterile PBS.

### 2.3.5 Recombinant human cytokines

Recombinant human IL-8, CXCL2, CXCL3, IL-1 alpha and VEGFA were purchased from R&D Systems. These were used in *in vitro* assays at optimal

concentrations of: 100ng/ml for IL-8, 1ng/ml for IL-1α, and 10ng/ml of CXCL2, CXCL3 and VEGFA.

### 2.3.6 Argininosuccinic Acid (ASA)

Argininosuccinic acid disodium salt hydrate was purchased from Sigma-Aldrich (UK). This was dissolved in distilled water to give a stock concentration of 50mg/ml (MW 334.24g/mol). This was used at concentrations of 0.25mmol/l - 2mmol/l.

## 2.4 Cell viability assays (MTS)

### 2.4.1 ADI-PEG20

Cells were seeded at 2.5 x $10^3$ cells per well on 96 well plates and cultured in 100µl RPMI 10% FBS for 24 hrs. The following day the media was changed and 100µl of ADI-PEG20 was added to achieve a final concentration range of between 0 and 20,000ng/ml. Cell viability was determined after 6 days, using the Cell Proliferation assay kit (Promega) that contains the tetrazolium salt 3-(4,5-dimethylthiazol-2-yl)-5-(3-carboxymethoxyphenyl)-2-(4-sulfophenyl)-2H-tetrazolium known as MTS, used in conjunction with the electron coupling reagent phenazine methosulfate (PMS). Mitochondrial enzymatic activity in viable cells reduces MTS to the water-soluble product formazan, and this reduction is facilitated by PMS. The number of living cells is directly proportional to the concentration of formazan in the sample, determined by the absorbance at 490nm. After 6 days media was removed and replaced with 20µl of MTS/PMS in a 20:1 ratio added to a final volume of 100µl RPMI per well. Plates were incubated for up to 4 hours and following this the plate was read at 490nm using an OpsysMR plate reader (DynexTechnologies Inc, Chantilly, US). Cell survival was normalised for background absorbance and expressed as a percentage of the untreated cells (control).

### 2.4.2 Liposomal Clodronate (CLIP)

Cells were seeded at 2.5 x $10^3$ cells per well on 96 well plates and cultured in 100µl RPMI 10% FBS for 24 hrs. The following day the media was changed and 125µl CLIP was added to achieve a final range of between 0 and 125µl. Cell viability was determined after 6 days, as described above.

### 2.4.3 ADI-PEG20 plus argininosuccinic acid (ASA)

Cells were seeded at 2.5 x $10^3$ cells per well on 96 well plates and cultured in 100µl RPMI 10% FBS for 24 hrs. The following day the media was changed and ADI-PEG20 was added at a concentration of 750ng/ml, plus ASA at concentrations of 0.25mmol/l, 0.5mmol/l, 1mmol/l and 2mmol/l, in 100µl RPMI 10% FBS. Cell viability was determined after 4 days as described above.

## 2.5 Real-time PCR analysis

### 2.5.1 RNA extraction

Cells were washed 3 times in PBS and 350µl Buffer RLT lysis buffer (Qiagen) was added to each well to disrupt the cells. RNA was then extracted according to tailored protocols from the RNeasy Mini Handbook (Qiagen).

Each of the 350µl cell lysate samples was transferred into a QIAshredder spin column placed in a 2 ml collection tube and spun for 2 minutes at full speed in an Eppendorf Microcentrifuge. The supernatant was transferred to a fresh 2ml collection tube. 350µl of 70% Ethanol was added and thoroughly mixed by pipetting. 700µl of each sample was transferred to an RNeasy spin column placed in a 2 ml collection tube and spun for 15 seconds at 10,000G. The flow through was discarded. On-column DNase digestion was then performed.

350µl of Buffer RW1 was added to each sample and spun for 15 seconds at 10,000G. The flow through was discarded and 80µl of DNase solution in Buffer RDD was added directly to the RNeasy spin column and left at room temperature for 15 minutes. 350µl of Buffer RW1 was then added to the RNeasy spin column and spun for 15 seconds at 10000G, with the flow through being discarded. 500µl Buffer RPE was added to the RNeasy spin column and spun for 15 seconds at 10,000G, and the flow through discarded. This step was repeated but spinning for 2 minutes to dry the RNeasy spin column membrane, and the flow trough discarded. The RNeasy spin column was placed in a new 2ml collection tube and spun for a further 1minute at full speed without the addition of buffers to ensure there was no ethanol carry over. The column was then carefully removed and placed in a fresh collection tube. Between 15µl and 30µl (depending on the expected yield of RNA) of RNase-free water was added directly to the column and spun for 1 minute at 10,000G to elute the RNA. The flow through was collected in a labelled 1.5ml collection tube and stored at -80°C until required.

### 2.5.2 RNA analysis

Purity and quantity was analysed using the ND1000 Spectophotometer, reading absorbance at 260/280nm (NanoDrop, Wilmington, US). All samples were expected to exhibit a 260/280 ratio of approximately 2, indicating that the RNA was pure and free of contaminants.

### 2.5.3 Reverse transcription of RNA to yield cDNA

Complimentary DNA (cDNA) synthesis was carried out using the Applied Biosystems High Capacity cDNA Reverse Transcription (RT) Kit on a thermal cycler as per the manufacturer's instructions.

The 2x RT mastermix was prepared as follows:

Per 20µl reaction:
2µl 10x RT Buffer
2µl 10x Random Primers
1µl MultiScribe™ Reverse Transcriptase (50Units/µl)
0.8µl 25x dNTP mix (100mM)
4.2µl Nuclease-free water

This was mixed gently and added to 10µl of RNA sample.
Each sample was briefly centrifuged to eliminate air bubbles before being before being placed in the thermal cycler. The reaction conditions in the thermal cycle were as follows: 25°C for 10 minutes, 37°C for 120 minutes, 85°C for 5 minutes. Samples were then cooled to 4°C.
Each 20µl tumour cell cDNA sample was then diluted with distilled water to give a final concentration of 20ng/µl cDNA. Each 20µl macrophage cDNA sample was diluted to give a final concentration of 5ng/µl (due to less RNA being yielded). Samples were stored at -20ºC until required.

### 2.5.4 Quantitative RT-PCR (qRT-PCR)

Analyses were performed using the ABI Prism 7500 Sequence Detection system Instrument and software (PE Applied Biosystems). qRT-PCR was performed using sample cDNA (FAM), an internal control 18sRNA (VIC) and specific TaqMan® probes.

qRT-PCR was carried out using the TaqMan® Universal PCR Master Mix (PE Applied Biosystems) in a 96 well plate. Each well contained the following reagents to make up a total volume of 25µl:

| | |
|---|---|
| 12.5µl | TaqMan® Universal PCR Master Mix |
| 8µl | DEPC $H_20$ |
| 2µl | Sample cDNA |
| 1.25µl | Probe/primer set for gene of interest |

1.25µl Probe/primer set for 18sRNA

The cycling program consisted of 10min at 95°C followed by 40 cycles of 95°C for 15 sec and 1 min at 60°C.
All samples were tested in duplicate.
Target mRNA was normalised (∆CT) to 18sRNA by subtracting the cycle threshold (CT) of the 18sRNA sample from the cycle threshold (CT) of each sample.

The expression level of each target gene in the treatment group samples was determined relative to the initial experimental controls:

$$\Delta\Delta CT = \Delta CT \text{ treatment} - \Delta CT \text{ control group}$$

This was expressed as a fold change in gene expression using the formula:

$$\text{Fold change} = 2^{-\Delta\Delta CT}$$

## 2.6 Western Blot

### 2.6.1 Protein Extraction

For extraction, NP40 lysis buffer (50mM Tris-HCL pH 8, 150mM NaCl, 1% NP40) was used with a proteinase inhibitor added at a concentration of 1 in 50 and a phosphatase inhibitor added at a concentration of 1 in 20 (Roche Diagnostics, UK).

To remove any traces of medium, cells were washed twice with cold PBS. The plates were then placed on ice, to prevent evaporation and reduce protein degradation, and protein was extracted by adding 50µl NP40 lysis buffer directly into wells (6-well plates). Cells were harvested using a cell scraper (BD Falcon, UK) and collected in a 1.5 ml Eppendorf tube. Samples were vortexed and incubated on ice for 15 minutes before centrifugation at

14000G for 10 minutes at 4ºC to pellet the cell debris. The supernatant containing the protein was removed and stored at -80°C until required for immunoblotting.

### 2.6.2 Protein concentration assay

For protein quantification a working reagent was prepared by combining 1 part Bio-Rad with 4 parts water. Protein standards were produced by performing serial dilutions of the provided albumin (BSA) stock (2µg/µl; Sigma-Aldrich) in dd$H_20$ to give standards at the following concentrations: 0.1, 0.25, 0.5, 0.8, 1, 1.4µg/µl protein. The standards could be kept at 4°C for two to three weeks, or at -20°C for long-term storage. Protein samples were diluted 1 in 10 and 10µl of diluted protein or standard (in triplicate) was plated in a 96 well plate with 200µl of working reagent and incubated at room temperature for 30 minutes. Samples were then read using a plate reader at 595nm.

### 2.6.3 Western Blotting

The range of protein concentrations amongst all the samples from the same experiment as determined by the plate reader was examined and then the same amount of protein for each sample (10-30µg) was made up to the same total volume with distilled water. The protein samples were then mixed with Sample Buffer (62.5mm tris-HCl, 2% SDS, 25% glycerol, 0.01% bromophenol blue, 1mM DTT) at a ratio of 1 in 4 (sample buffer to protein sample). Prior to loading, the protein samples were denatured by heating at 95ºC for 10 minutes. Samples were then spun down and allowed to cool. For each gel, 10µl of Color Pre-stained Protein Standard, Broad Range (11-245 kDa) (NEB) was also mixed with sample loading buffer at the same ratio as the samples and made up to the same total volume as the samples using distilled water.

Protein was separated in pre-cast 4-12% Bis-Tris NuPAGE gels (Invitrogen, UK) using 1 x MOPS buffer (50mM MOPS, 50mM Tris Base, 0.1% SDS, 1mM

EDTA). The gel was run at 150V for 45 minutes-1 hour, until the bromophenol blue marker ran off the bottom of the gel.
Next, proteins on the gel were transferred onto a nitrocellulose membrane at 20 V for 45 min using a semi-dry transfer apparatus (Bio-Rad) and transfer buffer. Prior to transfer the membrane was activated by being soaked in methanol for 1 minute, washed in distilled water, then equilibrated in transfer buffer (9.6mM glycine, 1.2mM Tris base, 10% methanol in distilled water). All Extra ThickBlot Paper (Bio-Rad) used for the transfer was previously soaked in transfer buffer and the negative electrode of the transfer apparatus was wet with transfer buffer.

Following transfer, the membrane was blocked in blocking solution (5% (w/v)) milk powder in PBS) for 1 hour at room temperature. The membrane was then incubated in primary antibody diluted in blocking buffer (normally 5% milk powder unless the manufacturer's instructions specified blocking in 5% BSA, 1x TBS, 0.1% Tween® 20 as for phosphorylated NFκB) overnight at 4ºC on a roller mixer. The primary antibodies used and the dilutions at which they were used are listed in Table 2.1. The membrane was then washed 3 times for 10 minutes in wash buffer (PBS/Tween® 20 0.05%) and incubated with the appropriate horse-radish peroxidase (HRP) conjugated secondary antibody diluted 1/1000 in blocking solution and incubated for 1 hour at room temperature on a roller mixer. The secondary antibodies used are listed in Table 2.2. The membrane was washed a further 3 times for 10 minutes in wash buffer before incubation in Amersham ECL (GE Healthcare, UK). For ECL, Reagents 1 and 2 were mixed 1:1 and used to completely cover the membrane for 3 minutes incubation at room temperature. Excess ECL was removed from the membrane and the resulting chemiluminescence signal was detected with Amersham Hyperfilm™ ECL (GE Healthcare).
Re-incubation with a β-actin antibody for 1 hour provided a loading control.

After development, ECL was washed off with 3 x 10 minute washes at room temperature. The membrane was then incubated with Restore™ Western Blot Stripping Buffer (ThermoScientific) for 10 min at room temperature with

rocking. The stripping buffer was removed with 3 x 10 minute washes at room temperature. The membrane was then dried out, wrapped in clingfilm and stored at -20°C.

| Protein | Raised in | Made by | Clone | Dilution | Reagent |
|---|---|---|---|---|---|
| ASS1 | Mouse | BD Biosciences | Monoclonal | 1:200 | ECL |
| ASL | Rabbit | Sigma-Aldrich | Polyclonal | 1:200 | ECL |
| XBP1 | Rabbit | Santa Cruz | Polyclonal | 1:50 | ECL |
| β-actin | Mouse | Dako | Monoclonal | 1:10000 | ECL |
| NFκB | Rabbit | Cell Signalling | Monoclonal | 1:200 | ECL |

**Table 2.1. Primary antibodies used for Western Blotting**

| Raised in | Anti- | Made by | Dilution |
|---|---|---|---|
| Rat | Mouse | Dako | 1:1000 |
| Goat | Rabbit | Dako | 1:1000 |

**Table 2.2. Secondary antibodies used for Western Blotting**

## 2.7 Enzyme-linked immunosorbent assay (ELISA)

### 2.7.1 Cell Supernatants

Quantikine ELISA kits (R&D Systems) were used to measure levels of VEGFA, IL-8 and IL-1α in the supernatant. For the cell line MSTO, measurement of these cytokines was repeated using Meso Scale Discovery® (MSD) ELISA kits (see section 2.7.2 for further detail on MSD ELISAs) to confirm the high concentration of these cytokines present in MSTO cell supernatant. Human GRO-beta and GRO-gamma ELISA Construction kits

(Antigenix America Inc.) were used to measure supernatant levels of CXCL2 and CXCL3, respectively.

#### *2.7.1.1 Quantikine ELISA (VEGFA, IL-8 and IL-1α)*

##### 2.7.1.1.1. Assay Principle

This is a Sandwich immunoassay. The 96-well plate is pre-coated with capture antibody. Samples or standards are added and any analyte present is bound by immobilised antibody. Unbound materials are washed away. Secondary HRP-labeled (detection) antibody is added and binds to the captured analyte. Tetramethylbenzidine (TMB) substrate solution is added to the well and a blue colour develops in proportion to the amount of analyte present. Colour development is stopped and absorbance of the colour at 450nm is then measured.

##### 2.7.1.1.2 Reagent preparation

All reagents were brought to room temperature before use.
The substrate solution was prepared by mixing Colour reagents A + B in equal volumes 15 minutes prior to use.

Standards were reconstituted with the appropriate Diluent to create an 8-point standard curve, described in Table 2.3 below.

| Cytokine Standard | Calibrator Diluent | Standard Range (pg/ml) | Minimum Detection Dose (pg/ml) |
|---|---|---|---|
| VEGFA | RD5K | 2000 – 0 | 5 |
| IL-8 | RD5P | 2000 – 0 | 3.5 |
| IL-1α | RD5-5 | 250 – 0 | <1 |

**Table 2.3. Standard range and Minimum Detection Dose (MDD) for each of the cytokines analysed**

#### 2.7.1.1.3 Assay procedure

50µl of the appropriate assay Diluent was added to each well, followed by 200µl of the standard or sample. The plate was sealed and incubated at room temperature for 2 hours. The plate was aspirated and thoroughly washed three times with PBS plus 0.05% Tween®20, and 200µl of conjugate was added to each well, the plate sealed and incubated for a further 2 hours. The plate was then aspirated and washed as before and 200µl of substrate solution was added to each well for 20 minutes, protected from the light. 50µl of stop solution was the added directly to each well of the plate and the plate was read within 30 minutes.

### *2.7.1.2 Antigenix America (CXCL2 and CXCL3)*

#### 2.7.1.2.1 Assay principle

The assay principle is as described in 2.7.1.1.1

#### 2.7.1.2.2 Reagent preparation

All reagents were brought to room temperature before use.
The substrate solution was prepared by mixing Colour reagents A + B in equal volumes 15 minutes prior to use.
Capture antibody was diluted to 1µg/ml in PBS
Detection antibody was diluted to 0.25µg/ml in PBS

Standards were reconstituted with 0.05% Tween®20, 0.1% BSA in PBS to create an 8-point standard curve, to give a concentration range of 625pg/ml-0.

#### 2.7.1.2.3 Assay procedure

A portion of the capture antibody was diluted with PBS to a concentration of 1µg/ml, and 100µl of this was added to each well of a 96 well plate. The plate

was sealed and left overnight at room temperature. The following day the wells were aspirated and plate washed 3 times with PBS plus 0.05% Tween®20. The plate was then blocked in 1% BSA for 1 hour followed by a washing step as previously described. 100µl standard or sample was added to each well in duplicate and the plate was sealed and incubated at room temperature for 2 hours. The plate was washed as previously described, followed by the addition of 100µl of 0.25µg/ml (Biotin tracer) detection antibody. The plate was sealed and incubated for 2 hours at room temperature. The plate was then washed as previously described. 100µl of Streptavidin-HRP conjugate (diluted 1:2000) was added to each well for 30 minutes. The plate was washed as previously described and 100µl of substrate solution was added. After 20 minutes the stop solution was added (2N Sulfuric acid) and the plate was immediately read at 450nm.

### 2.7.2 Human Plasma

ELISA-based assays for analysis of cytokine concentrations in human plasma samples were purchased from Meso Scale Discovery® (MSD), (Maryland, USA). Sample cytokines (VEGFA, IL-1α and IL-8) were measured using a Custom V-PLEX Assay, specifically designed to analyse the cytokines of interest. CXCL2 and CXCL3 concentrations were analysed using the ELISA construction Kits from Antigenix America (see section 2.7.1.2).

#### *2.7.2.1 MSD Assay principle*

The MSD plates are sandwich immunoassays. Each well of a 96-well plate contains independent and well-defined spots, each with a separate pre-coated specific capture antibody bound to a base-plate that can act as an electrode. The sample is added and binds to the capture antibody. A detection antibody is then added and will bind any sample antigen held by the capture antibody. The detection antibody is conjugated with electrochemiluminescent labels (MSD SULFO-TAG™). After incubation and washing steps, a read buffer is

added and the plate loaded to a MSD SECTOR™ Imager 6000 reader instrument. Here, a voltage is applied across the base plate electrode, causing any bound SULF-TAG molecules to emit light at an intensity proportional to the amount of bound sample. Multiple excitation cycles provide signal amplification, adding to the sensitivity of this technique.

The Custom V-PLEX Assay I used contained the human pro-inflammatory panel 1 (for IL-8) and the human cytokine panel 1 (for VEGFA and IL-1α). There were individual spots in the wells of a 96 well plate, each coated with these cytokines.

#### *2.7.2.2 Reagent preparation*

All reagents were brought to room temperature except the Calibrator stock, which was thawed on ice.

In order that an 8-point standard curve could be constructed, 4-fold serial dilutions of Calibrator were made from a first standard point solution prepared by combining 200µl of the human pro-inflammatory panel 1 V-PLEX calibrator blend with 200µl of the human cytokine panel 1 V-PLEX calibrator blend, brought to a final volume of 800µl with diluent 43. The final standard was Diluent 43 alone. This gave a range for the standard curves for each cytokine (detailed in table 2.4).

| Cytokine Standard | Standard range (pg/ml) |
|---|---|
| VEGFA | 1010-0 |
| IL-1α | 374-0 |
| IL-8 | 539-0 |

**Table 2.4. Standard curve range for each cytokine.**

60µl of each Detection antibody was added to Diluent 3 to make up a final volume of 3000µl.

Equal volumes of 4X Read Buffer and deionized water were mixed to give a 2x working solution.

***2.7.2.3 Assay protocol***.

25µl of Diluent 2 was dispensed to each well of the pre-coated plate.
25µl of sample plasma or Calibrator standard was then dispensed to individual wells in duplicate (resulting in a 2-fold dilution of sample plasma). The plate was sealed and agitated at 700rpm at room temperature for 2 hours. The plate was washed 3 times with PBS plus 0.05% Tween®20. 25µl of 1X Detection Antibody Solution was dispensed to each well, and the plate sealed and agitated as before at room temperature for 2 hours.
The plate was washed 3 times as before. 150µl of 2X Read Buffer was then dispensed using careful reverse pipetting into each well of the plate. This was to ensure no fluid bubbles were formed that might interfere with the subsequent plate reading process.
The plate was read using MSD SECTOR ™ Imager 6000. This imager uses a charge-coupled device (CCD) camera. This digital imaging technology allows high quality images to be constructed from emitted light by converting incoming photons into readable electric charges.

## 2.8 Immunostaining

### 2.8.1 Immunohistochemistry

Paraffin sections were dewaxed in xylene and immersed in 100% ethanol for 5 minutes. Following this, endogenous peroxidase was blocked using 100% methanol and 3% hydrogen peroxide for 10 minutes, followed by rehydration of sections in graded alcohols. Antigens were retrieved by microwaving in pre-heated 0.1M citrate (pH 6) buffer for 10 minutes (buffer: 2.94g Tri-sodium Citrate in 1000ml distilled water; pH adjustment using Acetic acid). Sections were incubated in horse serum (1:75) for 15 minutes and then drained. The appropriate primary antibody was then applied for 1hour at optimal dilution.

The primary antibodies and the dilutions at which they were used are listed in Table 2.5. After 1 hour sections were washed in two changes of PBS (5 minutes each). This was followed by incubation with biotinylated secondary (1:200) for 40 minutes, further washes in two changes of PBS (5 minutes each), and incubation with horseradish peroxidise-conjugated avidin (ABC Standard: Vector Laboratories). After two more washes in PBS (5 minutes each), formation was detected by the use of 3,3'diaminobenzidine (DAB) chromogen (DakoCytomation) for 2 minutes. Sections were then counterstained in Mayer Haematoxylin for 2 minutes. Once the antibodies were optimised manually, the slides were stained using the Ventana Classic Automated machine.

## 2.8.2 Immunofluorescence

### *2.8.2.1 Cell staining*

Cells were plated on cover slides in 500µl RPMI 10% FBS in a 24 well plate and incubated overnight. After incubation, media was aspirated and cells were washed twice with cold PBS. Cells were fixed in 4% paraformaldehyde for 15 minutes at room temperature, washed twice in PBS and permeabilised in 0.5% Triton PBS for 10 minutes. Cells were then washed in PBS and blocked with 300µl of 10% goat serum for 45 minutes at room temperature. Blocking solution was removed and cells were incubated with primary antibody for 1 hour at room temperature. Cells were washed 3 times with PBS and incubated for 1 hour with secondary antibody at room temperature in the dark. Wells were then washed 3 times with PBS in the dark, counter-stained with DAPI and mounted using Mowiol (5µl/slide) (Sigma-Aldrich).

### *2.8.2.2 Tissue staining*

Paraffin sections were dewaxed in xylene, and immersed in 100% ethanol for 5 minutes, followed by rehydration of sections in graded alcohols. Antigens were retrieved by microwaving for 10 minutes in Citra Solution (Vecton

Antigen Unmasking Solution 2.5mls in 250mls distilled water). Slides were then washed in PBS three times (5 minutes each) and cells were permeabilised with 0.1% Triton-X100 in PBS for 5 minutes at room temperature followed by washing with PBS. Using 50mM $NH_4Cl$ in PBS, cells were then quenched for 15 minutes at room temperature and washed in PBS. Sections were blocked using 20% goat serum and 2% BSA in PBS for 1 hour at room temperature and then drained. The primary antibody was then applied in block solution (5% goat serum, 2.5% BSA, 0.3% fish gelatine, glycine) for 1hr in the dark at room temperature at optimal dilution and then washed 3 times in PBS (5 minutes each). The primary antibodies used and the dilutions at which they were used are listed in Table 7. Following this, the secondary antibody was added in block solution and incubated in the dark at room temperature for 1 hour. The secondary antibodies used were anti-mouse AlexaFluor 488 and anti-rabbit AlexaFluor 568, 1:1000 (Invitrogen). Sections were washed twice in PBS (5 minutes each) and once in distilled water. They were then dehydrated in 100% isobutanol followed by xylene and mounted in Prolong Gold antifade reagent with DAPI (Invitrogen, UK).

| Protein | Raised in | Made by | Clone | Dilution |
|---|---|---|---|---|
| CD68 | Mouse | Dako | Monoclonal | 1:200 |
| F4/80 | Rat | Abcam | Monoclonal | 1:100 |
| ASS1 | Rabbit | Aviva Systems Biology | Polyclonal | 1:200 |

**Table 2.5. Primary antibodies used for Immunostaining**

### *2.8.2.3 Confocal Microscopy*

All confocal microscopy images were acquired using the Zeiss 510 confocal microscope

#### *2.8.2.4 Ariol Imaging*

The ARIOL imaging system (Genetix, San Jose, CA) was used to quantify antibody staining of the tissue microarrays (TMAs) and murine tumours. The specimens were scanned at a low resolution (1.25×) and high resolution (20×) using the Olympus BX 61 microscope with an automated platform (Prior). The slides were loaded in the automated slide loader (Applied Imaging SL 50). The images with high resolution were used for training and quantification purposes. The system was trained to select the stained and unstained cells by the colour of staining and shape of nuclei, such that brown staining was considered positive and blue staining was considered negative. The number of cells stained was calculated and represented as percentage of total cells stained positively, using the following formula:

Percentage area of total cells stained positively = colour 1 (brown)/ colour 2 (blue) x 100.

This method has been previously validated (300).

##### 2.8.2.4.1 Tissue Microarrays (TMAs)

Prior to randomisation, patients considered for the ADAM trial had their biopsies analysed by IHC for ASS1 status. The cut off for inclusion in the trial was >50% ASS1 negativity within an individual's tumour biopsy (ASS1 'low'). TMAs of ASS1 'low' and 'high' biopsies were then created for further analysis in our lab (by Ms Fiona Luong). Core biopsies from 108 patients were used to make the TMAs, with each individual having between 1 and 4 biopsy cores, creating a total of 5 TMAs. TMA maps were formulated in order to identify individual patients and their ASS1 status. Each TMA was then stained with the macrophage marker CD68. Prior to calculation of the percentage area of CD68 positive staining, all TMA cores were first reviewed manually and only included in the analysis if the core was intact with minimal fibrotic or acellular areas. This was to standardise tumour area and cellularity and enable valid

comparisons. The Ariol image analyser was then trained to select the stained and unstained cells as described above.

## 2.9 Flow Cytometry

### 2.9.1 FACS antibody staining of co-cultured tumour cells

Tumour cells were harvested using 1% trypsin-EDTA, centrifuged at 1500rpm for 5 minutes, the supernatant aspirated from each sample and the cells re-suspended in 1ml of PBS. The washed cells were then re-centrifuged, the supernatant discarded and the cells ($<1x10^6$) re-suspended in 100µl annexin binding buffer (Invitrogen, UK). 5µl of Alexa Fluor 488 Annexin V (FITC, Invitrogen, UK), 5µl of CD14 (APC, BD Pharmingen) and 5µl of CD11b (PE, BD Pharmingen) were added to each 100µl cell suspension and the samples were incubated at 4ºC for 30 minutes. After the incubation period, 400µl of annexin binding buffer was added to each sample, gently mixed and the samples were then kept on ice. Finally, DAPI (1:10,000; 1mg/ml stock) was added to each sample prior to cell analysis by flow cytometry.

### 2.9.2 FACS antibody staining of monocytes

To check purity of monocytes following CD14-positive selection, a sample of cells were centrifuged at 1500rpm for 5 minutes, the supernatant aspirated and the cells re-suspended in 1ml PBS. The washed cells ($< 1x10^6$) were then re-centrifuged, the supernatant discarded and the cells re-suspended in 100µl PBS. 5µl of CD14 (APC) was added to each 100µl cell suspension and the samples were then incubated at 4ºc. After 30 minutes, the cells were washed with a further 2mls of PBS and re-centrifuged at 1500rpm for 5 minutes. The supernatant was discarded and the cells were re-suspended in 350µl PBS.

Cells were then taken to be analysed by flow cytometry to ensure >95% purity.

### 2.9.3 FACS antibody staining of macrophages

Macrophages were harvested using cold PBS, centrifuged at 1500rpm for 5 minutes, the supernatant aspirated from each sample and the cells re-suspended in PBS. The washed cells (<1x$10^6$) were then re-centrifuged, the supernatant discarded and the cells re-suspended in 100µl PBS. 5µl of CD11b (APC; BD Pharmingen), 5µl CD80 (PE), 5µl of CD163 (PECy7), 5 µl of CD206 (FITC), and 5µl of HLA-DR (Alexa Fluor 700) (all Biolegend) were added to each 100µl cell suspension (with each fluorochrome having a control sample plus a no stain control for the purposes of compensation) and the samples were then incubated at 4ºC. After 30 minutes, the cells were washed with a further 2mls of PBS and re-centrifuged at 1500rpm for 5 minutes. The supernatant was discarded and the cells were re-suspended in 350µl PBS. Cells were then taken for analysis by flow cytometry. Immediately prior to analysis, DAPI was added to each sample.

### 2.9.4 FACS antibody staining of co-cultured cells for live sorting

Co-cultured tumour cells that were used for proteomics analysis went through live sorting to separate them from macrophages. Cells were harvested using cold PBS and centrifuged at 1500rpm for 5 minutes. The supernatant was aspirated and the cells re-suspended in 1ml PBS. The washed cells (< 1x$10^6$) were then re-centrifuged, the supernatant discarded and the cells re-suspended in 100µl PBS. 5µl of CD14 (APC) and 5µl of CD11b (PE) were added to each 100µl cell suspension and the samples were then incubated at 4ºC. After 30 minutes, the cells were washed with a further 2mls of PBS and

re-centrifuged at 1500rpm for 5 minutes. The supernatant was discarded and the cells were re-suspended in 350µl PBS. Immediately prior to sorting, DAPI was added to each sample.

### 2.9.5 FACS analysis

Samples were read using the BD LSR Fortessa™ Cell Analyser platform. Accurate analysis of fluorochrome detection was achieved with unstained and isotype controls, and compensation was performed with positively staining cellular samples.
Data was analysed using FlowJo 7.6.5 version software

## 2.10 Preparation of supernatant for Mass Spectrometry analysis

Supernatant from tumour cells and macrophages in co-culture and cultured individually, together with control samples of dialysed FBS and complete RPMI (no FBS), were collected and centrifuged at 1500rpm for 5 minutes. 100µl of supernatant from each sample was added to 300µl of cold methanol and immediately vortexed for 5 minutes then put on ice. After 30 minutes the samples were centrifuged at 10000rpm for 15 minutes at 4ºc and the supernatant was transferred in to another 1.5ml Eppendorf. The samples were then placed in a speed vac for 1 hour, collected and stored for analysis by mass spectrometry.

## 2.11 Preparation of cells for proteomics analysis

Preparation of cell lysates was carried out by Dr Pedro-Maria Casado (observed by Melissa Phillips). Proteomics analysis was performed by Dr Pedro Cutillas.

Proteins were lysed in Urea lysis buffer (8M urea and 20mM HEPES) for 15 minutes on ice to ensure they were homogenised. Samples were then sonicated (3 pulses of 15 seconds) to ensure protein breakdown. Samples were centrifuged at 20000G for 10 minutes at 5°C to pellet cell debris and the supernatant was transferred to new 1.5ml tubes. Protein concentration was measured using a BCA protein assay kit. Each protein sample was added to buffer to give the same amount of protein across conditions (made up to 200µl). Protein was then denatured by adding 10µl of Dithiothretiol (DTT) to each sample and incubating for 1 hour in the dark (with agitation). This was followed by the addition of 20µl of 415mM Iodoacetamide (IAM) to each sample for alkylation of cysteines, again with incubation for 1 hour in the dark with agitation. Samples were then diluted with 20mM HEPES (1 in 4) to remove the urea. Protein digestion was achieved with the use of immobilised trypsin beads. Samples with trypsin beads added were incubated at 37°C for 16 hours with shaking. After this incubation, the tryptic protein digests were de-salted (using trifluoroacetic acid (TFA) and acetonitrile (ACN)). Samples were stored at -80°C until required for analysis.

## 2.12 In vitro co-culture experiments

### 2.12.1 Co-culture experiments to assess tumour viability

1x $10^5$ MSTO cells were seeded wells of three 6 well plates, in 2mls RPMI 10% FBS for plate1, and in 1ml RPMI 10% FBS for plates 2 and 3. At the same time macrophages were plated in different conditions: alone in 2mls RPMI with 10% FBS (plate 4; control), in co-culture with the MSTO cells

without direct cell contact (plate 2), in co-culture with the MSTO cells in direct cell contact (plate 3). In the wells without direct cell contact, a 0.4µm pore transwell cell culture insert (BD Falcon) was placed in each well to allow free flow of media but no cell contact. $2x10^5$ macrophages were then added on top of the insert in 1ml of RPMI 10% FBS for a ratio of 1:2 tumour cells to macrophages. In the wells with direct cell contact, $2x10^5$ macrophages in 1ml RPMI with 10% FBS were added to the MSTO cells directly (therefore all wells had a total of 2mls RPMI media). After 24 hours (tumour cells approx. 70% confluent) the media in each well was discarded and the cells were gently washed three times with PBS. Media was replaced with 2mls RPMI 10% FBS, with ADI-PEG20 added at a concentration of 750ng/ml for the treatment wells. The plates were then incubated for 4 days. Following this, the cells were collected as described for FACS staining in section 2.9.1. The cell viability was then analysed by flow cytometry.

### 2.12.2 Co-culture experiments for qRT-PCR and Western blot analysis

Co-culture experiments were set up as described above but without a 'direct cell contact' condition. Thus, co-cultured tumour cells and macrophages were always separated by a 0.4µm transwell insert. For qRT-PCR and western blot analysis, cells were incubated for 48 hours +/- ADI-PEG20 750ng/ml. The media was then discarded and cells washed three times with PBS. Cells were lysed with Buffer RLT lysis buffer (for qRT-PCR) or NP40 (for western blot) (please refer to sections 2.5.1 and 2.6.1, respectively, for more detail) and stored at -80°C until required.

### 2.12.3 Co-culture experiments for mass spectrometry

Co-culture experiments were set up as described in section 2.12.1 but 10% dialysed FBS (Gibco®, Life Technologies) was used with the RPMI to ensure no false positives on mass spectrometry analysis. Supernatant from each condition was collected at 48 hours and prepared as detailed in section 2.10.

### 2.12.4 Co-culture experiments for Proteomics

$1x10^6$ MSTO cells were seeded on each of sixteen $10cm^3$ plates (Corning) in 10mls RPMI 10% dialysed FBS for plates 1-8 and 5mls RPMI 10% dialysed FBS for plates 9-16. $2x10^6$ macrophages were added to plates 9-16 in 5mls 10% dialysed FBS. After 24 hours media was removed and cells were washed three times with PBS. Media was replaced to achieve the following six different conditions:

1. MSTO cells alone in 10mls SILAC media (Thermo Scientific) with added arginine and lysine (Thermo Scientific) at concentrations representative of RPMI (0.2g/l arginine, 0.04g/l lysine), 10% dialysed FBS (two plates)
2. Co-cultured tumour cells and macrophages in SILAC media with added arginine and lysine at concentrations representative of RPMI 10% dialysed FBS (two plates)
3. MSTO cells alone in 10mls SILAC media (with added $^{13}C$ arginine (Thermo Scientific) and lysine at concentrations representative of RPMI) 10% dialysed FBS plus ADI-PEG20 750ng/ml (three plates)
4. Co-cultured tumour cells and macrophages in SILAC media (with added $^{13}C$ arginine and lysine at concentrations representative of RPMI) 10% dialysed FBS plus ADI-PEG20 750ng/ml (three plates)
5. MSTO cells alone in 10mls SILAC media (with added $^{13}C$ arginine and lysine at concentrations representative of RPMI) 10% dialysed FBS (three plates)
6. Co-cultured tumour cells and macrophages in SILAC media (with $^{13}C$ arginine and lysine at concentrations representative of RPMI) 10% dialysed FBS (three plates).

Cells were incubated for 48 hours. After 48 hours, media was removed and cells were gently washed three times with PBS. Cells were detached with cold

PBS and a gentle cell scraper. Cells were prepared for live flow cytometric sorting as detailed in section 2.9.4. Using his method, tumour cells were separated from the macrophages with 99% purity. Tumour cells were then washed with PBS and centrifuged at 1500rpm. The cell pellets were lysed in 8M urea lysis buffer. They were stored at -80°C in preparation for proteomic analysis.

## 2.13 Cytokine Stimulation of macrophages

### 2.13.1 Determining the optimal concentration of individual cytokines

$2x10^5$ macrophages were seeded into wells of eight 6 well plates, in 2mls RPMI 10% FBS. After 24 hours, media was removed and cells gently washed three times with PBS. Media was replaced with 2mls RPMI 10% FBS plus either IL-8 at 0ng/ml, 1ng/ml, 10ng/ml and 100ng/ml; IL1α at 0ng/ml, 0.1ng/ml, 1ng/ml and 10ng/ml; CXCL2 at 0ng/ml, 1ng/ml, 10ng/ml and100ng/ml; CXCL3 at 0ng/ml, 1ng/l, 10ng/ml and 100ng/ml, or VEGFA at 0ng/ml, 1ng/ml, 10ng/ml and100ng/ml, with a combination of all five as a final condition. Each condition was in duplicate. After 48 hours, media was removed and cells were washed three times in PBS. Cells were lysed in 350µl RLT lysis buffer and stored at -80°C until required.

### 2.13.2 Cytokine stimulation of macrophages

Once the optimum concentration was identified by qRT-PCR analysis of macrophage ASS1 expression relative to no cytokine control, the experiment was repeated again using the identified optimum concentration in triplicate plus a no cytokine control for each cytokine. After 48 hours, the cells were washed three times with PBS and lysed with 350µl RLT lysis buffer. Cells were stored at -80°C until required.

### 2.13.3 Cytokine stimulation of tumour cells

This was performed as detailed in section 2.13.2 using $2x10^5$ MSTO cells.

## 2.14 *In vitro* assays to validate the Affymetrix data

### 2.14.1 ADI-PEG20

For each tumour cell line (2591, MSTO, Ju77 wild-type, Ju77 ASS1, H28, H226) $2x10^5$ tumour cells were seeded in wells of four 6 well plates in 2mls RPMI 10% FBS. After 24 hours (approx. 70% confluent), media was removed and cells were washed three times with PBS. Media was replaced with 2mls RPMI +/- ADI-PEG20 750ng/ml. At specific time points (0 hours, 8 hours, 24 hours and 48 hours), media was collected into labelled 1.5ml collection tubes for later ELISA analysis, and cells were washed three times with PBS. Cells were lysed with 350µl Buffer RLT for later qRT-PCR analysis. Cells lysates and supernatant were stored at -80°C until required.

### 2.14.2 Arginine-deficient media

The tumour cells were seeded as detailed in section 2.14.1. After 24 hours, media was replaced with either 2mls RPMI 10% FBS or 2mls SILAC media (deficient in arginine; ThermoScientific) plus added citrulline (1mM concentration) and lysine 0.04g/l, 10% dialysed FBS. Cells and supernatant were collected as detailed in section 2.14.1 and stored at -80°C until required.

## 2.15 Animal Studies

### 2.15.1 Mouse xenograft model

5 week old female CD-1 homozygous Nu/Nu mice were purchased from Charles River Laboratories for xenograft studies. All mice were housed with a maximum of 6 mice per cage in a temperature-controlled pathogen-free animal facility. Water and food were freely available. All experiments were commenced at age 6 weeks and were conducted under the scope of my personal licence, awarded after completion of accredited training, and under

the Project Licence of Professor Nicholas Lemoine, in accordance with the Home Office Animals (Scientific Procedures) Act in 1986. All animals weighed between 22-24lbs at the start of experiments and were weighed weekly. Animals were culled if they lost greater than 10% of their body weight.

## 2.15.2 Mesotheliomal cell preparation and transplantation

MSTO cells were cultured as previously described in section 2.1.1, in 175cm$^3$ flasks. Prior to use for animal experiments, cells were detached with 1x trypsin-EDTA, washed twice in PBS and re-suspended in filtered PBS at a concentration of 30x10$^6$ cells/ml. Subcutaneous xenografts were seeded into the right flank of each mouse with 100µl volume containing 3x10$^6$ MSTO cells. MSTO cells were seeded for each experiment by Dr Ming Yuan. Once the tumours were palpable (approximately 5-6mm in diameter), treatment was initiated.

## 2.15.3 Injections

Intraperitoneal injections were administered into the mouse peritoneum using a 1ml capacity syringe and a 25-gauge needle (BD microlance).

## 2.15.4 Treatment schedules

### *2.15.4.1 ADI-PEG20 plus CLIP*

Mice were placed into 5 different groups with 12 mice per group. Groups were as follows:

- PBS (100µl)
- CLIP (200µl)

- PLIP (200µl)
- ADI-PEG20 (100µl at a dose of 5IU/100µl)
- ADI-PEG20+CLIP

200µl of CLIP (or PLIP as vehicle control) was injected twice a week for the first 3 doses to initiate macrophage depletion (Friday, Monday, Wednesday), and then continued on a weekly basis (every Wednesday) for the duration of the experiment for maintenance.

100µl of ADI PEG20 (or PBS as vehicle control) was injected on a weekly basis (every Thursday) after the first 3 doses of CLIP (or PLIP) had been administered.

#### *2.15.4.2 ADI-PEG20 plus SB225002 (Pilot)*

Mice were placed into 4 different groups with 5 mice per group.Groups were as follows:

- PBS (100µl)
- ADI-PEG20 (100µl at a dose of 5IU/100µl)
- SB225002 (100µl at a dose of 1mg/kg)
- ADI-PEG20 + SB225002

SB225002 was given daily and ADI-PEG20 was given weekly (every Wednesday). ADI-PEG20 was initiated 48 hours after SB225002 to ensure CXCR2 blockade.

### 2.15.5 Mesothelioma tumour progression assessment

This was performed with the observer blinded to the therapy received by each group. Assessment of tumour volume initially involved measurement of the long axis and perpendicular axis of the tumours using 0-200mm electronic digital callipers with 0.01mm resolution. Tumour volumes were then calculated according to the following formula (301):

$$\text{Tumour Volume} = 0.5 \ (\text{length} \times \text{width}^2)$$

Tumours were measured twice weekly.

### 2.15.6 Sacrifice and tumour removal

Mice were sacrificed by cervical dislocation. Subcutaneous tumours were immediately removed and placed in appropriate storage depending on subsequent intended use.

| | |
|---|---|
| FFPE sections | 10% Formalin |
| RNA extraction | 2ml micro-centrifuge tube on dry ice |

## 2.16 Statistical analysis

All statistical analysis was undertaken in GraphPad Prism 5.
Standard error of the mean (SEM) was used to determine the confidence limits for all experiments which had been performed in replicate. SEM is a method used to estimate the standard deviation (SD) of a sampling distribution.

To determine whether the difference between two experimental conditions was significant, *p* values were calculated using a two-sided unpaired Student's t test. To determine the difference between three or more

experimental conditions, *p* values were calculated using a 1 way ANOVA with Newman-Keuls multiple comparison post test analysis. A p-value of <0.05 was considered to be statistically significant. To determine the difference in plasma cytokine levels in one group of patients before and after the administration of ADI-PEG20, p values were calculated using a paired t test. A p-value of <0.05 was considered to be statistically significant.

# Chapter 3. ADI-PEG20 induces pro-inflammatory cytokine production by ASS1-negative malignant mesothelioma cells

## 3.1 Introduction

Despite promising results observed *in vitro* and *in vivo* as a targeted therapy for arginine auxotrophic tumours, drug resistance remains a significant challenge for effective use of arginine depletors in the clinical setting. Understanding and identifying novel tumoural mechanisms involved in the efficacy and resistance of arginine depletors will be critical in exploiting arginine deprivation with rationally selected drugs for cancer therapy. Ultimately, identifying tumoural resistance mechanisms may improve the treatment efficacy of many different ASS1 deficient cancers.

Therefore, to investigate mechanisms of tumoural resistance to ADI-PEG20, the gene expression profile of three ASS1 negative mesothelioma cell lines (plus one bladder cell line) was analysed using the Affymetrix Human Genome U133 plus 2.0 microarray platform, in order to gain a better understanding of the response of these cells to ADI-PEG20 treatment. The Affymetrix data, generated by our laboratory, was analysed by the Bioinformatics team at the Barts Cancer Institute. This analysis produced a number of key findings that required further investigation and validation, including a significant pro-inflammatory cytokine gene expression profile induced by ADI-PEG20 treatment in ASS1 negative mesothelioma cells.

## 3.2 Aims

The aims of this chapter were:

1. To confirm that ADI-PEG20 causes cell death in ASS1 negative mesothelioma cell lines

2. To validate the pro-inflammatory gene expression signature induced by ADI-PEG20 treatment and to ascertain whether these changes in gene expression are specific to ASS1 negative mesothelioma cells

3. To evaluate whether a similar pro-inflammatory response is seen in ASS1 negative mesothelioma cells following culture in arginine-deficient media

4. To determine how ADI-PEG20 provokes a pro-inflammatory cytokine response in ASS1 negative mesothelioma cells.

5. To assess whether the *in vitro* pro-inflammatory cytokine response is relevant *in vivo*, using patient plasma samples from the ADAM clinical trial

## 3.3 ADI-PEG20 causes cell death in ASS1 negative mesothelioma cells

First, I confirmed the ASS1 status of a panel of mesothelioma cell lines by western blot. This panel included three representative wild-type ASS1 negative mesothelioma cell lines, 2591(epithelioid), MSTO (biphasic) and Ju77 (sarcomatoid), two representative wild-type ASS1 positive mesothelioma cell lines, H28 and H226, and one ASS1 over-expressing cell line, Ju77ASS1 (Figure 3.1A).

Having confirmed the ASS1 status of each mesothelioma cell line in my panel, I next assessed the effect of ADI-PEG20 treatment on cell viability. To do this, the three validated ASS1 negative cell lines, 2591, MSTO and Ju77, plus the three ASS1 positive controls, H28, H226 and Ju77ASS1, were treated with increasing concentrations of ADI-PEG20. As expected, after six days of treatment with ADI-PEG20, a significant reduction in ASS1 negative mesothelioma cell viability was observed using the MTS assay. In contrast, the viability of ASS1 positive controls was not affected (Figure 3.1B).

**A**

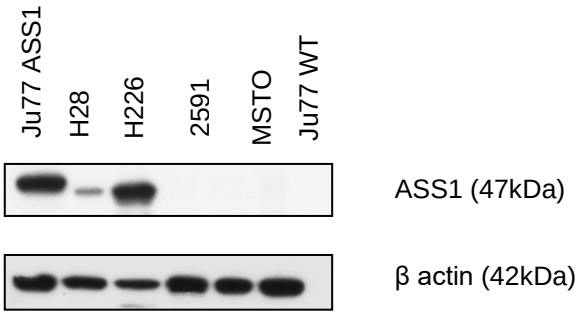


**B**

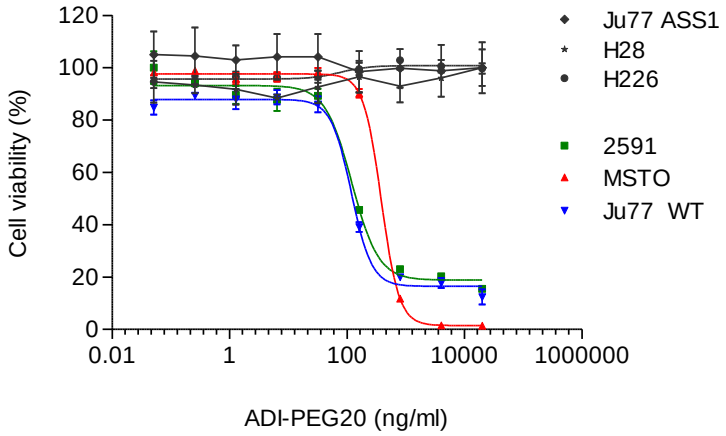


**Figure 3.1.**

**A) ASS1 expression in a panel of malignant mesothelioma cell lines.** Confirmation of loss of ASS1 expression in three wild-type ASS1 negative cell lines 2591, MSTO and Ju77, and of the presence of ASS1 protein in wild-type cell lines H226 and H28, and in the ASS1 overexpressing cell line, Ju77 ASS1, as shown by western blot.

**B) Response of ASS1 negative cells to ADI-PEG20 treatment.** MTS assay demonstrating the effect of ADI-PEG20 on cell viability in the three ASS1 negative cell lines and the three positive controls at six days post ADI-PEG20 exposure. Viability decreases to less than 20% in the ASS1 negative cell lines, whereas the ASS1 positive cell lines are unaffected. Experiments were repeated three times in triplicate with values representing the mean (+/- SEM).

## 3.4 Validation of the pro-inflammatory gene expression signature induced by ADI-PEG20 treatment

To elucidate mechanisms mediating tumoural resistance to arginine deprivation, I studied the gene expression profile of the three ASS1 negative wild-type mesothelioma cell lines treated with ADI-PEG20, generated using the Affymetrix Human Genome U133 plus 2.0 microarray platform. Ju77-ASS1 overexpressing cells were also assessed in this Affymetrix analysis as controls. Raw Affymetrix data had already been analysed in detail by the bioinformatics team and differentially expressed genes were determined by applying a double threshold of false discovery rate (0.05) and fold change (at least 2). Following exposure to ADI-PEG20, over 7,000 genes are modulated in the three wild-type ASS1 negative mesothelioma cell lines by 24 hours. However, only 30 genes were found to be modulated greater than log 2-fold (as specified by the bioinformatics team) across all three ASS1 negative cell lines. Notably, among the most highly modulated genes identified in this group were up-regulation of the pro-inflammatory cytokines IL-8 (CXCL8), CXCL2, CXCL3, VEGFA and IL-1α, whereas JU77-ASS1 overexpressing cells were unaffected by 24hrs of ADI-PEG20 treatment (Table 3.1).

| GENE | 2591 | MSTO | Ju77 (wild-type) | Ju77 ASS1 +ve |
|---|---|---|---|---|
| **VEGFA** | 4.03 | 4.17 | 3.33 | 0.37 |
| **IL-1α** | 4.29 | 4.44 | 2.22 | 0.26 |
| **CXCL2** | 7.77 | 2.58 | 7.45 | 0.51 |
| **CXCL3** | 3.38 | 5.00 | 4.47 | 0.52 |
| **IL-8** | 3.82 | 3.48 | 4.11 | 0.66 |

**Table 3.1. Table showing the significant up-regulation of pro-inflammatory cytokine gene expression in ASS1 negative mesothelioma cells following ADI-PEG20 treatment.** The table illustrates the fold increases in expression of the most highly up-regulated genes (VEGFA, IL-1 alpha, CXCL2, CXCL3 and IL-8) across all three wild-type ASS1 negative mesothelioma cell lines (2591, MSTO and Ju77) at 24hours post ADI-PEG20 (750ng/ml) treatment. This pro-inflammatory gene expression signature was not seen in the Ju77 ASS1 overexpressing (control) cells.

To validate this gene expression data, I analysed the induction of cytokine mRNA (Figure 3.2) following ADI-PEG20 exposure by qRT-PCR, in the three ASS1 negative and three ASS1 positive cell lines, and induction of cytokine protein (Figure 3.3) in the three ASS1 negative cell lines by ELISA. Results confirmed that the cytokine gene expression signature was specific to the ASS1 negative mesothelioma cell lines.

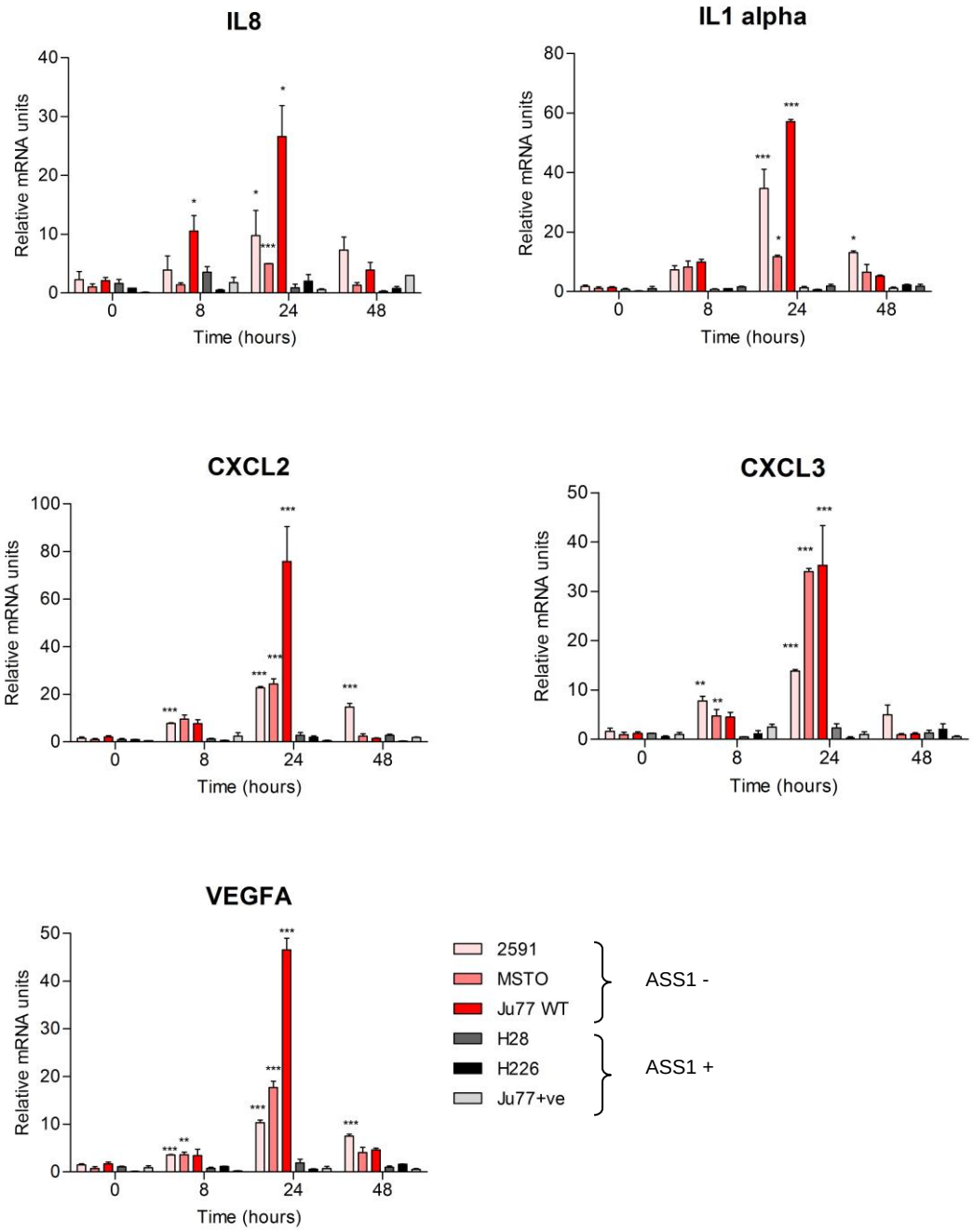


**Figure 3.2. Validation of the pro-inflammatory gene expression by qRT-PCR.** Three ASS1 negative and three ASS1 positive cell lines were analysed for induction of cytokine mRNA following ADI-PEG20 treatment at 0, 8, 24 and 48 hours. The no drug control for each cell line is normalised to one at every time point (not shown). All experiments were performed 3 times in triplicate for each cell line, with values representing the mean (+/- SEM). Statistical significance (1 way ANOVA with Newman Keul's multiple comparison post-test) * = $p<0.05$, ** = $p<0.01$, *** = $p<0.001$.

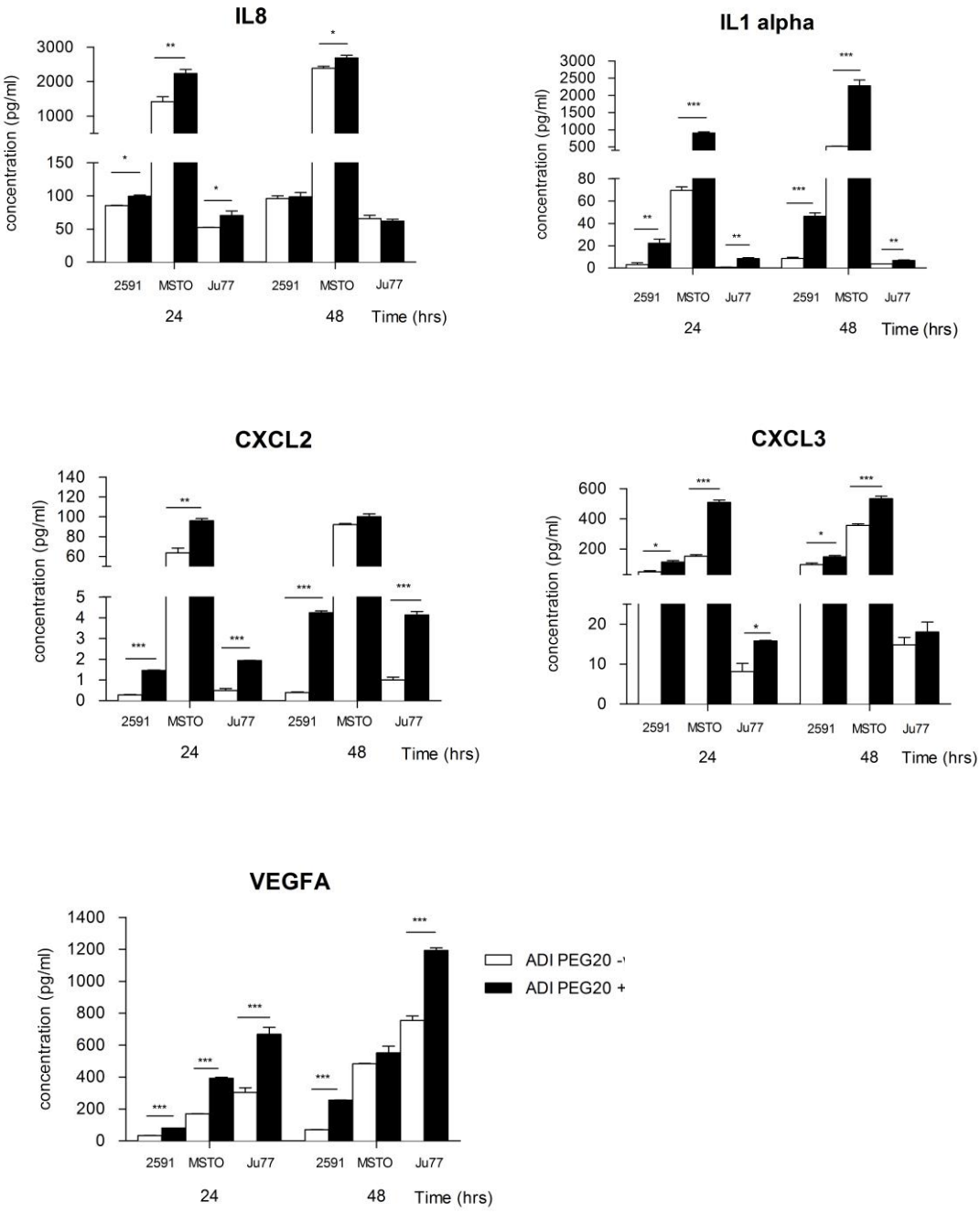


**Figure 3.3. Assessment of pro-inflammatory cytokines by ELISA (ASS1 negative MPM cells only).** Graphs represent the concentration of each pro-inflammatory cytokine at 24 and 48 hours following ADI-PEG20 treatment (750ng/ml) in the three ASS1 negative cell lines. ELISA-based assays to assess the concentrations of IL-8, IL-1α, CXCL2, CXCL3 and VEGFA were each performed twice in triplicate according to the manufacturer's protocol, with values representing the mean (+/- SEM). Statistical significance: (1-way ANOVA with Newman Keul's multiple comparison post-test) * =p<0.05, ** =p<0.01, *** =p<0.001.

## 3.5 Arginine-deficient media replicates the cytokine response in ASS1 negative mesothelioma cells

The qRT-PCR and ELISA experiments described above were repeated with the wild-type ASS1 negative cell lines, 2591, MSTO and Ju77, substituting ADI-PEG20 with arginine-deficient media. Results revealed that arginine-deficient media stimulates a similar cytokine response in ASS1 negative mesothelioma cells, highlighting that nutrient depletion is key to inducing the inflammatory reaction seen following ADI-PEG20 treatment (Figures 3.4 and 3.5).

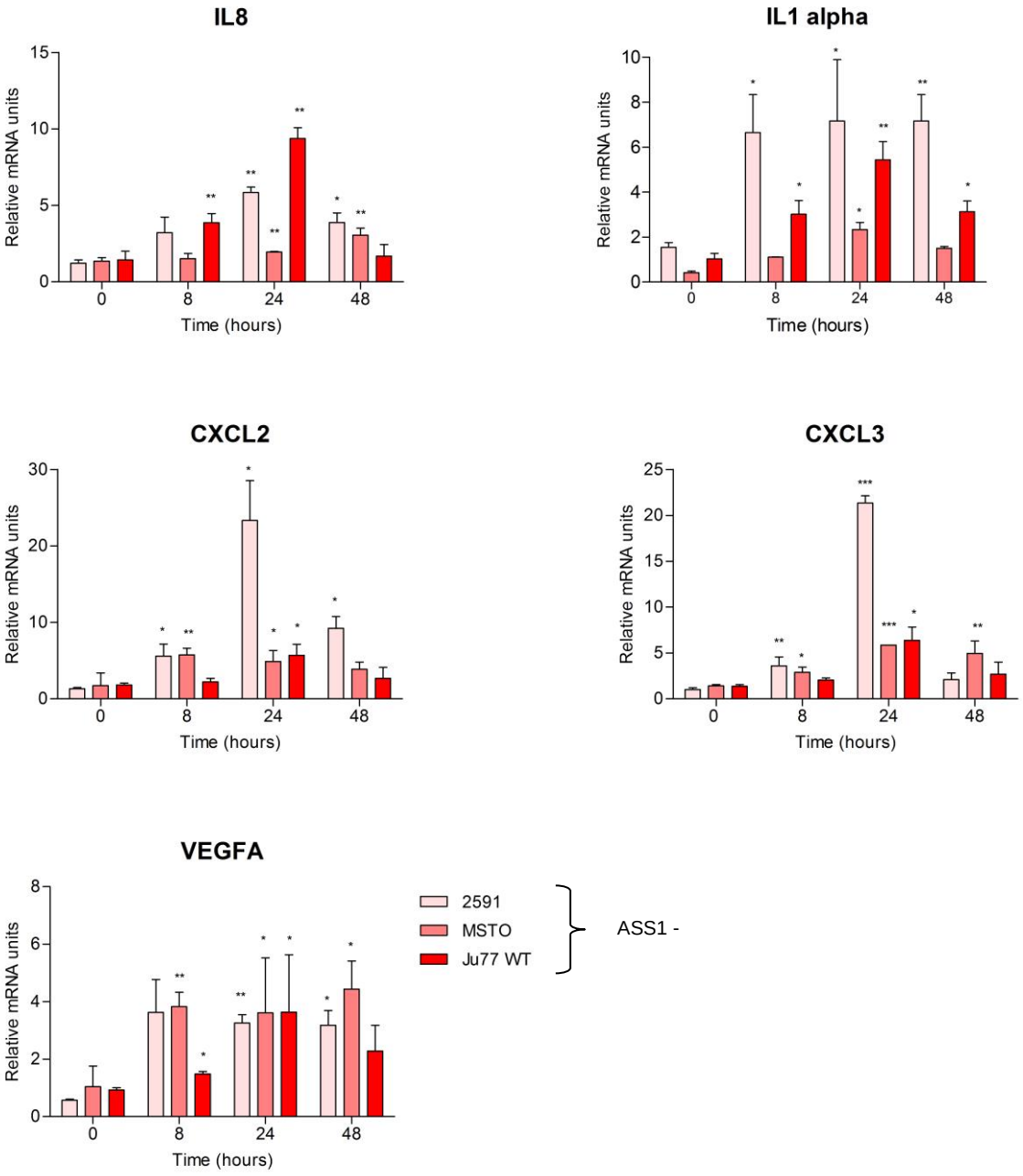


**Figure 3.4. Pro-inflammatory gene expression signature induced by arginine-deficient media in ASS1 negative MPM cells lines**. Three ASS1 negative cell lines 2591, MSTO and Ju77, were analysed for induction of cytokine mRNA following exposure to arginine deplete media at 0, 8, 24 and 48 hours. The graphs represent the relative increase in expression of individual genes in each cell line following substitution with arginine-deficient media, compared with control. The arginine control for each cell line is normalised to one at every time point (not shown). Experiments were performed twice in triplicate for each cell line, with values representing the mean (+/- SEM). Statistical significance (1 way ANOVA with Newman Keul's multiple comparison post-test) * = $p<0.05$, ** = $p<0.01$, *** = $p<0.001$

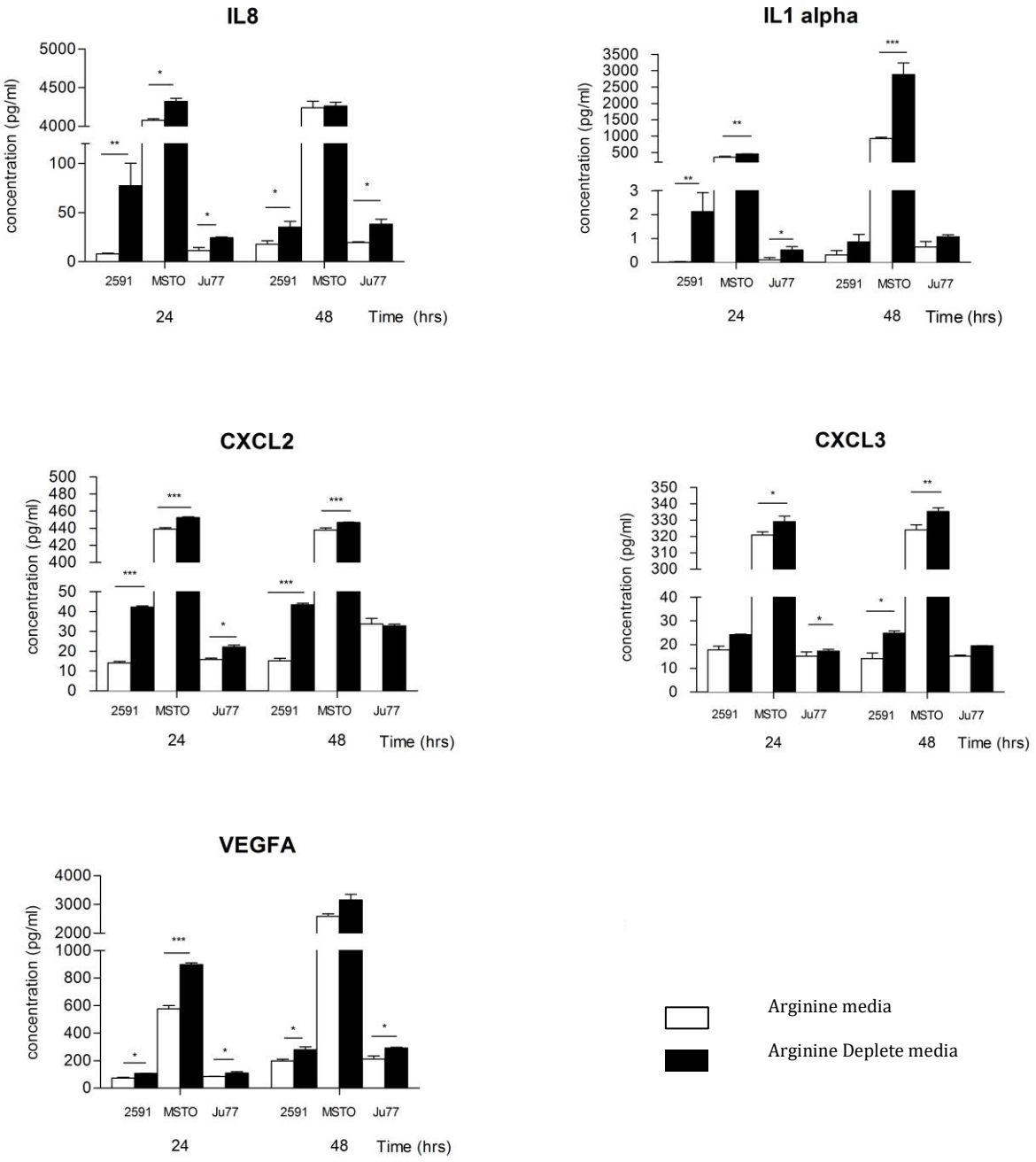


**Figure 3.5. Pro-inflammatory cytokine response induced by arginine-deficient media in ASS1 negative MPM cells.** Graphs represent the concentration of each pro-inflammatory cytokine at 24 and 48 hours following culture in arginine deficient media in the three ASS1 negative cell lines. ELISA-based assays to assess the concentrations of IL-8, IL-1α, CXCL2, CXCL3 and VEGFA were each performed twice in triplicate according to the manufacturer's protocol, with values representing the mean (+/- SEM). Statistical significance: (1-way ANOVA with Newman Keuls multiple comparison post-test) * =p<0.05, ** =p<0.01, *** =p<0.001.

## 3.6 Endoplasmic reticulum stress induces pro-inflammatory cytokine response

Since nutrient deprivation is a known endoplasmic reticulum (ER) stress signal (302), I explored its homeostatic role in ADI-PEG20-induced cytokine secretion in the ASS1 negative cells. One of the early cellular responses to endoplasmic reticulum (ER) stress is the activation of the unfolded protein response (UPR) (reviewed in the discussion). This is accompanied by increases in several well-recognised ER stress related proteins: data generated from the Affymetrix U133 2.0 platform demonstrated robust up-regulation of the ER stress-responsive genes, XBP1 and GADD34, at 24 hours, in parallel with the ADI-PEG20-induced pro-inflammatory gene expression (Table 3.2), suggesting a possible role for ER stress in the initiation of the inflammatory response following ADI-PEG20 treatment.

| GENE | 2591 | MSTO | Ju77 |
|---|---|---|---|
| XBP1 | 1.6 | 2.39 | 3.37 |
| GADD34 | 2.25 | 3.66 | 4.20 |

**Table 3.2. Gene expression analysis using the Affymetrix U133 plus 2.0 microarray platform.** The table illustrates the log-fold increase in expression of individual genes in the three wild-type ASS1 negative mesothelioma cell lines at 24hrs following exposure to ADI-PEG20 (750ng/ml), compared with the no-treatment controls.

To validate this gene expression data, I analysed the induction of XBP1 mRNA (Figure 3.6A) and spliced XBP1 protein (Figure 3.6B) following ADI-PEG20 exposure, by qRT-PCR and western blot, respectively, in the three wild-type ASS1 negative MPM cell lines and one ASS1 positive control cell line (H28). Results confirmed that XBP1 is significantly up-regulated by 24

hours following ADI-PEG20 treatment in the ASS1 negative MPM cell lines. No increase in XBP1 expression was seen in the ASS1 positive control.

**A**

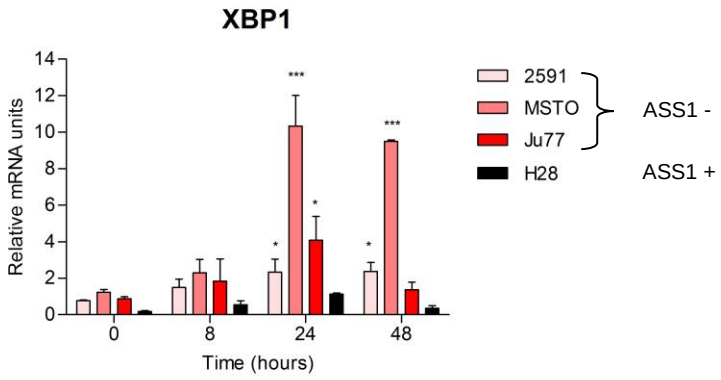


**B**

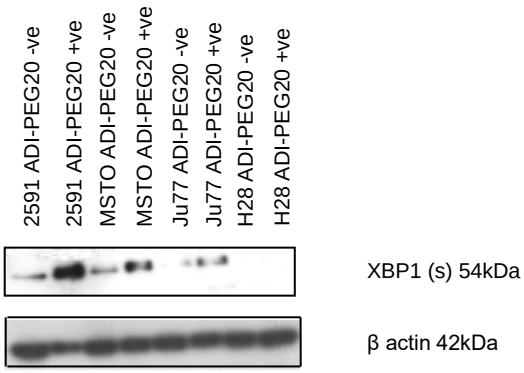


**Figure 3.6.**

**A) Validation of the up-regulation of ER stress marker, XBP1, by qRT-PCR**. Three ASS1 negative MPM cell lines (2591, MSTO and Ju77) and one ASS1 positive MPM cell line (H28) were analysed for induction of XBP1 mRNA following ADI-PEG20 treatment at 0, 8, 24 and 48 hours. Graph shows relative increase in XBP1 gene expression in each cell line compared with no drug control. The no drug control for each cell line is normalised to 1 at every time point (not shown). Experiments were performed twice in triplicate for each cell line with values representing the mean (+/- SEM). Statistical analysis: (1 way ANOVA with Newman Keul's multiple comparison post test analysis) * = $p<0.05$, *** = $p<0.001$.

**B) Western Blot validation of up-regulation of XBP1 (spliced)**. Three ASS1 negative MPM cell lines (2591, MSTO and Ju77) and one ASS1positive MPM cell line (H28) were analysed for expression of XBP1 (spliced) at 24 hours following ADI-PEG20 treatment by western blot. Results show an increase in XBP1 (s) protein in the ASS1 negative MPM cells. No expression was seen in the positive control (H28).

To corroborate the role of ER stress in the inflammatory response, the three ASS1 negative and the two wild-type ASS1 positive mesothelioma cell lines were treated with Tunicamycin (TM), an established ER stress inducing agent that blocks all N-glycosylation of proteins and causes cell cycle arrest in G1 phase (303). An increase in XBP1 mRNA expression was observed in all TM-treated cells, including the ASS1 positive cell lines (as TM will induce ER stress regardless of ASS1 status), by 24 hours (Figure 3.7). Furthermore, the pro-inflammatory genes that were up-regulated following ADI-PEG20 treatment, were also significantly up-regulated in the TM-treated cells (Figure 3.8). Thus, ADI-PEG20 stimulates a gene expression profile in ASS1 negative MPM cell lines that corresponds with that elicited by the well-recognised ER stress inducer, TM.

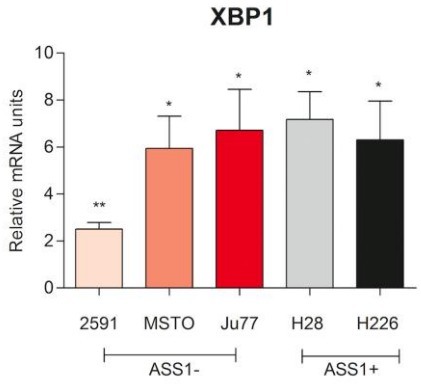


**Figure 3.7. Up-regulation of XBP1 mRNA at 24 hours following TM treatment.** Three wild-type ASS1 negative cell lines (2591, MSTO and Ju77) and two ASS1 positive cell lines (H28 and H226) were analysed to evaluate changes in expression of XBP1 at 24 hours following treatment with TM (5µg/ml). Graph represents the relative increase in XBP1 gene expression in each cell line after 24hrs of treatment with TM, compared with the no drug control. The no drug control is normalised to 1 (not shown). Experiments were repeated twice in triplicate for each cell line. Statistical analysis (unpaired two-tailed Student's t test): * = $p<0.05$, ** =$p<0.01$.

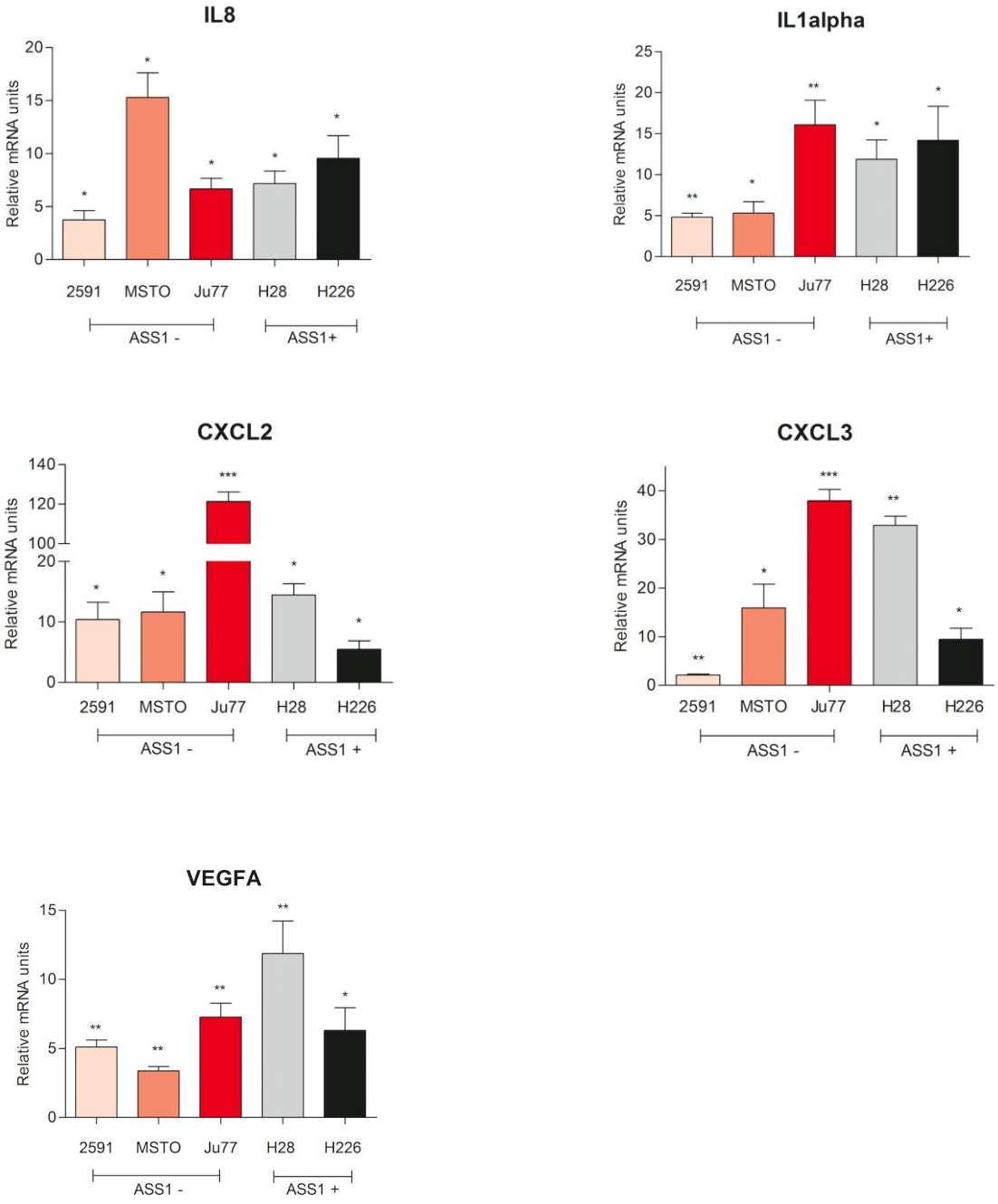


**Figure 3.8. Pro-inflammatory cytokine gene expression in a panel of mesothelioma cell lines at 24hrs following TM treatment.** Three ASS1 negative (2591, MSTO and Ju77) and two ASS1 positive cell lines (H28 and H226) were analysed for induction of cytokine mRNA at 24 hours following TM treatment. Graphs represent the relative increase in gene expression of the individual cytokines IL-8, IL1α, CXCL2, CXCL3 and VEGFA, compared with the no drug control. The no drug control is normalised to 1 (not shown). Experiments were repeated twice in triplicate for each cell line. Statistical analysis (unpaired two-tailed T Test): * = $p<0.05$, ** =$p<0.01$.

Having demonstrated a link between ER stress, XBP1 up-regulation, and pro-inflammatory cytokine secretion following ADI-PEG20-induced arginine depletion, I explored whether silencing of XBP1 would reduce the expression of pro-inflammatory genes following ADI-PEG20 treatment. To test this hypothesis, XBP1 knockdown was performed, using a SiRNA SMARTpool (Dharmacon). Good knockdown was achieved in two ASS1 negative cell lines, 2591 and MSTO; however, effective knockdown was not seen in Ju77, despite repeated attempts at various concentrations and cell densities (Figure 3.9).

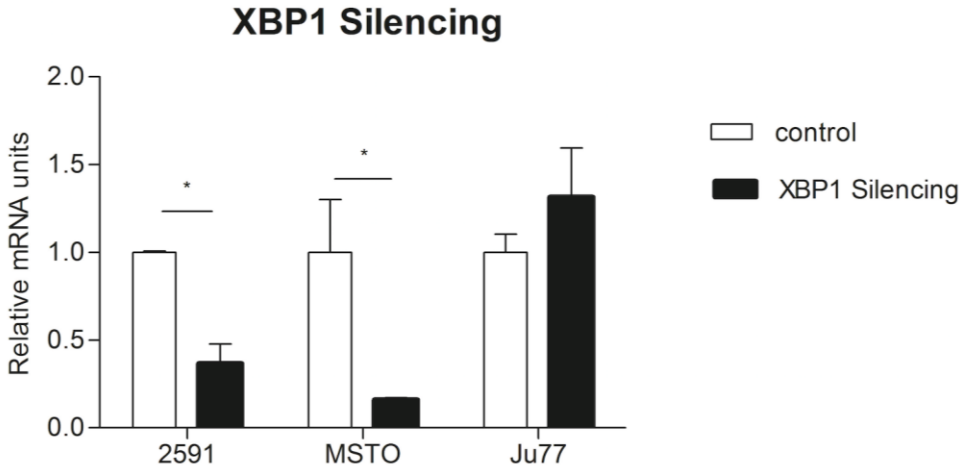


**Figure 3.9. Confirmation of XBP1 Silencing in ASS1 negative MPM cell lines 2591 and MSTO at 24hrs by qRT-PCR.** ASS1 negative MPM cell lines (2591, MSTO and Ju77) were analysed to evaluate XBP1 knockdown at 24 hours following SiRNA transfection. Graph represents the relative decrease in XBP1 gene expression compared with SiControl in 2591 and MSTO. Knockdown was not achieved in Ju77. Experiments were performed twice in triplicate for 2591 and MSTO, and threes times for Ju77. Graph represents the mean (+/- SEM). Statistical analysis: (unpaired two-tailed Student's t test) * =$p<0.05$.

Following confirmation of XBP1 knockdown by qRT-PCR, XBP1 silencing in the two ASS1 negative cell lines, 2591 and MSTO, was repeated and the cells were then treated with ADI-PEG20 for 24 hours. However, qRT-PCR results contradicted the hypothesis, revealing instead that XBP1 knockdown did not significantly dampen the pro-inflammatory cytokine response to ADI-PEG20. In fact, expression of IL-8 and CXCL3 actually increased significantly in both cell lines analysed (Figure 3.10).

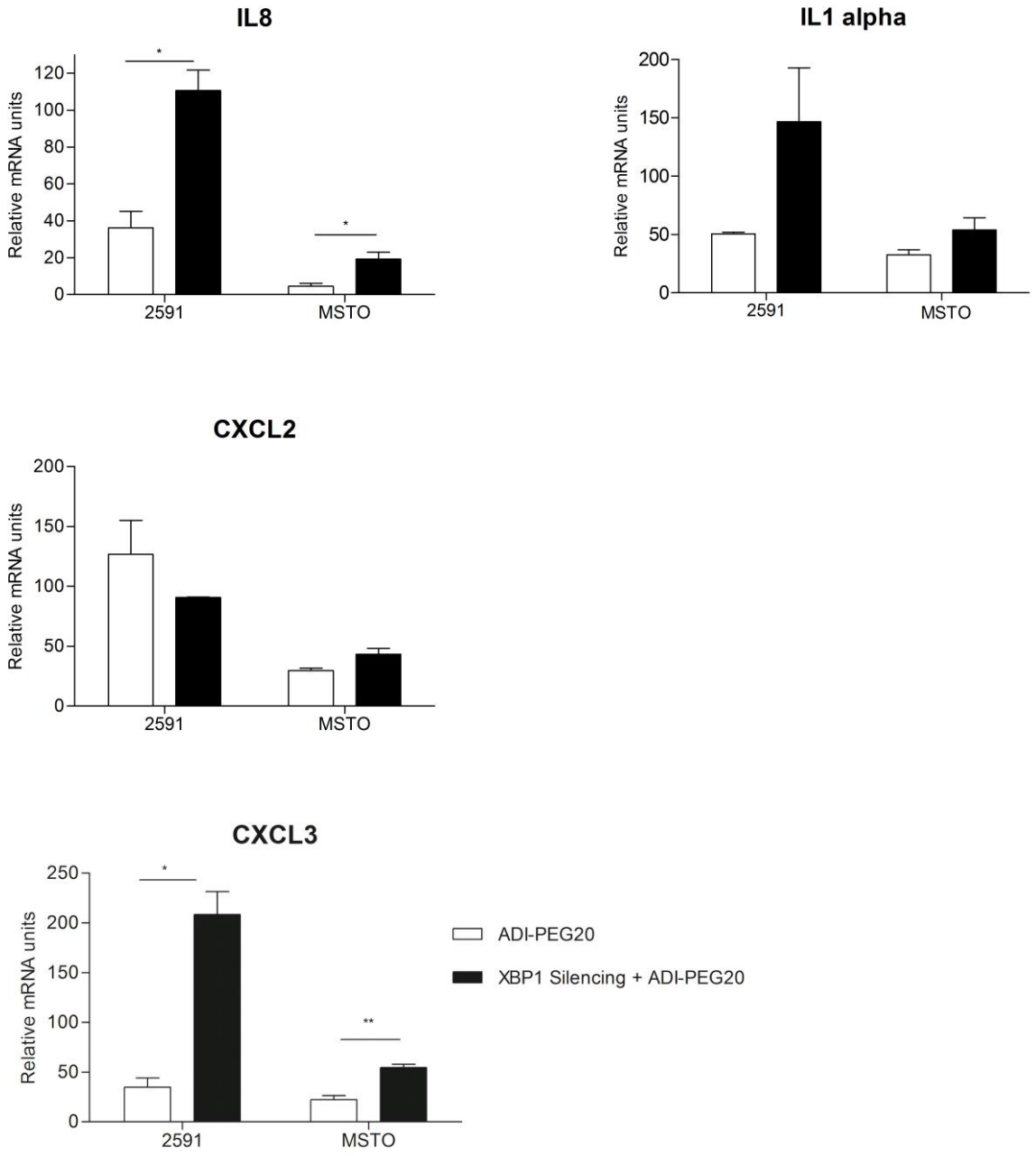


**Figure 3.10. ADI-PEG20-induced pro-inflammatory cytokine gene expression signature following XBP1 silencing in ASS1 negative cells (qRT-PCR).** ASS1 negative cell lines 2591 and MSTO, transfected with XBP1 SiRNA or SiControl, were analysed to evaluate changes in gene expression of individual cytokines at 24 hours following ADI-PEG20 treatment. Graphs represent the relative increase or decrease in expression of individual genes in each cell line transfected with either SiControl or XBP1 SiRNA, following ADI-PEG20 treatment, compared with no drug control. The no drug control for each cell line is normalised to one (not shown). Experiments were performed twice in triplicate for each cell line, with values representing the mean (+/- SEM). Statistical analysis (Unpaired two-tailed Student's t test) *=$p<0.05$, ** = $p<0.01$.

The UPR is a homeostatic signaling network that orchestrates the recovery of ER function (this will be reviewed in more detail in the discussion). Three separate UPR branches regulate ER homeostasis and the results here imply that the silencing of an ER-stress responsive gene from one UPR branch is insufficient to reduce the robust inflammatory response, as there is likely to be significant signaling crosstalk between branches which may provide compensatory regulation, whereby loss of one gene stimulates other pathways in order to maintain cell homeostasis. Thus, the inflammatory response is maintained, or, as seen here, heightened.

However, although maintenance of the inflammatory cytokine response following XBP1 knockdown was observed, I saw a significant decrease in tumour cell viability in XBP1 knockdown cells, at 24hrs following ADI-PEG20 treatment, highlighting the importance of the UPR pathways in maintaining cell homeostasis following ER stress (Figure 3.11).

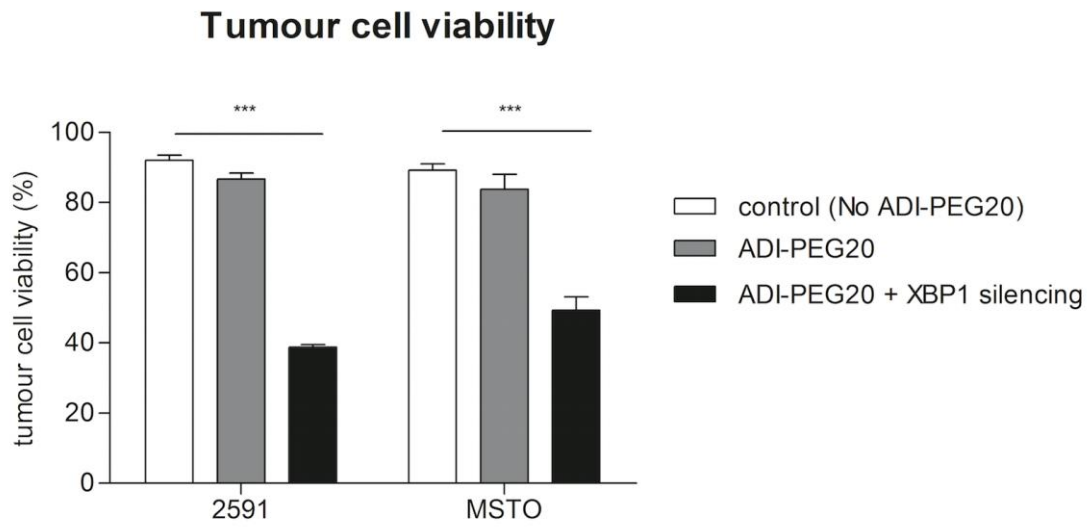


**Figure 3.11. Tumour cell viability in XBP1 silenced ASS1 negative cell lines at 24hrs following ADI-PEG20 treatment.** Two ASS1 negative cell lines, 2591 and MSTO, were transfected with XBP1 SiRNA or SiControl and analysed to assess cell viability at 24 hours following ADI-PEG20 treatment (750ng/ml). Cell viability was assessed by trypan blue exclusion assay using the Beckman Coulter ViCELL™ cell viability analyser. Graph shows the decrease in XBP1 knockdown tumour cell viability at 24hrs following ADI-PEG20 treatment. Typically treatment does not have an effect on tumour cell viability until 72 hours. Experiments were performed twice in triplicate for each cell line, with values representing the mean (+/- SEM). Statistical analysis (unpaired two-tailed Student's t test) *** = $p<0.001$.

In view of the maintained pro-inflammatory response following XBP1 knockdown, the next step was to look at factors regulated by more than one branch of the UPR. The transcription factor NF-κB is a key regulator of inflammation and is also reported to become activated by a number of cellular pathways during the UPR as a consequence of ER stress (304). Therefore, I sought to ascertain whether ADI-PEG20 treatment activated NF-κB in the ASS1 negative MPM cell lines. Western blot analysis confirmed phosphorylation (therefore activation) of NF-κB in the three ASS1 negative cell lines at 24 hours following ADI-PE20, with no evidence of phosphorylation in the ASS1 positive control, further supporting a link between ADI-PEG20, the ER stress response and inflammation (Figure 3.12).

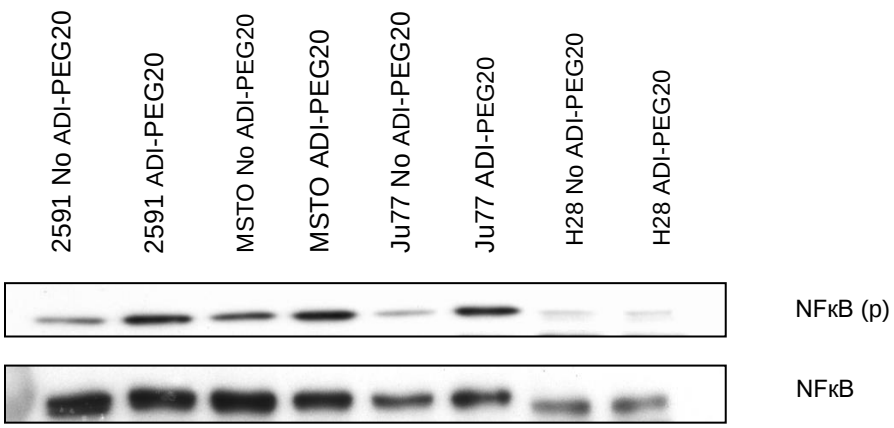


**Figure 3.12. NFκB phosphorylation following ADI-PEG20 treatment in ASS1 negative MPM cell lines.** The three ASS1 negative MPM cell lines (2591, MSTO and Ju77) and an ASS1 positive control (H28) were analysed for NFκB phosphorylation at 24 hours following ADI-PEG20 treatment. Western blot demonstrates increased protein expression of phosphorylated NFκB (NFκB (p)) in the three ASS1 negative cell lines at 24 hours following ADI-PEG20. There was no evidence of NFκB phosphorylation following ADI-PEG20 in ASS1 positive cells. Non-phosphorylated NFκB (NFκB) was used as a loading control.

## 3.7 *In vivo* induction of pro-inflammatory cytokines by ADI-PEG20

To determine whether the *in vitro* ADI-PEG20-induced pro-inflammatory cytokine response is relevant *in vivo*, I analysed plasma samples from a cohort of patients with ASS1-deficient ('ASS1 low') mesothelioma treated with or without ADI-PEG20 as part of the Arginine Deiminase and Mesothelioma or ADAM trial (clinicaltrials.gov identifier NCT01279967). This recently completed phase II national clinical trial was the first randomised trial to explore the role of arginine deprivation using ADI-PEG20 in patients selected for an ASS1-deficient tumour. For a diagrammatic summary of the ADAM trial design, please see Figure 3.13.

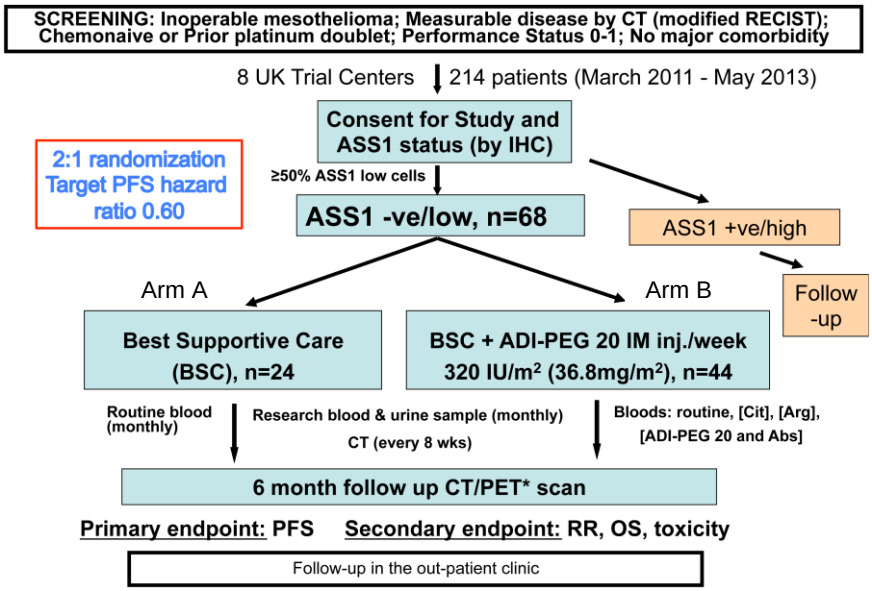


**Figure 3.13. Diagrammatic summary of ADAM trial design.** ASS1-deficient (ASS1 'low') patients were randomised (2:1 randomisation) to either best supportive care (BSC) (Arm A; 24 patients) or ADI-PEG20 + BSC (Arm B; 44 patients). In Arm B, ADI-PEG20 was given weekly as an intramuscular injection. Radiological assessment of response was performed every 2 months. PFS, progression-free survival; RR, response rate; OS, overall survival.

Patient plasma samples were analysed by ELISA for pro-inflammatory cytokines in response to ADI-PEG20 treatment. Results demonstrated that in patients with 'ASS1 low' tumours randomised to Arm B, the initial treatment dose of ADI-PEG20 induced an increase in all the cytokines analysed, with statistically significant increases seen in plasma IL-8 (p=0.002) CXCL2 (p=0.02) and VEGFA concentrations (p=0.002) (Figure 3.14). Furthermore, IL-8 and VEGFA remained significantly elevated at the two month assessment in the ADI-PEG20 treated group. No significant change from baseline was seen in IL-1α, CXCL2 or CXCL3 at the two month assessment in the ADI-PEG20 group. IL1-α was in fact unrecordable in the majority of plasma samples analysed and therefore it is difficult to make any conclusions from the IL1-α data. The untreated control group showed no change in any plasma cytokine levels from baseline (Figure 3.15). In addition, patients in the ADI-PEG20 group whose disease had progressed by the first assessment at two months, were found to have significantly higher levels of IL-8 (p=0.004), CXCL2 (p=0.02) and VEGFA (p=0.04) compared with those who demonstrated disease control at two months (Figure 3.16). Collectively, the ADAM data validate the *in vitro* studies and support the hypothesis that pro-inflammatory cytokines may be important in modulating resistance to ADI-PEG20.

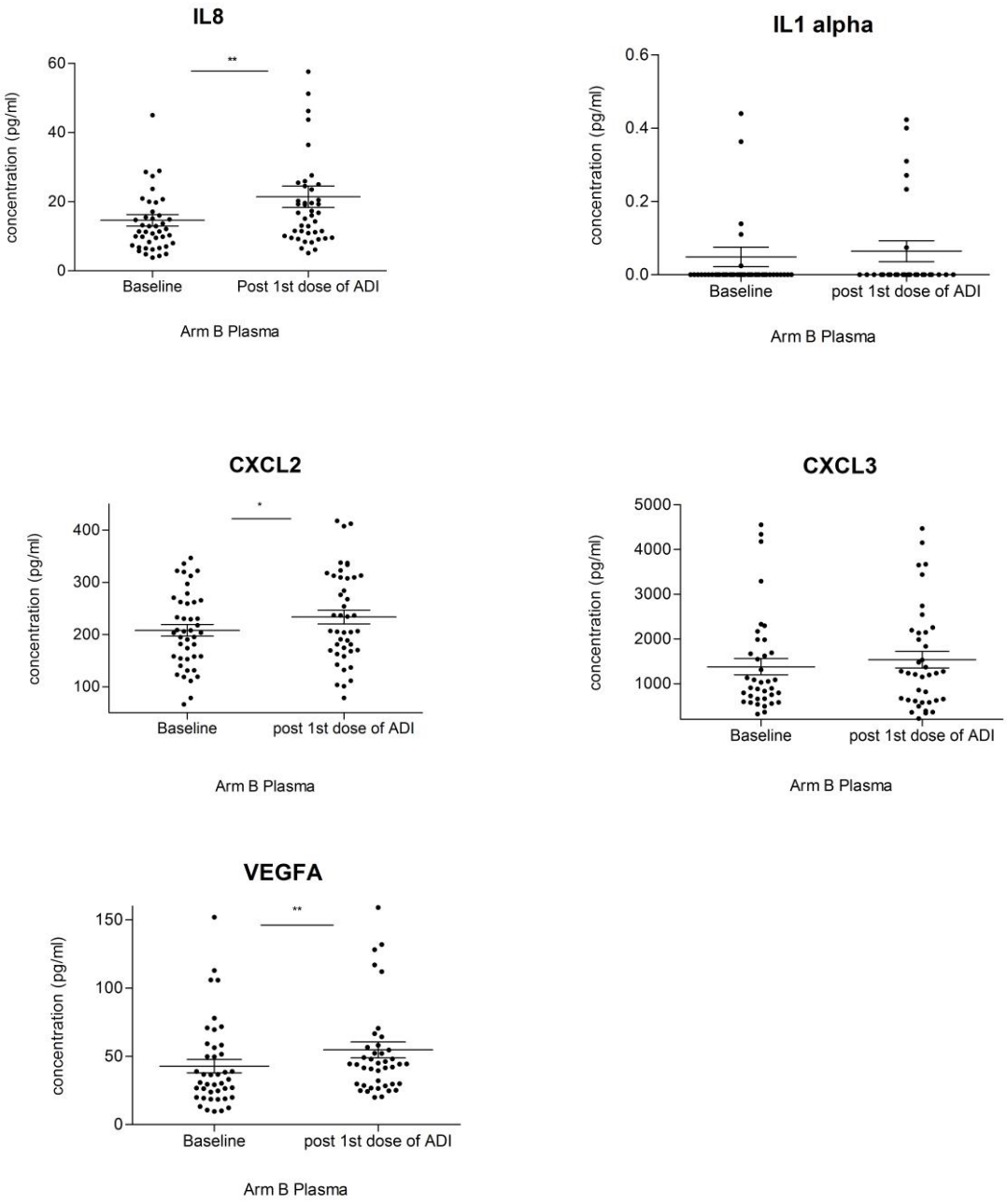


**Figure 3.14. Plasma concentrations of pro-inflammatory cytokines at baseline and following 1st administration of ADI-PEG20.** Patients enrolled on the ADAM clinical trial consented to having blood taken for research. Patients in Arm B (n=44) had weekly blood samples taken. After centrifugation, plasma was removed from each sample of blood and stored at -80°C until ELISA analysis. For ELISA analysis, plasma samples from patients in arm B at baseline and week 2 (1 week post 1st dose of ADI-PEG20), were thawed on ice and centrifuged a 12,000 rpm to remove debris. ELISAs were performed according to the manufacturer's instructions to assess plasma concentrations of each pro-inflammatory cytokine previously studied *in vitro* (1L-1α, IL-8, CXCL2, CXCL3, VEGFA). Graphs represent plasma concentrations of each pro-inflammatory cytokine at baseline and following 1$^{st}$ dose of ADI-PEG20. Plasma IL-1α was undetectable in the majority of samples; this has been shown as '0' on the graph. Statistical analysis (paired two-tailed T Test): * p=<0.05, ** p<0.01.

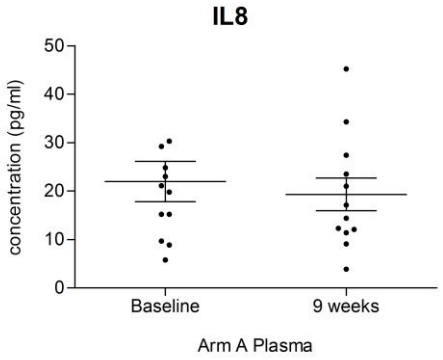
IL8
concentration (pg/ml)
50
40
30
20
10
0
Baseline
9 weeks
Arm A Plasma

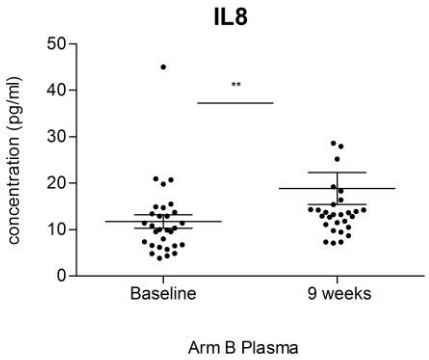
IL8
concentration (pg/ml)
50
40
30
20
10
0
**
Baseline
9 weeks
Arm B Plasma

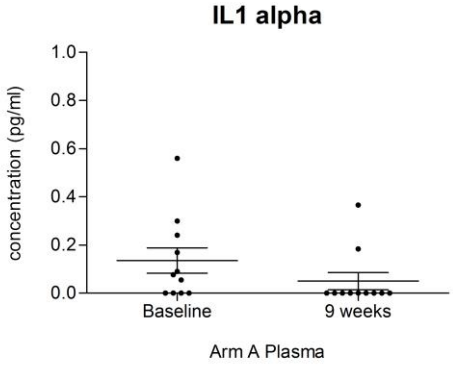
IL1 alpha
concentration (pg/ml)
1.0
0.8
0.6
0.4
0.2
0.0
Baseline
9 weeks
Arm A Plasma

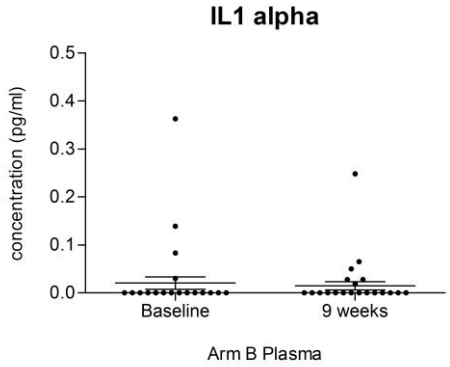
IL1 alpha
concentration (pg/ml)
0.5
0.4
0.3
0.2
0.1
0.0
Baseline
9 weeks
Arm B Plasma

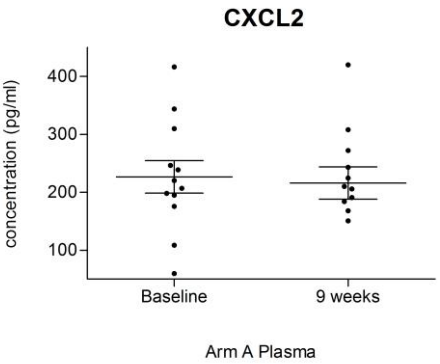
CXCL2
concentration (pg/ml)
400
300
200
100
Baseline
9 weeks
Arm A Plasma

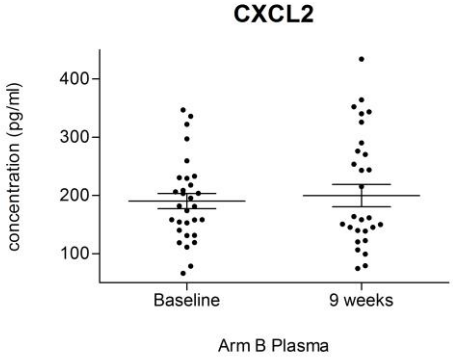
CXCL2
concentration (pg/ml)
400
300
200
100
Baseline
9 weeks
Arm B Plasma

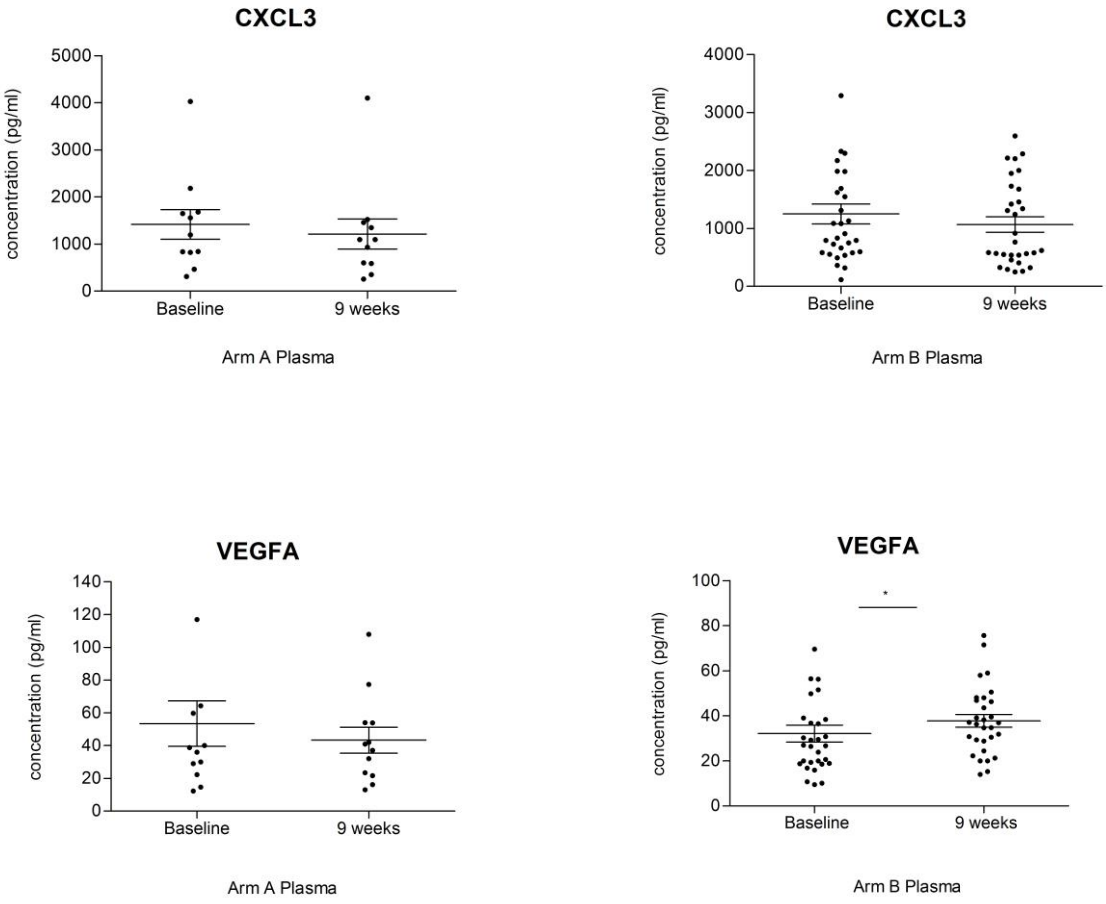


**Figure 3.15. Plasma concentrations of pro-inflammatory cytokines at baseline and the 9 week follow-up for patients in both trial groups.** Plasma samples taken at baseline and 9 weeks from patients randomised to both Arm A and Arm B, were analysed by ELISA, according to the manufacturer's protocol. Graphs represent the plasma concentrations of each pro-inflammatory cytokine at baseline and at 9 weeks following BSC or ADI-PEG20 plus BSC, in Arm A and Arm B, respectively. Graphs on the left hand side represent Arm A and graphs on the right represent Arm B. Statistical analysis (paired two-tailed T Test): * p=<0.05, ** p<0.01.

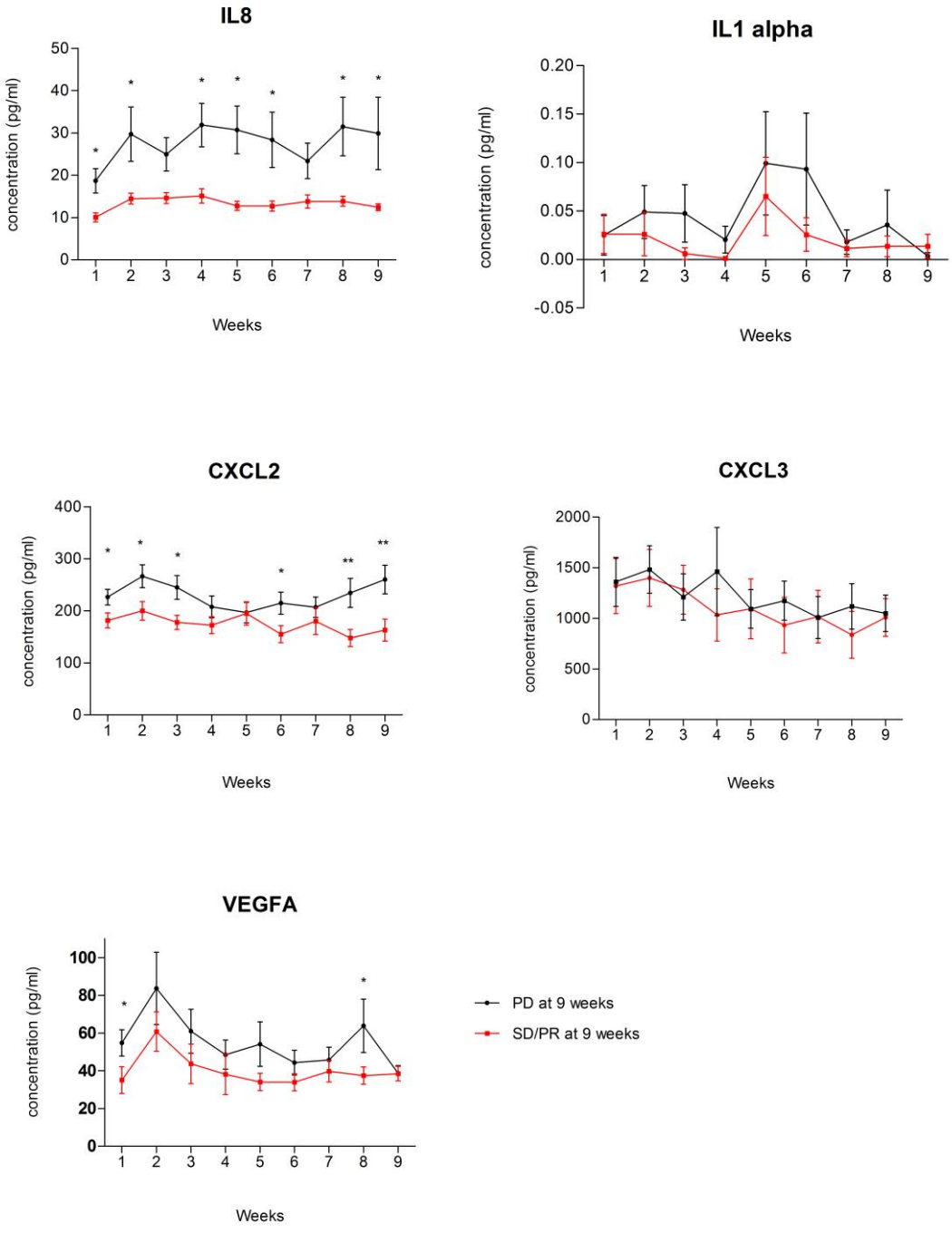


**Figure 3.16 a. Difference in plasma concentrations of pro-inflammatory cytokines in patients receiving ADI-PEG20 (Arm B) whose disease progressed at 9 week follow up compared with those who showed stable disease or a partial response**. Patients were assessed at 2 months (week 9) following initiation of ADI-PEG20. Patients whose disease had progressed (radiological assessment) whilst receiving ADI-PEG20 discontinued the drug, whilst patients with stable disease/partial response continued weekly treatment. Plasma samples from each week were analysed by ELISA, according to the manufacturer's protocol. Week 1 is baseline, prior to administration of the initial dose of ADI-PEG20. Week 2 is the 1st blood sample following ADI-PEG20 treatment initiation. Graphs represent the difference in

plasma concentrations of each pro-inflammatory cytokine in patients whose disease progressed (black line) compared with patients who had stable disease/partial response (red line). Statistical analysis (unpaired two-tailed t test for each week) * p=<0.05, ** p<0.01. PD; progressive disease, SD; stable disease, PR; partial response

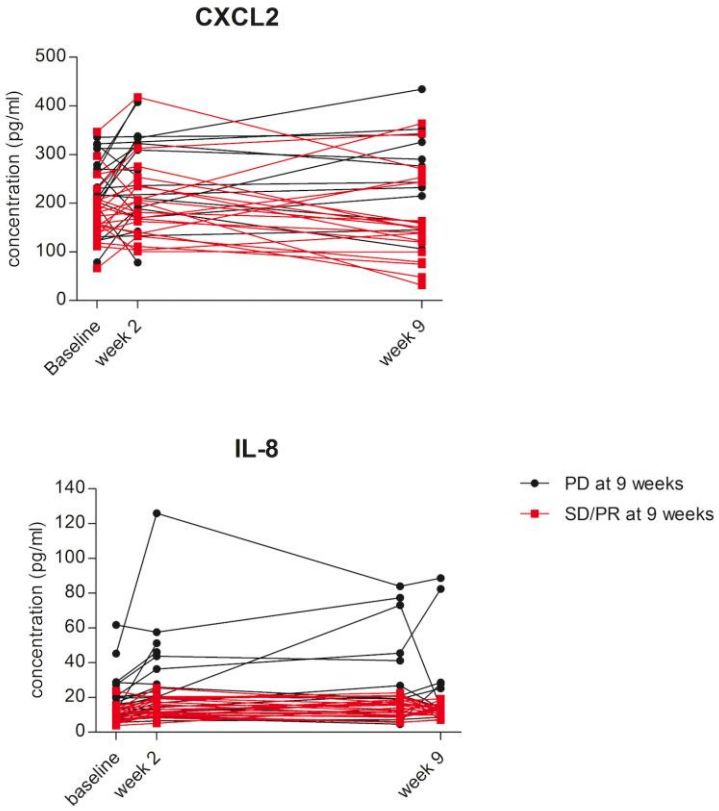


**Figure 3.16 b: Graphs plotting the individual patient plasma concentrations of IL-8 and CXCL2 at baseline, following initial ADI-PEG20 treatment (week 2) and at 9 weeks.** Individual patient plasma concentrations of IL-8 and CXCL2 were plotted to assess individual differences in these cytokine levels at baseline and following ADI-PEG20 exposure (week 2). Individual results were plotted for IL-8 and CXCL2 as these cytokines showed the most significant differences between patients who progressed at 9 weeks and patients who had stable disease/partial response. With IL-8, in particular, there were a number of individuals in the progressors group who had significantly higher concentrations of IL-8 than the majority of both progressors (black) and responders (red). PD; progressive disease, SD; stable disease, PR; partial response.

## 3.8 Discussion

A distinct pro-inflammatory gene expression signature was identified in ASS1 negative mesothelioma cell lines following exposure to ADI-PEG20. Specifically, IL-8, CXCL2, CXCL3, IL-1α and VEGFA were all found to be significantly up-regulated in the Affymetrix data analysis, and this was validated by qRT-PCR and ELISA. Furthermore, the pro-inflammatory cytokine production was also clinically relevant and supports a link between inflammation and ADI-PEG20 resistance in ASS1 negative mesothelioma.

Macrophages are key regulators of inflammation in cancer (305). Within a tumour, the cytokine network influencing these immune cells is intricate and extensive, and macrophage recruitment into tumours is mediated by multiple cytokines (230, 306), including the cytokines described above. Indeed, it is widely accepted that both VEGFA and IL-8 contribute to macrophage recruitment and activation (305, 307). Interestingly, IL-8 (CXCL8) belongs to the CXC family of chemokines, which also includes CXCL2 and CXCL3.This family is a chemotactic group of cytokines, characterized by the presence of four conserved cysteine amino acid residues in the amino terminus of the protein, in which the first two are separated by one non-conserved amino acid residue (hence the CXC designation). This family of molecules can be further subdivided based on the presence (+) or absence (-) of the amino acid sequence glutamic acid-leucine-arginine (ELR) immediately preceding the first cysteine. The ELR (+) family of CXC chemokines, to which IL-8, CXCL2 and CXCL3 belong, are potent pro-inflammatory agents and have increasingly been found to promote tumour growth, metastasis and angiogenesis as well as mediate tumour resistance to chemotherapeutic agents (308). CXCL2 and CXCL3 are better recognised for their role in neutrophil recruitment (309); however, all three of these ELR (+) chemokines bind to the CXC chemokine receptor 2 (CXCR2), a 7-transmembrane G-protein-coupled receptor that is also expressed on human blood monocytes and macrophages (211). Indeed, IL-4 and IL-13, cytokines that are typically increased within the TME (310, 311), induce CXCR2 in monocytes, therefore rendering these cells extremely

sensitive to IL-8 and related molecules (i.e. CXCL2 and CXCL3), which may contribute to regulating the positioning and functioning of TAM (312). Through CXCR2, CXCL2 and CXCL3 are also able to mediate robust monocyte arrest, an important step in monocyte recruitment (313). Moreover, research into cardiovascular disease has demonstrated that CXCR2 has a major impact on macrophage recruitment and accumulation in advanced atherosclerotic lesions (314), further supporting a role for CXCL2 and CXCL3, in addition to IL-8 and VEGFA, in macrophage recruitment. Further discussion on CXCR2 can be found in Chapter 5.

Other well-recognised chemokines involved in macrophage recruitment into tumour sites are CCL2 (MCP-1) and CCL5 (RANTES) (218). Affymetrix data analysis revealed that CCL5 gene expression was increased in ASS1 negative MPM cell lines following ADI-PEG20 treatment, but this increase did not meet the stringent criteria of greater than log 2-fold across all three ASS1 negative cell lines. No change in CCL2 expression was seen. This finding is similar to a recent study investigating the molecular signals induced by androgen blockade therapy that could recruit and modulate the function of TAM in Myc-CaP prostate cancer cells. Investigators found that CCL2 was expressed at very low levels, with no change seen following treatment, despite evidence of increased TAM infiltration (315). Indeed, although CCL2 is recognised to play a key role in macrophage recruitment, it has also been shown that in CCL2-deficient (CCL2 (-/-)) mice displaying abnormalities in wound repair, the number of macrophages within the wounded site was not affected by the absence of CCL2, suggesting that monocyte/macrophage recruitment can be independent of CCL2 (316).

A similar pro-inflammatory cytokine signature to that identified following ADI-PEG20 treatment was also seen in ASS1 negative mesothelioma cells following culture in arginine-deficient media. This result implies that the response is due to arginine depletion, rather than any off-target effects of ADI-PEG20. Interestingly, an IL-8-dependent pro-inflammatory response was seen in U20S osteosarcoma cells following deprivation of the amino acid glutamine (317). Here, the authors demonstrated that short-term glutamine restriction

triggers an endoplasmic reticulum (ER) stress response that leads to production of IL-8. In view of this finding, and the fact that there is an established link between ER stress, inflammation and malignancy (318-320), I considered the role of ER stress in induction of the inflammatory response following ADI-PEG20 treatment.

The endoplasmic reticulum (ER) is a multifunctional organelle essential for the synthesis, folding, and processing of secretory and transmembrane proteins. In order for proteins to fold properly, vital for normal cell function, a balance between the ER protein load and the folding capacity to process this load must be established (ER homeostasis). However, ER homeostasis can be disturbed by a number of different pathological processes, including hypoxia, nutrient overload or deprivation, infections, toxins and inflammatory cytokines (302), resulting in the accumulation of unfolded and misfolded proteins in the ER, a condition known as 'ER stress'. ER stress then activates a complex signaling network referred to as the Unfolded Protein response (UPR) (319). The UPR is initiated by three ER transmembrane proteins: Inositol Requiring 1 (IRE1), PKR-like ER kinase (PERK), and Activating Transcription Factor 6 (ATF6). These three master regulators sense and interpret protein-folding conditions in the ER and translate this information across the ER membrane to regulate downstream effectors. All three activate specialised transcriptional programs mediated by distinct transducers: ATF4 (for PERK), cleaved ATF6 (for ATF6), and spliced XBP1 (sXBP1) (for IRE1) (for a diagrammatic summary of the UPR and its role in inflammatory response, please see Figure 3.17). Ultimately, the aim of the UPR is to restore normal ER homeostasis. If this fails, the UPR tends to mediate cell death (321). UPR signaling is emerging as a contributing factor to the pathology of several human diseases, including cancer. Indeed, it has been shown to contribute to the growth and survival of tumours (322, 323).

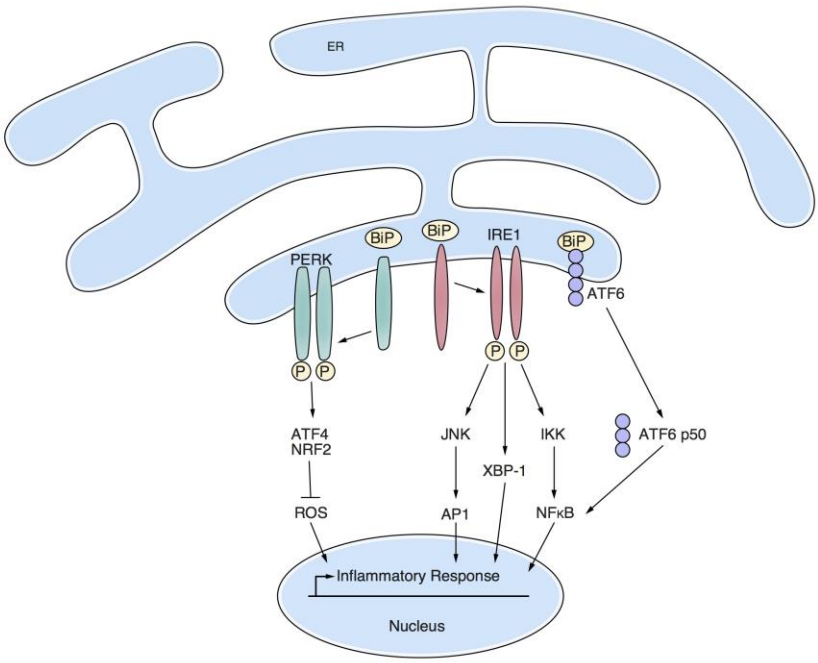


**Figure 3.17. ER stress and activation of the UPR: implication in the inflammatory response following ADI-PEG20 treatment.** The figure represents a simplified diagram of the core elements of the UPR signaling network. In unstressed conditions, the BiP chaperone interacts with the luminal domain of the three ER transmembrane sensors, AF6, IRE1 and PERK (representing the three branches of he UPR), and maintains them in an inactive state. Upon ER stress, caused by several pathological processes, including hypoxia, nutrient depletion or overload, infection and toxins, BiP interacts with unfolded proteins, leading to the activation of the UPR transducers. Activation of each sensor produces a transcription factor (ATF6(N), XBP-1 and ATF4, respectively) that activates genes to increase the protein folding capacity in the ER. IRE1 and PERK also decrease the load of proteins entering the ER. Both the increase in protein folding capacity and the decrease in protein load act to mitigate ER stress. The UPR is associated with inflammation via a variety of mechanisms involving ROS, JNK and NFκB. PERK promotes ATF4 and NRF2, which then suppress ROS production by activating antioxidant pathway. Upon activation, IRE1/TRAF2 recruits IKK, leading to the phosphorylation of IκBα and subsequent activation of NFκB. IRE1/TRAF2 can also activate AP1, resulting in the activation of JNK. XBP-1 induced by IRE1/TRAF2 can further induce the expression of various genes implicated in inflammation. Furthermore, ATF6 can promote inflammation via activating NFκB.

ATF, activating transcription factor; BiP, immunoglobulin heavy-chain-binding protein; IRE1, inositol-requiring enzyme-1; PERK, PKR-like ER kinase; XBP-1, X-box binding protein 1; ROS, reactive oxygen species; NRF2 nuclear factor-erythroid-derived 2-related factor 2; AP1, activator protein 1; JNK, c-Jun N-terminal kinase; IKK, IκB kinase; TRAF2, TNF receptor-associated factor 2

Adapted from Zhong et al (324)

The Affymetrix data generated in our laboratory supports data from the glutamine study and also demonstrates an association between ER stress and the pro-inflammatory gene expression profile following ADI-PEG20-induced arginine deprivation. A number of transcriptional changes associated with ER stress were noted, and increased expression of the critical transcription factor XBP1 was confirmed by qRT-PCR and western blot.

XBP1 is activated by an IRE1-mediated splicing event, and the spliced form of XBP1 (XBP1s) encodes a protein with a novel C terminus that acts as a potent transcriptional activator of many genes involved in the UPR. The IRE1-XBP1 pathway, the most conserved branch of the UPR, is required for ER biogenesis, as well as for efficient protein folding, maturation, and degradation in the ER (325). Furthermore, it has been shown to be an important component of tumour development and an essential survival factor (326). It is therefore not surprising that tumour cell viability was found to be significantly decreased after 24 hours of ADI-PEG20 treatment in XBP1 knockdown ASS1 negative cells, compared with the wild-type ASS1 negative control cells. This finding supports results from other studies showing that loss of XBP1 severely inhibits tumour cell survival. Indeed, under hypoxia, another inducer of ER stress, cell death was also increased following loss of XBP1 in the fibrosarcoma cell line HT1080 (323). Additionally, in this study, the IRE1-XBP1 pathway was also found to promote tumour growth in xenograft models. Depletion of XBP1 resulted in cell sensitization to ER stress–induced cell death and smaller tumours, and expression of XBP1(s) restored tumour growth under these conditions. Notably, investigators reported that although tumour cell death increased, loss of XBP1 had little influence on VEGFA expression in these cells (323). Likewise, I saw no significant decrease in pro-inflammatory cytokine expression following XBP1 knockdown in ASS1 negative cells, despite a decrease in cell viability. In fact, there was a compensatory increase. It is well recognized that all three main branches of the UPR have been shown to mediate pro-inflammatory gene expression (327, 328). This perhaps explains why the siRNA silencing of XBP1 (representing one branch) in ASS1 negative cells did not significantly dampen the inflammatory response to ADI-PEG20.

In addition, XBP1 mRNA splicing is also reported to trigger the autophagic response through regulation of BECLIN-1 transcriptional activation. BECLIN-1 plays a fundamental role in the initiation of autophagy (329). As autophagy is a recognized tumoural resistance mechanism following arginine depletion, providing a temporary supply of arginine, this may also explain why cell viability significantly decreased at 24hrs following ADI-PEG20 in the XBP1 knockdown ASS1 negative cells, compared to wild-type ASS1 negative cells.

Activation of the transcription factor NF-κB has been reported to be a consequence of ER stress (328). NF-κB is recognized as one of the key mediators of pro-inflammatory pathways, with genes transcribed by NF-κB including those that encode essential pro-inflammatory cytokines (330). Generally, NF-κB is kept in an inactive form within the cytoplasm; however, the UPR is able to activate NF-κB via different mechanisms (318). Therefore, in view of this, the next step was to evaluate whether NF-κB was activated following ADI-PEG20 treatment of ASS1 negative mesothelioma cells, to further validate the link between nutrient depletion, ER stress and inflammation. Western blot analysis confirmed phosphorylation (therefore activation) of NF-κB in these cells following treatment, with no evidence of phosphorylation in the ASS1 positive control. Further confirmation of NF-κB involvement would require inhibiting NF-κB activity in combination with ADI-PEG20 to see whether this combination attenuates pro-inflammatory cytokine production. This may, however, still be insufficient because of the redundancy demonstrated earlier with XBP1 blockade.

In cancer, ER stress has the capacity to activate cells of the adaptive immune system. Remarkably, it has also been suggested that ER stress may be transmissible from tumour cells to cells of the immune system. For example, when cultured in media conditioned by murine cancer cells experiencing ER stress, macrophages show activation of the UPR in a TLR-dependent manner (331). It is therefore possible that this acquired UPR in macrophages might influence their phenotype and result in the release of inflammatory mediators that further contribute to tumour inflammation and progression.

It is important to highlight here that the potential role of ER stress in modulating the pro-inflammatory cytokine response to ADI-PEG20 in ASS1 negative mesothelioma cells has not been confirmed by the data presented in this chapter. This is preliminary work and requires further validation.

To determine the clinical relevance of the pro-inflammatory gene signature, plasma samples obtained from the ADAM trial were analysed to look for changes in cytokine levels in response to ADI-PEG20. Results revealed that all the pro-inflammatory cytokines identified in the *in vitro* studies increased to some extent in patients one week following the initial dose of ADI-PEG20, with the increase in IL-8, VEGFA and CXCL2 being statistically significant at this time point. Furthermore, plasma IL-8 and VEGFA levels remained significantly higher than baseline at the two month follow up. In addition, IL-8, CXCL2 and VEGFA were significantly increased in patients whose mesothelioma progressed whilst on ADI-PEG20 therapy, compared with patients who demonstrated disease control to treatment, by two months. These findings validate the pre-clinical data and support a link between inflammation and ADI-PEG20 resistance. Moreover, they are in concordance with several independent reports showing a link between increased pro-inflammatory cytokines and therapeutic resistance. For example, IL-8 serum levels were assessed in melanoma patients treated with both BRAF inhibitors and immunotherapy. Here, decreased IL-8 correlated with best clinical response and increased IL-8 correlated with progressive disease (332). A decrease in IL8 levels during treatment has also been associated with improved response to chemotherapy and radiotherapy (333, 334). In addition, IL-8 was found to mediate resistance to PI3K-mTOR inhibitors in breast cancer (335). Furthermore, it was recently reported that mouse mammary tumours that developed resistance to chemotherapy had high expression of CXCL2 (336) and it has been suggested that elevated VEGF levels may also contribute to increased resistance to chemotherapy or endocrine therapy in advanced breast cancer (337). Accordingly, VEGF status has been shown to be of value in predicting the effectiveness of radiotherapy, chemotherapy, and hormonal therapy, as well as the likelihood of relapse, in a variety of cancers (338, 339). My data show that the increase in plasma IL-8, CXCL2 and

VEGFA corresponds with disease progression at 2 months in patients receiving ADI-PEG20. These cytokines may therefore have utility as early resistance biomarkers to ADI-PEG20 in the future.

However, plasma IL-8 could also be reflecting tumour burden in ADAM trial patients. It has been reported that in both melanoma and colorectal cancer xenografts, IL-8 concentrations precisely correlated with tumour burden, supporting the hypothesis that IL-8 output is a relatively constant parameter for a single tumour cell and that, as suggested by Sanmamed et al (332), IL-8 levels may accurately reflect the amount of tumour cells. However, as the ADI-PEG20 treatment Arm (Arm B) showed an increase in PFS compared with the BSC Arm (Arm A) overall (3.3 months versus 1.9 months; p=0.02), this indicates that the pro-inflammatory cytokine signature involving IL-8, CXCL2 and VEGFA, is linked to resistance and disease progression on ADI-PEG20.

Finally, the pro-inflammatory gene expression signature identified by Affymetrix in response to ADI-PEG20 was specific to ASS1 negative mesothelioma cells. It was not seen in the ASS1 negative bladder cell line, 253J. In fact, in 253J, the only cytokine that demonstrated a statistically significant increase compared with the no treatment control, was VEGFA, indicating that the response to ADI-PEG20 is not consistent across different tumour types. Further studies are required to assess the cytokine response to ADI-PEG20 in other ASS1 negative tumour types.

Collectively, the pre-clinical and clinical data support a link between the pro-inflammatory cytokine response and ADI-PEG20 resistance in malignant mesothelioma. Therefore, I sought to study further the relationship between these pro-inflammatory cytokines and resistance to arginine deprivation therapy in arginine-auxotrophic mesothelioma cells.

# Chapter 4. Macrophages promote resistance to ADI-PEG20 in ASS1 negative mesothelioma

## 4.1 Introduction

The pre-clinical and clinical data presented in Chapter 3 support a link between the pro-inflammatory cytokine response and ADI-PEG20 resistance in malignant pleural mesothelioma. Macrophages, well-recognised inflammatory cells, are recruited and activated by the pro-inflammatory cytokines identified in the previous chapter. Furthermore, they are reported to be abundant in mesothelioma, playing a central role in mesothelioma tumourigenesis (248, 279). Indeed, given the close relationship between macrophages and tumour cells within the mesothelioma tumour microenvironment, I sought to study further the link between the pro-inflammatory cytokines, macrophages and resistance to arginine deprivation therapy in arginine-auxotrophic mesothelioma cells.

## 4.2 Aims

The aims of this chapter were:

1. To confirm that macrophages resident within the mesothelioma microenvironment express ASS1

2. To establish whether there is a difference in macrophage number between ASS1 ‘high’ and ASS1 ‘low’ expressing mesotheliomas using patient biopsies from the ADAM trial

3. To evaluate the phenotype of co-cultured macrophages in the presence and absence of ADI-PEG20

4. To investigate whether macrophages are able to modulate the therapeutic response of ASS1 negative mesothelioma cells to ADI-PEG20

5. To identify the mechanism behind macrophage-mediated tumoural resistance to ADI-PEG20

## 4.3 Mesothelioma is enriched with ASS1-expressing macrophages

First I assessed the expression of ASS1 in macrophages residing in the mesothelioma tumour microenvironment. Analysis of human mesothelioma tissue confirmed co-localisation of ASS1 with the macrophage-marker CD68, indicating that macrophages are capable of synthesizing the arginine precursor, argininosuccinate (Figure 4.1 A+B).

**A**

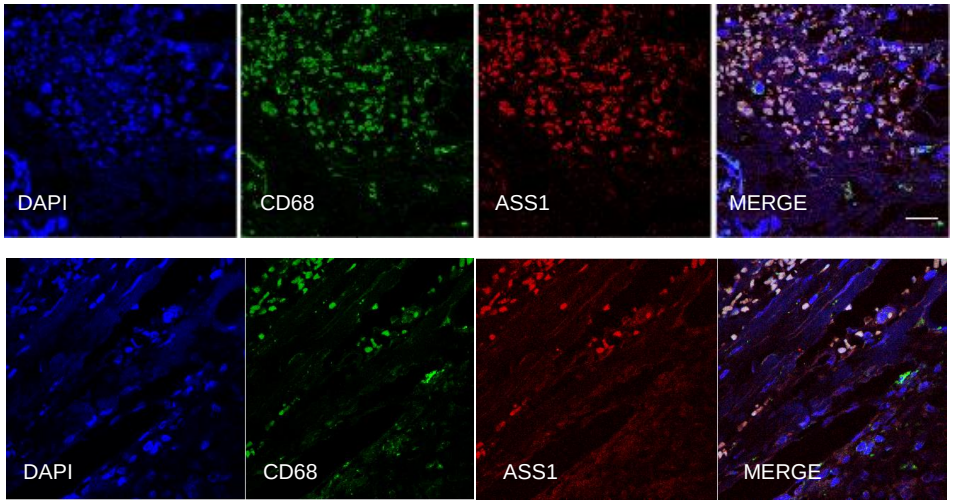


**B**

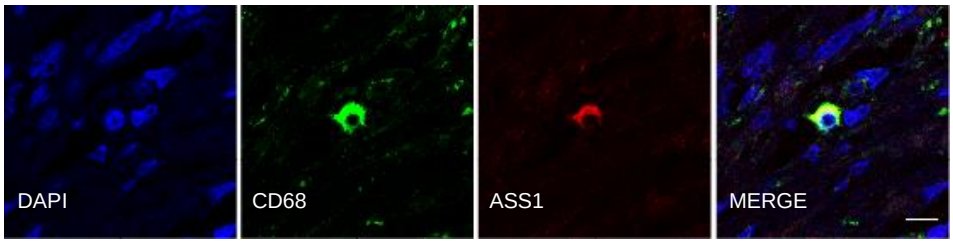


**Figure 4.1 A+B. Human mesothelioma is enriched with ASS1 expressing macrophages.** Human mesothelioma sections were assessed by immunofluorescence (IF). Each figure demonstrates representative examples of IF stains against CD68 (green) and ASS1 (red), clearly showing CD68 and ASS1 co-localisation (merged cells). DAPI (blue) was used as a counter-stain to identify cell nuclei. Co-localisation was identified by 63x magnification confocal microscopy. Figure A: the scale bar represents 20µm. Figure B: this image is zoomed in x2 and the scale bar represents 10µm.

## 4.4 Quantification of macrophage number in ASS1 ‘high’ and ASS1 ‘low’ mesothelioma

Biopsies obtained from ADAM clinical trial patients were used to create tissue microarrays (TMAs). These TMAs were stained for the macrophage marker CD68 by immunohistochemistry. CD68-positive macrophages were then quantified using a validated imaging analysis program on the Ariol Imaging System (300). Results showed that there was no significant difference in macrophage number between ‘low’ and ‘high’ expressing mesotheliomas (Figure 4.2).

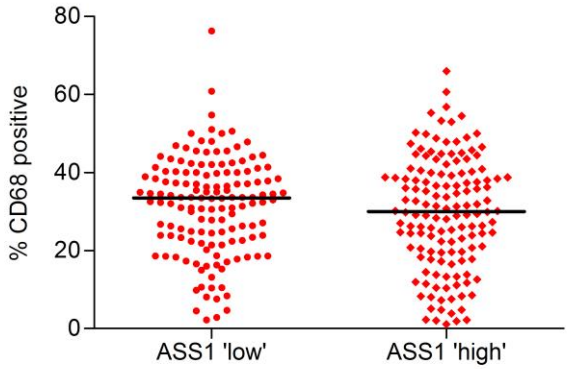


**Figure 4.2. Percentage of CD68 positive macrophages in human mesothelioma tissue.** Tissue microarrays (TMAs) from the ADAM clinical trial were stained with the macrophage marker CD68. Prior to calculation of the percentage area of CD68 positive staining, all TMA cores were first reviewed manually and only included in the analysis if the core was intact with minimal fibrotic or acellular areas. This was to standardise tumour area and cellularity and enable valid comparisons. Each reviewed core was then entered into the Ariol imaging analysis program, to quantify CD68 antibody staining of the TMAs. Graph represents the percentage of CD68 positive macrophages in both ASS1 ‘low’ and ASS1 ‘high’ biopsies. The black line represents the median.

## 4.5 Macrophages mediate resistance to ADI-PEG20 in ASS1 negative mesothelioma cells *in vitro*

Having established that mesothelioma-associated macrophages are abundant in human mesothelioma tissue and express ASS1, I sought to evaluate the effect of ADI-PEG20 on the three ASS1 negative mesothelioma cell lines in the presence of macrophages using an *in vitro* co-culture model. Human PBMC-derived macrophages were co-cultured with the ASS1 negative cell lines 2591, MSTO and Ju77, both with and without direct cell contact (i.e. using a 0.4µM transwell insert), in the presence and absence of ADI-PEG20. Tumour cell viability was assessed at four days. Results revealed that macrophages partially protected the mesothelioma cells from arginine depletion (Figure 4.3 and 4.4). Indeed, while macrophage viability was unaffected by exposure to ADI-PEG20 (Figure 4.5), there was a significant increase in tumour cell viability of up to 30% when tumour cells were co-cultured with macrophages, compared with tumour cells cultured alone, following ADI-PEG20. This increase in viability was apparent when cells were cultured with and without direct macrophage contact, implying a soluble factor in mediating resistance.

Notably, similar increases in viability were seen across all three ASS1 negative cell lines, but both 2591 and Ju77 were not as sensitive to ADI-PEG20 at four days as MSTO. As MSTO was the more sensitive cell line (i.e. there was significantly more MSTO cell death (80%) than Ju77 and 2591 by 4 days), this was the cell line used in all following experiments.

**A. 2591**

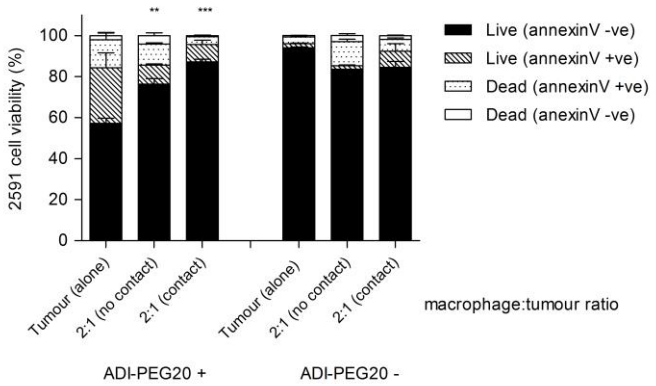


**B. MSTO**

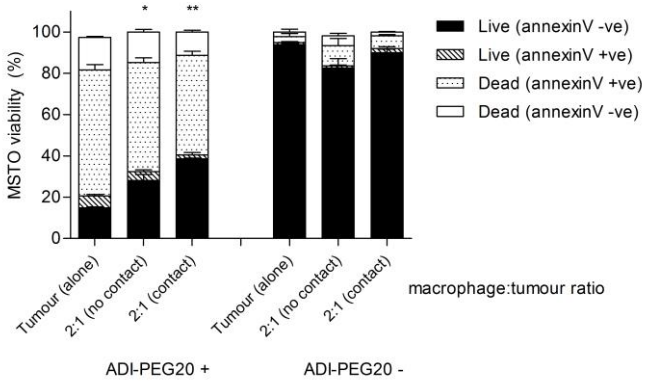


**C. Ju77**

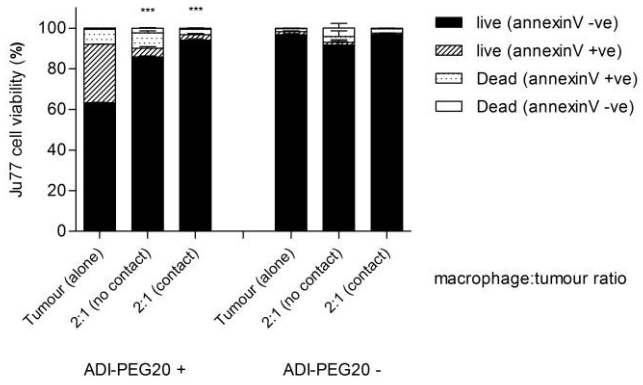


**Figure 4.3. Tumour cell viability at 4 days post ADI-PEG20 treatment.** The three ASS1 negative cell lines, 2591, MSTO and Ju77 were analysed. Each cell line was cultured alone and in co-culture with macrophages, either with or without direct cell contact (using a 0.4µM transwell insert), in the presence and absence of ADI-PEG20. The 2:1 macrophage:tumour cell ratio was chosen following extensive optimisation of the ratios, using 1:1, 2:1 and 5:1

initially. In addition, the 2:1 macrophage:tumour ratio has previously been used in a recent study evaluating the crosstalk between macrophages and colon cancer cells (340).Viability was assessed at 4 days by FACS. Apoptotic cells were taken to be the number of annexin V positive cells (see raw FACS data, Figure 4.4). Experiments were repeated three times for each cell line with values representing the mean (+/- SEM). Statistical analysis (1 way ANOVA with Newman Keuls post-test analysis using 'live cells annexin V negative'): * = $p<0.05$, ** = $p<0.01$, *** = $p<0.001$.

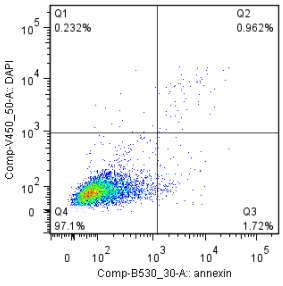


ADI-PEG20 -ve

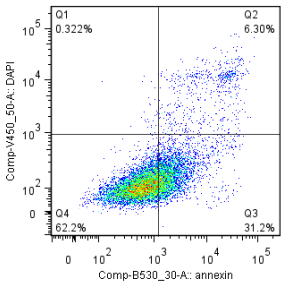


ADI-PEG20+ve

**B.**

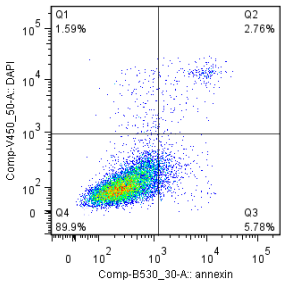


ADI-PEG20 -ve

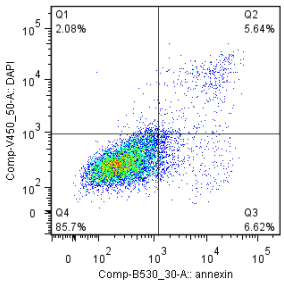


ADI-PEG20 +ve

**C.**

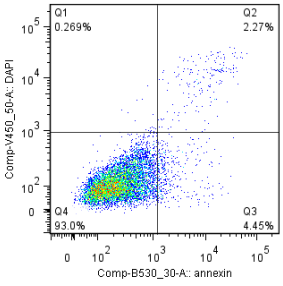


ADI-PEG20 -ve

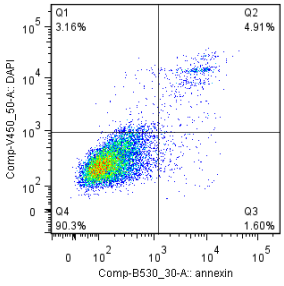


ADI-PEG20 +ve

**Figure 4.4. 2591 tumour cell viability following ADI-PEG20 treatment.** A) tumour cells cultured alone; B) tumour cells co-cultured with macrophages without direct cell contact; C) tumour cells co-cultured with macrophages with direct cell contact. Graphs represent one of three experiments analysed by FACS. Key: Q1=DAPI +ve dead cells, Q2=DAPI +ve and

annexin V +ve dead cells (apoptosis), Q3=annexin V +ve live cells (undergoing apoptosis), Q4=live cells. 10,000 events were recorded for each condition. Prior to analysis of tumour cell viability, the macrophages from co-culture conditions were identified (using CD14 and CD11b stains) and excluded. Only tumour cells are shown in the graphs.

**A.**

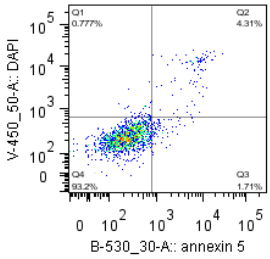


ADI-PEG20 -ve

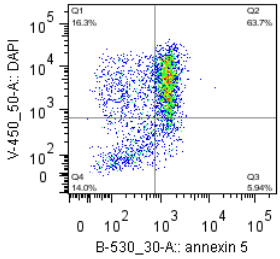


ADI-PEG20 +ve

**B.**

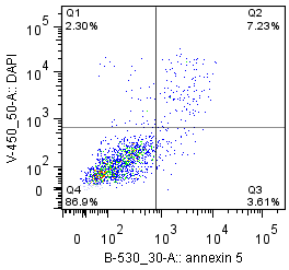


ADI-PEG20 -ve

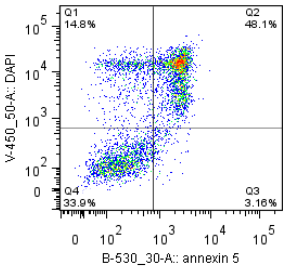


ADI-PEG20+ve

**C.**

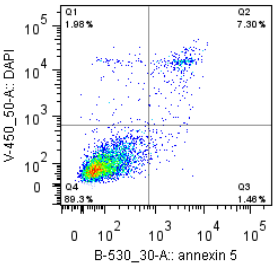


ADI-PEG20 -ve

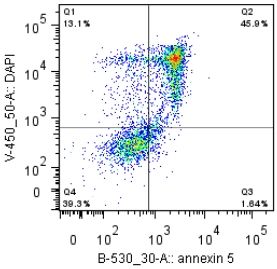


ADI-PEG20 +ve

**Figure 4.5. MSTO tumour cell viability following ADI-PEG20 treatment.** A) tumour cells cultured alone; B) tumour cells co-cultured with macrophages without direct cell contact; C) tumour cells co-cultured with macrophages with direct cell contact. Graphs represent one of

three experiments analysed by FACS. Key: Q1=DAPI +ve dead cells, Q2=DAPI +ve and annexin V +ve dead cells (apoptosis), Q3=annexin V +ve live cells (undergoing apoptosis), Q4=live cells. 10,000 events were recorded for each condition. Prior to analysis of tumour cell viability, the macrophages from co-culture conditions were identified (using CD14 and CD11b stains) and excluded. Only tumour cells are shown in the graphs.

**A.**

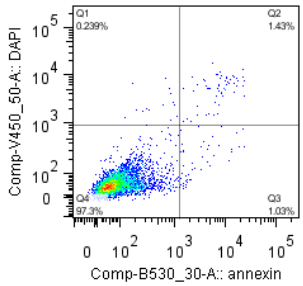


ADI-PEG20 -ve

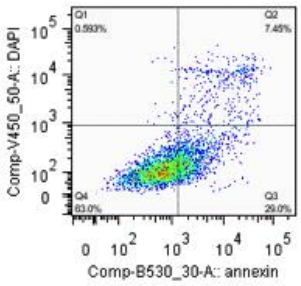


ADI-PEG20 +ve

**B.**

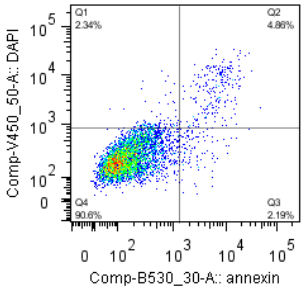


ADI-PEG20-ve

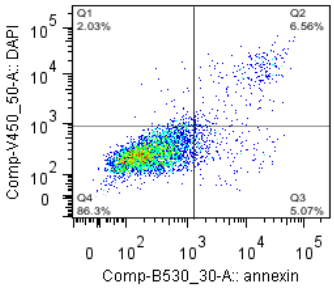


ADI-PEG20 +ve

**C.**

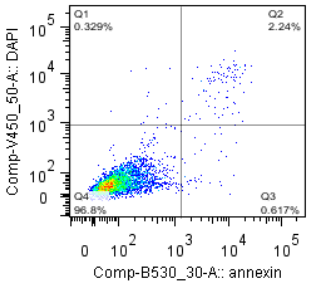


ADI-PEG20 -ve

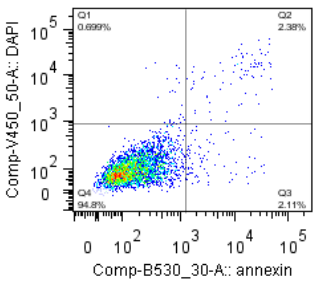


ADI-PEG20 +ve

**Figure 4.6. Ju77 tumour cell viability following ADI-PEG20 treatment.** A) tumour cells cultured alone; B) tumour cells co-cultured with macrophages without direct cell contact; C) tumour cells co-cultured with macrophages with direct cell contact. Graphs represent one of

three experiments analysed by FACS. Key: Q1=DAPI +ve dead cells, Q2=DAPI +ve and annexin V +ve dead cells (apoptosis), Q3=annexin V +ve live cells (undergoing apoptosis), Q4=live cells. 10,000 events were recorded for each condition. Prior to analysis of tumour cell viability, the macrophages from co-culture conditions were identified (using CD14 and CD11b stains) and excluded. Only tumour cells are shown in the graphs.

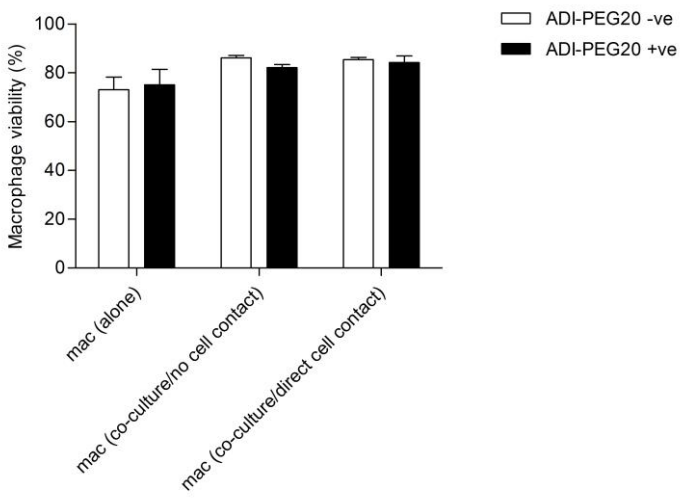


**Figure 4.7. Macrophage viability at 4 days post ADI-PEG20 treatment.** Macrophages were cultured alone and in co-culture with each ASS1 negative tumour cell line (2591, MSTO and Ju77, either with or without direct cell contact (using a 0.4µM transwell insert), in the presence and absence of ADI-PEG20. Viability was assessed at 4 days by FACS. Annexin V positivity denoted apoptotic cells. Graph shows the percentage of viable macrophages cultured alone and with MSTO cells (both with and without direct contact) in the presence and absence of ADI-PEG20. Similar viability was observed when macrophages were co-cultured with the cell lines Ju77 and 2591. ADI-PEG20 does not appear to affect macrophage viability. Experiments were repeated three times for each tumour cell line, with values representing the mean (+/- SEM).

## 4.6 ADI-PEG20 exposure leads to coordinate up-regulation of ASS1 in macrophages and ASL in tumour cells

To explore the mechanism behind this observed resistance, I tested the effect of ADI-PEG20 on the key urea cycle enzymes, ASS1 and ASL, in macrophages and ASS1 negative mesothelioma cells. A significant increase in ASS1 expression was detected in macrophages co-cultured with tumour cells by 48 hours following ADI-PEG20 exposure, compared with macrophages cultured alone (Figure 4.8 A+B). In contrast, there was no corresponding increase in macrophage ASL (Figure 4.9 A+B). Notably, in the tumour cells, re-expression of ASS1, an important early mechanism of resistance to ADI-PEG20 in other tumour types (173), was not seen (Figure 4.10 A+B). However, there was a significant increase in ASL expression in tumour cells co-cultured with macrophages, compared with tumour cells cultured alone (Figure 4.11 A+B). Taken together, these findings suggest that the macrophages are cooperating metabolically with ASS1 negative mesothelioma cells via a coordinate up-regulation of the urea cycle enzymes ASS1 and ASL, following ADI-PEG20 treatment.

**A.**

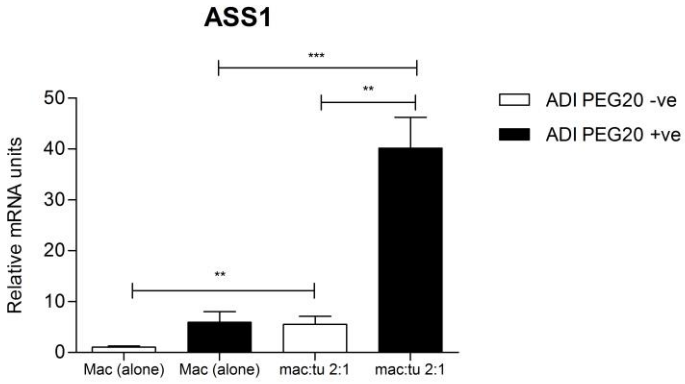


**B.**

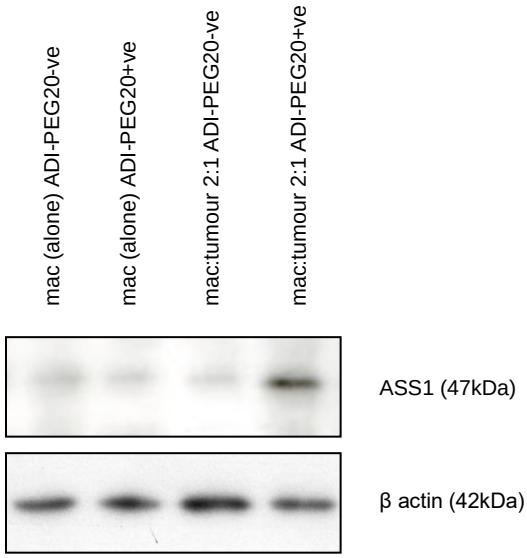


**Figure 4.8. Increase in ASS1 expression in co-cultured macrophages at 48 hours following treatment with ADI-PEG20**

**A) qRT-PCR .** Macrophages were cultured alone and in co-culture with MSTO cells (without direct cell contact) at a ratio of 2:1 macrophages to tumour cells, in the presence and absence of ADI-PEG20. ASS1 gene expression was assessed at 48 hours following ADI-PEG20 treatment. Graph represents the relative increase in ASS1 mRNA expression in co-cultured macrophages following treatment with ADI-PEG20, compared with macrophages cultured alone in the absence of ADI-PEG20 (normalised to 1). Experiments were performed three times in triplicate with values representing the mean (+/- SEM). Statistical analysis (I way ANOVA with Newman Keuls post-test analysis) ** = $p<0.01$, *** = $p<0.001$.

**B) Western Blot**. Blot shows the increase in expression of ASS1 protein in co-cultured macrophages at 48 hours following treatment with ADI-PEG20, with βactin as a control protein. Experiments were performed three times in triplicate.

**A**

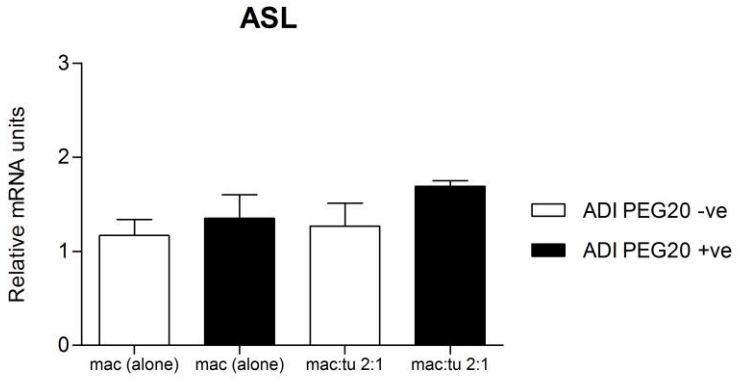


**B**

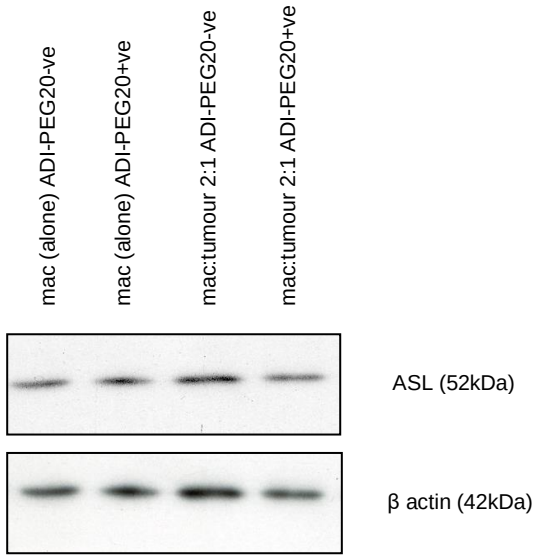


**Figure 4.9. Macrophage ASL expression at 48 hours following ADI-PEG20 treatment.**

**A) qRT-PCR.** Graph shows no difference in ASL mRNA expression in macrophages cultured alone and with tumour cells at 48 hours following ADI-PEG20 treatment, compared with macrophages cultured alone in the absence of ADI-PEG20 (normalised to 1). Experiments performed three times in triplicate with values representing the mean (+/- SEM).

**B) Western Blot.** Following ASS1 analysis (see 4.8 B), the blot was stripped using stripping buffer for 5 minutes, washed three times for ten minutes in PBS-Tween[20], and re-probed for ASL. Western Blot shows expression of macrophage ASL protein 48 hours following ADI-PEG20 treatment. No change in protein expression was

observed. βactin was used as a control protein. Experiment was performed three times in triplicate.

**A**

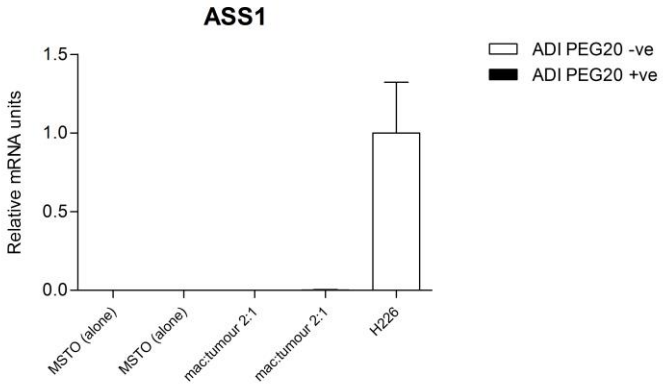


**B**

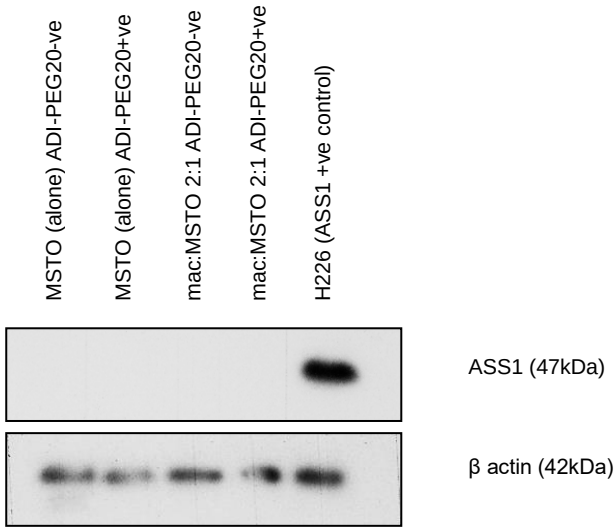


**Figure 4.10. ASS1 expression in MSTO tumour cells cultured alone and with macrophages ± ADI-PEG20 treatment**

**A)** **qRT-PCR.** MSTO cells were cultured alone and with macrophages (without direct cell contact) in the presence and absence of ADI-PEG20. MSTO ASS1 gene expression was assessed at 48 hours following ADI-PEG20 treatment. There is no re- expression of tumoural ASS1 mRNA following ADI-PEG20 treatment in cells cultured alone or with macrophages. ASS1 expression in MSTO cells is shown relative to an ASS1 positive control (H226), normalised to 1. Experiments were performed three times in triplicate, with the graph representing the mean (+/- SEM).

**B)** Western blot assessing ASS1 protein expression in MSTO tumour cells, cultured alone and in co-culture with macrophages, in the presence and absence of ADI-PEG20. No re-expression of ASS1 is seen in MSTO cells cultured alone or with

macrophages, following ADI-PEG20 treatment. The ASS1 positive cell line, H226, was used as a positive control. Experiments were performed three times in triplicate.

**A**

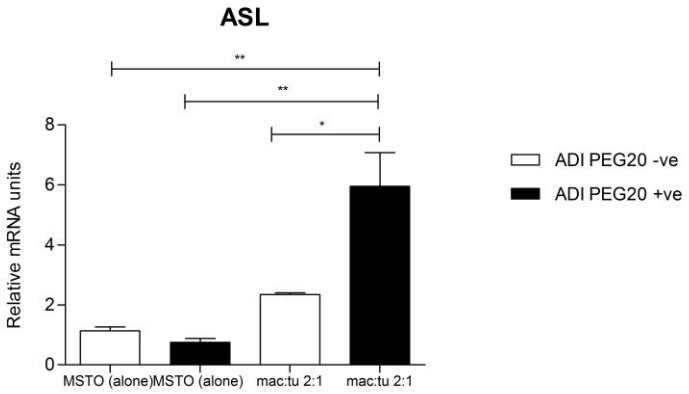


**B**

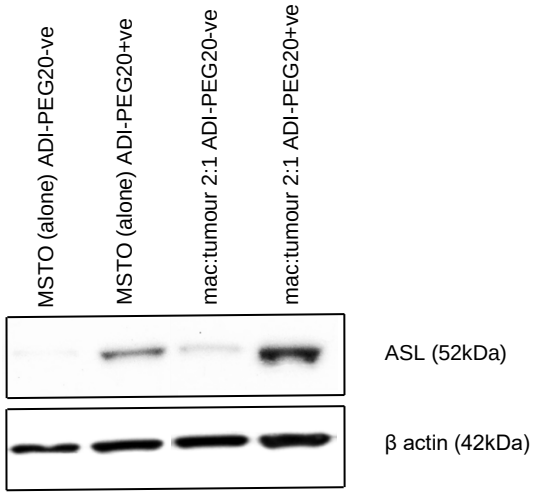


**Figure 4.11. Tumoural ASL expression ± ADI-PEG20 treatment**

**A) qRT-PCR**. Graph shows the relative increase in expression of ASL mRNA in co-cultured MSTO tumour cells at 48 hours following ADI-PEG20 treatment. Experiments were performed three times in triplicate with the values representing the mean (+/- SEM).Statistical analysis (1 way ANOVA with Newman Keuls post-test comparison analysis) * = $p<0.05$, ** = $p<0.01$.

**B) Western Blot**. A significant increase in ASL protein expression is seen in MSTO cells co-cultured with macrophages at 48 hours post ADI-PEG20 treatment, supporting the increased expression in ASL mRNA seen by qRT-PCR. There is also an increase in ASL protein following ADI-PEG20 in macrophages cultured alone, but this is not seen

at mRNA level. Experiment was repeated twice in triplicate with β actin used as a control protein.

## 4.7 Tumour-derived pro-inflammatory cytokines induced by ADI-PEG20 modulate macrophage ASS1 expression

Next, I studied whether the tumour-derived pro-inflammatory cytokines induced by ADI-PEG20 (IL-1α, lL-8, CXCL2, CXCL3 and VEGFA) and associated with ADI-PEG20 resistance in ADAM trial patients (IL-8, CXCL2 and VEGFA; Chapter 3), modulated ASS1 and ASL expression. I found that macrophages stimulated with lL1α, CXCL2, CXCL3 and lL-8, but not VEGFA, increased ASS1 expression to levels comparable to that seen in co-culture. Moreover, the cytokine combination was the most potent inducer of ASS1 (Figure 4.12 A+B), confirming a link between inflammatory and metabolic signalling pathways.

In contrast, tumoural ASL expression was unaffected by cytokine stimulation (Figure 4.13), nor by the addition of the product of ASS1 activity, argininosuccinate, at lower concentrations (Figure 4.14). There was, however, a small decrease in tumoural ASL protein expression following addition of argininosuccinate at higher concentrations.

**A**

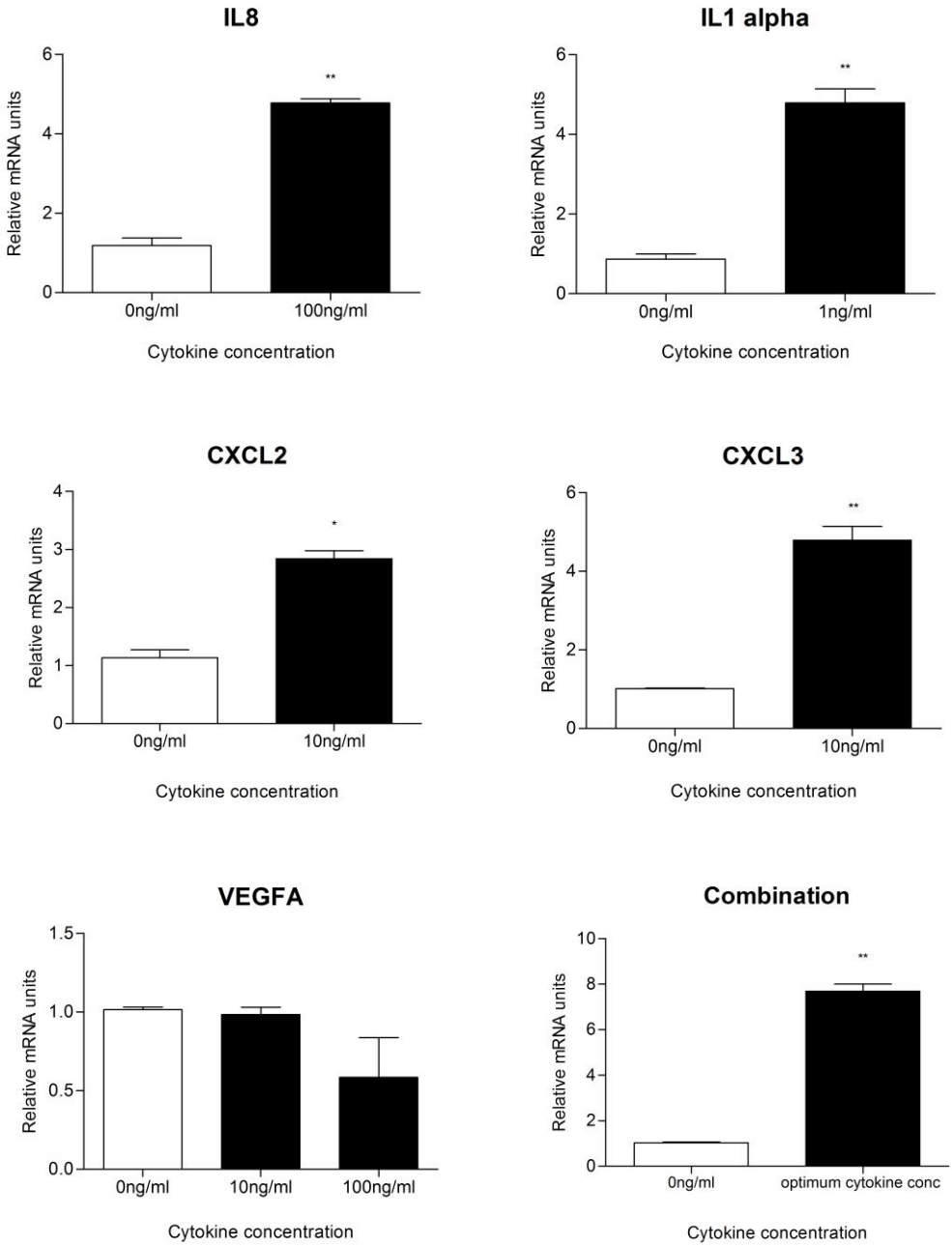


**Figure 4.12 A. Induction of ASS1 in macrophages by pro-inflammatory cytokines (qRT-PCR).** Macrophages were stimulated with pro-inflammatory cytokines for 48 hours. Graphs show the relative increase in expression of ASS1 mRNA following the addition of individual cytokines IL-8, IL-1α, CXCL2 and CXCL3, and a combination of all five. The concentration of individual cytokines added to the combination were: IL-8, 100ng/ml; IL-1α, 1ng/ml; CXCL2, CXCL3 and VEGFA, 10ng/ml. No change is seen in VEGFA expression. Experiments were repeated twice in triplicate with the values representing the mean (+/- SEM). Statistical analysis (unpaired two-tailed t-test), * = $p<0.05$, ** = $p<0.01$.

**B**

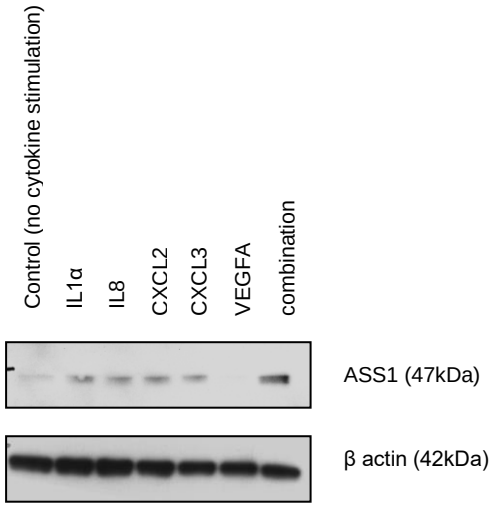


**Figure 4.12 B. Induction of ASS1 in macrophages by pro-inflammatory cytokines (western blot).** Blot shows the increase in macrophage ASS1 protein expression at 48 hours following stimulation with the individual cytokines IL-8 (100ng/ml), IL-1α (1ng/ml), CXCL2 (10ng/ml) and CXCL3 (10ng/ml), and the cytokine combination. The combination results in the most significant increase. Expression of ASS1 protein following VEGFA (10ng/ml) stimulation actually decreases. Experiments were performed twice with βactin used as the protein control.

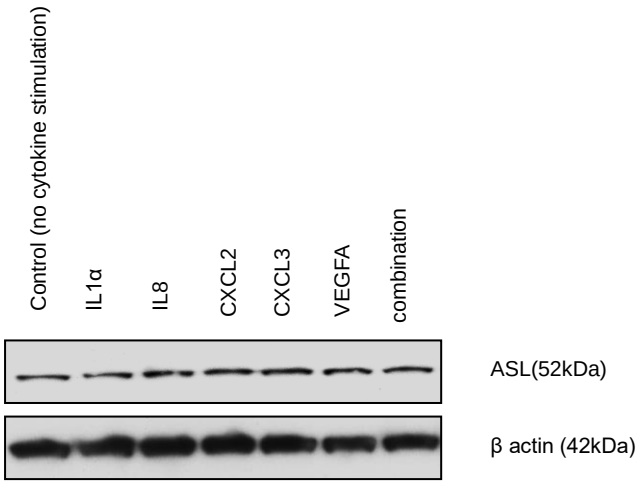


**Figure 4.13. ASL expression in MSTO mesothelioma cells ± pro-inflammatory cytokines.** Western blot shows the expression of ASL protein in tumour cells at 48 hours following stimulation with IL8 (100ng/ml), IL1α (1ng/ml), CXCL2 (10ng/ml), CXCL3 (10ng/ml), VEGFA (10ng/ml) and a combination of all five. There is no difference in expression of ASL, compared with the un-stimulated MSTO control. Experiments were performed twice, with β actin used as the control protein.

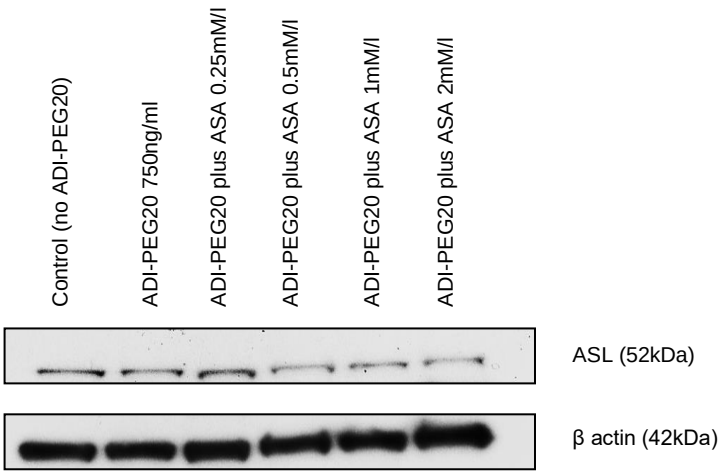


**Figure 4.14. ASL expression in MSTO mesothelioma cells ± ADI-PEG20 and argininosuccinic acid (ASA).** Western blot shows tumour ASL protein expression at 48 hours following treatment with ADI-PEG20 plus ASA at increasing concentrations, compared with the no drug control. There appears to be a decrease in ASL expression at the higher concentrations of ASA. Experiment was performed twice with β actin used as the control protein.

## 4.8 Co-cultured macrophages secrete argininosuccinate following ADI-PEG20

Given the coordinate increase in urea cycle enzymes in macrophages and tumour cells, it was hypothesised that the arginine precursor, argininosuccinate, may be critical to macrophage-mediated resistance to ADI-PEG20. Therefore, I analysed the cell supernatant levels of arginine, citrulline and argininosuccinate from tumour cells and macrophages, alone and in co-culture, by mass spectrometry. As expected, across all conditions, the arginine concentration decreased to negligible levels, with a doubling in citrulline, by 48 hours following ADI-PEG20 treatment (Figure 4.15 A and B). The argininosuccinate concentration in cell supernatant from macrophages cultured alone did not change following ADI-PEG20. Conversely, upon co-culture with ASS1 negative tumour cells, a relative doubling in the argininosuccinate concentration was observed by 48 hours following ADI-PEG20 treatment, indicating that macrophages secrete this amino acid precursor in response to pro-inflammatory signalling from arginine-deprived ASS1 negative mesothelioma cells (Figure 4.16).

**A**

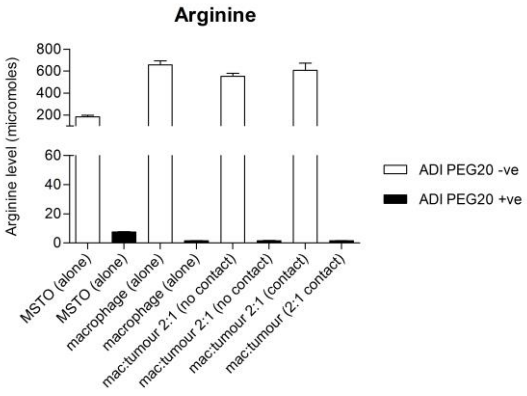


**B**

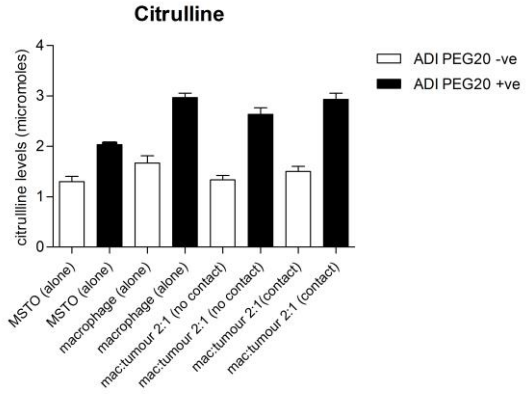


**Figure 4.15. Arginine and Citrulline in supernatant of co-cultured cells ± ADI-PEG20.** Graphs show; A) the decrease in arginine levels by 48 hours following ADI-PEG20 treatment; B) Citrulline levels are almost double following ADI-PEG20 treatment in all conditions. Experiments performed three times in triplicate with the graphs representing the mean (+/- SEM). Cell preparation for mass spectrometry was performed by Melissa Phillips. Mass spectrometry was kindly performed by Dr Essam Ghazaly.

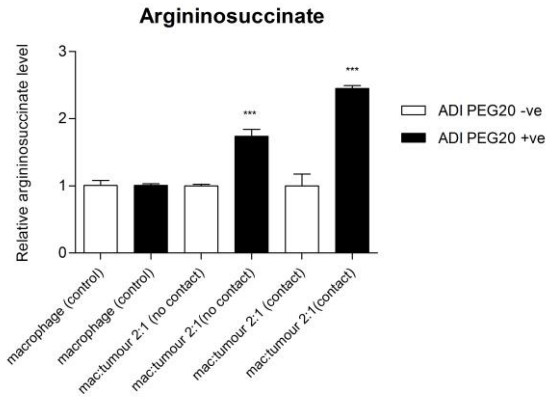


**Figure 4.16. Argininosuccinate in supernatant of co-cultured cells ± ADI-PEG20.** Graph shows the significant increase in argininosuccinate concentration in the supernatant from co-cultured cells at 48 hours following ADI-PEG20 treatment. This is seen in conditions where there is both no direct cell contact and direct cell contact. Each condition with no ADI-PEG20 treatment is normalised to 1 and the ADI-PEG20 treated conditions are shown relative to the no drug control for that condition. The graph is presented in this way due to differences in argininosuccinate baseline levels across the three experiments when analysed by mass spectrometry. Argininosuccinate concentration in the supernatant of tumour cells cultured alone was negligible and is therefore not shown on the graph. Experiments were performed three times in triplicate with values representing the mean (+/- SEM). Statistical analysis (unpaired two-tailed t test) *** = $p<0.001$. Cell preparation for mass spectrometry was performed by Melissa Phillips, mass spectrometry was kindly performed by Dr Essam Ghazaly.

## 4.9 Argininosuccinate rescues ASS1 negative mesothelioma cells from ADI-PEG20-induced cytoxicity

The above results suggest that macrophages mediate resistance to ADI-PEG20 in ASS1 negative mesothelioma cells *via* the delivery of argininosuccinate, in this way bypassing the ADI-PEG20-induced tumour cytotoxicity. To further explore the role of argininosuccinate, ASS1 negative tumour cells were treated with ADI-PEG20 and argininosuccinic acid (ASA; Sigma) was added at increasing concentrations. For consistency with previous co-culture experiments, tumour cell viability was assessed at 4 days. MTS assay results revealed that tumour cell viability increased with escalating concentrations of argininosuccinate, confirming that ASS1 negative tumour cells are able to uptake and utilise argininosuccinate (Figure 4.17). Therefore, argininosuccinate rescues ASS1 negative tumour cells from ADI-PEG20 cytotoxicity.

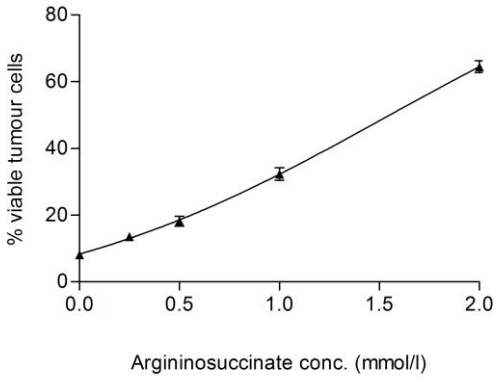


**Figure 4.17. Effect of argininosuccinate on MSTO cell viability following treatment with ADI-PEG20.** MSTO cells were treated with ADI-PEG20 plus argininosuccinic acid (ASA) at increasing concentrations. After four days, cell viability was assessed by MTS. Graph shows the increase in MSTO cell viability with the addition of argininosuccinate, following ADI-PEG20 treatment. Experiment was repeated three times in triplicate with values representing the mean (+/-SEM).

## 4.10 Macrophage-mediated resistance to ADI-PEG20 is reversed by tumoural ASL knockdown

Results from the previous section led to the hypothesis that cytokine-induced argininosuccinate is key to macrophage-mediated resistance. To confirm this, MSTO cells were transfected with SiRNA directed against ASL. Efficient knockdown of ASL mRNA expression knockdown was achieved in MSTO cells by 48 hours and remained below 50% of control levels by 96 hours, enabling the knockdown cells to be used in co-culture experiments (Figure 4.18). I found that cell viability in ASL knockdown tumour cells co-cultured with macrophages was similar to tumour cells cultured alone following ADI-PEG20 treatment. Therefore, macrophage-mediated resistance of ADI-PEG20 is abrogated by silencing ASL (Figure 4.19).

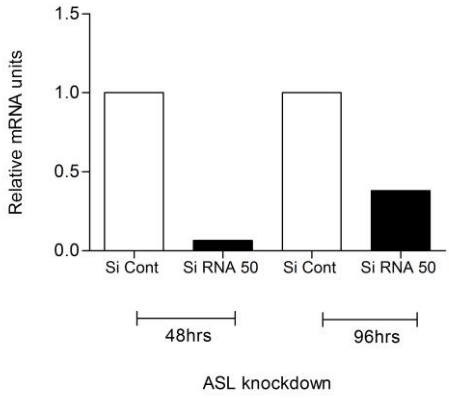


**Figure 4.18. SiRNA knockdown of tumoural ASL mRNA expression.** Graph shows ASL knockdown in MSTO cells after 48 and 96 hours, compared with the SiControl (normalised to 1 at both time points). Experiment was performed once in triplicate.

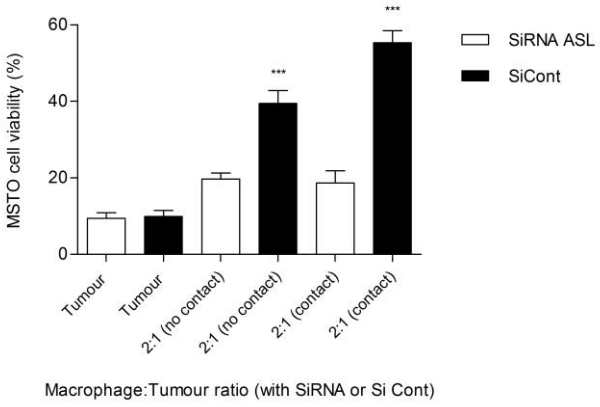


**Figure 4.19. MSTO cell viability following ASL mRNA knockdown and ADI-PEG20.** MSTO tumour cells were transfected with ASL SiRNA or SiControl 50nM as in Figure 4.18. After 8 hours, media was removed and cells were washed three times with PBS. Using one control well, the tumour cells were counted. MSTO cells were then cultured alone and in co-culture with macrophages (with and without direct cell contact at a ratio of 2:1 macrophages to MSTO tumour cells) in the presence and absence of ADI-PEG20. Cell viability was assessed at 4 days by FACS. The graph represents live cells only and shows that ASL mRNA knockdown abrogates the metabolic resistance conferred by macrophages. Experiments and FACS analysis were repeated three times with values representing the mean (+/- SEM). Statistical analysis (1 way ANOVA with Newman Keuls post test analysis ) *** = $p<0.001$.

**A.**

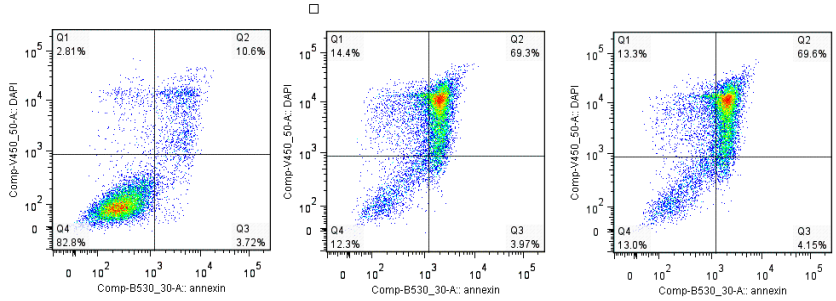


ADI-PEG20 -ve | ADI-PEG20 +ve | ADI-PEG20 +ve SiControl

**B.**

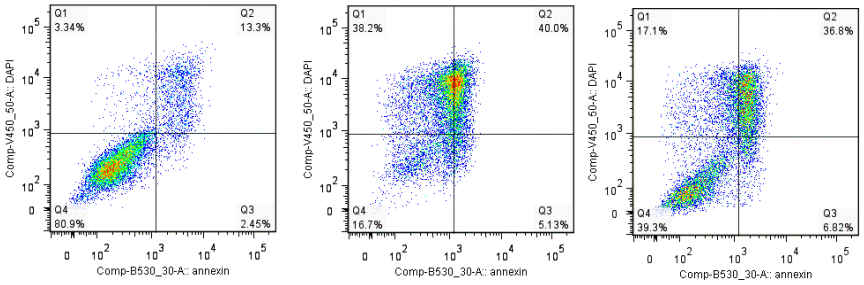


ADI-PEG20 -ve | ADI-PEG20 +ve SiRNA knockdown | ADI-PEG20 +ve SiControl

**C.**

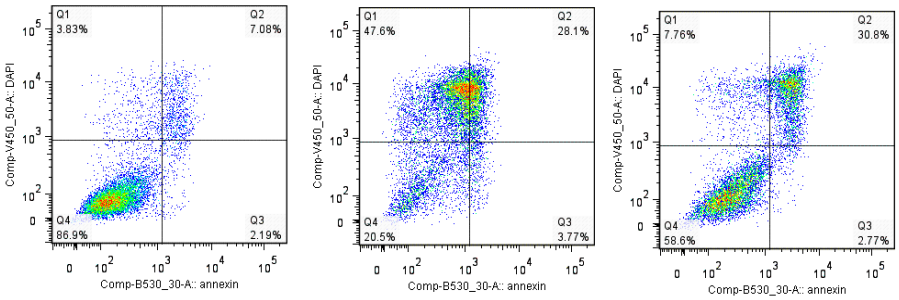


ADI-PEG20 -ve | ADI-PEG20 +ve SiRNA knockdown | ADI-PEG20 +ve SiControl

**Figure 4.20. MSTO tumour cell viability following ASL mRNA knockdown and ADI-PEG20.** A) tumour cells cultured alone; B) tumour cells co-cultured with macrophages without direct cell contact; C) tumour cells co-cultured with macrophages with direct cell contact. Graphs represent one of three experiments analysed by FACS. Key: Q1=DAPI +ve dead cells, Q2=DAPI +ve and annexin V +ve dead cells (apoptosis), Q3=annexin V +ve live cells (undergoing apoptosis), Q4=live cells. 10,000 events were recorded for each condition. Prior to analysis of tumour cell viability, the macrophages from co-culture conditions were identified (using CD14 and CD11b stains) and excluded. Only tumour cells are shown in the graphs.

## 4.11 Proteomic analysis of arginine-labelled peptides in ASS1 negative tumour cells cultured alone and with macrophages

To further validate the mechanism of resistance, proteomic analysis to identify the percentage of arginine-labelled peptides present in ASS1 negative tumour cells cultured alone and with macrophages, was performed. By replacing arginine in the media with $^{13}C$ arginine, the label could be traced through the cells. Arginine-labelled peptides were then identified in tumour cells cultured with and without macrophages by 48 hours of ADI-PEG20 treatment. Results show a small increase in the percentage of arginine labelled peptides identified in the lysates of tumour cells co-cultured with macrophages, compared with tumour cells cultured alone. However, results are difficult to interpret due to the fact that the triplicate results for tumour cells cultured alone across two separate experiments were very different and, furthermore, it is surprising to observe any arginine-labelled peptide in these tumour cells, given that no ASS1 expression was identified. Further experiments are required to understand the results presented here.

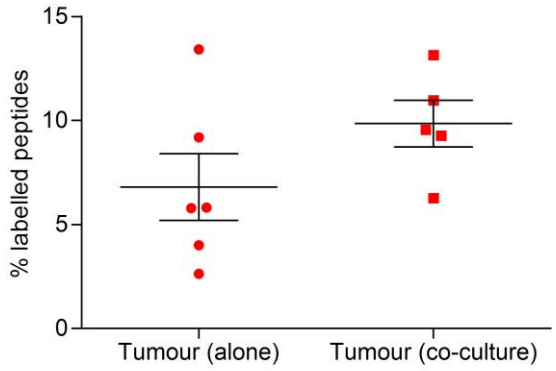


**Figure 4.21. Proteomic analysis identifying the percentage of arginine labelled peptides present in MSTO tumour cells following ADI-PEG20 treatment.** MSTO tumour cells were cultured in SILAC media, ±$^{13}$C arginine, alone and in co-culture with macrophages (with direct cell contact) in the presence and absence of ADI-PEG20. After 48 hours, cells were collected and the tumour cells were separated from the macrophages by live cell sorting, with 99% purity. Tumour cells were then washed with PBS, lysed in 8M urea lysis buffer and stored at -80°C in preparation for proteomic analysis. For proteomics, cell preparation was performed by Dr Pedro-Maria Casado with Melissa Phillips observing. Proteomic analysis was performed by Dr Pedro Cutillas. Graph represents the percentage of arginine labelled peptides identified in tumour cells cultured alone and with macrophages at 48 hours following ADI-PEG20 treatment. Graph is representative of two experiments performed in triplicate. Error bars represent the mean (+/- SEM) of the replicates.

## 4.12 Analysis of macrophage phenotype in the presence and absence of ADI-PEG20

Having demonstrated that macrophages are involved in mediating tumoural resistance to ADI-PEG20, I next wanted to study macrophage phenotype in co-culture in the presence and absence of ADI-PEG20. Macrophage phenotype was assessed by analysing expression of several recognised 'M1' and 'M2' specific cell surface markers (high expression of HLADR in M1skewed macrophages and high expression of CD163 and CD206 in M2skewed macrophages), in addition to expression of the 'M2' intracellular cytokine, IL10, and the enzyme arginase. FACS analysis revealed a cell surface phenotype typical of alternative activation, with increased expression of CD163 and CD206 and a significant decrease in HLA-DR in macrophages co-cultured with tumour cells, compared with macrophages cultured alone in the absence of ADI-PEG20 (Figure 4.22 and 4.23). Interestingly, treatment of co-cultured macrophages with ADI-PEG20 resulted in a decrease in the percentage staining for CD163 and CD206. However, there was also a significant decrease in HLA-DR expression in co-cultured macrophages following ADI-PEG20.

qRT-PCR results showed a significant increase in macrophage expression of IL-10 in macrophages co-cultured with tumour cells, compared with macrophages cultured alone in the absence of ADI-PEG20 (Figure 4.24). Gene expression of IL-10 did not change significantly in co-cultured macrophages following ADI-PEG20 treatment. Conversely, macrophage expression of arginase significantly decreased following ADI-PEG20 treatment (Figure 4.25). Therefore, taken together, results suggest that changes in co-cultured macrophage phenotype following ADI-PEG20 do not fit classic M1or M2 stereotypes, instead displaying heterogeneity. More work is needed to establish the functional relevance of the changes in response to ADI-PEG20.

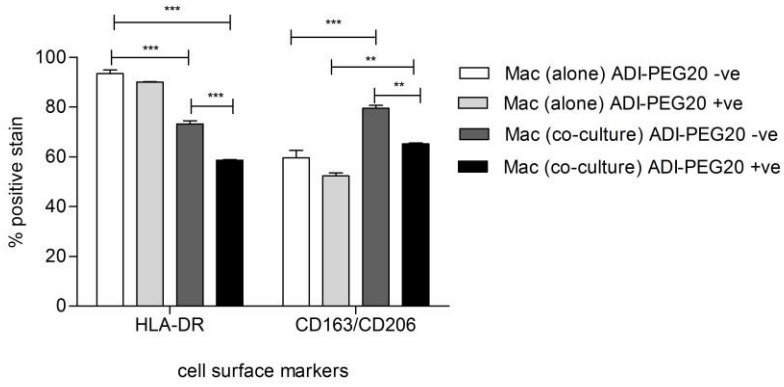


**Figure 4.22. Cell surface marker expression in macrophages cultured alone and with MSTO tumour cells ±ADI-PEG20.** Macrophages were cultured alone and in co-culture with MSTO tumour cells without direct cell contact at a ratio of 2:1 macrophages to tumour cells, in the presence and absence of ADI-PEG20. After three days macrophage cell surface marker expression was analysed by FACS. Graph shows the increase in expression of recognised M2 markers CD163 and CD206 in co-cultured macrophages. Expression of these markers decreases in co-cultured macrophages following ADI-PEG20 treatment. HLA-DR, recognised as being increased in M1 skewed macrophages, significantly decreases in co-cultured macrophages. There is a further decrease following ADI-PEG20 treatment. Experiments were performed three times, with values representing the mean (+/-SEM). Statistical analysis (1 way ANOVA with Newman Keuls multiple comparison post test analysis for each stain; HLA-DR and CD163/CD206) ** = $p<0.01$, *** = $p<0.001$.

**A.** HLA-DR expression

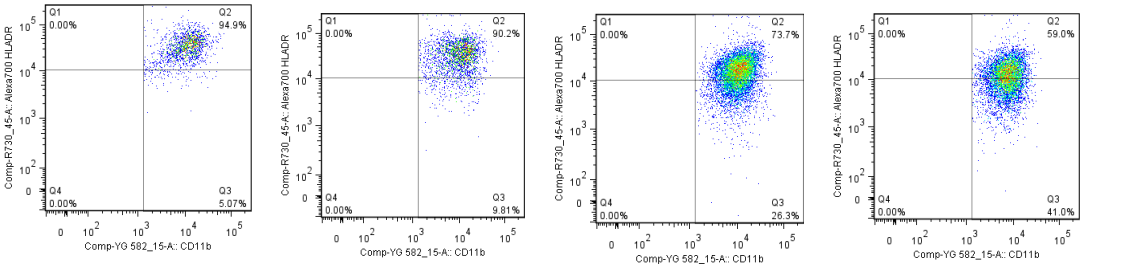


Macrophage (alone) ADI-PEG20 -ve | Macrophage (alone) ADI-PEG20 +ve | Macrophage (co-culture) ADI-PEG20 -ve | Macrophage (co-culture) ADI-PEG20 +ve

**B.** CD163/CD206 expression

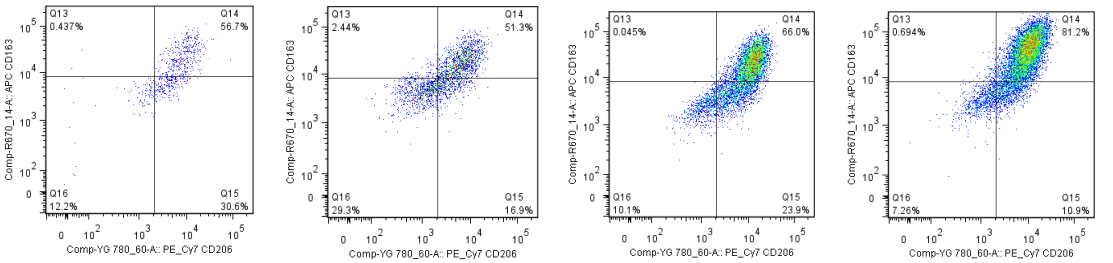


Macrophage (alone) ADI-PEG20 -ve | Macrophage (alone) ADI-PEG20 +ve | Macrophage (co-culture) ADI-PEG20 -ve | Macrophage (co-culture) ADI-PEG20 +ve

**Figure 4.23. Macrophage cell surface marker expression ± ADI-PEG20.** FACS data shown represents one of three experiments performed. Following 3 days of culture ± ADI-PEG20, macrophages were analysed by FACS. A) HLADR expression, B) CD163/CD206 expression. Graphs represent live cells (dead cells were identified using DAPI and excluded).

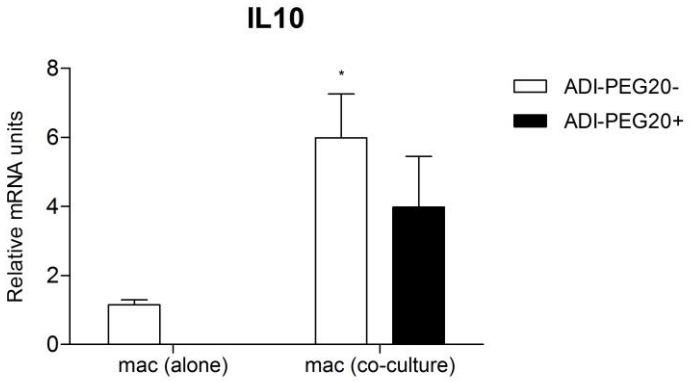


**Figure 4.24. Induction of IL-10 mRNA expression in co-cultured macrophages ± ADI-PEG20.** Macrophages were cultured alone and in co-culture with MSTO tumour cells without direct cell contact at a ratio of 2:1 macrophages to tumour cells, ± ADI-PEG20. After 3 days, macrophages were collected for qRT-PCR analysis. Graph shows an increase in expression of IL-10 in macrophages co-cultured with tumour cells with and without ADI-PEG20, relative to macrophages cultured alone in the absence of ADI-PEG20 (normalised to 1). Experiments performed twice in triplicate with values representing the mean (+/- SEM). Statistical analysis (unpaired two-tailed t test) * = $p<0.05$.

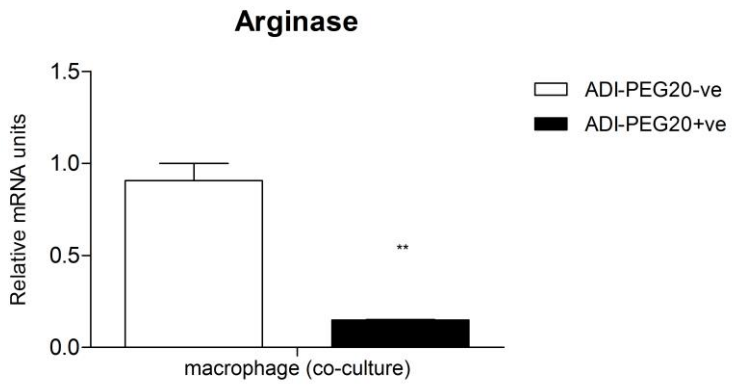


**Figure 4.25. Co-cultured macrophage arginase expression following ADI-PEG20 treatment.** Graph shows the relative decrease in arginase expression in co-cultured macrophages at three days following ADI-PEG20 treatment, compared with co-cultured macrophages in the absence of ADI-PEG20 (normalised to 1). Experiment was repeated twice in triplicate with values representing the mean (+/- SEM). Statistical analysis (unpaired two-tailed t test) ** = $p<0.01$.

## 4.13 Discussion

The metabolic role of macrophages, as abundant host cells within the MPM tumour microenvironment, was examined in ASS1-deficient mesothelioma cells exposed to ADI-PEG20. The results show that TAM have a key modulatory effect on the impact of ADI-PEG20 in the arginine auxotrophic cancer, mesothelioma. The data indicate that ASS1-deficient mesothelioma tumour cells co-opt macrophages to release argininosuccinate, which bypasses the anti-tumour effects of ADI-PEG20 (for a diagrammatic summary, please see Figure 4.26).

Thus, there was a significant pro-inflammatory cytokine response by ASS1 negative mesothelioma cells following ADI-PEG20 which plays a central role in the up-regulation of ASS1 in co-cultured macrophages. Previously, it has been shown that a number of pro-inflammatory cytokines can induce up-regulation of ASS1 in endothelial and inflammatory cells, including TNF alpha, IL1 and TGF beta (112). Here, I have identified members of the ELR +ve CXC subgroup of pro-inflammatory chemokines, CXCL2, CXCL3 and IL-8, as novel regulators of ASS1 expression in macrophages. Furthermore, as this up-regulation is coupled with an increased capacity to protect the tumour cells from ADI-PEG20 cytotoxicity via argininosuccinate secretion, it suggests a key mechanistic link between the inflammatory response and macrophage-mediated resistance evident in co-culture.

ASL expression, although not modulated in macrophages, was found to be significantly increased in co-cultured tumour cells following ADI-PEG20 treatment. However, the stimulus for the increase in ASL expression is unclear, as neither the pro-inflammatory cytokines, nor the addition of argininosuccinate, induced expression. The metabolic crosstalk between ASS1 negative tumour cells and macrophages is likely to involve multiple signalling pathways and identifying signals that induce ASL expression requires further investigation.

It is interesting to note, however, that ASL has been shown to be transcriptionally induced by ER stress (138). In this study, ER stress was induced *in vitro* and *in vivo* using tunicamycin. Results revealed significant up-regulation of ASL mRNA and protein in human hepatoma cell lines *in vitro*. Moreover, ASL was also induced in the livers of C57BL/6 mice following intraperitoneal tunicamycin administration, confirming that ASL expression was induced by ER stress. Further study into the effect of tunicamycin-induced ER stress on ASL expression in the ASS1 negative mesothelioma cell lines would be helpful to identify whether ER stress is a contributing factor in the modulation of ASL expression seen here.

Less is known about the tumoural role of ASL. Recently, ASL has been found to be up-regulated in hepatocellular carcinoma (HCC), with increased expression linked to increased aggressiveness mediated by NO and cyclin A2 signaling (138). In addition, in fumarate hydratase (FH) deficient renal cell cancer (RCC), where ASL is intact, the enzyme's activity is reversed producing high levels of argininosuccinate from arginine and fumarate. (140). As seen with ASS1, the role of ASL in human cancer appears to be dependent on tumour type and further work is needed to gain a better understanding of the significance of ASL expression in tumours.

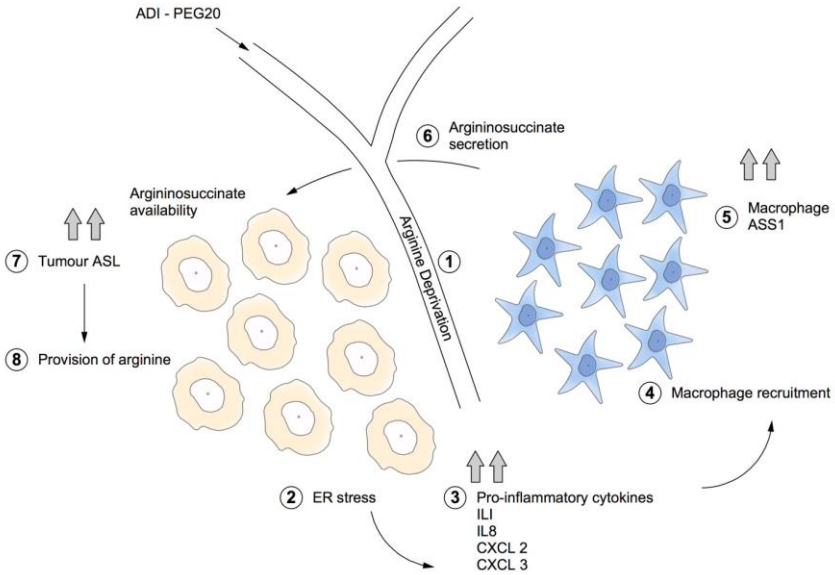


**Figure 4.26. Proposed mechanism of macrophage-mediated resistance to ADI-PEG20 in ASS1 negative mesothelioma.** It is hypothesised that ADI-PEG20-induced arginine deprivation leads to ER stress in ASS1 negative mesothelioma cells, activating the UPR and resulting in pro-inflammatory cytokine secretion. This pro-inflammatory cytokine response induces up-regulation of macrophage ASS1, associated with macrophage secretion of the arginine precursor, argininosuccinate. Via ASL, tumour cells are able to uptake and utilize argininosuccinate to synthesise arginine.

This is the first time that metabolic cooperation resulting in the provision of arginine has been demonstrated between ASS1 negative tumour cells and macrophages in the context of arginine depletion. However, previous research into childhood citrullinemia, an autosomal recessive urea cycle disorder caused by mutations in the ASS1 gene, found that metabolic cooperation also exists between co-cultured fibroblasts deficient in either ASS1 or ASL. Similar to my findings, the coordinate regulation of these urea cycle enzymes resulted in protection of both cell types from arginine depletion (341). In this study, however, it was hypothesised that the delivery of argininosuccinate was primarily via intercellular junctions, and this resulted in almost 100% fibroblast viability. Results from the tumour/macrophage co-cultures instead suggest that a soluble factor is mediating resistance, as tumour cells are not required to be in direct contact with macrophages, and this leads to a smaller increase in tumour cell viability. The protection provided by macrophage-secreted argininosuccinate is also substrate dependent, with tumour cell viability increasing with increasing amounts of argininosuccinate. As the concentration of argininosuccinate in co-culture supernatant was in µM range, this may explain why smaller increases in cell viability were observed. In support of this, a study examining arginine synthesis in cattle kidney cortex also reported that in similar *in vitro* experiments to assess arginine production by HPLC, synthesis of arginine from argininosuccinate was also strongly dependent on substrate concentration. Here, the synthesis of arginine from argininosuccinate was found to be very sensitive to concentrations up to 1mmol/l, and maximum production of arginine was found at 15mmol/l (342). Importantly, this study also demonstrates that argininosuccinate can be utilised by cells to synthesise arginine.

To validate the role of argininosuccinate in ADI-PEG20 resistance, siRNA knockdown of ASL was performed. Results showed that the observed resistance is abrogated following silencing of ASL in the tumour cells, demonstrating that a functioning ASL in ASS1 negative mesothelioma cells is critical for macrophage-mediated resistance to ADI-PEG20. Indeed, ASL is required for the conversion of argininosuccinate to arginine, key to this proposed resistance mechanism. This finding also supports results from a

recent study investigating arginine depletion in glioblastoma multiforme (GBM); Syed and colleagues reported that methylated ASL contributes to the arginine auxotrophy of GBM, with the loss of ASL as well as ASS1 conferring greater sensitivity to ADI-PEG20 (139).

As an alternative method of validation of the described resistance mechanism, proteomic analysis of $^{13}C$ arginine-labelled peptides present in tumour cells cultured alone or with macrophages following ADI-PEG20 treatment, was performed. It was hypothesised that treating the media containing $^{13}C$ labelled arginine with ADI-PEG20 prior to adding it to the MSTO tumour cells ± macrophages, would result in the breakdown of labelled arginine to labelled citrulline before contact with cells. As ASS1 negative cells would be unable to synthesise this citrulline to arginine due to the loss of ASS1 expression, it was proposed that in tumour cells cultured alone, no $^{13}C$ arginine labelled peptides would be identified. In contrast, it was postulated that in tumour cells co-cultured with macrophages, the macrophages could convert the labelled citrulline to argininosuccinate via ASS1 and as shown in the previous experiments, MSTO cells could utilise available argininosuccinate secreted by the macrophages to synthesise arginine. In this way $^{13}C$ arginine labelled peptides would be detectable in co-cultured tumour cells. However, there were technical issues with this experiment. The arginine labelled peptides identified in tumour cells cultured alone were unexpected. This may be because media was added to the cells immediately following the addition of ADI-PEG20, which may have not allowed enough time for the complete breakdown of the labelled arginine. Therefore, tumour cells would have readily taken up any available labelled arginine, altering the results. Future work would require confirmation of arginine depletion in the media prior to adding it to the cells.

It is now widely recognised that cancer cells cooperate with stromal cells and optimise the resources present within their environment to promote tumour growth. Until recently, most research on the mechanisms by which the stromal cells promote tumour growth has focused on changes in the ECM and the increased secretion of tumour promoting cytokines, such as IL-6, IL-8 and

VEGFA (343, 344). Now, increasingly, investigators are considering the metabolic properties of the tumour stroma and the contribution that metabolic cooperation between tumour cells and stromal cells makes to tumour progression (197). Indeed, several independent studies have recently highlighted the importance of metabolic-coupling, where stromal cells serve as 'food donors' for cancer cells, thereby promoting proliferation and invasion (345). For example, CAFs have been shown to serve as a key source of high energy nutrients to fuel cancer cell mitochondrial activity (346). In the crosstalk between CAFs and tumour cells, production of ROS by the tumour cells leads to oxidative stress and activation of key transcription factor HIF1α. By inducing autophagy, HIF1α promotes degradation of Caveolin-1 (Cav-1) in CAFs, leading to dysfunctional mitochondria. As CAFs attempt to remove the dysfunctional mitochondria via mitophagy, they rely on enhanced glycolysis, leading to increased production of energy-rich nutrients. Thus, a 'reversed Warburg' effect occurs in these cells, which secrete the high energy nutrients, including lactate, ketone bodies and glutamine. These molecules are then used by anabolic cancer cells in more oxygenated areas to serve as a source of energy and/or intermediates to biosynthesis (347, 348). Via this metabolic-coupling, CAFs therefore 'feed' cancer cells. The loss of Cav-1 as a result of this coupling is associated with poor clinical outcome in prostate and breast cancers (349, 350).

Adipocytes have also been shown to fuel mitochondrial oxidation and promote tumour growth. Indeed, it was recently reported that in ovarian cancer, tumour cells reprogram the metabolism of adipocytes to become catabolic, leading to lipolysis in adipocytes, with the release of free fatty acids that can be used as a fuel for cancer cells. Ovarian cancer cells adjacent to these activated adipocytes show increased fatty acid uptake and utilisation via β-oxidation in mitochondria, demonstrating that metabolic-coupling also occurs between these two cellular compartments (351).

Here, I have found that tumour cells co-opt macrophages to secrete argininosuccinate, critical to the survival of ASS1-deficient mesothelioma

cells, following arginine depletion. In this situation the argininosuccinate is therefore ‘feeding’ these cancer cells.

Interestingly, macrophage plasticity has previously been shown to be modulated by metabolites and metabolic enzymes within the tumour microenvironment (TME) (352). Both the increased production of lactate by tumour cells and the acidic TME have a profound impact on the secretory profile of TAM, promoting tumour angiogenesis (353, 354). This environment also promotes the development of MDSCs and immune suppression (355). Thus, a metabolic symbiosis is formed with innate immune cells to facilitate tumour growth.

Importantly, tumour-stromal metabolic-coupling also induces drug resistance, as energy-rich metabolites derived from stromal cells are able to maintain mitochondrial ‘well-being’ in cancer cells. Indeed, it was recently discovered that the enhanced mitochondrial activity in epithelial cancer cells promotes tamoxifen resistance in breast cancer. Here, co-culture of oestrogen receptor positive (ER+) MCF7 breast cancer cells with fibroblasts resulted in a 4.4-fold reduction in tumour cell apoptosis following tamoxifen treatment, compared with tumour cells cultured alone. The authors found that combination treatment with a mitochondrial ‘poison’ such as metformin was able to re-sensitise breast cancer cells to tamoxifen (356).

Furthermore, following asparaginase- induced depletion of asparagine, mesenchymal-derived stromal cells are able to ‘feed’ this amino acid to asparagine-auxotrophic leukaemic cells in ALL, thereby protecting these cells from asparaginase cytotoxicity (described in the introduction)(357).

The pro-tumoural effects of TAM, including drug resistance, are generally attributed to the M2-skewed phenotype. It was therefore of interest that macrophages co-cultured with ASS1 negative mesothelioma cells demonstrated cell surface marker expression typical of alternative activation, with increased expression of CD206 and CD163, recognised M2 markers. Furthermore, IL-10 mRNA was significantly increased in co-cultured

macrophages and HLA-DR significantly decreased, compared with macrophages cultured alone, both linked to alternative activation. These findings are consistent with a previous *in vitro* study that analysed ovarian cancer cells in co-culture with macrophages. Investigators here found that following co-culture there were dynamic changes in macrophage expression of IL-10 and development of a cell surface phenotype typical of alternative activation (358). Notably, they also found that one of the genes significantly up-regulated in co-cultured macrophages compared with macrophages cultured alone, was ASS1, which increased 5-fold (using semi-quantitative PCR). mRNA expression of macrophage ASS1 also increased following co-culture with ASS1 negative mesothelioma cells, which may indicate another marker of alternative activation.

However, the phenotype of macrophages following ADI-PEG20 is more difficult to understand. Findings suggest a more complex situation, resulting in functional polarisation towards a mixed M1/M2 phenotype. Indeed, the expression of M2 cell surface markers were decreased and were more comparable with the expression observed in macrophages cultured alone. However, HLR-DR significantly decreased following ADI-PEG20, suggesting an even more immunosuppressive phenotype. It is well-established that plasticity and diversity are hallmarks of macrophages and that these immune cells undergo intense functional re-programming in response to different signals from within the TME, including cytokines and metabolic products of cancer cells (e.g. lactate) (359). Therefore, perhaps exposure to ADI-PEG20, the cytokine response by the tumour to this arginine-depleting agent, and the modulation of metabolic pathways as a result of the loss of arginine, result in the dynamic changes observed in the co-cultured macrophages. Further investigation is required to establish the functional relevance of these changes.

Another significant change in co-cultured macrophages following ADI-PEG20 exposure is the decrease in mRNA expression of arginase. Indeed, arginase is another key marker of alternative activation. However, the decrease here may to be due to the sudden need to endogenously synthesise arginine

following ADI-PEG20-induced arginine depletion, and it has previously been shown that macrophages are able to effectively synthesise arginine (360). Arginine is either catabolised by iNOS to give NO and citrulline, or arginase, to give ornithine and urea. Therefore, as arginine synthesis is essential for macrophage survival in the context of arginine depletion, it is hypothesised that catabolism of arginine may become dominated by iNOS, and the citrulline produced re-cycled to synthesise arginine. This may explain the decrease in arginase expression in co-cultured macrophages following ADI-PEG20 treatment.

It is important to note that arginase expression in TAM has been shown to have a key role in tumour growth, possibly via an arginase-dependent pathway responsible for producing polyamines, substrates that play a critical role in cell proliferation (361). The functional change in arginase expression may therefore have a longer term effect on tumour growth under continued depletion of arginine. This requires further study.

In addition to evaluating macrophage phenotype, macrophage number in human mesothelioma tissue was also assessed, to determine whether numbers differed between ASS1 ‘low’ and ASS1 ‘high’ expressing tumours. Results demonstrated that there was no significant difference in macrophage number between low and high expressing ASS1 mesotheliomas, although there was a trend towards an increase in ASS1 ‘low’ tumours. In view of this observed trend, a more significant difference may be seen with more biopsy analyses. Furthermore, for macrophage quantification, immunohistochemical staining against the pan-macrophage marker CD68 was used. This has a number of limitations, which may affect the results. Firstly, in humans, although CD68 expression is predominantly found on macrophages, it can also be expressed on granulocytes, dendritic cells, fibroblasts, endothelial cells and some lymphoid subsets (236, 245). Secondly, CD68 is not a specific marker for determining macrophage phenotype. As it has previously been shown that high numbers of M2-skewed TAM predict poor prognosis in mesothelioma (283), and, indeed, in many other tumour types (244), perhaps immunohistochemical staining against the M2 cell surface marker CD163 may

be useful in identifying differences in ASS1 ‘low’ and ASS1 ‘high’ expressing mesotheliomas.

In summary, results presented in this chapter clearly demonstrate that as a result of metabolic cooperation, macrophages are able to partially protect ASS1 negative mesothelioma cells from ADI-PEG20 cytotoxicity via provision of the arginine precursor, argininosuccinate. Furthermore, the crosstalk between inflammatory and metabolic signalling pathways is central to this resistance mechanism.

# Chapter 5. Macrophage depletion potentiates the cytotoxic effect of ADI-PEG20 *in vivo*

## 5.1 Introduction

Results presented in the previous chapters have demonstrated that macrophages are able to mediate tumoural resistance to ADI-PEG20 in ASS1 negative MPM, and that the crosstalk between inflammatory and metabolic signalling pathways is critical to this resistance. Therefore, having established a link between pro-inflammatory cytokine signalling, macrophage activation and ADI-PEG20 resistance, the next step was to consider methods to overcome this resistance. This chapter evaluates two methods to overcome macrophage-mediated resistance in MPM; blockade of the CXCL/CXCR2 signalling pathway in vitro and in vivo, and depletion of macrophages in vivo. Ultimately, the aim was to establish whether targeting macrophages in combination with ADI-PEG20 improved the efficacy of ADI-PEG20 in ASS1 negative MPM.

## 5.2 Aims

The aims of this chapter were:

1. To investigate the role of CXCR2 in macrophage-mediated resistance to ADI-PEG20

2. To study the effect of CXCR2 blockade on macrophage-mediated resistance to ADI-PEG20

3. To quantify macrophage number in murine tumours in the presence and absence of ADI-PEG20, to determine whether ADI-PEG20 induces macrophage recruitment into the tumour site.

4. To evaluate whether macrophage depletion potentiates the cytotoxic effect of ADI-PEG20 *in vivo.*

## 5.3 CXCR2 expression is up-regulated in co-cultured macrophages following ADI-PEG20 treatment

As discussed previously, three of the ADI-PEG20-induced chemokines found to up-regulate ASS1 expression in macrophages, IL-8, CXCL2 and CXCL3, promote tumour angiogenesis, proliferation and inflammatory cell recruitment via binding to the G protein-coupled receptor, CXCR2. This indicates that CXCR2 signalling may play a key role in macrophage-mediated resistance to ADI-PEG20. Macrophage CXCR2 expression was therefore evaluated to determine whether there was any modulation following ADI-PEG20 treatment. Results revealed a significant increase in CXCR2 mRNA expression in co-cultured macrophages compared with macrophages cultured alone. A further increase in CXCR2 mRNA expression was seen in co-cultured macrophages following ADI-PEG20 treatment, suggesting that expression of this receptor increases in response to the inflammatory cytokines released by the tumour (Figure 5.1).

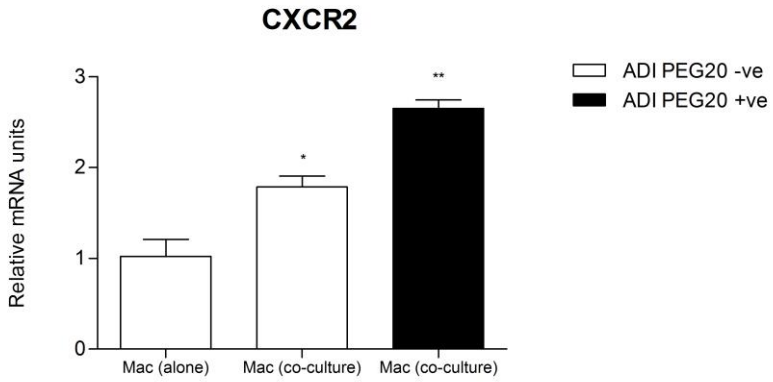


**Figure 5.1. Co-cultured macrophage CXCR2 expression following ADI-PEG20 treatment.** Macrophages were cultured alone and in co-culture with MSTO tumour cells without direct cell contact ±ADI-PEG20 for 24 hours. Graph shows the relative increase in CXCR2 mRNA expression in macrophages co-cultured with tumour cells, compared with macrophages cultured alone (normalised to 1). A further increase is seen following ADI-PEG20 therapy. Experiments were performed twice in triplicate with values representing the mean (+/-SEM). Statistical analysis (unpaired two-tailed t test) * = $p<0.05$, ** = $p<0.01$.

## 5.4 CXCR2 blockade fails to prevent up-regulation of macrophage ASS1 in response to ADI-PEG20

Having identified that CXCR2 is up-regulated in co-cultured macrophages following ADI-PEG20 treatment, it was hypothesised that the CXCR2-axis may be an important link between the inflammatory and metabolic signalling pathways leading to increased macrophage ASS1 expression and subsequently ADI-PEG20 resistance. To investigate this, a small molecule inhibitor of CXCR2, SB225002, was used in combination with ADI-PEG20 in macrophages co-cultured with tumour cells, to determine whether CXCR2 blockade attenuates the increase in expression of macrophage ASS1 following ADI-PEG20 treatment. Results revealed that CXCR2 blockade had no effect on co-cultured macrophage ASS1 expression following ADI-PEG20 treatment, with the increased expression identified on western blot analysis comparable to that seen following ADI-PEG20 alone (Figure 5.2). This implies that blocking CXCR2 alone is not sufficient to dampen the macrophage metabolic response to ADI-PEG20 treatment, indicating that other signalling pathways are able to compensate.

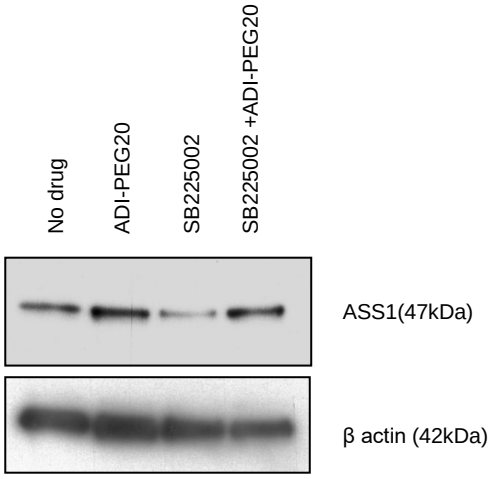


**Figure 5.2. Co-cultured macrophage ASS1 expression following ADI-PEG20 treatment and CXCR2 blockade.** Macrophages were co-cultured with MSTO tumour cells without direct cell contact ±ADI-PEG20 and SB225002 for 48 hours. Blot shows an increase in co-cultured macrophage ASS1 expression following ADI-PEG20 treatment. ASS1 expression also increases with ADI-PEG20 in combination withSB225002.Experiment repeated twice with βactin used as the control protein

## 5.5 CXCR2 blockade has no effect on the anti-tumour efficacy of ADI-PEG20 *in vivo*.

In parallel with evaluating the effect of CXCR2 blockade on macrophage ASS1 expression *in vitro*, a pilot xenograft study was set up to look at the influence of CXCR2 blockade on ADI-PEG20-induced tumour cytotoxicity *in vivo*. Nude mice bearing subcutaneous xenografts of MSTO were treated with SB225002, ADI-PEG20, or a combination of both. Results revealed that ADI-PEG20 suppressed tumour growth ($p=0.07$ with $n=5$) compared with vehicle control. However, although there was a small reduction in tumour volume in mice receiving SB225002 compared with vehicle control ($p=0.28$ with $n=5$), there was no additive effect in supressing mesothelioma growth when combined with ADI-PEG20, compared with ADI-PEG20 alone (Figure 5.3). In view of the results from this pilot study, no further *in vivo* studies evaluating CXCR2 were undertaken.

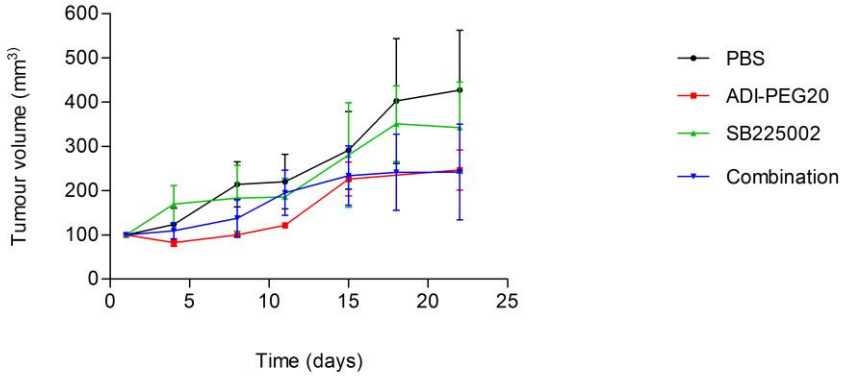


**Figure 5.3. CXCR2 blockade plus ADI-PEG20 in vivo.** In this pilot study 5 mice were used in each of the four conditions (n=20). Tumours were measured twice weekly for the duration of the study. Dosing schedule for both agents is explained in detail in the methods section. Graph shows the difference in tumour volume following ADI-PEG20, SB225002, or a combination of both, compared with vehicle control. Pilot experiment performed once. Statistical analysis (unpaired two-tailed t test at final time point comparing ADI-PEG20 (red) and SB225002 (green) with vehicle control).

## 5.6 Liposomal Clodronate (CLIP) does not affect tumour cell viability *in vitro*

Given that CXCR2 blockade did not demonstrate any additive effect in combination with ADI-PEG20, I next sought to evaluate the effect of depleting macrophages in combination with arginine deprivation *in vivo*. Clodronate-containing liposomes (Liposomal Clodronate; CLIP) were used to deplete macrophages *in vivo*. Previous studies have shown that CLIP is cytotoxic to phagocytic cells of the monocyte/macrophage lineage (282). However, in order to determine the effect of macrophage depletion on tumour growth *in vivo*, it was first necessary to investigate any direct effect of CLIP on ASS1 negative mesothelioma cells. MTS results demonstrate that CLIP has no effect on tumour cell viability *in vitro*, implying that any observed effect of CLIP on tumour growth *in vivo* is due to indirect effects (Figure 5.4).

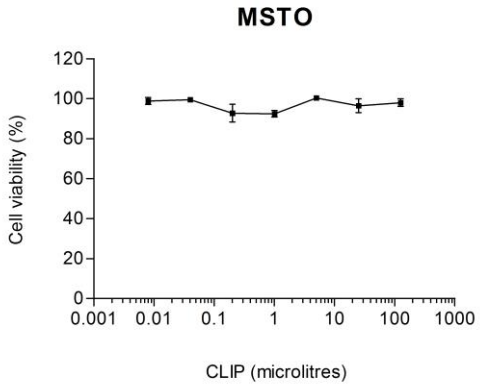


**Figure 5.4. MSTO cell viability at 6 days following treatment with CLIP.** MSTO tumour cells were treated with increasing volumes of CLIP. After 6 days, cell viability was determined by MTS. Graph shows that CLIP has no significant effect on tumour cell viability. Experiments were performed three times in triplicate with values representing the mean (+/- SEM).

## 5.7 Macrophage depletion enhances the cytotoxic effect of ADI-PEG20 *in vivo*

To evaluate the effect of macrophage depletion on ADI-PEG20 cytotoxicity in ASS1 negative mesothelioma cells, nude mice bearing subcutaneous xenografts of MSTO were treated with PBS, CLIP, ADI-PEG20, or a combination of ADI-PEG20 and CLIP. Both ADI-PEG20 and CLIP therapy individually demonstrated similar tumour suppression effects in the mice, compared with vehicle control. Furthermore, the combination of ADI-PEG20 and CLIP therapy had an additive effect in suppressing tumour growth significantly more than ADI-PEG20 or CLIP alone (Figure 5.5).

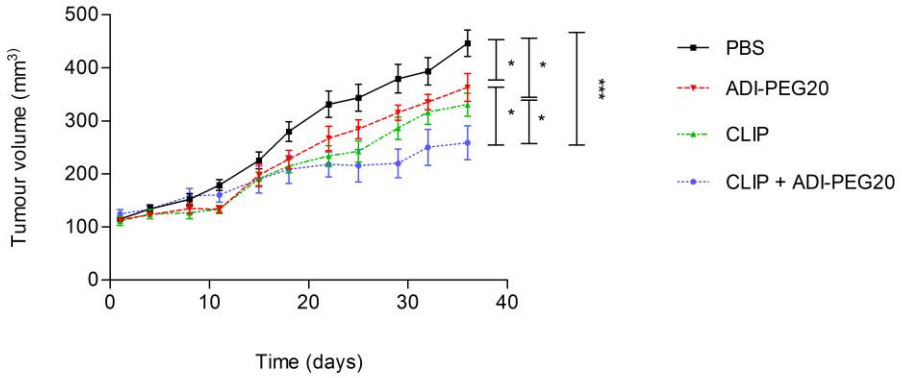


**Figure 5.5. ADI-PEG20 combined with macrophage depletion suppression in the MSTO xenograft model.** For this study nude mice bearing subcutaneous xenografts of MSTO were randomised to the following five groups: PBS, CLIP, PLIP (PBS-containing liposomes as the CLIP control), ADI-PEG20, or a combination of ADI-PEG20 and CLIP, with 12 mice in each group (n=60). The treatment schedule is described in detail in Chapter 2. Tumour volumes for each group were measured twice weekly over a 5 week period. Graph represents the difference in tumour volume between the groups and shows that ADI-PEG20, CLIP, and the combination of ADI-PEG20 and CLIP, all significantly suppress tumour growth, compared with the vehicle control. Furthermore, the combination of ADI-PEG20 with CLIP significantly enhances the tumour suppression effect of ADI-PEG20. Values represent the mean (+/- SEM) tumour volume for each group at specific time points. No difference was seen between PLIP and PBS (data not shown). Two other mouse studies were also completed; one was a pilot with 5 mice per group, and one compared the difference between ADI-PEG20 and ADI-PEG20/CLIP combination with 10 mice per group (without the controls). Similar results were observed (data not shown). Statistical analysis (1 way ANOVA of all 5 groups at the last time point with Newman-Keuls multiple comparison post-test) * = $p<0.05$, ** = $p< 0.01$, *** = $p<0.001$.

## 5.8 ADI-PEG20 stimulates recruitment of macrophages into ASS1 negative xenografts

Having observed that *in vivo*, macrophage depletion in combination with ADI-PEG20 potentiates ADI-PEG20-induced tumour cytotoxicity, I sought to study whether ADI-PEG20 treatment had an effect on macrophage number in tumours. Immunohistochemical staining and analysis of formulin fixed, paraffin embedded (FFPE) tumour sections using the murine macrophage marker, F4/80, demonstrated a significant increase in the number of macrophages present in the tumours of mice treated with ADI-PEG20 therapy compared with vehicle control. CLIP therapy alone effectively depleted macrophages, with a significant decrease in macrophage number also observed in tumours from mice treated with ADI-PEG20/CLIP combination therapy. These results imply that ADI-PEG20 therapy stimulates macrophage recruitment and activation in tumours, which then contributes to ADI-PEG20 resistance (Figure 5.6 and 5.7).

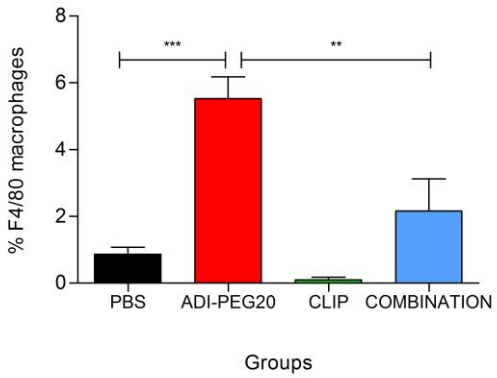


**Figure 5.6. Difference in macrophage number in xenograft tumours following ADI-PEG20 treatment.** The tumours of five mice from each group were analysed for comparison of macrophage number. Graph represents the percentage of F4/80 stained macrophages in each of the five mice from the different experimental conditions. Statistical analysis (1 way ANOVA with Newman Keuls post-test multiple comparison analysis) ** = $p<0.01$, *** = $p<0.001$.

A

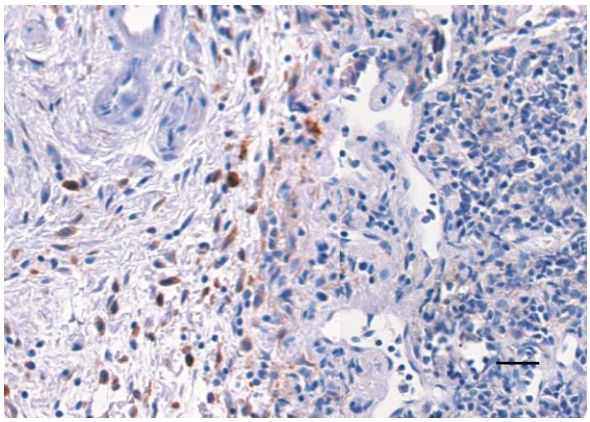

B

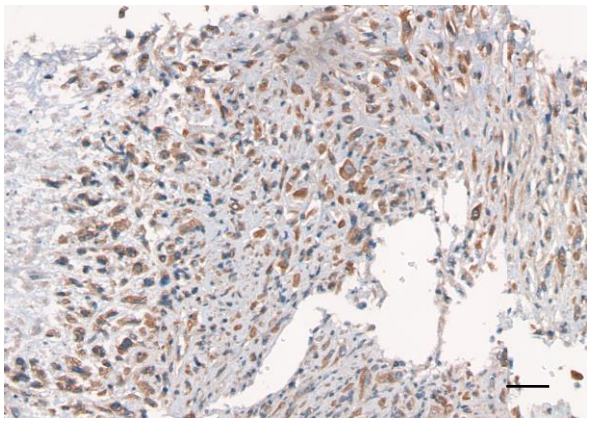

C

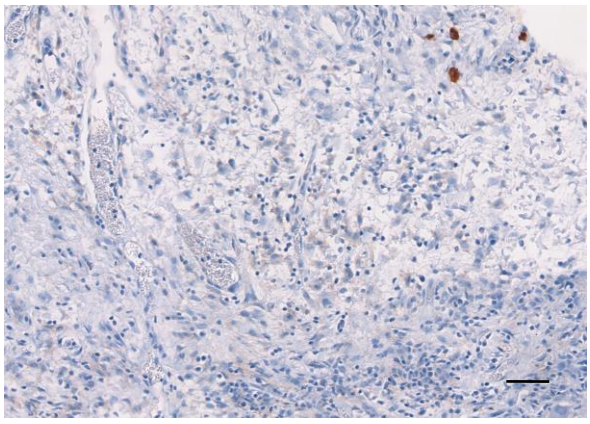

D

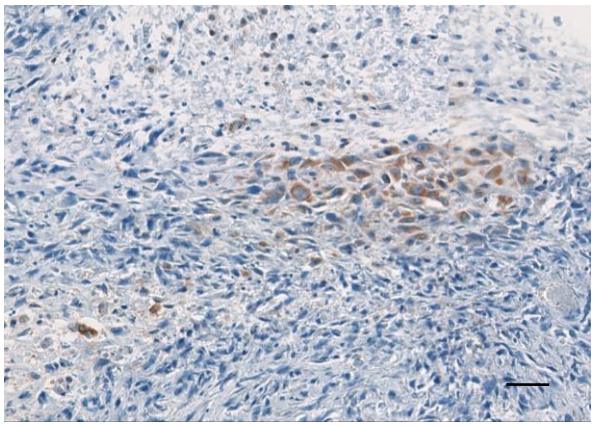

**Figure 5.7. F4/80 expression in mouse xenografts.** Representative examples of tumours treated with A) PBS (vehicle control), B) ADI-PEG20, C) CLIP, D) ADI-PEG20/CLIP combination (magnification x200. Scale bars represent 20µm). Tumours were stained with F4/80, an adhesion protein expressed on the surface of murine macrophages, and counterstained with haemotoxylin. Macrophages are conspicuous as large, brown staining cells with branching cytoplasmic processes. ADI-PEG20 therapy results in a significant increase in F4/80 positive macrophages.

## 5.9 Discussion

The aim of this chapter was to find a method to overcome the macrophage-mediated ADI-PEG20 resistance and in this way enhance the anti-tumour efficacy of ADI-PEG20 *in vivo*. Given that *in vitro* studies had identified abundant secretion of several CXC chemokines by ASS1 negative cells following ADI-PEG20 treatment, all signaling through the G protein-coupled receptor, CXCR2, it was hypothesized that this signaling axis might be playing a role in ADI-PEG20 resistance.

The ELR+ CXC chemokines were originally considered to be chemoattractants for neutrophils via the chemokine receptor CXCR2, but more recently CXCR2 expression has been also identified on other stromal cells, including endothelial cells, mast cells, monocytes and macrophages, as well as on multiple tumour cells (362, 363). Indeed, CXCR2 has become the subject of much interest recently because of a number of studies indicating its involvement in cancer. It has recently been reported that CXCR2 and its ligands are intimately involved in tumour regulation, growth and metastasis of various cancers, including colorectal cancer, melanoma, lung cancer, pancreatic cancer, HCC and head and neck cancers, with blockade of the CXCL/CXCR2 axis reducing tumourigenesis/angiogenesis (364-369).

In addition, the CXCR2 axis has also been linked to therapeutic resistance. For example, an increase in the transcription and secretion of IL-8 and CXCL1, in parallel with increased CXCR2 expression, was observed after oxaliplatin treatment in androgen-independent prostate cancer, and this autocrine signaling was implicated in the attenuation of chemotherapy induced apoptosis (370). More recently, Sharma and colleagues reported a novel role of CXCR2 and its ligands in maintaining chemotherapy resistance in breast cancer. Here, targeting CXCR2 signaling re-sensitised cells to chemotherapy (371).

Importantly, in addition to autocrine signaling, there have been several interesting reports regarding the relationship between the CXCL/CXCR2 paracrine network and tumour development. Indeed, Ijichi and co-workers reported that in a Kras+ TGF-beta receptor type II knockout (Kras+TGFbr2KO) mouse model of pancreatic cancer, the PDAC cells secreted much higher levels of several CXC chemokines compared with mouse pancreatic intraepithelial neoplasia cells, which are preinvasive. The CXC chemokines induced connective tissue growth factor (CTGF) expression in the pancreatic stromal fibroblasts, not in the PDAC cells themselves. Subcutaneous grafting studies revealed that the fibroblasts enhanced growth of PDAC cell allografts, which was attenuated by CXCR2 inhibition. Moreover, treating the Kras+Tgfbr2KO mice with the CXCR2 inhibitor reduced tumour progression. The authors concluded that pancreatic cancer-stromal interactions via a CXCR2-dependent chemokine and connective tissue growth factor axis regulate the progression of pancreatic cancer (372). Moreover, another study has demonstrated a network of endothelial-cancer cells-myeloid signaling mediated by CXCL/CXCR2. Here, overexpression of CXCL1 and CXCL2 (both CXCR2 ligands) in breast cancer cells was found to attract CXCR2-expressing myeloid cells to the tumour. These cells produced S100A8/9 chemokines which enhanced cancer cell survival (336). In line with this study, I found that macrophage CXCR2 expression was significantly increased when macrophages were co-cultured with ASS1 negative mesothelioma cells, with a further increase in expression seen following ADI-PEG20 treatment. This suggested that overexpression and secretion of the CXCR2 ligands by ASS1 negative mesothelioma cells following ADI-PEG20 treatment is attracting and activating CXCR2-expressing macrophages, resulting in ADI-PEG20 resistance. Therefore, it was proposed that these molecules driving the inflammatory response to ADI-PEG20 could have considerable potential as therapeutic targets to overcome macrophage-mediated resistance to ADI-PEG20 in mesothelioma.

However, results showed that CXCR2 blockade was insufficient to attenuate the increase in macrophage ASS1 expression following treatment with ADI-PEG20, implying that there is redundancy, with other pro-inflammatory

signaling pathways able to compensate for the loss of CXCR2. Furthermore, findings from the small pilot xenograft study using CXCR2 blockade in combination with ADI-PEG20 demonstrated no additive effect in suppressing mesothelioma growth *in vivo*, supporting the view that other factors are involved in the signaling crossalk between cell types.

Several limitations which need to be considered when interpreting my results. Firstly, CXCR2 blockade was performed using SB225002, a potent nonpeptide inhibitor of CXCR2. Although this has been validated as an effective inhibitor, with a number of independent studies using this as a method for CXCR2 blockade (373, 374), it would have been helpful to have performed CXCR2 knockdown studies *in vitro*, in addition to using SB225002, to confirm the results observed. Furthermore, due to unforseen circumstances in the animal unit housing the mice, the study had to be terminated early; differences between groups may only have been identified at later time points.

Nevertheless, CXCR2 blockade in combination with ADI-PEG20 does not appear to increase the anti-tumour efficacy of ADI-PEG20.

Given that there was no apparent effect in suppressing mesothelioma growth *in vivo* by blocking CXCR2, the next step was to evaluate the effect of macrophage depletion on ADI-PEG20 cytotoxicity. Macrophages were depleted *in vivo* using Liposomal Clodronate (CLIP). Liposomes are artificially prepared lipid vessels consisting of concentric phospholipid bilayers. They can be used to encapsulate strongly hydrophilic molecules such as clodronate, a non-toxic bisphosphonate. Clodronate will not cross liposomal or cellular phospholipid membranes. After injection, liposomes are ingested and digested by macrophages, followed by intracellular release and accumulation of clodronate. Clodronate then induces apoptosis of the macrophage.

Results revealed that CLIP as a single agent significantly suppressed tumour growth compared with vehicle control, emphasizing the critical role macrophages play in mesothelioma growth. Furthermore, this finding supports results from a previous study demonstrating that macrophage depletion

following CLIP therapy significantly reduced the number of tumours, the area of tumour burden and the percentage of liver and lung metastasis in an orthotopic murine model of mesothelioma (282).

Similarly, ADI-PEG20 has been shown to suppress tumour growth in various ASS1 negative xenograft models (130, 133, 145). In this study, ADI-PEG20 treatment resulted in a small but significant stabilisation of mesothelioma growth *in vivo*; however, it did not prevent subsequent tumour outgrowth. In contrast, a similar study using a xenograft model of ASS1 negative bladder cancer demonstrated superior anti-tumour efficacy using ADI-PEG20 as a single –agent, compared with mesothelioma, by effectively halting tumour growth (133).It is interesting to note again here that results from our lab's Affymetrix analysis revealed that the ASS1negative bladder cell line 253J did not demonstrate the same robust pro-inflammatory gene expression signature as the ASS1 negative mesothelioma cell lines in response to ADI-PEG20 treatment . Given that I have demonstrated a link between pro-inflammatory cytokines and ADI-PEG20 resistance in ASS1 negative MPM, this difference may explain in part the difference in response to ADI-PEG20. Further studies are required to validate this Affymetrix data.

Macrophage number also increased significantly in the MSTO xenografts, to an average of almost 6% of the mesothelioma tumour area, following ADI-PEG20 treatment, implying an increase in TAM infiltration in response to treatment. As described above, the use of CLIP effectively depleted the macrophages and in parallel suppressed tumour growth as efficiently as ADI-PEG20. Furthermore, there was an additive effect when using CLIP in combination with ADI-PEG20, suppressing mesothelioma growth significantly more than ADI-PEG20 or CLIP alone, further supporting a role for macrophages in mediating mesothelioma resistance to ADI-PEG20.

Increased TAM infiltration causing drug resistance has recently been demonstrated in prostate cancer. Similar to my findings, macrophages comprised a significant component of the TME in implanted Myc-CaP murine prostate tumours, as well as in the parental transgenic Hi-Myc spontaneous

prostate cancer model, constituting 2-5% of viable cells within the tumour. Furthermore, there was a significant increase in TAM infiltration following androgen blockade therapy (ABT) (315), associated with drug resistance. Investigators found that inhibition of macrophage recruitment using a CSF-1 receptor inhibitor re-sensitised the tumour cells to ABT and reversed macrophage-mediated resistance. For this study, two murine models were used; a xenograft and a spontaneous prostate cancer model. I used only a xenograft model for studying macrophage infiltration following ADI-PEG20 therapy in mesothelioma. This has its limitations: although the CD1 nu/nu mice do have macrophages, they lack a functioning thymus and therefore have an altered immune system due to the absence of B cells and T cells. When studying the role of immune cells and immune response, the optimal model would be an immunocompetent orthotopic murine model. However, an ASS1 negative orthotopic model was not available. Perhaps creating a stable murine mesothelioma ASS1 knockdown cell line using the CRISPR-Cas9 system may help with future studies investigating ASS1 negative mesothelioma and immune response. Nevertheless, my results provide evidence which suggests that targeting macrophages in combination with ADI-PEG20 in mesothelioma may be a rational combination for increasing its anti-tumour efficacy.

A number of methods can be used to target macrophages. The Liposomal Clodronate used in this study, although well validated in mice, is not used in humans due to the concern over systemic toxicities caused by pan-macrophage depletion. It is interesting to note, however, that it was recently demonstrated for the first time that targeting TAM plays a central role in the anti-tumour activity of the clinically approved agent, Trabectedin. This natural product, derived from the marine organism Ecteinascidia turbinate, is specifically cytotoxic for human and murine macrophages and inhibits the production of CCL2 and IL-6 (375). The selective monocyte/macrophage cytotoxicity has now been shown to be a major component of its potent anti-tumour activity. This finding provides proof-of-principle for macrophage depletion in humans and therefore has implications for the future design of combination therapies. Indeed, a single arm phase 2 study evaluating

Trabectedin as second line therapy in epithelioid MPM and as first/second line therapy in biphasic/sarcomatoid MPM, was recently presented at ASCO 2015 (NCT02194231). Results from the completed cohort of biphasic/sarcomatoid patients demonstrated Trabectedin activity in terms of PFS (29.4% of patients had a PFS >18weeks), and reported that it was well tolerated in this population of patients with advanced disease, concluding that these results merit further investigation with a larger cohort (376).

In addition, there is increasing interest in the development of novel methods for targeting macrophages in human cancers in an effort to eliminate their pro-tumorigenic properties. This is based on pre-clinical data from a number of independent laboratories indicating that macrophage presence and/or activity are malleable *in vivo* (212). Key strategies under investigation include targeting macrophage recruitment, blocking pro-tumour polarisation, or directly promoting macrophage activation. A number of agents are being evaluated in clinical trial in several solid tumour types in an effort to augment the response to cytotoxic therapy (please refer to Table 5.1). To date, the major strategy for inhibiting macrophage recruitment has been to target CSF-1 or the CSF-1 receptor (CSF-1R). Several clinical trials are underway targeting CSF-1R signalling, and a recently completed trial using an anti-CSF-1R antibody reported objective clinical responses in diffuse-type giant cell tumours (377). Alternatively, re-polarising macrophages toward an anti-tumour phenotypic state, either by blocking signals that drive pro-tumour polarisation or by delivering signals that enhance anti-tumour polarisation, could perhaps provide a more efficacious approach. Indeed, a phase I clinical trial of the fully human CD40 agonist antibody CP-870,893 in combination with gemcitabine chemotherapy in patients with advanced pancreatic cancer, demonstrated efficacy via the anti-tumour activities of macrophages (378). Using this agent, investigators identified a modified macrophage phenotype displaying upregulated MHC Class II and CD86 (M1-skewed) expression (379). Importantly, the two studies described here are among the first clinical studies to demonstrate the potential efficacy of macrophage- targeted agents in human cancer.

| Pathway | Target[a] | Efficacy in murine models | Clinical Compounds | Clinical Trials in Solid Tumours[b] |
|---|---|---|---|---|
| **Recruitment** | CD11b | RT, chemotherapy | Rovelizumab | |
| | CSF-1R | Single agent (GBM, PDAC), chemotherapy, RT, angiogenesis inhibitors | PLX3397, AMG820<br><br>IMC-CS4/LY3022855<br><br>RG7155/RO5509554 | NCT01596751 (O)<br>NCT01444404 (C)<br>NCT01349036 (O)<br>NCT01004861 (O)<br>NCT01346358 (O)<br>NCT02265536 (O)<br>NCT01494688 (O)<br>NCT02323191 (O) |
| | CCL2 | Single agent (metastasis PDAC) | Carlumab | NCT00992186 (C)<br>NCT01204996 (C) |
| | Neuropilin-1 | angiogenesis inhibitors | MNRP1685A | NCT00747734 (C)<br>NCT00954642 (C) |
| | ANG2 | single agent (mammary) chemotherapy, angiogenesis inhibitors | Nesvacumab | NCT01271972 (O)<br>NCT01688960 (O) |
| **Polarisation** | IL-4 | single agent (metastasis) chemotherapy, RT | Pascolizumab | |
| | IL-13 | chemotherapy | Lebrikizumab, tralokinumab, GSK679586 | |
| **Function** | IL-6 | | clazakizumab, olokizumab, siltuximab, sirukumab | NCT00433446 (C);<br>NCT00385827 (C)<br>NCT00841191 (C) |
| | TNF-alpha | mitogen-activated protein kinase (MAPK) inhibitors | adalimumab, certolizumab, etanercept, golimumab, infliximab | |
| **Activation** | CD40 | single agent (PDAC), chemotherapy | CP-870,893 | NCT00711191 (C);<br>NCT01456585 (C)<br>NCT02157831 (C);<br>NCT01008527 (O)<br>NCT02225002 (C);<br>NCT00607048 (C)<br>NCT01103635 (O) |

O, ongoing; C, completed

[a]Only targets with clinical compounds are listed

GBM, Glioblastoma multiforme; PDAC, Pancreatic ductal adenocarcinoma; RT, radiotherapy

[b]Data obtained from https://clinicaltrials.gov

**Table 5.1. Macrophage Therapeutic Targeting.** Table shows macrophage targets currently under investigation. Adapted from Ruffell and Coussens (212)

When considering targeting macrophages in combination with other anti-cancer therapies, the question still remains which of these approaches will be the most efficacious? With regards to ADI-PEG20, my *in vitro* work suggests a mixed M1/M2 macrophage phenotype. The functional relevance of the changes seen in co-cultured macrophages in response to ADI-PEG20 remains unclear, which may make re-polarisation more difficult in combination with ADI-PEG20. However, as the phenotype was immunosuppressive, with a significant decrease in MHC Class II expression observed following ADI-PEG20, perhaps directly promoting M1-skewed macrophage activation and increasing the antigen presentation, as seen with the anti-CD40 antibody, may prove an effective combination. Certainly, going forward, it will be critical to understand the best therapeutic approach to accompany combination therapy, as this is likely to vary for different tumour types and at different stages of tumour progression. Toxicity also remains a key concern for combinatorial studies. Nevertheless, data presented in this thesis suggests that, with the right agent, targeting macrophages in combination with ADI-PEG20 in the clinical setting may increase its anti-tumour efficacy in mesothelioma. Ultimately, with further research, this combination may improve the treatment efficacy of many cancers that depend on arginine for survival.

# Chapter 6. Conclusions and future research

## 6.1 Summary

An investigation into mechanisms of tumoural resistance to ADI-PEG20 in the arginine-auxotrophic cancer, MPM, led to the discovery that macrophages within the mesothelioma tumour microenvironment have a key modulatory effect on the impact of ADI-PEG20 therapy in this disease. Thus, ASS1-deficient malignant mesothelioma cells co-opt macrophages to release argininosuccinate, which bypasses the anti-tumour effects of ADI-PEG20.

The main findings of the work presented in this thesis are:

Identification and validation of a robust pro-inflammatory gene expression signature specific to ASS1-negative mesothelioma cells and patients in response to ADI-PEG20 treatment (chapter 3).

- Discovery of a role for ER stress in modulating the inflammatory response to ADI-PEG20-induced arginine depletion.

Macrophages promote resistance to ADI-PEG20 therapy in ASS1 negative MPM (chapter 4).

- Macrophages are able to partially protect ASS1 negative MPM cells from ADI-PEG20 cytotoxicity.
- ADI-PEG20 causes coordinate up-regulation of ASS1 and ASL in macrophages and tumour cells, respectively. Pro-inflammatory cytokines IL-1α, IL-8, CXCL2 and CXCL3 induce up-regulation of ASS1 in macrophages.

- Co-cultured macrophages secrete argininosuccinate in response to ADI-PEG20 treatment.
- Silencing of tumoural ASL abrogates macrophage-mediated resistance to ADI-PEG20.

Macrophage depletion potentiates ADI-PEG20 cytotoxicity *in vivo* (chapter 5).

- ADI-PEG20 in combination with macrophage depletion has an additive effect in suppressing MPM tumour growth significantly more than ADI-PEG20 alone.

## 6.2 Conclusions

In recent years, medical oncology has placed significant focus on personalizing therapeutic approaches, with the aim of identifying patient subpopulations that would benefit from specific targeted therapies. The use of the arginine-depleting agent ADI-PEG20 in patients with ASS1-deficient malignancies, including MPM, is an example of a promising novel single target therapeutic approach. However, resistance to targeted therapies remains the major obstacle to their effective use in the clinical setting. A better understanding of tumoural resistance mechanisms is therefore critical to improving outcome. The exploration of therapeutic resistance has largely focused on the tumour cell; however, increasingly, the influence of the local tumour microenvironment is being identified as an important contributor to drug resistance (380) . Macrophages are recognised as abundant cells within the tumour microenvironment, with evidence indicating that they promote tumour growth and metastasis in a wide range of solid tumours. However, despite advances in our understanding of the pro-tumourigenic function of TAM, less is known about the microenvironmental and metabolic factors which enable tumour cells to co-opt macrophages to promote tumour growth and drug resistance (381) . The work presented here shows for the first time

that macrophages within the mesothelioma tumour microenvironment are able to mediate tumoural resistance to ADI-PEG20, and that it is the cross-talk between inflammatory and metabolic signaling pathways that is critical to this resistance mechanism. This data highlights the importance of the dynamic and adaptive dialogue that exists between tumour cells and their surrounding microenvironment in promoting tumour growth and drug resistance and raises the question; in the clinical setting, can durable responses result from combination therapies that target both the ASS1 negative mesothelioma tumour cells and the tumour stroma?

## 6.3 Future work

### 6.3.1 Alternative methods of targeting macrophages

#### *6.3.1.1 Inhibition of macrophage recruitment*

For this thesis, macrophage depletion was achieved *in vivo* using liposomal clodronate. It would be interesting to use an alternative method of targeting macrophages, such as targeting macrophage recruitment via CSF-1/CSF-1R blockade, to evaluate whether this has the same additive effect in combination with ADI-PEG20. Furthermore, if an additive effect in combination with ADI-PEG20 is observed, this agent could also potentially be used in the clinical setting. Indeed, trials of novel CSF-1R antagonists have commenced in other solid tumours and results are awaited (please see table 5.1 for details).

#### *6.3.1.2 Targeting ER Stress*

ER stress and the UPR function as a 'double-edge sword', by supporting or repressing cancer initiation and progression under different circumstances (382). Data presented in chapter 3 demonstrates that in ASS1 negative mesothelioma cells, activation of the UPR following ADI-PEG20-induced arginine depletion supports mesothelioma cell survival by leading to induction of the pro-inflammatory cytokine response that is critical to the macrophage-

mediated resistance to ADI-PEG20. Furthermore, as mentioned previously, ER stress has been reported to trigger tumour cells to modulate macrophage phenotype (331) via the release of soluble factors, resulting in both the induction of an ER stress response and a robust pro-inflammatory phenotype in macrophages, further supporting tumour cell survival. Therefore, as the UPR can promote tumour cell adaptation and drug resistance, and activate macrophages within the tumour cell microenvironment, combination therapies that include drugs targeting ER stress and the UPR with ADI-PEG20 in ASS1-deficient MPM may enhance the sensitivity of mesothelioma cells to ADI-PEG20. Indeed, in other examples, an IRE1α inhibitor sensitized resistant human glioblastoma cells to oncolytic virus therapy both *in vitro* and *in vivo* (383). Inhibition of PERK was also shown to kill hypoxic tumour cells that are radioresistant *in vivo* (384). Following on from work presented in this thesis, a potential target of UPR signalling to consider investigating further is NFκB. I have shown in chapter 3 that NFκB is induced in ASS1 negative cell lines following ADI-PEG20. NFκB is activated by the UPR signalling pathways and is well-recognised as a master transcriptional regulator of pro-inflammatory pathways. Therefore, it would be interesting to evaluate whether blocking NFκB would dampen the inflammatory response to ADI-PEG20 therapy and in this way attenuate macrophage-mediated resistance.

### 6.3.2 Assessment of ADI-PEG20 in combination with chemotherapy

When considering rational drug combinations to enhance the efficacy of ADI-PEG20, it is also important to evaluate the effect of ADI-PEG20 in combination with chemotherapy. Chemotherapy can promote an inflammatory microenvironment (385). On the other hand, chemotherapy has been shown to stimulate antigen presentation on infiltrating immune cells, leading to enhanced adaptive anti-tumour immune response (386, 387). Chemotherapy in combination with ADI-PEG20 may therefore affect macrophage phenotype and in this way modulate macrophage-mediated resistance. Furthermore,

dexamethasone is used in chemotherapy regimes, and this anti-inflammatory agent may suppress the pro-inflammatory cytokine response to ADI-PEG20, in this way enhancing ADI-PEG20 cytotoxicity. There is currently a clinical trial assessing ADI-PEG20 in combination with chemotherapy and recruitment will be completed by the end of 2016.

#### *6.3.2.1 ADI-PEG20 with pemetrexed and cisplatin for lung cancer and mesothelioma (TRAP) study.*

The TRAP study is a phase 1 study that is currently recruiting patients with mesothelioma and other ASS1-deficient tumours, to assess ADI-PEG20 in combination with pemetrexed and cisplatin chemotherapy. Plasma samples are being collected from this cohort of patients with ASS1 'low' disease each week, and these samples will be analysed by ELISA for the pro-inflammatory cytokines identified previously (IL-1α, IL-8, CXCL2, CXCL3 and VEGFA) in response to ADI-PEG20 plus pemetrexed and cisplatin. The objective is to assess whether the addition of chemotherapeutic agents in combination with ADI-PEG20 modulates the pro-inflammatory cytokine response, and the impact this may have on macrophage-mediated resistance.

In parallel with this analysis, it would be interesting to set up *in vitro* co-culture experiments using ASS1 negative tumour cells and macrophages, to evaluate the effect of ADI-PEG20 in combination with pemetrexed and cisplatin on macrophage phenotype (analysed by FACS as in Chapter 4) and macrophage-mediated resistance.

### 6.3.3 Further assessment of the regulation of ASL

Results presented in Chapter 4 demonstrated that ASL expression was significantly increased in co-cultured ASS1 negative tumour cells following ADI-PEG20 treatment. However, the stimulus for the increase in ASL expression was not clear, as neither the pro-inflammatory cytokines, nor the

addition of argininosuccinate, induced expression. Identifying signals that induce ASL expression in ASS1 negative tumour cells therefore requires further investigation. Indeed, a better understanding of the regulation of ASL expression may allow therapeutic intervention here, in this way abrogating macrophage-mediated resistance. As previously discussed, ASL has been shown to be transcriptionally induced by ER stress (138). Assessment of ASL expression in ASS1 negative mesothelioma cells following exposure to tunicamycin would therefore be interesting.

### 6.3.4 Further Proteomics analysis of the macrophage-mediated resistance pathway

Proteomic analysis of ASS1 negative tumour cell lysates was performed to identify the percentage of $^{13}C$ arginine-labelled peptides in tumour cells co-cultured with macrophages, compared with tumour cells cultured alone, as an alternative method of validating the macrophage-mediated resistance pathway. However, results were difficult to interpret due to technical issues with the experiment. It would therefore be helpful to confirm depletion of the $^{13}C$ arginine by ADI-PEG20 prior to adding this media to the cells, in this way reducing the risk of false positives.

### 6.3.5 Assessment of the effect of arginine depletion on other stromal cells within the MPM tumour microenvironment

For this thesis, macrophages were considered to be the optimal stromal cell type to evaluate for a number of reasons. Firstly, macrophages are abundant and important host-derived cells within the MPM tumour microenvironment. Secondly, they are recruited and activated by the pro-inflammatory cytokines initially identified at the beginning of the project. However, many other cell types make up this microenvironment and a key cell type requiring further investigation is the fibroblast. Indeed, as discussed in the introduction, fibroblasts are also found in abundance in MPM. Moreover, previous co-

culture studies using fibroblasts and mesothelioma cells demonstrated that fibroblasts promoted MPM tumour progression via a malignant cytokine network (196). Can fibroblasts partially protect ASS1 negative MPM cells from ADI-PEG20 cytotoxicity? Certainly, previous research into citrullinaemia demonstrated that fibroblasts deficient in ASS1 and ASL, when cultured together, were able to ‘feed’ each other the required amino acid, highlighting their ability to cooperate metabolically with each other (341). Perhaps metabolic cooperation also exists between fibroblasts and ASS1 negative MPM tumour cells as well? This requires further investigation, initially by evaluating whether the pro-inflammatory cytokines identified induce up-regulation of ASS1 in fibroblasts, a key step in macrophage-mediated resistance.

Ultimately, a better understanding of the cross-talk between cells of the tumour microenvironment and potential resistance pathways will help lead to new therapeutic targets, with the aim of overcoming this microenvironment-conferred survival advantage to tumour cells.

# Bibliography

1. Robinson BW, Lake RA. Advances in malignant mesothelioma. N Engl J Med. 2005;353(15):1591-603.

2. Porpodis K, Zarogoulidis P, Boutsikou E, Papaioannou A, Machairiotis N, Tsakiridis K, et al. Malignant pleural mesothelioma: current and future perspectives. J Thorac Dis. 2013;5(Suppl 4):S397-S406.

3. Carbone M, Ly BH, Dodson RF, Pagano I, Morris PT, Dogan UA, et al. Malignant mesothelioma: facts, myths, and hypotheses. J Cell Physiol. 2012;227(1):44-58.

4. Wagner JC, Sleggs CA, Marchand P. Diffuse pleural mesothelioma and asbestos exposure in the North Western Cape Province. British journal of industrial medicine. 1960;17:260-71.

5. Armstrong BK, Musk AW, Baker JE, Hunt JM, Newall CC, Henzell HR, et al. Epidemiology of malignant mesothelioma in Western Australia. The Medical journal of Australia. 1984;141(2):86-8.

6. Gennaro V, Ceppi M, Boffetta P, Fontana V, Perrotta A. Pleural mesothelioma and asbestos exposure among Italian oil refinery workers. Scandinavian journal of work, environment & health. 1994;20(3):213-5.

7. Morinaga K, Kishimoto T, Sakatani M, Akira M, Yokoyama K, Sera Y. Asbestos-related lung cancer and mesothelioma in Japan. Industrial health. 2001;39(2):65-74.

8. Ribak J, Lilis R, Suzuki Y, Penner L, Selikoff IJ. Malignant mesothelioma in a cohort of asbestos insulation workers: clinical presentation, diagnosis, and causes of death. British journal of industrial medicine. 1988;45(3):182-7.

9. Lievense LA, Bezemer K, Aerts JG, Hegmans JP. Tumor-associated macrophages in thoracic malignancies. Lung Cancer. 2013;80(3):256-62.

10. Yang H, Rivera Z, Jube S, Nasu M, Bertino P, Goparaju C, et al. Programmed necrosis induced by asbestos in human mesothelial cells causes high-mobility group box 1 protein release and resultant inflammation.

Proceedings of the National Academy of Sciences of the United States of America. 2010;107(28):12611-6.

11. Jaurand MC, Fleury-Feith J. Pathogenesis of malignant pleural mesothelioma. Respirology. 2005;10(1):2-8.

12. Christensen BC, Houseman EA, Godleski JJ, Marsit CJ, Longacker JL, Roelofs CR, et al. Epigenetic profiles distinguish pleural mesothelioma from normal pleura and predict lung asbestos burden and clinical outcome. Cancer research. 2009;69(1):227-34.

13. Tsou JA, Galler JS, Wali A, Ye W, Siegmund KD, Groshen S, et al. DNA methylation profile of 28 potential marker loci in malignant mesothelioma. Lung cancer. 2007;58(2):220-30.

14. Christensen BC, Godleski JJ, Marsit CJ, Houseman EA, Lopez-Fagundo CY, Longacker JL, et al. Asbestos exposure predicts cell cycle control gene promoter methylation in pleural mesothelioma. Carcinogenesis. 2008;29(8):1555-9.

15. Fischer JR, Ohnmacht U, Rieger N, Zemaitis M, Stoffregen C, Kostrzewa M, et al. Promoter methylation of RASSF1A, RARbeta and DAPK predict poor prognosis of patients with malignant mesothelioma. Lung cancer. 2006;54(1):109-16.

16. Carbone M, Kratzke RA, Testa JR. The pathogenesis of mesothelioma. Semin Oncol. 2002;29(1):2-17.

17. Carbone M, Emri S, Dogan AU, Steele I, Tuncer M, Pass HI, et al. A mesothelioma epidemic in Cappadocia: scientific developments and unexpected social outcomes. Nat Rev Cancer. 2007;7(2):147-54.

18. Metintas S, Metintas M, Ucgun I, Oner U. Malignant mesothelioma due to environmental exposure to asbestos: follow-up of a Turkish cohort living in a rural area. Chest. 2002;122(6):2224-9.

19. Goodman JE, Nascarella MA, Valberg PA. Ionizing radiation: a risk factor for mesothelioma. Cancer causes & control : CCC. 2009;20(8):1237-54.

20. Travis LB, Fossa SD, Schonfeld SJ, McMaster ML, Lynch CF, Storm H, et al. Second cancers among 40,576 testicular cancer patients: focus on long-term survivors. J Natl Cancer Inst. 2005;97(18):1354-65.

21. Hodgson DC, Gilbert ES, Dores GM, Schonfeld SJ, Lynch CF, Storm H, et al. Long-term solid cancer risk among 5-year survivors of Hodgkin's lymphoma. J Clin Oncol. 2007;25(12):1489-97.
22. Cutrone R, Lednicky J, Dunn G, Rizzo P, Bocchetta M, Chumakov K, et al. Some oral poliovirus vaccines were contaminated with infectious SV40 after 1961. Cancer Res. 2005;65(22):10273-9.
23. Bocchetta M, Eliasz S, De Marco MA, Rudzinski J, Zhang L, Carbone M. The SV40 large T antigen-p53 complexes bind and activate the insulin-like growth factor-I promoter stimulating cell growth. Cancer Res. 2008;68(4):1022-9.
24. Gazdar AF, Butel JS, Carbone M. SV40 and human tumours: myth, association or causality? Nat Rev Cancer. 2002;2(12):957-64.
25. Carbone M, Pass HI, Rizzo P, Marinetti M, Di Muzio M, Mew DJ, et al. Simian virus 40-like DNA sequences in human pleural mesothelioma. Oncogene. 1994;9(6):1781-90.
26. Cicala C, Pompetti F, Carbone M. SV40 induces mesotheliomas in hamsters. Am J Pathol. 1993;142(5):1524-33.
27. Robinson C, van Bruggen I, Segal A, Dunham M, Sherwood A, Koentgen F, et al. A novel SV40 TAg transgenic model of asbestos-induced mesothelioma: malignant transformation is dose dependent. Cancer research. 2006;66(22):10786-94.
28. Kroczynska B, Cutrone R, Bocchetta M, Yang H, Elmishad AG, Vacek P, et al. Crocidolite asbestos and SV40 are cocarcinogens in human mesothelial cells and in causing mesothelioma in hamsters. Proceedings of the National Academy of Sciences of the United States of America. 2006;103(38):14128-33.
29. Ashburner M, Ball CA, Blake JA, Botstein D, Butler H, Cherry JM, et al. Gene ontology: tool for the unification of biology. The Gene Ontology Consortium. Nature genetics. 2000;25(1):25-9.
30. Roe OD, Stella GM. Malignant pleural mesothelioma: history, controversy and future of a manmade epidemic. European respiratory review : an official journal of the European Respiratory Society. 2015;24(135):115-31.
31. Sekido Y. Molecular pathogenesis of malignant mesothelioma. Carcinogenesis. 2013;34(7):1413-9.

32. Lee AY, Raz DJ, He B, Jablons DM. Update on the molecular biology of malignant mesothelioma. Cancer. 2007;109(8):1454-61.
33. James MF, Han S, Polizzano C, Plotkin SR, Manning BD, Stemmer-Rachamimov AO, et al. NF2/merlin is a novel negative regulator of mTOR complex 1, and activation of mTORC1 is associated with meningioma and schwannoma growth. Molecular and cellular biology. 2009;29(15):4250-61.
34. Takeda M, Kasai T, Enomoto Y, Takano M, Morita K, Kadota E, et al. Genomic gains and losses in malignant mesothelioma demonstrated by FISH analysis of paraffin-embedded tissues. Journal of clinical pathology. 2012;65(1):77-82.
35. Murakami H, Mizuno T, Taniguchi T, Fujii M, Ishiguro F, Fukui T, et al. LATS2 is a tumor suppressor gene of malignant mesothelioma. Cancer research. 2011;71(3):873-83.
36. Altomare DA, Vaslet CA, Skele KL, De Rienzo A, Devarajan K, Jhanwar SC, et al. A mouse model recapitulating molecular features of human mesothelioma. Cancer research. 2005;65(18):8090-5.
37. Lopez-Lago MA, Okada T, Murillo MM, Socci N, Giancotti FG. Loss of the tumor suppressor gene NF2, encoding merlin, constitutively activates integrin-dependent mTORC1 signaling. Molecular and cellular biology. 2009;29(15):4235-49.
38. Pan D. The hippo signaling pathway in development and cancer. Developmental cell. 2010;19(4):491-505.
39. Carbone M, Yang H, Pass HI, Krausz T, Testa JR, Gaudino G. BAP1 and cancer. Nature reviews Cancer. 2013;13(3):153-9.
40. Testa JR, Cheung M, Pei J, Below JE, Tan Y, Sementino E, et al. Germline BAP1 mutations predispose to malignant mesothelioma. Nature genetics. 2011;43(10):1022-5.
41. Carbone M, Yang H. Molecular pathways: targeting mechanisms of asbestos and erionite carcinogenesis in mesothelioma. Clinical cancer research : an official journal of the American Association for Cancer Research. 2012;18(3):598-604.
42. Bott M, Brevet M, Taylor BS, Shimizu S, Ito T, Wang L, et al. The nuclear deubiquitinase BAP1 is commonly inactivated by somatic mutations

and 3p21.1 losses in malignant pleural mesothelioma. Nature genetics. 2011;43(7):668-72.

43. Yoshikawa Y, Sato A, Tsujimura T, Emi M, Morinaga T, Fukuoka K, et al. Frequent inactivation of the BAP1 gene in epithelioid-type malignant mesothelioma. Cancer science. 2012;103(5):868-74.

44. Villanova F, Procopio A, Rippo MR. Malignant mesothelioma resistance to apoptosis: recent discoveries and their implication for effective therapeutic strategies. Current medicinal chemistry. 2008;15(7):631-41.

45. British Thoracic Society Standards of Care C. BTS statement on malignant mesothelioma in the UK, 2007. Thorax. 2007;62 Suppl 2:ii1-ii19.

46. Hodgson JT, McElvenny DM, Darnton AJ, Price MJ, Peto J. The expected burden of mesothelioma mortality in Great Britain from 2002 to 2050. Br J Cancer. 2005;92(3):587-93.

47. Krupoves A, Camus M, De Guire L. Incidence of malignant mesothelioma of the pleura in Quebec and Canada from 1984 to 2007, and projections from 2008 to 2032. American journal of industrial medicine. 2015;58(5):473-82.

48. Joshi TK, Bhuva UB, Katoch P. Asbestos ban in India: challenges ahead. Annals of the New York Academy of Sciences. 2006;1076:292-308.

49. Luo S, Liu X, Mu S, Tsai SP, Wen CP. Asbestos related diseases from environmental exposure to crocidolite in Da-yao, China. I. Review of exposure and epidemiological data. Occupational and environmental medicine. 2003;60(1):35-41; discussion -2.

50. Takahashi K, Karjalainen A. A cross-country comparative overview of the asbestos situation in ten Asian countries. International journal of occupational and environmental health. 2003;9(3):244-8.

51. Nasreen N, Khodayari N, Mohammed KA. Advances in malignant pleural mesothelioma therapy: targeting EphA2 a novel approach. American journal of cancer research. 2012;2(2):222-34.

52. Pinto C, Novello S, Torri V, Ardizzoni A, Betta PG, Bertazzi PA, et al. Second Italian consensus conference on malignant pleural mesothelioma: state of the art and recommendations. Cancer Treat Rev. 2013;39(4):328-39.

53. Henderson DW, Reid G, Kao SC, van Zandwijk N, Klebe S. Challenges and controversies in the diagnosis of mesothelioma: Part 1. Cytology-only

diagnosis, biopsies, immunohistochemistry, discrimination between mesothelioma and reactive mesothelial hyperplasia, and biomarkers. Journal of clinical pathology. 2013;66(10):847-53.
54. Yaziji H, Battifora H, Barry TS, Hwang HC, Bacchi CE, McIntosh MW, et al. Evaluation of 12 antibodies for distinguishing epithelioid mesothelioma from adenocarcinoma: identification of a three-antibody immunohistochemical panel with maximal sensitivity and specificity. Mod Pathol. 2006;19(4):514-23.
55. Husain AN, Colby T, Ordonez N, Krausz T, Attanoos R, Beasley MB, et al. Guidelines for pathologic diagnosis of malignant mesothelioma: 2012 update of the consensus statement from the International Mesothelioma Interest Group. Archives of pathology & laboratory medicine. 2013;137(5):647-67.
56. Ascoli. Pathologic diagnosis of malignant
mesothelioma: chronological prospect
and advent of recommendations
and guidelines. Ann Ist Super Sanità. 2015;51(1):52-9.
57. Hiddinga BI, van Meerbeeck JP. Surgery in mesothelioma--where do we go after MARS? Journal of thoracic oncology : official publication of the International Association for the Study of Lung Cancer. 2013;8(5):525-9.
58. Treasure T, Lang-Lazdunski L, Waller D, Bliss JM, Tan C, Entwisle J, et al. Extra-pleural pneumonectomy versus no extra-pleural pneumonectomy for patients with malignant pleural mesothelioma: clinical outcomes of the Mesothelioma and Radical Surgery (MARS) randomised feasibility study. The Lancet Oncology. 2011;12(8):763-72.
59. Rusch V, Baldini EH, Bueno R, De Perrot M, Flores R, Hasegawa S, et al. The role of surgical cytoreduction in the treatment of malignant pleural mesothelioma: meeting summary of the International Mesothelioma Interest Group Congress, September 11-14, 2012, Boston, Mass. The Journal of thoracic and cardiovascular surgery. 2013;145(4):909-10.
60. Rimner A, Rosenzweig KE. Novel radiation therapy approaches in malignant pleural mesothelioma. Annals of cardiothoracic surgery. 2012;1(4):457-61.
61. Vogelzang NJ, Rusthoven JJ, Symanowski J, Denham C, Kaukel E, Ruffie P, et al. Phase III study of pemetrexed in combination with cisplatin

versus cisplatin alone in patients with malignant pleural mesothelioma. J Clin Oncol. 2003;21(14):2636-44.

62. van Meerbeeck JP, Gaafar R, Manegold C, Van Klaveren RJ, Van Marck EA, Vincent M, et al. Randomized phase III study of cisplatin with or without raltitrexed in patients with malignant pleural mesothelioma: an intergroup study of the European Organisation for Research and Treatment of Cancer Lung Cancer Group and the National Cancer Institute of Canada. Journal of clinical oncology : official journal of the American Society of Clinical Oncology. 2005;23(28):6881-9.

63. Nowak AK. Chemotherapy for malignant pleural mesothelioma: a review of current management and a look to the future. Annals of cardiothoracic surgery. 2012;1(4):508-15.

64. Zucali PA, Simonelli M, Michetti G, Tiseo M, Ceresoli GL, Collova E, et al. Second-line chemotherapy in malignant pleural mesothelioma: results of a retrospective multicenter survey. Lung cancer. 2012;75(3):360-7.

65. Stebbing J, Powles T, McPherson K, Shamash J, Wells P, Sheaff MT, et al. The efficacy and safety of weekly vinorelbine in relapsed malignant pleural mesothelioma. Lung cancer. 2009;63(1):94-7.

66. Zucali PA, Ceresoli GL, Garassino I, De Vincenzo F, Cavina R, Campagnoli E, et al. Gemcitabine and vinorelbine in pemetrexed-pretreated patients with malignant pleural mesothelioma. Cancer. 2008;112(7):1555-61.

67. Okuno SH, Delaune R, Sloan JA, Foster NR, Maurer MJ, Aubry MC, et al. A phase 2 study of gemcitabine and epirubicin for the treatment of pleural mesothelioma: a North Central Cancer Treatment Study, N0021. Cancer. 2008;112(8):1772-9.

68. Fennell DA, Steele JP, Shamash J, Evans MT, Wells P, Sheaff MT, et al. Efficacy and safety of first- or second-line irinotecan, cisplatin, and mitomycin in mesothelioma. Cancer. 2007;109(1):93-9.

69. Okuda K, Sasaki H, Kawano O, Yukiue H, Yokoyama T, Yano M, et al. Epidermal growth factor receptor gene mutation, amplification and protein expression in malignant pleural mesothelioma. Journal of cancer research and clinical oncology. 2008;134(10):1105-11.

70. Mezzapelle R, Miglio U, Rena O, Paganotti A, Allegrini S, Antona J, et al. Mutation analysis of the EGFR gene and downstream signalling pathway in

histologic samples of malignant pleural mesothelioma. British journal of cancer. 2013;108(8):1743-9.

71. Garland LL, Rankin C, Gandara DR, Rivkin SE, Scott KM, Nagle RB, et al. Phase II study of erlotinib in patients with malignant pleural mesothelioma: a Southwest Oncology Group Study. J Clin Oncol. 2007;25(17):2406-13.

72. Govindan R, Kratzke RA, Herndon JE, 2nd, Niehans GA, Vollmer R, Watson D, et al. Gefitinib in patients with malignant mesothelioma: a phase II study by the Cancer and Leukemia Group B. Clinical cancer research : an official journal of the American Association for Cancer Research. 2005;11(6):2300-4.

73. Jahan T, Gu L, Kratzke R, Dudek A, Otterson GA, Wang X, et al. Vatalanib in malignant mesothelioma: a phase II trial by the Cancer and Leukemia Group B (CALGB 30107). Lung cancer. 2012;76(3):393-6.

74. Nowak AK, Millward MJ, Creaney J, Francis RJ, Dick IM, Hasani A, et al. A phase II study of intermittent sunitinib malate as second-line therapy in progressive malignant pleural mesothelioma. Journal of thoracic oncology : official publication of the International Association for the Study of Lung Cancer. 2012;7(9):1449-56.

75. Campbell NP, Kunnavakkam R, Leighl N, Vincent MD, Gandara DR, Koczywas M, et al. Cediranib in patients with malignant mesothelioma: a phase II trial of the University of Chicago Phase II Consortium. Lung cancer. 2012;78(1):76-80.

76. Kindler HL, Karrison TG, Gandara DR, Lu C, Krug LM, Stevenson JP, et al. Multicenter, double-blind, placebo-controlled, randomized phase II trial of gemcitabine/cisplatin plus bevacizumab or placebo in patients with malignant mesothelioma. Journal of clinical oncology : official journal of the American Society of Clinical Oncology. 2012;30(20):2509-15.

77. Zalcman G MJ, Scherpereel A, Astoul P, Monnet I, Milleron B, Paule L, M. André, D. Moro-Sibilot, J. Mazieres on behalf of IFCT. Bevacizumab 15mg/kg plus cisplatin-pemetrexed (CP) triplet versus CP doublet in Malignant Pleural Mesothelioma (MPM): Results of the IFCT-GFPC-0701 MAPS randomized phase 3 trial. Journal Of Clinical Oncology. 2015;33 (suppl; abstr 7500)((suppl; abstr 7500)).

78. Krug LM, Wozniak AJ, Kindler HL, Feld R, Koczywas M, Morero JL, et al. Randomized phase II trial of pemetrexed/cisplatin with or without CBP501 in patients with advanced malignant pleural mesothelioma. Lung cancer. 2014;85(3):429-34.
79. Bianchi AB, Mitsunaga SI, Cheng JQ, Klein WM, Jhanwar SC, Seizinger B, et al. High frequency of inactivating mutations in the neurofibromatosis type 2 gene (NF2) in primary malignant mesotheliomas. Proceedings of the National Academy of Sciences of the United States of America. 1995;92(24):10854-8.
80. Dolly S BJ, Kindler H, et al. Evaluation of tolerability and anti-tumor activity of GDC-0980, an oral PI3K/mTOR inhibitor, administered to patients with advanced solid tumors or non-Hodgkin's lymphoma. . In ECCO-ESMO-ESTRO 2013 Amsterdam: EJC 2013. 2013.
81. Ou SH, Moon J, Garland LL, Mack PC, Testa JR, Tsao AS, et al. SWOG S0722: phase II study of mTOR inhibitor everolimus (RAD001) in advanced malignant pleural mesothelioma (MPM). Journal of thoracic oncology : official publication of the International Association for the Study of Lung Cancer. 2015;10(2):387-91.
82. Villena-Vargas J, Adusumilli PS. Mesothelin-targeted immunotherapies for malignant pleural mesothelioma. Annals of cardiothoracic surgery. 2012;1(4):466-71.
83. Ma J, Tang WK, Esser L, Pastan I, Xia D. Recognition of mesothelin by the therapeutic antibody MORAb-009: structural and mechanistic insights. The Journal of biological chemistry. 2012;287(40):33123-31.
84. Hassan R, Cohen SJ, Phillips M, Pastan I, Sharon E, Kelly RJ, et al. Phase I clinical trial of the chimeric anti-mesothelin monoclonal antibody MORAb-009 in patients with mesothelin-expressing cancers. Clinical cancer research : an official journal of the American Association for Cancer Research. 2010;16(24):6132-8.
85. Hassan R, Kindler HL, Jahan T, Bazhenova L, Reck M, Thomas A, et al. Phase II clinical trial of amatuximab, a chimeric antimesothelin antibody with pemetrexed and cisplatin in advanced unresectable pleural mesothelioma. Clinical cancer research : an official journal of the American Association for Cancer Research. 2014;20(23):5927-36.

86. Kreitman RJ, Hassan R, Fitzgerald DJ, Pastan I. Phase I trial of continuous infusion anti-mesothelin recombinant immunotoxin SS1P. Clinical cancer research : an official journal of the American Association for Cancer Research. 2009;15(16):5274-9.
87. Hassan R, Miller AC, Sharon E, Thomas A, Reynolds JC, Ling A, et al. Major cancer regressions in mesothelioma after treatment with an anti-mesothelin immunotoxin and immune suppression. Science translational medicine. 2013;5(208):208ra147.
88. Calabro L, Morra A, Fonsatti E, Cutaia O, Amato G, Giannarelli D, et al. Tremelimumab for patients with chemotherapy-resistant advanced malignant mesothelioma: an open-label, single-arm, phase 2 trial. The Lancet Oncology. 2013;14(11):1104-11.
89. Calabro L, Maio M. Immune checkpoint blockade in malignant mesothelioma: A novel therapeutic strategy against a deadly disease? Oncoimmunology. 2014;3(1):e27482.
90. Kotova S, Wong RM, Cameron RB. New and emerging therapeutic options for malignant pleural mesothelioma: review of early clinical trials. Cancer management and research. 2015;7:51-63.
91. Hegmans JP, Veltman JD, Lambers ME, de Vries IJ, Figdor CG, Hendriks RW, et al. Consolidative dendritic cell-based immunotherapy elicits cytotoxicity against malignant mesothelioma. Am J Respir Crit Care Med. 2010;181(12):1383-90.
92. Le DT, Brockstedt DG, Nir-Paz R, Hampl J, Mathur S, Nemunaitis J, et al. A live-attenuated Listeria vaccine (ANZ-100) and a live-attenuated Listeria vaccine expressing mesothelin (CRS-207) for advanced cancers: phase I studies of safety and immune induction. Clinical cancer research : an official journal of the American Association for Cancer Research. 2012;18(3):858-68.
93. Hassan R. Antimesothelin vaccine CRS-207 plus chemotherapy as front-line treatment for malignant pleural mesothelioma (MPM). J Clin Oncol 32:5s, 2014 (suppl; abstr 7532). 2014.
94. Sterman DH, Recio A, Vachani A, Sun J, Cheung L, DeLong P, et al. Long-term follow-up of patients with malignant pleural mesothelioma receiving high-dose adenovirus herpes simplex thymidine kinase/ganciclovir suicide

gene therapy. Clinical cancer research : an official journal of the American Association for Cancer Research. 2005;11(20):7444-53.

95. Astoul P, Picat-Joossen D, Viallat JR, Boutin C. Intrapleural administration of interleukin-2 for the treatment of patients with malignant pleural mesothelioma: a Phase II study. Cancer. 1998;83(10):2099-104.

96. Sterman DH, Recio A, Haas AR, Vachani A, Katz SI, Gillespie CT, et al. A phase I trial of repeated intrapleural adenoviral-mediated interferon-beta gene transfer for mesothelioma and metastatic pleural effusions. Molecular therapy : the journal of the American Society of Gene Therapy. 2010;18(4):852-60.

97. Sterman DH, Haas A, Moon E, Recio A, Schwed D, Vachani A, et al. A trial of intrapleural adenoviral-mediated Interferon-alpha2b gene transfer for malignant pleural mesothelioma. American journal of respiratory and critical care medicine. 2011;184(12):1395-9.

98. Hanahan D, Weinberg RA. Hallmarks of cancer: the next generation. Cell. 2011;144(5):646-74.

99. Warburg O, Wind F, Negelein E. The Metabolism of Tumors in the Body. The Journal of general physiology. 1927;8(6):519-30.

100. Vander Heiden MG, Cantley LC, Thompson CB. Understanding the Warburg effect: the metabolic requirements of cell proliferation. Science. 2009;324(5930):1029-33.

101. Groves AM, Win T, Haim SB, Ell PJ. Non-[18F]FDG PET in clinical oncology. The Lancet Oncology. 2007;8(9):822-30.

102. Dang CV. Links between metabolism and cancer. Genes & development. 2012;26(9):877-90.

103. Cantor JR, Sabatini DM. Cancer cell metabolism: one hallmark, many faces. Cancer discovery. 2012;2(10):881-98.

104. Phillips MM, Sheaff MT, Szlosarek PW. Targeting arginine-dependent cancers with arginine-degrading enzymes: opportunities and challenges. Cancer research and treatment : official journal of Korean Cancer Association. 2013;45(4):251-62.

105. Vander Heiden MG. Targeting cancer metabolism: a therapeutic window opens. Nature reviews Drug discovery. 2011;10(9):671-84.

106. Richards NG, Kilberg MS. Asparagine synthetase chemotherapy. Annual review of biochemistry. 2006;75:629-54.
107. Jaffe N, Traggis D, Das L, Frauenberger G, Hann HW, Kim BS, et al. Favorable remission induction rate with twice weekly doses of L-asparaginase. Cancer research. 1973;33(1):1-4.
108. Douer D. Is asparaginase a critical component in the treatment of acute lymphoblastic leukemia? Best practice & research Clinical haematology. 2008;21(4):647-58.
109. Gilroy E. The influence of arginine upon the growth rate of a transplantable tumour in the mouse. Biochem J. 1930;24(3):589-95.
110. Boger RH, Bode-Boger SM. The clinical pharmacology of L-arginine. Annu Rev Pharmacol Toxicol. 2001;41:79-99.
111. Wu G, Morris SM, Jr. Arginine metabolism: nitric oxide and beyond. The Biochemical journal. 1998;336 ( Pt 1):1-17.
112. Delage B, Fennell DA, Nicholson L, McNeish I, Lemoine NR, Crook T, et al. Arginine deprivation and argininosuccinate synthetase expression in the treatment of cancer. International journal of cancer Journal international du cancer. 2010;126(12):2762-72.
113. Yerushalmi HF, Besselsen DG, Ignatenko NA, Blohm-Mangone KA, Padilla-Torres JL, Stringer DE, et al. Role of polyamines in arginine-dependent colon carcinogenesis in Apc(Min) (/+) mice. Mol Carcinog. 2006;45(10):764-73.
114. Yerushalmi HF, Besselsen DG, Ignatenko NA, Blohm-Mangone KA, Padilla-Torres JL, Stringer DE, et al. The role of NO synthases in arginine-dependent small intestinal and colonic carcinogenesis. Mol Carcinog. 2006;45(2):93-105.
115. Yeatman TJ, Risley GL, Brunson ME. Depletion of dietary arginine inhibits growth of metastatic tumor. Archives of surgery. 1991;126(11):1376-81; discussion 81-2.
116. Closs EI, Simon A, Vekony N, Rotmann A. Plasma membrane transporters for arginine. J Nutr. 2004;134(10 Suppl):2752S-9S; discussion 65S-67S.

117. Husson A, Brasse-Lagnel C, Fairand A, Renouf S, Lavoinne A. Argininosuccinate synthetase from the urea cycle to the citrulline-NO cycle. European journal of biochemistry / FEBS. 2003;270(9):1887-99.
118. Xie L, Gross SS. Argininosuccinate synthetase overexpression in vascular smooth muscle cells potentiates immunostimulant-induced NO production. The Journal of biological chemistry. 1997;272(26):16624-30.
119. Summar ML, Koelker S, Freedenberg D, Le Mons C, Haberle J, Lee HS, et al. The incidence of urea cycle disorders. Molecular genetics and metabolism. 2013;110(1-2):179-80.
120. Haberle J. Clinical and biochemical aspects of primary and secondary hyperammonemic disorders. Archives of biochemistry and biophysics. 2013;536(2):101-8.
121. Erez A, DeBerardinis RJ. Metabolic dysregulation in monogenic disorders and cancer - finding method in madness. Nature reviews Cancer. 2015;15(7):440-8.
122. Su TS, Bock HG, O'Brien WE, Beaudet AL. Cloning of cDNA for argininosuccinate synthetase mRNA and study of enzyme overproduction in a human cell line. The Journal of biological chemistry. 1981;256(22):11826-31.
123. Ensor CM, Holtsberg FW, Bomalaski JS, Clark MA. Pegylated arginine deiminase (ADI-SS PEG20,000 mw) inhibits human melanomas and hepatocellular carcinomas in vitro and in vivo. Cancer Res. 2002;62(19):5443-50.
124. Szlosarek PW, Klabatsa A, Pallaska A, Sheaff M, Smith P, Crook T, et al. In vivo loss of expression of argininosuccinate synthetase in malignant pleural mesothelioma is a biomarker for susceptibility to arginine depletion. Clin Cancer Res. 2006;12(23):7126-31.
125. Dillon BJ, Prieto VG, Curley SA, Ensor CM, Holtsberg FW, Bomalaski JS, et al. Incidence and distribution of argininosuccinate synthetase deficiency in human cancers: a method for identifying cancers sensitive to arginine deprivation. Cancer. 2004;100(4):826-33.
126. Yoon CY, Shim YJ, Kim EH, Lee JH, Won NH, Kim JH, et al. Renal cell carcinoma does not express argininosuccinate synthetase and is highly sensitive to arginine deprivation via arginine deiminase. Int J Cancer. 2007;120(4):897-905.

127. Kim RH, Coates JM, Bowles TL, McNerney GP, Sutcliffe J, Jung JU, et al. Arginine deiminase as a novel therapy for prostate cancer induces autophagy and caspase-independent apoptosis. Cancer Res. 2009;69(2):700-8.

128. Feun L, You M, Wu CJ, Kuo MT, Wangpaichitr M, Spector S, et al. Arginine deprivation as a targeted therapy for cancer. Curr Pharm Des. 2008;14(11):1049-57.

129. Tsai WB, Aiba I, Lee SY, Feun L, Savaraj N, Kuo MT. Resistance to arginine deiminase treatment in melanoma cells is associated with induced argininosuccinate synthetase expression involving c-Myc/HIF-1alpha/Sp4. Mol Cancer Ther. 2009;8(12):3223-33.

130. Kobayashi E, Masuda M, Nakayama R, Ichikawa H, Satow R, Shitashige M, et al. Reduced argininosuccinate synthetase is a predictive biomarker for the development of pulmonary metastasis in patients with osteosarcoma. Mol Cancer Ther. 2010;9(3):535-44.

131. Lan J, Tai HC, Lee SW, Chen TJ, Huang HY, Li CF. Deficiency in expression and epigenetic DNA Methylation of ASS1 gene in nasopharyngeal carcinoma: negative prognostic impact and therapeutic relevance. Tumour Biol. 2014;35(1):161-9.

132. Nicholson LJ, Smith PR, Hiller L, Szlosarek PW, Kimberley C, Sehouli J, et al. Epigenetic silencing of argininosuccinate synthetase confers resistance to platinum-induced cell death but collateral sensitivity to arginine auxotrophy in ovarian cancer. International journal of cancer Journal international du cancer. 2009;125(6):1454-63.

133. Allen MD, Luong P, Hudson C, Leyton J, Delage B, Ghazaly E, et al. Prognostic and Therapeutic Impact of Argininosuccinate Synthetase 1 Control in Bladder Cancer as Monitored Longitudinally by PET Imaging. Cancer Res. 2014;74(3):896-907.

134. Thompson CB. Metabolic enzymes as oncogenes or tumor suppressors. The New England journal of medicine. 2009;360(8):813-5.

135. Rabinovich S, Adler L, Yizhak K, Sarver A, Silberman A, Agron S, et al. Diversion of aspartate in ASS1-deficient tumours fosters de novo pyrimidine synthesis. Nature. 2015;527(7578):379-83.

136. Huang CC, Tsai ST, Kuo CC, Chang JS, Jin YT, Chang JY, et al. Arginine deprivation as a new treatment strategy for head and neck cancer. Oral oncology. 2012;48(12):1227-35.
137. Erez A, Nagamani SC, Shchelochkov OA, Premkumar MH, Campeau PM, Chen Y, et al. Requirement of argininosuccinate lyase for systemic nitric oxide production. Nature medicine. 2011;17(12):1619-26.
138. Huang HL, Hsu HP, Shieh SC, Chang YS, Chen WC, Cho CY, et al. Attenuation of argininosuccinate lyase inhibits cancer growth via cyclin A2 and nitric oxide. Molecular cancer therapeutics. 2013;12(11):2505-16.
139. Syed N, Langer J, Janczar K, Singh P, Lo Nigro C, Lattanzio L, et al. Epigenetic status of argininosuccinate synthetase and argininosuccinate lyase modulates autophagy and cell death in glioblastoma. Cell Death Dis. 2013;4:e458.
140. Zheng L, Mackenzie ED, Karim SA, Hedley A, Blyth K, Kalna G, et al. Reversed argininosuccinate lyase activity in fumarate hydratase-deficient cancer cells. Cancer & metabolism. 2013;1(1):12.
141. Adam J, Yang M, Bauerschmidt C, Kitagawa M, O'Flaherty L, Maheswaran P, et al. A role for cytosolic fumarate hydratase in urea cycle metabolism and renal neoplasia. Cell reports. 2013;3(5):1440-8.
142. Qiu F, Chen YR, Liu X, Chu CY, Shen LJ, Xu J, et al. Arginine starvation impairs mitochondrial respiratory function in ASS1-deficient breast cancer cells. Science signaling. 2014;7(319):ra31.
143. Szlosarek P. A randomised phase II trial of pegylated arginine deiminase (ADI-PEG20) in patients with malignant pleural mesothelioma (MPM). In: 2013 World Conference on Lung Cancer 2013 Oct 27-30; Sydney, Australia. 2013; Abstract number: MO09.02.
144. Feun LG, Marini A, Walker G, Elgart G, Moffat F, Rodgers SE, et al. Negative argininosuccinate synthetase expression in melanoma tumours may predict clinical benefit from arginine-depleting therapy with pegylated arginine deiminase. Br J Cancer. 2012;106(9):1481-5.
145. Huang HY, Wu WR, Wang YH, Wang JW, Fang FM, Tsai JW, et al. ASS1 as a novel tumor suppressor gene in myxofibrosarcomas: aberrant loss via epigenetic DNA methylation confers aggressive phenotypes, negative

prognostic impact, and therapeutic relevance. Clin Cancer Res. 2013;19(11):2861-72.
146. Delage B, Luong P, Maharaj L, O'Riain C, Syed N, Crook T, et al. Promoter methylation of argininosuccinate synthetase-1 sensitises lymphomas to arginine deiminase treatment, autophagy and caspase-dependent apoptosis. Cell death & disease. 2012;3:e342.
147. Lagarde SM, Ver Loren van Themaat PE, Moerland PD, Gilhuijs-Pederson LA, Ten Kate FJ, Reitsma PH, et al. Analysis of gene expression identifies differentially expressed genes and pathways associated with lymphatic dissemination in patients with adenocarcinoma of the esophagus. Annals of surgical oncology. 2008;15(12):3459-70.
148. Bowles TL, Kim R, Galante J, Parsons CM, Virudachalam S, Kung HJ, et al. Pancreatic cancer cell lines deficient in argininosuccinate synthetase are sensitive to arginine deprivation by arginine deiminase. Int J Cancer. 2008;123(8):1950-5.
149. Kim JH, Kim JH, Yu YS, Kim DH, Min BH, Kim KW. Anti-tumor activity of arginine deiminase via arginine deprivation in retinoblastoma. Oncology reports. 2007;18(6):1373-7.
150. Kelly MP, Jungbluth AA, Wu BW, Bomalaski J, Old LJ, Ritter G. Arginine deiminase PEG20 inhibits growth of small cell lung cancers lacking expression of argininosuccinate synthetase. Br J Cancer. 2012;106(2):324-32.
151. Qiu F, Huang J, Sui M. Targeting arginine metabolism pathway to treat arginine-dependent cancers. Cancer Lett. 2015;364(1):1-7.
152. Morris SM, Jr. Enzymes of arginine metabolism. The Journal of nutrition. 2004;134(10 Suppl):2743S-7S; discussion 65S-67S.
153. Ni Y, Schwaneberg U, Sun ZH. Arginine deiminase, a potential anti-tumor drug. Cancer letters. 2008;261(1):1-11.
154. Holtsberg FW, Ensor CM, Steiner MR, Bomalaski JS, Clark MA. Poly(ethylene glycol) (PEG) conjugated arginine deiminase: effects of PEG formulations on its pharmacological properties. Journal of controlled release : official journal of the Controlled Release Society. 2002;80(1-3):259-71.
155. Dillon BJ, Holtsberg FW, Ensor CM, Bomalaski JS, Clark MA. Biochemical characterization of the arginine degrading enzymes arginase and arginine deiminase and their effect on nitric oxide production. Medical science

monitor : international medical journal of experimental and clinical research. 2002;8(7):BR248-53.
156. Cheng PN, Lam TL, Lam WM, Tsui SM, Cheng AW, Lo WH, et al. Pegylated recombinant human arginase (rhArg-peg5,000mw) inhibits the in vitro and in vivo proliferation of human hepatocellular carcinoma through arginine depletion. Cancer research. 2007;67(1):309-17.
157. Mauldin JP, Zeinali I, Kleypas K, Woo JH, Blackwood RS, Jo CH, et al. Recombinant human arginase toxicity in mice is reduced by citrulline supplementation. Translational oncology. 2012;5(1):26-31.
158. Laplante M, Sabatini DM. mTOR signaling in growth control and disease. Cell. 2012;149(2):274-93.
159. Rhoads JM, Chen W, Gookin J, Wu GY, Fu Q, Blikslager AT, et al. Arginine stimulates intestinal cell migration through a focal adhesion kinase dependent mechanism. Gut. 2004;53(4):514-22.
160. Fu YM, Zhang H, Ding M, Li YQ, Fu X, Yu ZX, et al. Specific amino acid restriction inhibits attachment and spreading of human melanoma via modulation of the integrin/focal adhesion kinase pathway and actin cytoskeleton remodeling. Clinical & experimental metastasis. 2004;21(7):587-98.
161. Park IS, Kang SW, Shin YJ, Chae KY, Park MO, Kim MY, et al. Arginine deiminase: a potential inhibitor of angiogenesis and tumour growth. British journal of cancer. 2003;89(5):907-14.
162. Stelter L, Evans MJ, Jungbluth AA, Longo VA, Zanzonico P, Ritter G, et al. Imaging of tumor vascularization using fluorescence molecular tomography to monitor arginine deiminase treatment in melanoma. Molecular imaging. 2013;12(1):67-73.
163. Gong H, Pottgen C, Stuben G, Havers W, Stuschke M, Schweigerer L. Arginine deiminase and other antiangiogenic agents inhibit unfavorable neuroblastoma growth: potentiation by irradiation. International journal of cancer Journal international du cancer. 2003;106(5):723-8.
164. Tsai WB, Aiba I, Long Y, Lin HK, Feun L, Savaraj N, et al. Activation of Ras/PI3K/ERK pathway induces c-Myc stabilization to upregulate argininosuccinate synthetase, leading to arginine deiminase resistance in melanoma cells. Cancer Res. 2012;72(10):2622-33.

165. You M, Savaraj N, Kuo MT, Wangpaichitr M, Varona-Santos J, Wu C, et al. TRAIL induces autophagic protein cleavage through caspase activation in melanoma cell lines under arginine deprivation. Mol Cell Biochem. 2013;374(1-2):181-90.

166. Vynnytska-Myronovska B, Bobak Y, Garbe Y, Dittfeld C, Stasyk O, Kunz-Schughart LA. Single amino acid arginine starvation efficiently sensitizes cancer cells to canavanine treatment and irradiation. International journal of cancer Journal international du cancer. 2012;130(9):2164-75.

167. Ascierto PA, Scala S, Castello G, Daponte A, Simeone E, Ottaiano A, et al. Pegylated arginine deiminase treatment of patients with metastatic melanoma: results from phase I and II studies. J Clin Oncol. 2005;23(30):7660-8.

168. Izzo F, Marra P, Beneduce G, Castello G, Vallone P, De Rosa V, et al. Pegylated arginine deiminase treatment of patients with unresectable hepatocellular carcinoma: results from phase I/II studies. J Clin Oncol. 2004;22(10):1815-22.

169. Yang TS, Lu SN, Chao Y, Sheen IS, Lin CC, Wang TE, et al. A randomised phase II study of pegylated arginine deiminase (ADI-PEG 20) in Asian advanced hepatocellular carcinoma patients. Br J Cancer. 2010;103(7):954-60.

170. Szlosarek PW, Luong P, Phillips MM, Baccarini M, Stephen E, Szyszko T, et al. Metabolic response to pegylated arginine deiminase in mesothelioma with promoter methylation of argininosuccinate synthetase. J Clin Oncol. 2013;31(7):e111-3.

171. Glazer ES, Piccirillo M, Albino V, Di Giacomo R, Palaia R, Mastro AA, et al. Phase II study of pegylated arginine deiminase for nonresectable and metastatic hepatocellular carcinoma. J Clin Oncol. 2010;28(13):2220-6.

172. Ott PA, Carvajal RD, Pandit-Taskar N, Jungbluth AA, Hoffman EW, Wu BW, et al. Phase I/II study of pegylated arginine deiminase (ADI-PEG 20) in patients with advanced melanoma. Invest New Drugs. 2013;31(2):425-34.

173. Manca A, Sini MC, Izzo F, Ascierto PA, Tatangelo F, Botti G, et al. Induction of arginosuccinate synthetase (ASS) expression affects the antiproliferative activity of arginine deiminase (ADI) in melanoma cells. Oncology reports. 2011;25(6):1495-502.

174. Rabinowitz JD, White E. Autophagy and metabolism. Science. 2010;330(6009):1344-8.
175. Kim RH, Bold RJ, Kung HJ. ADI, autophagy and apoptosis: metabolic stress as a therapeutic option for prostate cancer. Autophagy. 2009;5(4):567-8.
176. Delage B, Luong P, Maharaj L, O'Riain C, Syed N, Crook T, et al. Promoter methylation of argininosuccinate synthetase-1 sensitises lymphomas to arginine deiminase treatment, autophagy and caspase-dependent apoptosis. Cell Death Dis. 2012;3:e342.
177. Syed N, Langer J, Janczar K, Singh P, Lo Nigro C, Lattanzio L, et al. Epigenetic status of argininosuccinate synthetase and argininosuccinate lyase modulates autophagy and cell death in glioblastoma. Cell Death Dis. 2013;4:e458.
178. Wang Z, Shi X, Li Y, Zeng X, Fan J, Sun Y, et al. Involvement of autophagy in recombinant human arginase-induced cell apoptosis and growth inhibition of malignant melanoma cells. Appl Microbiol Biotechnol. 2013.
179. Iwamoto S, Mihara K, Downing JR, Pui CH, Campana D. Mesenchymal cells regulate the response of acute lymphoblastic leukemia cells to asparaginase. J Clin Invest. 2007;117(4):1049-57.
180. Ehsanipour EA, Sheng X, Behan JW, Wang X, Butturini A, Avramis VI, et al. Adipocytes cause leukemia cell resistance to L-asparaginase via release of glutamine. Cancer Res. 2013;73(10):2998-3006.
181. Witz IP, Levy-Nissenbaum O. The tumor microenvironment in the post-PAGET era. Cancer Lett. 2006;242(1):1-10.
182. Weber CE, Kuo PC. The tumor microenvironment. Surg Oncol. 2012;21(3):172-7.
183. Junttila MR, de Sauvage FJ. Influence of tumour micro-environment heterogeneity on therapeutic response. Nature. 2013;501(7467):346-54.
184. Chen F, Zhuang X, Lin L, Yu P, Wang Y, Shi Y, et al. New horizons in tumor microenvironment biology: challenges and opportunities. BMC medicine. 2015;13:45.
185. Dittmer J, Leyh B. The impact of tumor stroma on drug response in breast cancer. Seminars in cancer biology. 2015;31:3-15.

186. Valencia T, Kim JY, Abu-Baker S, Moscat-Pardos J, Ahn CS, Reina-Campos M, et al. Metabolic reprogramming of stromal fibroblasts through p62-mTORC1 signaling promotes inflammation and tumorigenesis. Cancer cell. 2014;26(1):121-35.
187. Scherz-Shouval R, Santagata S, Mendillo ML, Sholl LM, Ben-Aharon I, Beck AH, et al. The reprogramming of tumor stroma by HSF1 is a potent enabler of malignancy. Cell. 2014;158(3):564-78.
188. Witz IP. The tumor microenvironment: the making of a paradigm. Cancer Microenviron. 2009;2 Suppl 1:9-17.
189. Li H, Fan X, Houghton J. Tumor microenvironment: the role of the tumor stroma in cancer. Journal of cellular biochemistry. 2007;101(4):805-15.
190. Shimoda M, Mellody KT, Orimo A. Carcinoma-associated fibroblasts are a rate-limiting determinant for tumour progression. Seminars in cell & developmental biology. 2010;21(1):19-25.
191. Ungefroren H, Sebens S, Seidl D, Lehnert H, Hass R. Interaction of tumor cells with the microenvironment. Cell communication and signaling : CCS. 2011;9:18.
192. Romero IL, Mukherjee A, Kenny HA, Litchfield LM, Lengyel E. Molecular pathways: trafficking of metabolic resources in the tumor microenvironment. Clinical cancer research : an official journal of the American Association for Cancer Research. 2015;21(4):680-6.
193. Cirri P, Chiarugi P. Cancer associated fibroblasts: the dark side of the coin. American journal of cancer research. 2011;1(4):482-97.
194. Baglole CJ, Ray DM, Bernstein SH, Feldon SE, Smith TJ, Sime PJ, et al. More than structural cells, fibroblasts create and orchestrate the tumor microenvironment. Immunological investigations. 2006;35(3-4):297-325.
195. Harvey P, Warn A, Newman P, Perry LJ, Ball RY, Warn RM. Immunoreactivity for hepatocyte growth factor/scatter factor and its receptor, met, in human lung carcinomas and malignant mesotheliomas. The Journal of pathology. 1996;180(4):389-94.
196. Li Q, Wang W, Yamada T, Matsumoto K, Sakai K, Bando Y, et al. Pleural mesothelioma instigates tumor-associated fibroblasts to promote progression via a malignant cytokine network. The American journal of pathology. 2011;179(3):1483-93.

197. Ghesquiere B, Wong BW, Kuchnio A, Carmeliet P. Metabolism of stromal and immune cells in health and disease. Nature. 2014;511(7508):167-76.
198. Carmeliet P. VEGF as a key mediator of angiogenesis in cancer. Oncology. 2005;69 Suppl 3:4-10.
199. Li Q, Yano S, Ogino H, Wang W, Uehara H, Nishioka Y, et al. The therapeutic efficacy of anti vascular endothelial growth factor antibody, bevacizumab, and pemetrexed against orthotopically implanted human pleural mesothelioma cells in severe combined immunodeficient mice. Clinical cancer research : an official journal of the American Association for Cancer Research. 2007;13(19):5918-25.
200. Yano S, Shinohara H, Herbst RS, Kuniyasu H, Bucana CD, Ellis LM, et al. Production of experimental malignant pleural effusions is dependent on invasion of the pleura and expression of vascular endothelial growth factor/vascular permeability factor by human lung cancer cells. The American journal of pathology. 2000;157(6):1893-903.
201. Fridman WH, Pages F, Sautes-Fridman C, Galon J. The immune contexture in human tumours: impact on clinical outcome. Nature reviews Cancer. 2012;12(4):298-306.
202. Anraku M, Cunningham KS, Yun Z, Tsao MS, Zhang L, Keshavjee S, et al. Impact of tumor-infiltrating T cells on survival in patients with malignant pleural mesothelioma. The Journal of thoracic and cardiovascular surgery. 2008;135(4):823-9.
203. Balkwill FR, Capasso M, Hagemann T. The tumor microenvironment at a glance. Journal of cell science. 2012;125(Pt 23):5591-6.
204. Campbell DJ, Koch MA. Treg cells: patrolling a dangerous neighborhood. Nature medicine. 2011;17(8):929-30.
205. Bates GJ, Fox SB, Han C, Leek RD, Garcia JF, Harris AL, et al. Quantification of regulatory T cells enables the identification of high-risk breast cancer patients and those at risk of late relapse. Journal of clinical oncology : official journal of the American Society of Clinical Oncology. 2006;24(34):5373-80.
206. Wynn TA, Chawla A, Pollard JW. Macrophage biology in development, homeostasis and disease. Nature. 2013;496(7446):445-55.

207. Epelman S, Lavine KJ, Randolph GJ. Origin and functions of tissue macrophages. Immunity. 2014;41(1):21-35.
208. Bain CC, Bravo-Blas A, Scott CL, Gomez Perdiguero E, Geissmann F, Henri S, et al. Constant replenishment from circulating monocytes maintains the macrophage pool in the intestine of adult mice. Nature immunology. 2014;15(10):929-37.
209. McGovern N, Schlitzer A, Gunawan M, Jardine L, Shin A, Poyner E, et al. Human dermal CD14(+) cells are a transient population of monocyte-derived macrophages. Immunity. 2014;41(3):465-77.
210. Fogg DK, Sibon C, Miled C, Jung S, Aucouturier P, Littman DR, et al. A clonogenic bone marrow progenitor specific for macrophages and dendritic cells. Science. 2006;311(5757):83-7.
211. Gordon S, Taylor PR. Monocyte and macrophage heterogeneity. Nature reviews Immunology. 2005;5(12):953-64.
212. Ruffell B, Coussens LM. Macrophages and therapeutic resistance in cancer. Cancer cell. 2015;27(4):462-72.
213. Ruffell B, Affara NI, Coussens LM. Differential macrophage programming in the tumor microenvironment. Trends Immunol. 2012;33(3):119-26.
214. Biswas SK, Mantovani A. Macrophage plasticity and interaction with lymphocyte subsets: cancer as a paradigm. Nature immunology. 2010;11(10):889-96.
215. Mantovani A, Sozzani S, Locati M, Allavena P, Sica A. Macrophage polarization: tumor-associated macrophages as a paradigm for polarized M2 mononuclear phagocytes. Trends Immunol. 2002;23(11):549-55.
216. Mantovani A, Sica A. Macrophages, innate immunity and cancer: balance, tolerance, and diversity. Current opinion in immunology. 2010;22(2):231-7.
217. Gordon S. Alternative activation of macrophages. Nature reviews Immunology. 2003;3(1):23-35.
218. Mantovani A, Allavena P, Sica A, Balkwill F. Cancer-related inflammation. Nature. 2008;454(7203):436-44.
219. Gordon S, Martinez FO. Alternative activation of macrophages: mechanism and functions. Immunity. 2010;32(5):593-604.

220. Quatromoni JG, Eruslanov E. Tumor-associated macrophages: function, phenotype, and link to prognosis in human lung cancer. American journal of translational research. 2012;4(4):376-89.
221. Lawrence T, Natoli G. Transcriptional regulation of macrophage polarization: enabling diversity with identity. Nature reviews Immunology. 2011;11(11):750-61.
222. Sica A, Mantovani A. Macrophage plasticity and polarization: in vivo veritas. J Clin Invest. 2012;122(3):787-95.
223. Talmadge JE, Donkor M, Scholar E. Inflammatory cell infiltration of tumors: Jekyll or Hyde. Cancer Metastasis Rev. 2007;26(3-4):373-400.
224. Bronte V, Zanovello P. Regulation of immune responses by L-arginine metabolism. Nature reviews Immunology. 2005;5(8):641-54.
225. Classen A, Lloberas J, Celada A. Macrophage activation: classical versus alternative. Methods in molecular biology. 2009;531:29-43.
226. Phillips MM, Szlosarek P. Arginine metabolism and tumour-associated macrophages. Tumour -associated macrophages. 2012(Springer: Eds T Lawrence and T Hagemann):77-90.
227. Lin EY, Nguyen AV, Russell RG, Pollard JW. Colony-stimulating factor 1 promotes progression of mammary tumors to malignancy. The Journal of experimental medicine. 2001;193(6):727-40.
228. Qian BZ, Li J, Zhang H, Kitamura T, Zhang J, Campion LR, et al. CCL2 recruits inflammatory monocytes to facilitate breast-tumour metastasis. Nature. 2011;475(7355):222-5.
229. Mizutani K, Sud S, McGregor NA, Martinovski G, Rice BT, Craig MJ, et al. The chemokine CCL2 increases prostate tumor growth and bone metastasis through macrophage and osteoclast recruitment. Neoplasia. 2009;11(11):1235-42.
230. Balkwill F. Cancer and the chemokine network. Nat Rev Cancer. 2004;4(7):540-50.
231. Mantovani A, Allavena P, Sozzani S, Vecchi A, Locati M, Sica A. Chemokines in the recruitment and shaping of the leukocyte infiltrate of tumors. Seminars in cancer biology. 2004;14(3):155-60.
232. Allavena P, Mantovani A. Immunology in the clinic review series; focus on cancer: tumour-associated macrophages: undisputed stars of the

inflammatory tumour microenvironment. Clinical and experimental immunology. 2012;167(2):195-205.

233. Mantovani A, Vecchi A, Allavena P. Pharmacological modulation of monocytes and macrophages. Current opinion in pharmacology. 2014;17:38-44.

234. Heusinkveld M, van der Burg SH. Identification and manipulation of tumor associated macrophages in human cancers. Journal of translational medicine. 2011;9:216.

235. Movahedi K, Laoui D, Gysemans C, Baeten M, Stange G, Van den Bossche J, et al. Different tumor microenvironments contain functionally distinct subsets of macrophages derived from Ly6C(high) monocytes. Cancer research. 2010;70(14):5728-39.

236. Ruffell B, Au A, Rugo HS, Esserman LJ, Hwang ES, Coussens LM. Leukocyte composition of human breast cancer. Proceedings of the National Academy of Sciences of the United States of America. 2012;109(8):2796-801.

237. Redente EF, Dwyer-Nield LD, Merrick DT, Raina K, Agarwal R, Pao W, et al. Tumor progression stage and anatomical site regulate tumor-associated macrophage and bone marrow-derived monocyte polarization. The American journal of pathology. 2010;176(6):2972-85.

238. Massi D, Marconi C, Franchi A, Bianchini F, Paglierani M, Ketabchi S, et al. Arginine metabolism in tumor-associated macrophages in cutaneous malignant melanoma: evidence from human and experimental tumors. Human pathology. 2007;38(10):1516-25.

239. Zhang QW, Liu L, Gong CY, Shi HS, Zeng YH, Wang XZ, et al. Prognostic significance of tumor-associated macrophages in solid tumor: a meta-analysis of the literature. PloS one. 2012;7(12):e50946.

240. Ong SM, Tan YC, Beretta O, Jiang D, Yeap WH, Tai JJ, et al. Macrophages in human colorectal cancer are pro-inflammatory and prime T cells towards an anti-tumour type-1 inflammatory response. European journal of immunology. 2012;42(1):89-100.

241. Dumont P, Berton A, Nagy N, Sandras F, Tinton S, Demetter P, et al. Expression of galectin-3 in the tumor immune response in colon cancer. Laboratory investigation; a journal of technical methods and pathology. 2008;88(8):896-906.

242. Rahat MA, Hemmerlein B. Macrophage-tumor cell interactions regulate the function of nitric oxide. Frontiers in physiology. 2013;4:144.
243. Weigert A, Brune B. Nitric oxide, apoptosis and macrophage polarization during tumor progression. Nitric Oxide. 2008;19(2):95-102.
244. Komohara Y, Jinushi M, Takeya M. Clinical significance of macrophage heterogeneity in human malignant tumors. Cancer science. 2014;105(1):1-8.
245. Gottfried E, Kunz-Schughart LA, Weber A, Rehli M, Peuker A, Muller A, et al. Expression of CD68 in non-myeloid cell types. Scandinavian journal of immunology. 2008;67(5):453-63.
246. Obeid E, Nanda R, Fu YX, Olopade OI. The role of tumor-associated macrophages in breast cancer progression (review). International journal of oncology. 2013;43(1):5-12.
247. Wormann SM, Diakopoulos KN, Lesina M, Algul H. The immune network in pancreatic cancer development and progression. Oncogene. 2014;33(23):2956-67.
248. Burt BM, Rodig SJ, Tilleman TR, Elbardissi AW, Bueno R, Sugarbaker DJ. Circulating and tumor-infiltrating myeloid cells predict survival in human pleural mesothelioma. Cancer. 2011;117(22):5234-44.
249. Chen P, Huang Y, Bong R, Ding Y, Song N, Wang X, et al. Tumor-associated macrophages promote angiogenesis and melanoma growth via adrenomedullin in a paracrine and autocrine manner. Clinical cancer research : an official journal of the American Association for Cancer Research. 2011;17(23):7230-9.
250. Hao NB, Lu MH, Fan YH, Cao YL, Zhang ZR, Yang SM. Macrophages in tumor microenvironments and the progression of tumors. Clinical & developmental immunology. 2012;2012:948098.
251. Lin EY, Li JF, Gnatovskiy L, Deng Y, Zhu L, Grzesik DA, et al. Macrophages regulate the angiogenic switch in a mouse model of breast cancer. Cancer research. 2006;66(23):11238-46.
252. Lin EY, Li JF, Bricard G, Wang W, Deng Y, Sellers R, et al. Vascular endothelial growth factor restores delayed tumor progression in tumors depleted of macrophages. Molecular oncology. 2007;1(3):288-302.
253. De Palma M, Venneri MA, Galli R, Sergi Sergi L, Politi LS, Sampaolesi M, et al. Tie2 identifies a hematopoietic lineage of proangiogenic monocytes

required for tumor vessel formation and a mesenchymal population of pericyte progenitors. Cancer cell. 2005;8(3):211-26.

254. Forget MA, Voorhees JL, Cole SL, Dakhlallah D, Patterson IL, Gross AC, et al. Macrophage colony-stimulating factor augments Tie2-expressing monocyte differentiation, angiogenic function, and recruitment in a mouse model of breast cancer. PloS one. 2014;9(6):e98623.

255. Noy R, Pollard JW. Tumor-associated macrophages: from mechanisms to therapy. Immunity. 2014;41(1):49-61.

256. Egeblad M, Werb Z. New functions for the matrix metalloproteinases in cancer progression. Nature reviews Cancer. 2002;2(3):161-74.

257. Coussens LM, Tinkle CL, Hanahan D, Werb Z. MMP-9 supplied by bone marrow-derived cells contributes to skin carcinogenesis. Cell. 2000;103(3):481-90.

258. Gocheva V, Wang HW, Gadea BB, Shree T, Hunter KE, Garfall AL, et al. IL-4 induces cathepsin protease activity in tumor-associated macrophages to promote cancer growth and invasion. Genes & development. 2010;24(3):241-55.

259. Almholt K, Lund LR, Rygaard J, Nielsen BS, Dano K, Romer J, et al. Reduced metastasis of transgenic mammary cancer in urokinase-deficient mice. International journal of cancer Journal international du cancer. 2005;113(4):525-32.

260. Sangaletti S, Di Carlo E, Gariboldi S, Miotti S, Cappetti B, Parenza M, et al. Macrophage-derived SPARC bridges tumor cell-extracellular matrix interactions toward metastasis. Cancer research. 2008;68(21):9050-9.

261. Bonde AK, Tischler V, Kumar S, Soltermann A, Schwendener RA. Intratumoral macrophages contribute to epithelial-mesenchymal transition in solid tumors. BMC cancer. 2012;12:35.

262. Kuang DM, Zhao Q, Peng C, Xu J, Zhang JP, Wu C, et al. Activated monocytes in peritumoral stroma of hepatocellular carcinoma foster immune privilege and disease progression through PD-L1. The Journal of experimental medicine. 2009;206(6):1327-37.

263. Chen C, Shen Y, Qu QX, Chen XQ, Zhang XG, Huang JA. Induced expression of B7-H3 on the lung cancer cells and macrophages suppresses

T-cell mediating anti-tumor immune response. Experimental cell research. 2013;319(1):96-102.

264. Noman MZ, Desantis G, Janji B, Hasmim M, Karray S, Dessen P, et al. PD-L1 is a novel direct target of HIF-1alpha, and its blockade under hypoxia enhanced MDSC-mediated T cell activation. The Journal of experimental medicine. 2014;211(5):781-90.

265. Herbst RS, Soria JC, Kowanetz M, Fine GD, Hamid O, Gordon MS, et al. Predictive correlates of response to the anti-PD-L1 antibody MPDL3280A in cancer patients. Nature. 2014;515(7528):563-7.

266. Tumeh PC, Harview CL, Yearley JH, Shintaku IP, Taylor EJ, Robert L, et al. PD-1 blockade induces responses by inhibiting adaptive immune resistance. Nature. 2014;515(7528):568-71.

267. Torroella-Kouri M, Silvera R, Rodriguez D, Caso R, Shatry A, Opiela S, et al. Identification of a subpopulation of macrophages in mammary tumor-bearing mice that are neither M1 nor M2 and are less differentiated. Cancer research. 2009;69(11):4800-9.

268. Izzi V, Chiurchiu V, D'Aquilio F, Palumbo C, Tresoldi I, Modesti A, et al. Differential effects of malignant mesothelioma cells on THP-1 monocytes and macrophages. International journal of oncology. 2009;34(2):543-50.

269. Curiel TJ, Coukos G, Zou L, Alvarez X, Cheng P, Mottram P, et al. Specific recruitment of regulatory T cells in ovarian carcinoma fosters immune privilege and predicts reduced survival. Nature medicine. 2004;10(9):942-9.

270. Liu J, Zhang N, Li Q, Zhang W, Ke F, Leng Q, et al. Tumor-associated macrophages recruit CCR6+ regulatory T cells and promote the development of colorectal cancer via enhancing CCL20 production in mice. PloS one. 2011;6(4):e19495.

271. Sharda DR, Yu S, Ray M, Squadrito ML, De Palma M, Wynn TA, et al. Regulation of macrophage arginase expression and tumor growth by the Ron receptor tyrosine kinase. Journal of immunology. 2011;187(5):2181-92.

272. Rodriguez PC, Zea AH, DeSalvo J, Culotta KS, Zabaleta J, Quiceno DG, et al. L-arginine consumption by macrophages modulates the expression of CD3 zeta chain in T lymphocytes. Journal of immunology. 2003;171(3):1232-9.

273. Rodriguez PC, Quiceno DG, Zabaleta J, Ortiz B, Zea AH, Piazuelo MB, et al. Arginase I production in the tumor microenvironment by mature myeloid cells inhibits T-cell receptor expression and antigen-specific T-cell responses. Cancer research. 2004;64(16):5839-49.

274. Ellyard JI, Quah BJ, Simson L, Parish CR. Alternatively activated macrophage possess antitumor cytotoxicity that is induced by IL-4 and mediated by arginase-1. J Immunother. 2010;33(5):443-52.

275. Casazza A, Laoui D, Wenes M, Rizzolio S, Bassani N, Mambretti M, et al. Impeding macrophage entry into hypoxic tumor areas by Sema3A/Nrp1 signaling blockade inhibits angiogenesis and restores antitumor immunity. Cancer cell. 2013;24(6):695-709.

276. Mantovani A, Sica A, Sozzani S, Allavena P, Vecchi A, Locati M. The chemokine system in diverse forms of macrophage activation and polarization. Trends Immunol. 2004;25(12):677-86.

277. Tsutsui S, Yasuda K, Suzuki K, Tahara K, Higashi H, Era S. Macrophage infiltration and its prognostic implications in breast cancer: the relationship with VEGF expression and microvessel density. Oncol Rep. 2005;14(2):425-31.

278. Lewis CE, Pollard JW. Distinct role of macrophages in different tumor microenvironments. Cancer research. 2006;66(2):605-12.

279. Izzi V, Masuelli L, Tresoldi I, Foti C, Modesti A, Bei R. Immunity and malignant mesothelioma: from mesothelial cell damage to tumor development and immune response-based therapies. Cancer letters. 2012;322(1):18-34.

280. Hegmans JP, Hemmes A, Hammad H, Boon L, Hoogsteden HC, Lambrecht BN. Mesothelioma environment comprises cytokines and T-regulatory cells that suppress immune responses. Eur Respir J. 2006;27(6):1086-95.

281. Bielefeldt-ohmann. Potential for Interferon-a-Based Therapy in Mesothelioma:
Assessment in a Murine Model. JOURNAL OF INTERFERON AND CYTOKINE RESEARCH: (1995). 1995; 15(3):213-23.

282. Miselis NR, Wu ZJ, Van Rooijen N, Kane AB. Targeting tumor-associated macrophages in an orthotopic murine model of diffuse malignant mesothelioma. Mol Cancer Ther. 2008;7(4):788-99.

283. Cornelissen R, Lievense LA, Maat AP, Hendriks RW, Hoogsteden HC, Bogers AJ, et al. Ratio of intratumoral macrophage phenotypes is a prognostic factor in epithelioid malignant pleural mesothelioma. PloS one. 2014;9(9):e106742.
284. DeLong P, Carroll RG, Henry AC, Tanaka T, Ahmad S, Leibowitz MS, et al. Regulatory T cells and cytokines in malignant pleural effusions secondary to mesothelioma and carcinoma. Cancer biology & therapy. 2005;4(3):342-6.
285. Veltman JD, Lambers ME, van Nimwegen M, Hendriks RW, Hoogsteden HC, Hegmans JP, et al. Zoledronic acid impairs myeloid differentiation to tumour-associated macrophages in mesothelioma. Br J Cancer. 2010;103(5):629-41.
286. Gabrilovich DI, Ostrand-Rosenberg S, Bronte V. Coordinated regulation of myeloid cells by tumours. Nature reviews Immunology. 2012;12(4):253-68.
287. Miselis NR, Lau BW, Wu Z, Kane AB. Kinetics of host cell recruitment during dissemination of diffuse malignant peritoneal mesothelioma. Cancer microenvironment : official journal of the International Cancer Microenvironment Society. 2010;4(1):39-50.
288. Gabrilovich DI, Nagaraj S. Myeloid-derived suppressor cells as regulators of the immune system. Nature reviews Immunology. 2009;9(3):162-74.
289. Zheng Y, Cai Z, Wang S, Zhang X, Qian J, Hong S, et al. Macrophages are an abundant component of myeloma microenvironment and protect myeloma cells from chemotherapy drug-induced apoptosis. Blood. 2009;114(17):3625-8.
290. Nefedova Y, Landowski TH, Dalton WS. Bone marrow stromal-derived soluble factors and direct cell contact contribute to de novo drug resistance of myeloma cells by distinct mechanisms. Leukemia. 2003;17(6):1175-82.
291. DeNardo DG, Brennan DJ, Rexhepaj E, Ruffell B, Shiao SL, Madden SF, et al. Leukocyte complexity predicts breast cancer survival and functionally regulates response to chemotherapy. Cancer Discov. 2011;1(1):54-67.

292. Shree T, Olson OC, Elie BT, Kester JC, Garfall AL, Simpson K, et al. Macrophages and cathepsin proteases blunt chemotherapeutic response in breast cancer. Genes Dev. 2011;25(23):2465-79.
293. Weizman N, Krelin Y, Shabtay-Orbach A, Amit M, Binenbaum Y, Wong RJ, et al. Macrophages mediate gemcitabine resistance of pancreatic adenocarcinoma by upregulating cytidine deaminase. Oncogene. 2014;33(29):3812-9.
294. Smith MP, Sanchez-Laorden B, O'Brien K, Brunton H, Ferguson J, Young H, et al. The immune microenvironment confers resistance to MAPK pathway inhibitors through macrophage-derived TNFalpha. Cancer discovery. 2014;4(10):1214-29.
295. Wang T, Xiao M, Ge Y, Krepler C, Belser E, Lopez-Coral A, et al. BRAF Inhibition Stimulates Melanoma-Associated Macrophages to Drive Tumor Growth. Clinical cancer research : an official journal of the American Association for Cancer Research. 2015;21(7):1652-64.
296. Alizadeh D, Trad M, Hanke NT, Larmonier CB, Janikashvili N, Bonnotte B, et al. Doxorubicin eliminates myeloid-derived suppressor cells and enhances the efficacy of adoptive T-cell transfer in breast cancer. Cancer research. 2014;74(1):104-18.
297. Kodumudi KN, Woan K, Gilvary DL, Sahakian E, Wei S, Djeu JY. A novel chemoimmunomodulating property of docetaxel: suppression of myeloid-derived suppressor cells in tumor bearers. Clinical cancer research : an official journal of the American Association for Cancer Research. 2010;16(18):4583-94.
298. De Palma M, Lewis CE. Macrophage regulation of tumor responses to anticancer therapies. Cancer cell. 2013;23(3):277-86.
299. Van Rooijen N, Sanders, A. Liposome mediated depletion of macrophages: mechanism of action, preparation of liposomes and applications. J Immunol Methods. 1994;174(1-2):89-93.
300. Greaves P, Clear A, Coutinho R, Wilson A, Matthews J, Owen A, et al. Expression of FOXP3, CD68, and CD20 at diagnosis in the microenvironment of classical Hodgkin lymphoma is predictive of outcome. Journal of clinical oncology : official journal of the American Society of Clinical Oncology. 2013;31(2):256-62.

301. Jensen MM, Jorgensen JT, Binderup T, Kjaer A. Tumor volume in subcutaneous mouse xenografts measured by microCT is more accurate and reproducible than determined by 18F-FDG-microPET or external caliper. BMC medical imaging. 2008;8:16.
302. Hotamisligil GS. Inflammation and metabolic disorders. Nature. 2006;444(7121):860-7.
303. Samali A, Fitzgerald U, Deegan S, Gupta S. Methods for monitoring endoplasmic reticulum stress and the unfolded protein response. International journal of cell biology. 2010;2010:830307.
304. Tam AB, Mercado EL, Hoffmann A, Niwa M. ER stress activates NF-kappaB by integrating functions of basal IKK activity, IRE1 and PERK. PloS one. 2012;7(10):e45078.
305. Sica A, Allavena P, Mantovani A. Cancer related inflammation: the macrophage connection. Cancer Lett. 2008;267(2):204-15.
306. Lee HW, Choi HJ, Ha SJ, Lee KT, Kwon YG. Recruitment of monocytes/macrophages in different tumor microenvironments. Biochim Biophys Acta. 2013;1835(2):170-9.
307. Solinas G, Germano G, Mantovani A, Allavena P. Tumor-associated macrophages (TAM) as major players of the cancer-related inflammation. J Leukoc Biol. 2009;86(5):1065-73.
308. Vandercappellen J, Van Damme J, Struyf S. The role of CXC chemokines and their receptors in cancer. Cancer Lett. 2008;267(2):226-44.
309. Kolaczkowska E, Kubes P. Neutrophil recruitment and function in health and inflammation. Nat Rev Immunol. 2013;13(3):159-75.
310. Srabovici N, Mujagic Z, Mujanovic-Mustedanagic J, Muminovic Z, Softic A, Begic L. Interleukin 13 expression in the primary breast cancer tumour tissue. Biochemia medica. 2011;21(2):131-8.
311. Li Z, Chen L, Qin Z. Paradoxical roles of IL-4 in tumor immunity. Cellular & molecular immunology. 2009;6(6):415-22.
312. Bonecchi R, Facchetti F, Dusi S, Luini W, Lissandrini D, Simmelink M, et al. Induction of functional IL-8 receptors by IL-4 and IL-13 in human monocytes. J Immunol. 2000;164(7):3862-9.

313. Smith DF, Galkina E, Ley K, Huo Y. GRO family chemokines are specialized for monocyte arrest from flow. Am J Physiol Heart Circ Physiol. 2005;289(5):H1976-84.
314. Boisvert WA, Rose DM, Johnson KA, Fuentes ME, Lira SA, Curtiss LK, et al. Up-regulated expression of the CXCR2 ligand KC/GRO-alpha in atherosclerotic lesions plays a central role in macrophage accumulation and lesion progression. Am J Pathol. 2006;168(4):1385-95.
315. Escamilla J, Schokrpur S, Liu C, Priceman SJ, Moughon D, Jiang Z, et al. CSF1 receptor targeting in prostate cancer reverses macrophage-mediated resistance to androgen blockade therapy. Cancer research. 2015;75(6):950-62.
316. Low QE, Drugea IA, Duffner LA, Quinn DG, Cook DN, Rollins BJ, et al. Wound healing in MIP-1alpha(-/-) and MCP-1(-/-) mice. Am J Pathol. 2001;159(2):457-63.
317. Shanware NP, Bray K, Eng CH, Wang F, Follettie M, Myers J, et al. Glutamine deprivation stimulates mTOR-JNK-dependent chemokine secretion. Nature communications. 2014;5:4900.
318. Garg AD, Kaczmarek A, Krysko O, Vandenabeele P, Krysko DV, Agostinis P. ER stress-induced inflammation: does it aid or impede disease progression? Trends in molecular medicine. 2012;18(10):589-98.
319. Hotamisligil GS, Erbay E. Nutrient sensing and inflammation in metabolic diseases. Nat Rev Immunol. 2008;8(12):923-34.
320. Clarke HJ, Chambers JE, Liniker E, Marciniak SJ. Endoplasmic reticulum stress in malignancy. Cancer Cell. 2014;25(5):563-73.
321. Schroder M, Kaufman RJ. The mammalian unfolded protein response. Annual review of biochemistry. 2005;74:739-89.
322. Bi M, Naczki C, Koritzinsky M, Fels D, Blais J, Hu N, et al. ER stress-regulated translation increases tolerance to extreme hypoxia and promotes tumor growth. The EMBO journal. 2005;24(19):3470-81.
323. Romero-Ramirez L, Cao H, Nelson D, Hammond E, Lee AH, Yoshida H, et al. XBP1 is essential for survival under hypoxic conditions and is required for tumor growth. Cancer Res. 2004;64(17):5943-7.

324. Zhong J, Rao X, Xu JF, Yang P, Wang CY. The role of endoplasmic reticulum stress in autoimmune-mediated beta-cell destruction in type 1 diabetes. Experimental diabetes research. 2012;2012:238980.
325. Yu CY, Hsu YW, Liao CL, Lin YL. Flavivirus infection activates the XBP1 pathway of the unfolded protein response to cope with endoplasmic reticulum stress. Journal of virology. 2006;80(23):11868-80.
326. Ma Y, Hendershot LM. The role of the unfolded protein response in tumour development: friend or foe? Nature reviews Cancer. 2004;4(12):966-77.
327. Verfaillie T, Garg AD, Agostinis P. Targeting ER stress induced apoptosis and inflammation in cancer. Cancer Lett. 2013;332(2):249-64.
328. Zhang K, Kaufman RJ. From endoplasmic-reticulum stress to the inflammatory response. Nature. 2008;454(7203):455-62.
329. Margariti A, Li H, Chen T, Martin D, Vizcay-Barrena G, Alam S, et al. XBP1 mRNA splicing triggers an autophagic response in endothelial cells through BECLIN-1 transcriptional activation. The Journal of biological chemistry. 2013;288(2):859-72.
330. Pahl HL. Activators and target genes of Rel/NF-kappaB transcription factors. Oncogene. 1999;18(49):6853-66.
331. Mahadevan NR, Rodvold J, Sepulveda H, Rossi S, Drew AF, Zanetti M. Transmission of endoplasmic reticulum stress and pro-inflammation from tumor cells to myeloid cells. Proceedings of the National Academy of Sciences of the United States of America. 2011;108(16):6561-6.
332. Sanmamed MF, Carranza-Rua O, Alfaro C, Onate C, Martin-Algarra S, Perez G, et al. Serum interleukin-8 reflects tumor burden and treatment response across malignancies of multiple tissue origins. Clin Cancer Res. 2014;20(22):5697-707.
333. Brennecke S, Deichmann M, Naeher H, Kurzen H. Decline in angiogenic factors, such as interleukin-8, indicates response to chemotherapy of metastatic melanoma. Melanoma research. 2005;15(6):515-22.
334. Merchant TE, Li C, Xiong X, Gaber MW. Cytokine and growth factor responses after radiotherapy for localized ependymoma. Int J Radiat Oncol Biol Phys. 2009;74(1):159-67.

335. Britschgi A, Andraos R, Brinkhaus H, Klebba I, Romanet V, Muller U, et al. JAK2/STAT5 inhibition circumvents resistance to PI3K/mTOR blockade: a rationale for cotargeting these pathways in metastatic breast cancer. Cancer Cell. 2012;22(6):796-811.
336. Acharyya S, Oskarsson T, Vanharanta S, Malladi S, Kim J, Morris PG, et al. A CXCL1 paracrine network links cancer chemoresistance and metastasis. Cell. 2012;150(1):165-78.
337. Pegram MD, Reese DM. Combined biological therapy of breast cancer using monoclonal antibodies directed against HER2/neu protein and vascular endothelial growth factor. Seminars in oncology. 2002;29(3 Suppl 11):29-37.
338. Toi M, Matsumoto T, Bando H. Vascular endothelial growth factor: its prognostic, predictive, and therapeutic implications. The Lancet Oncology. 2001;2(11):667-73.
339. Poon RT, Fan ST, Wong J. Clinical implications of circulating angiogenic factors in cancer patients. Journal of clinical oncology : official journal of the American Society of Clinical Oncology. 2001;19(4):1207-25.
340. Zhang Y, Sime W, Juhas M, Sjolander A. Crosstalk between colon cancer cells and macrophages via inflammatory mediators and CD47 promotes tumour cell migration. European journal of cancer. 2013;49(15):3320-34.
341. Davidson JS BI, Harley EH. Metabolic Cooperation between Argininosuccinate Synthetase and Argininosuccinate lyase Deficient Human Fibroblasts. Experimental cell research. 1987;150:367-78
.
342. Sultana Hea. A quantitative study on arginine synthesis from argininosuccinic acid and citrulline by crude enzymes of cattle kidney. Animal Science Journal. 2003;74:289-94.
343. McAllister SS, Weinberg RA. Tumor-host interactions: a far-reaching relationship. Journal of clinical oncology : official journal of the American Society of Clinical Oncology. 2010;28(26):4022-8.
344. Orimo A, Gupta PB, Sgroi DC, Arenzana-Seisdedos F, Delaunay T, Naeem R, et al. Stromal fibroblasts present in invasive human breast carcinomas promote tumor growth and angiogenesis through elevated SDF-1/CXCL12 secretion. Cell. 2005;121(3):335-48.

345. Icard P, Kafara P, Steyaert JM, Schwartz L, Lincet H. The metabolic cooperation between cells in solid cancer tumors. Biochimica et biophysica acta. 2014;1846(1):216-25.
346. Pavlides S, Vera I, Gandara R, Sneddon S, Pestell RG, Mercier I, et al. Warburg meets autophagy: cancer-associated fibroblasts accelerate tumor growth and metastasis via oxidative stress, mitophagy, and aerobic glycolysis. Antioxidants & redox signaling. 2012;16(11):1264-84.
347. Lisanti MP, Martinez-Outschoorn UE, Chiavarina B, Pavlides S, Whitaker-Menezes D, Tsirigos A, et al. Understanding the "lethal" drivers of tumor-stroma co-evolution: emerging role(s) for hypoxia, oxidative stress and autophagy/mitophagy in the tumor micro-environment. Cancer biology & therapy. 2010;10(6):537-42.
348. Martinez-Outschoorn UE, Lisanti MP, Sotgia F. Catabolic cancer-associated fibroblasts transfer energy and biomass to anabolic cancer cells, fueling tumor growth. Seminars in cancer biology. 2014;25:47-60.
349. Ayala G, Morello M, Frolov A, You S, Li R, Rosati F, et al. Loss of caveolin-1 in prostate cancer stroma correlates with reduced relapse-free survival and is functionally relevant to tumour progression. The Journal of pathology. 2013;231(1):77-87.
350. Qian N, Ueno T, Kawaguchi-Sakita N, Kawashima M, Yoshida N, Mikami Y, et al. Prognostic significance of tumor/stromal caveolin-1 expression in breast cancer patients. Cancer science. 2011;102(8):1590-6.
351. Nieman KM, Kenny HA, Penicka CV, Ladanyi A, Buell-Gutbrod R, Zillhardt MR, et al. Adipocytes promote ovarian cancer metastasis and provide energy for rapid tumor growth. Nature medicine. 2011;17(11):1498-503.
352. Wang T, Liu G, Wang R. The Intercellular Metabolic Interplay between Tumor and Immune Cells. Frontiers in immunology. 2014;5:358.
353. Crowther M, Brown NJ, Bishop ET, Lewis CE. Microenvironmental influence on macrophage regulation of angiogenesis in wounds and malignant tumors. Journal of leukocyte biology. 2001;70(4):478-90.
354. Shime H, Yabu M, Akazawa T, Kodama K, Matsumoto M, Seya T, et al. Tumor-secreted lactic acid promotes IL-23/IL-17 proinflammatory pathway. Journal of immunology. 2008;180(11):7175-83.

355. Husain Z, Huang Y, Seth P, Sukhatme VP. Tumor-derived lactate modifies antitumor immune response: effect on myeloid-derived suppressor cells and NK cells. Journal of immunology. 2013;191(3):1486-95.
356. Martinez-Outschoorn UE, Goldberg A, Lin Z, Ko YH, Flomenberg N, Wang C, et al. Anti-estrogen resistance in breast cancer is induced by the tumor microenvironment and can be overcome by inhibiting mitochondrial function in epithelial cancer cells. Cancer biology & therapy. 2011;12(10):924-38.
357. Iwamoto S, Mihara K, Downing JR, Pui CH, Campana D. Mesenchymal cells regulate the response of acute lymphoblastic leukemia cells to asparaginase. J Clin Invest. 2007;117(4):1049-57.
358. Hagemann T, Wilson J, Burke F, Kulbe H, Li NF, Pluddemann A, et al. Ovarian cancer cells polarize macrophages toward a tumor-associated phenotype. J Immunol. 2006;176(8):5023-32.
359. Mantovani A, Allavena P. The interaction of anticancer therapies with tumor-associated macrophages. The Journal of experimental medicine. 2015;212(4):435-45.
360. Wu GY, Brosnan JT. Macrophages can convert citrulline into arginine. Biochem J. 1992;281 ( Pt 1):45-8.
361. Colegio OR, Chu NQ, Szabo AL, Chu T, Rhebergen AM, Jairam V, et al. Functional polarization of tumour-associated macrophages by tumour-derived lactic acid. Nature. 2014;513(7519):559-63.
362. Strieter RM, Burdick MD, Mestas J, Gomperts B, Keane MP, Belperio JA. Cancer CXC chemokine networks and tumour angiogenesis. European journal of cancer. 2006;42(6):768-78.
363. Heidemann J, Ogawa H, Dwinell MB, Rafiee P, Maaser C, Gockel HR, et al. Angiogenic effects of interleukin 8 (CXCL8) in human intestinal microvascular endothelial cells are mediated by CXCR2. The Journal of biological chemistry. 2003;278(10):8508-15.
364. Gabellini C, Trisciuoglio D, Desideri M, Candiloro A, Ragazzoni Y, Orlandi A, et al. Functional activity of CXCL8 receptors, CXCR1 and CXCR2, on human malignant melanoma progression. European journal of cancer. 2009;45(14):2618-27.

365. Baier PK, Wolff-Vorbeck G, Eggstein S, Baumgartner U, Hopt UT. Cytokine expression in colon carcinoma. Anticancer research. 2005;25(3B):2135-9.
366. Ohri CM, Shikotra A, Green RH, Waller DA, Bradding P. Chemokine receptor expression in tumour islets and stroma in non-small cell lung cancer. BMC cancer. 2010;10:172.
367. Liu Z, Yang L, Xu J, Zhang X, Wang B. Enhanced expression and clinical significance of chemokine receptor CXCR2 in hepatocellular carcinoma. The Journal of surgical research. 2011;166(2):241-6.
368. Han L, Jiang B, Wu H, Wang X, Tang X, Huang J, et al. High expression of CXCR2 is associated with tumorigenesis, progression, and prognosis of laryngeal squamous cell carcinoma. Medical oncology. 2012;29(4):2466-72.
369. Wente MN, Keane MP, Burdick MD, Friess H, Buchler MW, Ceyhan GO, et al. Blockade of the chemokine receptor CXCR2 inhibits pancreatic cancer cell-induced angiogenesis. Cancer letters. 2006;241(2):221-7.
370. Waugh DJ, Wilson C. The interleukin-8 pathway in cancer. Clin Cancer Res. 2008;14(21):6735-41.
371. Sharma B, Nawandar DM, Nannuru KC, Varney ML, Singh RK. Targeting CXCR2 enhances chemotherapeutic response, inhibits mammary tumor growth, angiogenesis, and lung metastasis. Molecular cancer therapeutics. 2013;12(5):799-808.
372. Ijichi H, Chytil A, Gorska AE, Aakre ME, Bierie B, Tada M, et al. Inhibiting Cxcr2 disrupts tumor-stromal interactions and improves survival in a mouse model of pancreatic ductal adenocarcinoma. The Journal of clinical investigation. 2011;121(10):4106-17.
373. Sueoka H, Hirano T, Uda Y, Iimuro Y, Yamanaka J, Fujimoto J. Blockage of CXCR2 suppresses tumor growth of intrahepatic cholangiocellular carcinoma. Surgery. 2014;155(4):640-9.
374. Grepin R, Guyot M, Giuliano S, Boncompagni M, Ambrosetti D, Chamorey E, et al. The CXCL7/CXCR1/2 axis is a key driver in the growth of clear cell renal cell carcinoma. Cancer research. 2014;74(3):873-83.

375. Germano G, Frapolli R, Belgiovine C, Anselmo A, Pesce S, Liguori M, et al. Role of macrophage targeting in the antitumor activity of trabectedin. Cancer cell. 2013;23(2):249-62.
376. Diego Luigi Cortinovis LHH, Irene Claudia Floriani, Federica Grosso, Alessandro Marinello, Giovanni Luca Ceresoli, Ilaria Pacchetti, Paolo Andrea Zucali, Maurizio D'Incalci, Stefania Canova, Maria Ida Abbate, Francesca Ugo, Suela Vukcaj, Paolo Bidoli; Az Ospedale S. Gerardo, Monza. Activity and safety of trabectedin in patients with sarcomatoid / biphasic malignant pleural mesothelioma (MPM). J Clin Oncol 33, 2015 (suppl; abstr 7561). 2015.
377. Ries CH, Cannarile MA, Hoves S, Benz J, Wartha K, Runza V, et al. Targeting tumor-associated macrophages with anti-CSF-1R antibody reveals a strategy for cancer therapy. Cancer cell. 2014;25(6):846-59.
378. Beatty GL, Torigian DA, Chiorean EG, Saboury B, Brothers A, Alavi A, et al. A phase I study of an agonist CD40 monoclonal antibody (CP-870,893) in combination with gemcitabine in patients with advanced pancreatic ductal adenocarcinoma. Clinical cancer research : an official journal of the American Association for Cancer Research. 2013;19(22):6286-95.
379. Beatty GL, Chiorean EG, Fishman MP, Saboury B, Teitelbaum UR, Sun W, et al. CD40 agonists alter tumor stroma and show efficacy against pancreatic carcinoma in mice and humans. Science. 2011;331(6024):1612-6.
380. Holohan C, Van Schaeybroeck S, Longley DB, Johnston PG. Cancer drug resistance: an evolving paradigm. Nature reviews Cancer. 2013;13(10):714-26.
381. Cullen SJ, Fatemie S, Ladiges W. Breast tumor cells primed by endoplasmic reticulum stress remodel macrophage phenotype. American journal of cancer research. 2013;3(2):196-210.
382. Wang M, Kaufman RJ. The impact of the endoplasmic reticulum protein-folding environment on cancer development. Nature reviews Cancer. 2014;14(9):581-97.
383. Mahoney DJ, Lefebvre C, Allan K, Brun J, Sanaei CA, Baird S, et al. Virus-tumor interactome screen reveals ER stress response can reprogram resistant cancers for oncolytic virus-triggered caspase-2 cell death. Cancer cell. 2011;20(4):443-56.

384. Rouschop KM, Dubois LJ, Keulers TG, van den Beucken T, Lambin P, Bussink J, et al. PERK/eIF2alpha signaling protects therapy resistant hypoxic cells through induction of glutathione synthesis and protection against ROS. Proceedings of the National Academy of Sciences of the United States of America. 2013;110(12):4622-7.
385. Vakkila J, Lotze MT. Inflammation and necrosis promote tumour growth. Nature reviews Immunology. 2004;4(8):641-8.
386. Zitvogel L, Apetoh L, Ghiringhelli F, Kroemer G. Immunological aspects of cancer chemotherapy. Nature reviews Immunology. 2008;8(1):59-73.
387. Grivennikov SI, Greten FR, Karin M. Immunity, inflammation, and cancer. Cell. 2010;140(6):883-99.

# Appendix